LC-Impact
Version 0.5

A spatially differentiated life cycle impact assessment approach

Francesca Verones[1,2]

Stefanie Hellweg[4]

Ligia B. Azevedo[1,3]

Abhishek Chaudhary[4]

Nuno Cosme[5]

Peter Fantke[5]

Mark Goedkoop[6]

Michael Hauschild[5]

Alexis Laurent[5]

Christopher L. Mutel[4]

Stephan Pfister[4]

Tommie Ponsioen[6]

Zoran Steinmann[1]

Rosalie van Zelm[1]

Marisa Vieira[1,6]

Mark A. J. Huijbregts[1]

[1] Department of Environmental Science, Radboud University Nijmegen, The Netherlands

[2] Industrial Ecology Programme, Department of Energy and Process Engineering, NTNU, Trondheim, Norway

[3] International Institute for Applied Systems Analysis (IIASA), Ecosystem Services and Management Program, Laxenburg, Austria

[4] Institute for Environmental Engineering, ETH Zürich, Zurich, Switzerland

[5] Quantitative Sust. Assessment, DTU Management Engineering, DTU, Denmark

[6] Pré Consultants, Amersfoort, The Netherlands

Table of Contents

1. Overall framework

Francesca Verones[1,2], Stefanie Hellweg[3], Mark A.J. Huijbregts[1]*

[1] Department of Environmental Science, Radboud University Nijmegen, The Netherlands

[2] Industrial Ecology Programme and Department of Energy and Process Engineering, NTNU, Trondheim, Norway

[3] Institute for Environmental Engineering, ETH Zürich, Zurich, Switzerland

*francesca.verones@ntnu.no

1.1. Introduction

1.1.1. General background

Life Cycle Assessment (LCA) is a methodology for assessing the environmental impacts of a product or a service throughout its whole life cycle. In general LCA consists of four phases (ISO 2006b), as shown in Figure 1.1. In the first phase an explicit goal is defined, including the definition of a functional unit for which the LCA is performed. The boundaries of the investigated system are set, the required impact categories chosen and assumptions and limitations identified. During the inventory analysis the materials and inputs required, as well as emissions and outputs created during the complete life cycle are collected. The third step is the Life Cycle Impact Assessment (LCIA) that aims at quantifying the potential environmental impacts and their significance, based on the life cycle inventory (LCI) results. Within the impact assessment characterization models, such as the ones presented here for the LC-IMPACT methodology, are applied. The characterization factors developed in these models indicate the environmental impact per unit of stressor (e.g. per kg of resource used or emission released). In order to make impacts comparable, results are calculated in equivalence units, such as for example DALYs – disability adjusted life years for human health impacts or PDFs – potentially disappeared fractions of species for ecosystem quality.

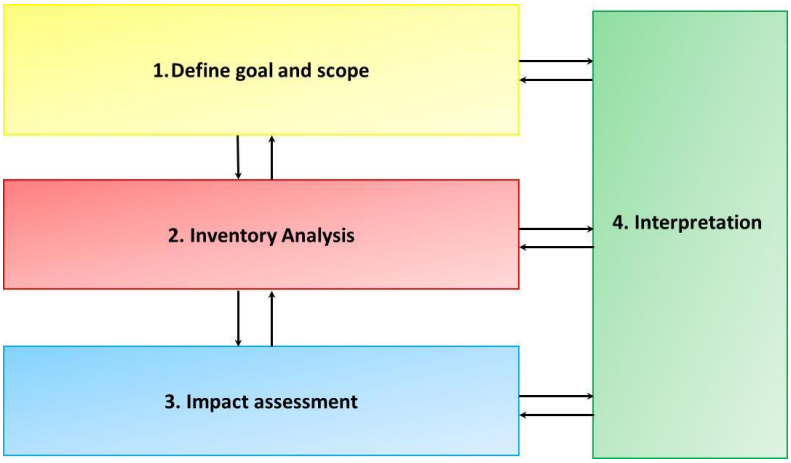

Figure 1.1: The four phases of performing an LCA according to ISO (ISO 2006a; ISO 2006b).

Optionally, normalization can be performed. Normalization factors are relating the characterised results of each impact category to a certain reference situation (e.g. global water consumption in the year 2010), thus introducing an adequate context. Typically, reference situations are chosen at the

global level since the analysed product system often stretches the entire world. In doing this, normalisation provides the relative contribution of a certain product to the chosen reference situation, thus facilitating interpretation (Wegener Sleswijk et al. 2008).

1.1.2. Aim

The development and refinement of LCIA methodologies has made large progress during the last couple of years, incorporating new impact pathways (e.g. water use) and including spatial differentiation if relevant. The LC-IMPACT methodology is at the forefront of these developments and aims to provide a "living" life cycle impact assessment methodology, which is regularly updated to include the most important developments in LCIA. In particular, LC-IMPACT aims to have global coverage for the three main areas of protection (humans, ecosystems, resources), including spatially differentiated information where appropriate.

Innovations include:

- Spatial resolution of CF according to the nature of impact (where possible) as well as spatially aggregated CF on country and global level, to facilitate coupling with LCI
- A new approach for assessing impacts to ecosystems, assessing global extinctions. This approach is more relevant and consistent than previous approaches, which mixed scales of extinctions.
- Explicit documentation of value judgments
- Explicit documentation of type of approach (marginal and/or average/linear)
- Quantitative uncertainty assessments for selected impact categories and qualitative discussion of uncertainties for all impact categories.
-

Normalization factors are also made available along with characterization factors.

The influence of value choices were quantified. Value choices are related to the level of robustness, temporal system boundary or certainty of impacts. This includes the separation of results between short-term and long-term impacts as well as impacts with more or less certainty (e.g. different diseases). This explicit distinction between short-term and certain impacts versus long-term and less certain impacts allows the practitioner to understand the nature of impact better (further explanation below).

In the first phase (2016) only results on an endpoint level will be made available for the impact categories. Harmonized and common midpoint indicators, as well as additional impact categories will be added in the future.

The main work of this harmonized methodology results from the outcomes of the FP7-funded project LC-IMPACT (http://www.lc-impact.eu/). After this framework chapter, individual chapters for all the impact categories follow. Each of them provides information on how the impact pathway affects the environment and the three areas of protection, and explains the value choices and modelling steps for both mid- and endpoints.

1.2. Areas of protection and environmental mechanisms

Human health, ecosystem quality and abiotic resources are commonly used in life cycle impact assessment (LCIA) methodologies (Goedkoop 2000; Goedkoop et al. 2009) as the three areas of protection. It was decided to keep the same three areas of protection for the implementation of the LC-IMPACT methodology.

The overview of the link between the environmental mechanisms and the three areas of protection is shown in Figure 1.2. The category "ecosystem quality" covers the terrestrial, aquatic and marine environments.

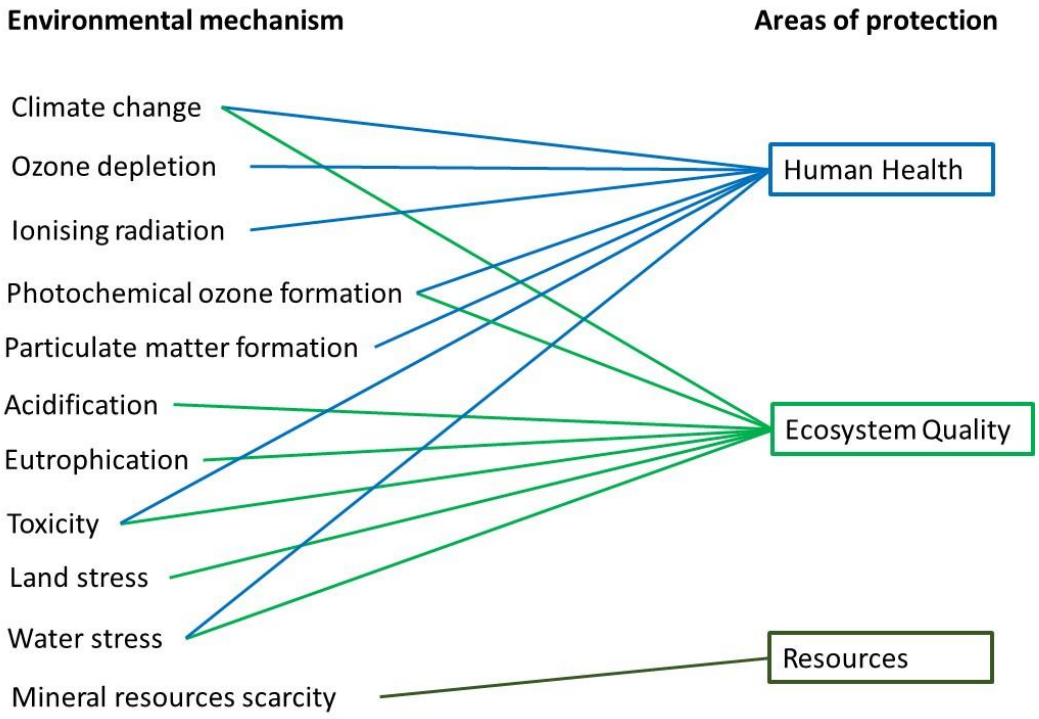

Figure 1.2: Overview of the environmental mechanisms that are covered in the LC-IMPACT methodology and their relation to the areas of protection. Note that "ecosystem quality" covers terrestrial, freshwater and marine ecosystems, thus multiple environmental compartments may be impacted (e.g. terrestrial and freshwater ecotoxicity)

The endpoints are related to the three areas of protection (see

Table **1.1**). Two basic equations for calculating endpoint characterization factors (CFs) are shown below. Equation 1.1 shows the basic CF for human health, with intake fraction iF, exposure factor XF, effect factor EF and damage factor DF. The intake fraction is a measure for the fate and exposure of people to a certain substance, the effect factor quantifies the effect of a certain substance on human health, while the damage factor is a measure for the severity of an impact on human health.

$$CF_{human} = iF \cdot XF \cdot EF \cdot DF$$

Equation 1.1

Equation 1.2 reflects the CF equation for ecosystems. Relative global species loss per unit of emission or extraction was calculated by the product of fate factor FF and effect factor EF.

$$CF_{ecosystems} = FF \cdot EF$$

Equation 1.2

What is special in LC-IMPACT compared to other LCIA methods is that the EF quantifies the relative global species loss by putting the regional species loss in perspective of the global species pool. This is done for one or more taxa (fish, mammals, birds, amphibians, reptiles, and/or plants), depending on the data availability per impact category. For land stress and water stress, we also added a vulnerability score (VS) to the EF calculation. The VS of a species varies between 0 and 1. A VS of 1 means that the species is highly threatened or probably endemic, while lower scores denote less vulnerable species (see also Verones et al. (2015)). We tested the differences between factors including a vulnerability score and those that do not include a vulnerability score, in order to avoid any bias. For land use, the ratio between the median aggregated regional and global CF is by definition 1 (see Chapter 11 on Land stress). Thus, we do not introduce a bias with the vulnerability scores.

Table 1.1: Overview of the areas of protection and respective endpoint units. DALY stands for disability adjusted life years and PDF stands for potentially disappeared fraction of species. kg_{ore} stands for the extra average amount of ore to be produced.

Area of protection	abbreviation	endpoint unit
damage to human health	HH	DALY
damage to ecosystem quality	EQ	PDF
damage to abiotic resources	R	kg_{ore}

The unit for resource is kilogram of ore (kg_{ore}) which represents the extra average amount of ore produced as a result of mineral resource extraction.

DALYs (disability adjusted life years) represent the years that are lost or that a person is disabled for due to a disease or accident. DALYs are typically based on health statistics from the World Health Organization on the global burden of disease (for example, WHO (2014)).

The unit for ecosystem quality is a global fraction of potentially disappeared species (PDF). Although this unit sounds similar to previous LCIA approaches, the underlying concept of how to arrive at these fractions differs from previous methodologies. Instead of local losses based on locally present species, losses of species are considered in relation to the globally present species, leading to a globally normalized PDF of species.

PDF and DALY are no standard units, a DALY basically being a year and a PDF being a fraction. The reason why the results are still presented including the DALY (instead of just year) or PDF (instead of nothing) notation is to clarify the targeted endpoint.

Although it has been argued that mineral resources are available in almost infinite amounts in the earth crust, the actual availability of a mineral primarily depends on ore grades (Gerst 2008). When a mineral is extracted, the overall ore grade of that mineral declines (Prior et al. 2012). The lower the ore grade, the larger the amount of ore that is produced for extracting the same amount of mineral. According to Prior et al. (2012), ore grade decline can be used as an indicator for a range of societal impacts. For instance, larger amounts of ore produced for the same unit of mineral output, implies more waste (waste rock, tailings) to be handled. This is the mechanism that is captured in the area of

protection 'Resources' for mineral resources as a means of extra future effort for resource extraction. The unit of the resource scarcity indicator is the extra amount of ore produced per unit of mineral extracted, averaged over the mining of the full mineral reserve that is currently available (see Figure 1.4 for illustration). Reserves are defined as economically proven reserves for the CF_{core} and ultimately extractable reserves for the $CF_{extended}$. Fossil resources will be included in a later stage of the LC-IMPACT method.

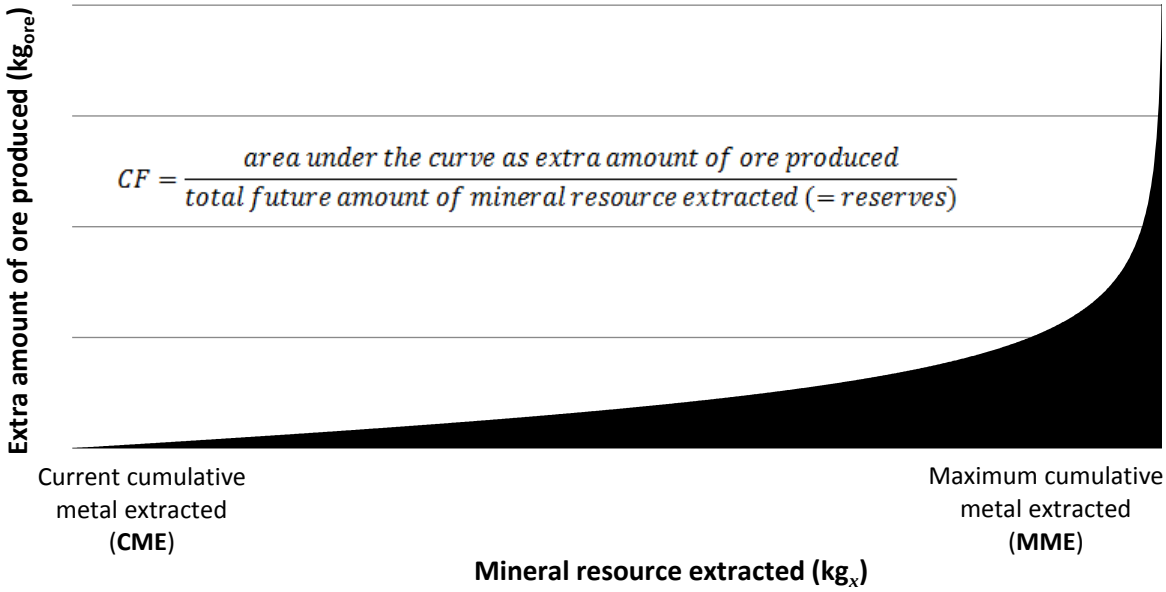

Figure 1.3: Illustrative example for the calculation of characterization factors for mineral resource scarcity.

1.3. Linear/average vs. marginal approach

There are different possible approaches for calculating effect factors, namely marginal, and average/linear (see also Figure 1.4). According to the marginal approach, the influence of raising the background concentration/pressure by an incremental amount is investigated. This means that the reference state is today's situation or the current background concentration and the additional impact of a marginal change is quantified. By contrast, in the case of average modeling, rather than taking the derivative of the curve at the point of current level of impact, the average effect change per unit of change is used. The reference state is the current situation, relating the change either to a zero effect, a preferred state (e.g. environmental targets) or a prospective future state. The main difference between linear and average is that for an average approach the background level is known (highlighted with an asterisk in Table 1.2), while it is assumed to be 0.5 for the linear approach due to the absence of information on background pollution levels.

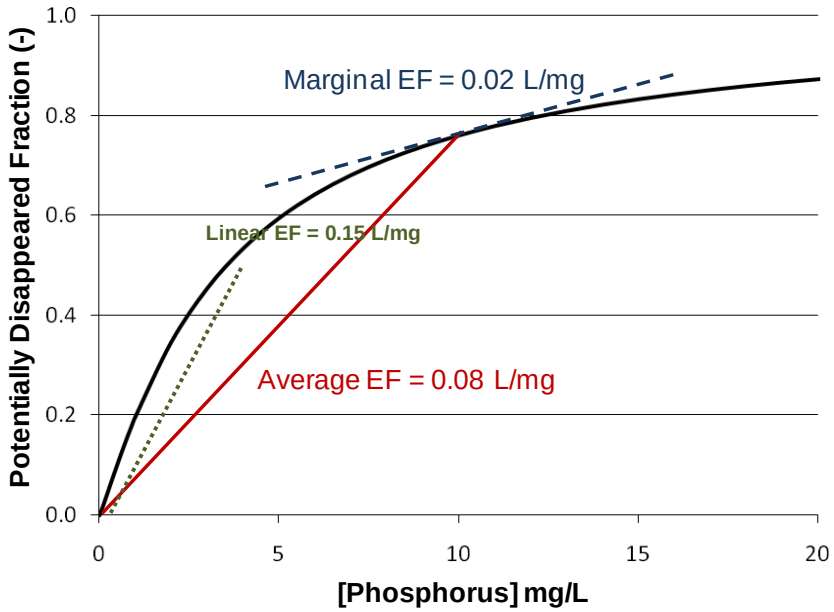

Figure 1.4: Derivation of effect factors (EF) following a linear approach, marginal approach and an average approach, for the impact of total phosphorus concentrations on freshwater macro-invertebrate diversity with a logistic response curve PDF = 1/(1+4.07·Cp-1.11) and working point of 10 mg/l (Huijbregts et al. 2011).

Different environmental mechanisms work with different approaches for calculating the required factors. If possible, more than one approach is used, in order to provide different factors. An overview of the approaches covered by environmental mechanism is given in Table 1.2. Table 1.3 shows that for various impact categories different approaches were chosen. This is not different from previous methods, but in contrast to other LCIA method, here we make the approach explicit so that the practitioner can consciously decide on which one to use. Depending on the scope of the study the practitioner may choose either marginal or linear/average values (if both are available). It is recommended to use, if possible, consistent sets of factors (e.g. either all marginal or all linear/average).

Table 1.2: Overview of approaches covered by each environmental mechanism. An asterisk indicates if the background level is known (average approach).

Environmental mechanism	marginal	average/linear
climate change	✓	✓*
stratospheric ozone depletion		✓
ionising radiation		✓
photochemical ozone formation		✓*
particular matter formation		✓
terrestrial acidification	✓	
freshwater eutrophication		✓
marine eutrophication		✓
freshwater ecotoxicity		✓
human toxicity (carcinogenic)		✓
human toxicity (non-carcinogenic)		✓
marine ecotoxicity		✓
terrestrial ecotoxicity		✓
land stress	✓	✓*
water stress (ecosystems)	✓	
water stress (human health)	✓	✓*
mineral resources extraction		✓

The different approaches have different strengths for applications. Approaches with marginal changes quantify the impact of small changes in emissions or resource uses (as stated in Huijbregts et al. (2011): "what do we add in terms of environmental impact with the consumption of one liter of coffee?"). However, if there are already high environmental impacts, the marginal impact may decrease and in extreme cases become zero, implying that if environmental impacts are already substantial, additional impacts are of no consequence. Average approaches, on the other hand, assess the impacts of larger changes than just marginal ones. Therefore, this type of approach potentially also opens a further field of application of life cycle impact assessment methods such as LC-Impact, by connecting it to the macro-scale assessments of input-output models. Input-output models quantify accurately what the resource use or footprint of a consumer is, but hardly ever attempt to quantify the environmental consequences related to this resource use. LC-Impact, as a spatially differentiated impact assessment method can potentially contribute to such an assessment.

1.4. Value choices

Important binary choices are the differentiation between low and high levels of robustness. Binary choices between the level of robustness can be related either (1) to the fact that it can be highly uncertain whether a specific effect is caused by the interventions that belong to an impact category (e.g. cataract for ozone depletion) and (2) to the timing of the impact (long-term or short-term effects), represented by the time horizon. In general, the further away in time the impact is, the more uncertain, i.e. the lower the level of robustness.

In contrast to the cultural perspectives (individualist, hierarchist and egalitarian) that are commonly used in LCA (e.g. Goedkoop et al. (2009)), we follow another approach here. Instead, the characterization factor is built in a modular way that allows the user to add or neglect impacts that are farther away (in a time perspective) and less certainly caused by a specific environmental mechanism. This is schematically shown in Figure 1.5 and Equation 1.3.

$$CF_{extended} = CF_{core} + \Delta CF_{long-term/low\ robustness}$$

Equation 1.3

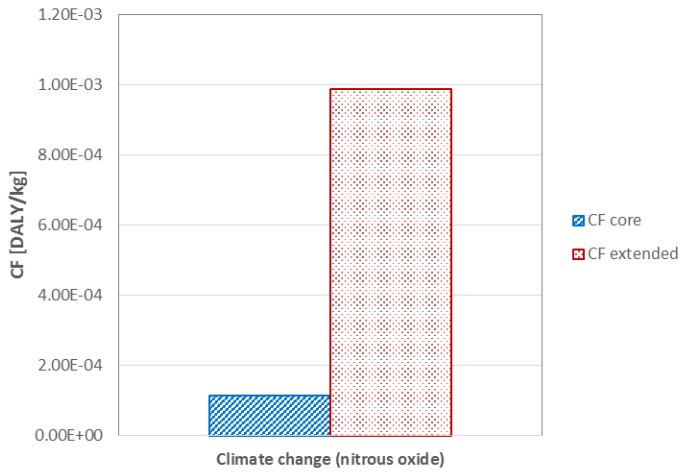

Figure 1.5: Schematic representation of the modularity of the characterization factors for damage calculation with the example of nitrous oxide (climate change). If only the core level factor is used, the characterization factor (CF) would be 1.13E-04 DALY/kg, while the extended version of the CF is 9.9E-04 DALY/kg (adding the long-term/low robustness part to the core CF).

We acknowledge that it is also theoretically possible to have four categories instead of two: 1) short time horizon and high level of certainty for impact of a specific intervention, 2) long time horizon and high level of certainty for impact of a specific intervention, 3) short time horizon and low level of certainty for impact of a specific intervention and 4) long time horizon and low level of certainty for impact of a specific intervention. However, this would overly complicate the application and thus it was decided to stick to only two levels of robustness and time frame. We recommend users to always calculate results with both sets of characterization factors (high level/short term and total), in order to understand the full extent and nature of potential impact.

Table 1.3 gives an overview of the value choices with low and high level of robustness for each environmental mechanism. Please note that these binary choices, in order to in- or exclude certain parts of a characterization factor do not reflect statistical uncertainty or confidence intervals.

Table 1.3: Overview of choices per impact category. Note that the time horizon for terrestrial acidification and mineral resources can be relevant (van Zelm et al. 2007; Vieira et al. 2012) but cannot be considered due to insufficient data (indicated with "not used" instead of "not relevant").

Environmental mechanism	Core CFs	addition to reach extended CFs
climate change	**Time horizon:** 100 yrs **Included effects:** diarrhoea, malaria, coastal flooding	**Time horizon:** 100-1000 yrs **Included effects:** malnutrition, cardiovascular diseases, inland flooding
stratospheric ozone depletion	**Time horizon:** 100 yrs **Included effects:** skin cancer	**Time horizon:** 100 yrs-infinite **Included effects:** cataract
ionising radiation	**Time horizon:** 100 yrs **Included effects:** Cancers: Thyroid, bone marrow, lung and breast. Hereditary disease	**Time horizon:** 100-1000 yrs **Included effects:** bladder, colon, ovary, skin, liver, oesophagus, stomach, bone surface and remaining cancer
photochemical ozone formation	**Time horizon:** not relevant **Included effects: -**	**Time horizon:** not relevant **Included effects: -**
particular matter formation	**Time horizon:** not relevant **Included effects:** from primary aerosols only	**Time horizon:** not relevant **Included effects:** secondary aerosols from SO2, NH3 and NOx
terrestrial acidification	**Time horizon:** not used **Included effects:** reduction of plant species richness due to N and S emissions to air	**Time horizon:** - **Included effects:**-
freshwater eutrophication	**Time horizon:** not relevant **Included effects:** reduction of fish species richness due to P emissions to water	**Time horizon:** - **Included effects:** -
marine eutrophication	**Time horizon:** not relevant **Included effects:** affected fractions via air and freshwater emissions of N, NH3 and NOx	**Time horizon:** - **Included effects:** same as core
freshwater ecotoxicity	**Time horizon:** 100 yrs **Included effects:**	**Time horizon:** 100 yrs - infinite **Included effects:**
human toxicity (carcinogenic)	**Time horizon:** 100 yrs **Included effects:** via air and drinking water only, only substances with strong evidence for carcinogenity (IARC-category 1, 2A and 2B)	**Time horizon:** 100 yrs - infinite **Included effects:** via food, remaining substances of the totally 844 potentially carcinogenic substances from IARC
human toxicity (non-carcinogenic)	**Time horizon:** 100 yrs **Included effects:** via air and drinking water only	**Time horizon:** 100 yrs - infinite **Included effects:** via food
marine ecotoxicity	**Time horizon:** 100 yrs **Included effects:** sea compartment only	**Time horizon:** 100 yrs - infinite **Included effects:** ocean compartment only
terrestrial ecotoxicity	**Time horizon:** 100 yrs **Included effects:**	**Time horizon:** 100 yrs **-** infinite **Included effects:**

land stress (occupation)	**Time horizon:** not relevant **Included effects:** occupation of 6 land use types	**Time horizon:** - **Included effects:** same as core
land stress (transformation)	**Time horizon:** 100 yrs **Included effects:** transformation of 6 land use types	**Time horizon:** 10 yrs - total recovery times (up to 1200 yrs, depending on ecosystem) **Included effects:** transformation of 6 land use types
water stress (ecosystems)	**Time horizon:** not relevant **Included effects:** surface water consumption impacts on wetlands	**Time horizon:** not relevant **Included effects:** groundwater consumption impacts on wetlands
water stress (human health)	**Time horizon:** not relevant **Included effects:** Malnutrition	**Time horizon:** - **Included effects:** same as core
mineral resources extraction	**Time horizon:** not used **Included effects:** uses (economic) 'reserves'	**Time horizon:** not used **Included effects:** uses 'ultimately extractable reserves'

1.5. Spatial variability

1.5.1. Level of spatial resolution

The level of spatial detail is varying greatly between the different environmental mechanisms, as is shown in Table 1.4. Some mechanisms, for example climate change do not need spatial detail in the application of the characterization factors, since the damages are spreading on a global level. Others, for example water stress, have very local and specific impacts and incorporating spatial details in the methodological development is thus a large benefit. The approach for including spatial variability is, wherever possible, reflecting the nature and spatial extend of impact. However, for some impact categories it was data driven (Table 1.4). We include spatial variability, as soon as information is available and adapt the spatial resolution on which the final characterization factors are provided to the resolution of the available data.

Table 1.4: Spatial resolution for the different parts of the environmental mechanisms.

environmental mechanism	Spatial resolution fate factor	Spatial resolution effect factor	Spatial resolution characterization factor
climate change (ecosystems)	none	none	none
climate change (human health)	none	none	none
stratospheric ozone depletion	none	none	none
ionising radiation	global values for air, freshwater, marine	none	global values for air, freshwater, marine
photochemical ozone depletion (ecosystems)	56 world regions (averages of base run of 1°x1°)	none	country level
photochemical ozone depletion (human health)	56 world regions (averages of base run of 1°x1°)	none	country level
particular matter formation	56 world regions (averages of base run of 1°x1°)	none	country level
terrestrial acidification	615'888 three dimensional compartments	2° x 2.5°	2° x 2.5°
freshwater eutrophication	0.5° x 0.5°	biogeographical habitats	0.5° x 0.5°

marine eutrophication	Country to large marine ecosystems (233 spatial units)	66 large marine ecosystems (5 climate zones)	Country to large marine ecosystems (233 spatial units)
freshwater ecotoxicity			sub-continental
human toxicity			sub-continental
marine ecotoxicity			sub-continental
terrestrial ecotoxicity			sub-continental
land stress	ecoregions	ecoregions	ecoregions
water stress (ecosystems)	more than 20'000 individual points	more than 20'000 individual points	0.05° x 0.05°
water stress (human health)	watersheds (11'000 units)	country level	watersheds (11'000 units)
mineral resources extraction	none		none

1.5.2. Ecosystem impacts: Procedures for maps of taxonomic classes

Maps with number of species present and, if possible, vulnerability scores (VS) are calculated for different taxonomic groups. An overview of the taxonomic groups covered in each impact category is given in Table 1.5.

Table 1.5: Overview of the taxonomic groups used for calculating maps of species counts and vulnerability scores (only possible for taxa with available IUCN data). All groups consist of animals except tracheophyta (vascular plants) and liliopsida (sea grass). FEOW stands for freshwater ecoregions of the world.

Environmental mechanism	taxonomic group	taxonomic classification	Spatial resolution	VS map available?	Data origin
Acidification	Tracheophyta	Phylum	0.53°x0.53°	no	Kier et al. (2009)
Freshwater eutrophication	Fish	Classes	FEOW	no	Abell et al. (Abell et al. 2008)
Marine eutrophication	Actinopterygii Chondrichthyes Liliopsida Anthozoa Halothuroidea Gastropoda	Classes (note: only species occurring in marine neritic habitats are included)	0.05°x0.05°	yes	IUCN (2013b)
Photochemical ozone formation	Tracheophyta	Phylum	0.53°x0.53°	no	Kier et al. (2009)
Water	Mammalia Aves Amphibia Reptilia	Classes	0.05°x0.05°	yes	IUCN (2013b)
Land	Mammalia Aves Amphibia Reptilia Traxcheophyta	Classes	0.05°x0.05°	yes	IUCN (2013b)
Climate change	Global average	-	-	no	
Ecotoxicity	Global average	-	-	no	

Species maps were calculated with as much and detailed data as possible according to the following data priority setting:

1) Maps calculated with IUCN data

For a wide variety of species IUCN provides geographic range sizes, including explicit spatial information, compatible for use in geographical information systems. As taxonomic classification level

we chose “classes” for calculating these maps (Table 1.5). Classes are the third level of the taxonomic classification after “Kingdom” (e.g. plants, animals) and “Phylum” (e.g. chordate, tracheophyta). In order to represent the number of species on a global grid, the geographical ranges of all relevant species were overlaid and summed in Matlab (MathWorks 2013). Species that are already extinct nowadays were excluded from the analysis, because the aim of the maps is to give present species counts. The procedure is also described in Verones et al. (2013b). The resolution of these maps is 0.05°x0.05°.

2) Species maps from other authors

If no species-specific information on geographic range sizes were available, a search for existing species maps was performed. The map for tracheophyta (vascular plants) is a map that was made available by Kreft et al. (2007). Tracheophyta is a phylum and not a class, but there is no map available for all 12 classes of vascular plants that are grouped into the phylum tracheophyta. The resolution is fixed and we do not have species lists available for different classes at each location.

3) Using relationships with abiotic parameters to estimate species occurrences

If the search for existing maps yielded no results, relationships with abiotic parameters were applied for estimating the number of species in a spatially differentiated way. This is the case for freshwater fish species. We used a species-discharge relationship (Oberdorff et al. 1995) and the modelled yearly average discharge from WaterGap (WATCH 2011) to come up with a map of estimated fish species numbers.

For the fish map (for freshwater eutrophication) the fate and effect factor are made compatible to the resolution of the species map because we have explicit relationships for modelling the fish counts at spatial level. However, the map of tracheophyta for terrestrial acidification cannot be resampled. Thus, we upsize the resolutions of the fate and effect factor for terrestrial acidification, in order to match the resolution of the tracheophyta map. This species map is an existing map we are using with species richness information. However, we do not know which species exactly are present in which cell. Thus we cannot resample the map, since the same species number (e.g. 3) in two pixels does not mean that the species composition is exactly the same (e.g. species A, B and C in pixel 1 and A, B and D in pixel 2).

1.5.3. Spatial aggregation

All spatially-differentiated characterization factors are also available on a country and a continental level to facilitate application. A single global default value will also be provided.

Spatial aggregation is done by calculating weighted averages. Averaging at higher spatial scales will be based on actual emissions, except for land and water stress, which will be based on water withdrawal and land use, respectively. Population density can be used as a fallback proxy weighting scheme. The aggregation based on emission and resource consumption patterns reflects the best knowledge we currently have about activity levels. Note that with this approach we assume that a new activity (emission, consumption) is more likely to happen in regions where activities are already taking place, i.e. this is an attributional assessment (Mutel et al. in preparation). Table 1.6 shows the data sources and method used for aggregating.

Table 1.6: Overview of data sources and aggregation type for impact categories that include spatial differentiation.

impact category	aggregation based on	Reference year	Data source for aggregation
freshwater eutrophication	emissions/ crop areas (for erosion)	2000	Scherer et al. (2015)
terrestrial acidification	population density	2000	CIESIN (2005)
water stress	water consumption	2010	WATCH (2011), Pfister et al. (2011a), UN (2011)
land stress	ecoregion size	-	Olson et al.(2001a)
particulate matter	emissions	2000	Lamarque et al. (2010)
photochemical ozone formation	emissions	2000	Lamarque et al. (2010)

1.6. Literature

Abell, R., Thieme, M. L., Revenga, C., Bryer, M., Kottelat, M., et al. (2008). "Freshwater Ecoregions of the World: A New Map of Biogeographic Units for Freshwater Biodiversity Conservation." BioScience **58**(5): 403-414.

CIESIN, (Center for Interantional Earth Science Information Network, Columbia University) and CIAT, (Centro Internacional de Agricultura Tropical) (2005). Gridded Population of the World, Version 3 (GPWv3): Population Density Grid. Palisades,NY: NASA Socieoeconomic Data and Applictions Center (SEDAC). http://dx.doi.org/10.7927/H4XK8CG2 (03.09.2014).

Gerst, M. D. (2008). "Revisiting the cumulative grade-tonnage relationship for major copper ore types." Economic Geology **103**(3): 615-628.

Goedkoop, M. (2000). The Eco-indicator 99 LCIA methodology - an introduction. Eco-Indicator 99 - eine schadensorientierte Bewertungsmethode. Nachbereitung zum 12. Diskussionsforum Ökobilanzen vom 30. Juni and der ETH Zürich. T. Baumgartner and A. Braunschweig. Zurich, Switzerland.

Goedkoop, M., Heijungs, R., Huijbregts, M. A. J., De Schryver, A., Struijs, J. and van Zelm, R. (2009). ReCiPe 2008: A life cycle impact assessment method which comprises harmonised category indicators at the midpoint and endpoint levels. First edition. Report i: Characterization. The Netherlands, Ruimte en Milieu, Ministerie van Volkshuisvesting, Ruimtelijke Ordening en Milieubeheer.

Huijbregts, M. A. J., Hellweg, S. and Hertwich, E. (2011). "Do We Need a Paradigm Shift in Life Cycle Assessment?" Environ. Sci. Technol. **45**: 3833-3834.

ISO (2006a). Environmental Management - Life Cycle Assessment - Principles and Framework. International Standard ISO 14040. International Organisation for Standardisation. Geneva, Switzerland.

ISO (2006b). Environmental management - Life Cycle Assessment - Requirements and guidelines. International Standard ISO 14044, International Organisation for Standardisation. Geneva, Switzerland.

IUCN, (International Union for Conservation of Nature and Natural Resources). (2013). "Spatial Data Download." Retrieved 3 October, 2013, from http://www.iucnredlist.org/technical-documents/spatial-data.

Kier, G., Kreft, H., Lee, T. M., Jetz, W., Ibisch, P. L., Nowicki, C., Mutke, J. and Barthlott, W. (2009). "A global assessment of endemism and species richness across island and mainland regions." PNAS **106**(23): 9322-9327.

Kreft, H. and Jetz, W. (2007). "Global patterns and determinants of vascular plant diversity." PNAS **104**(14): 5925-5930.

Lamarque, J. F., Bond, T. C., Eyring, V., Granier, C., Heil, A., et al. (2010). "Historical (1850-2000) gridded anthropogenic and biomass burning emissions of reactive gases and aerosols: methodology and application." Atmos. Chem. Phys. **10**(15): 7017-7039.

MathWorks (2013). "Matlab Version 2013b."

Mutel, C. L. and Hellweg, S. (in preparation). "Computational Methods for Regionalized Life Cycle Assessment." Environmental Science and Technology.

Oberdorff, T., Guégan, J.-F. and Hugueny, B. (1995). "Global scale patterns of fish species richness in rivers." Ecography **18**: 345-352.

Olson, D. M., Dinerstein, E., Wikramanayake, E. D., Burgess, N., Powell, G. V. N., Underwood, E., D'Amico, J. A., Itoua, I., Strand, H. E., Morrison, J. C., Loucks, C. J., Allnutt, T. F., Ricketts, T. H., Kura, Y., Lamoreux, J. F., Wettengel, W. W., Hedao, P. and Kassem, K. R. (2001). "Terrestrial Ecoregions of the World: A New Map of Life on Earth (Note: data update from 2004 used)." BioScience **51**(11): 933-938.

Pfister, S., Bayer, P., Koehler, A. and Hellweg, S. (2011). "Environmental Impacts of Water Use in Global Crop Production: Hotspots and Trade-Offs with Land Use." Environ. Sci. Technol. **45**(13): 5761-5768.

Prior, T., Giurco, D., Mudd, G., Mason, L. and Behrish, J. (2012). "Resource depletion, peak minerals and the implications for sustainable resource management." Global Environmental Change **22**(3): 577-587.

Scherer, L. and Pfister, S. (2015). "Modelling spatially explicit impacts from phosphorus emissions in agriculture." The International Journal of Life Cycle Assessment **20**(6): 785-795.

United Nations and Department of Economic and Social Affairs, Population Divison, (2011). "World Population Prospectes: The 2010 Revision, CD-ROM edition."

van Zelm, R., Huijbregts, M. A. J., van Jaarsveld, H. A., Reinds, G. J., de Zwart, D., Struijs, J. and van de Meent, D. (2007). "Time Horizon Dependent Characterization Factors for Acidification in Life-Cycle Assessment Based on Forest Plant Species Occurrence in Europe." Environmental Science & Technology **41**(3): 922-927.

Verones, F., Huijbregts, M. A. J., Chaudhary, A., De Baan, L., Koellner, T. and Hellweg, S. (2015). "Harmonizing the Assessment of Biodiversity Effects from Land and Water Use within LCA." Environ. Sci. Technol. **49**(6): 3584-3592.

Verones, F., Saner, D., Pfister, S., Baisero, D., Rondinini, C. and Hellweg, S. (2013). "Effects of consumptive water use on wetlands of international importance." Environ. Sci. Technol. **47**(21): 12248-12257.

Vieira, M. D. M., Goedkoop, M. J., Storm, P. and Huijbregts, M. A. J. (2012). "Ore Grade Decrease As Life Cycle Impact Indicator for Metal Scarcity: The Case of Copper." Environmental Science & Technology **46**(23): 12772-12778.

WATCH. (2011). "Water and global change." Retrieved August, 2012, from http://www.eu-watch.org/; download of data from: https://gateway.ceh.ac.uk/terraCatalog/Start.do.

Wegener Sleswijk, A., van Oers, L. F. C. M., Guinée, J. B., Struijs, J. and Huijbregts, M. A. J. (2008). "Normalisation in product life cycle assessment: An LCA of the global and European economic systems in the year 2000." Science of the total environment **390**(1): 227-240.

WHO, (World Health Organization). (2014). "Estimaters for 2002-2012: Disease burden." Retrieved 1 December, 2014, from http://www.who.int/healthinfo/global_burden_disease/estimates/en/index2.html.

2. Climate change

Zoran Steinmann[1], Mark A.J. Huijbregts[1]*

[1] Department of Environmental Science, Radboud University Nijmegen, The Netherlands

* z.steinmann@science.ru.nl

2.1. Areas of protection and environmental mechanisms covered

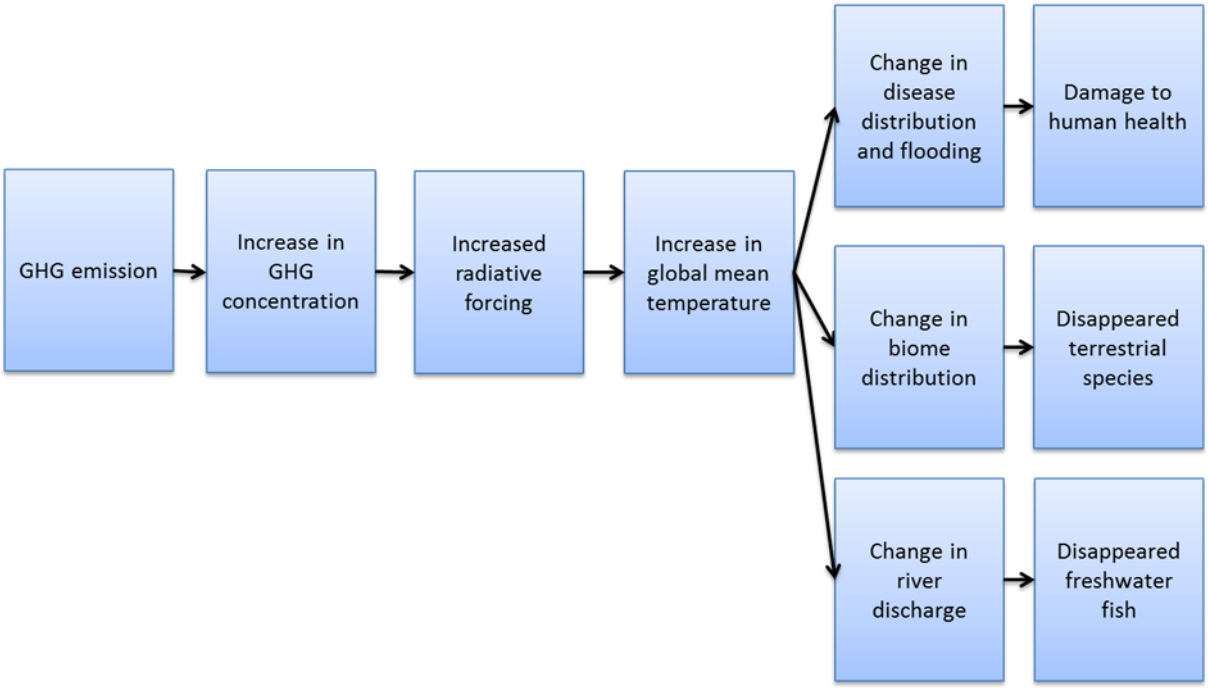

Figure 2.1: Cause and effect pathway of climate change (from Huijbregts et al., 2014)

The cause and effect pathway (Figure 2.1) of climate change starts with the emission of a greenhouse gas (GHG) to the atmosphere. The increased concentration of the GHGs causes the radiative forcing capacity of the atmosphere to increase, resulting in a larger part of the solar energy being retained in the atmosphere. This causes the global temperature to increase, thus affecting human health as well as the natural ecosystems. In this section we describe only those damages that are covered by our methodology. The areas of protection that are relevant for this environmental mechanism are human health and ecosystem quality (terrestrial and aquatic).

Human health can be affected through a shift in disease distributions. With increased temperatures certain parasites will be able to survive in areas where they previously were not able to live. Furthermore, the increased amount of energy in the atmosphere will give rise to more extreme weather in the form of coastal or inland flooding or droughts, all of which have an adverse effect on human health.

Terrestrial ecosystems will experience a shift in distribution as a result of increased temperatures. Not all species will be able to migrate quickly enough to follow the associated change in vegetation, causing them to go extinct. Freshwater ecosystems can be affected through a decrease in river discharge as a

result of the changed climate. Rivers with larger discharges can sustain more different species of fish than river with lower discharges. Therefore a decrease in discharge is likely to cause a number of species to go extinct in that river system.

The climate models, which are used to predict the impact on human health, assume an increase in global temperature of 0.5 to 0.68 degrees in the year 2030 relative to the average global temperature in the reference year 2000. The 0.18 degree difference between the two scenarios is used to derive the final CF, this is a relatively small change in temperature and hence a marginal approach. A temperature change of 1-3.5 degrees is modelled for terrestrial ecosystems, while a change of 1.9 to 4.4 degrees is used for the aquatic ecosystems, making these approaches more similar to a mix between a marginal and an average approach. Ideally, one would use the same model with the same temperature increase for both human health and ecosystem damage effect factors. However, because both models have been developed independently of each other, such synchronization was not possible. Because climate change is modelled as a global increase in radiative forcing there is no need to provide location-specific emission factors. Regardless of the emissions location the impact will be the same.

2.2. Calculation of the characterization factors at endpoint level

The endpoint characterization factors for climate change that are used for damage on human health represent Disability-Adjusted loss of Life Years (DALY). This is a metric for the potential loss of life years (plus the years in which people have to live with disease, weighted with the severity of the disease) among the total world population (in the unit yr/kg GHG). The factors for ecosystem damage represent the globally potentially disappeared fraction of species over a period of time due to the emission of 1 kg of GHG (unit yr/kg GHG). In order to calculate these factors several steps are needed, starting with the prospected increase in temperature due to the release of 1 kg GHG. The following equation (equation 2.1) shows the calculation of the endpoint characterization factor CF_{end} for greenhouse gas x. GWP is the greenhouse warming potential of greenhouse gas x, *TH* is the time horizon, δTEMP is the temperature increase due to the release of 1 kg of CO_2 and *EF* is the effect factor for a given Area Of Protection (*AOP,* i.e. human health, freshwater or terrestrial ecosystems).

$$CF_{end,x,TH,AOP} = GWP_{x,TH} \cdot \partial Temp_{CO_2,TH} \cdot EF_{AOP}$$

Equation 2.1.

2.2.1. From emission to temperature increase

The International Panel on Climate Change (IPCC) provides characterization factors called Absolute Global Warming Potentials (AGWPs) which can be used to compare different GHGs (IPCC, 2013). The AGWP of a GHG represents the amount of solar radiation that is retained within the atmosphere over a period of time. When the AGWP is expressed relative to the AGWP of the reference gas CO_2 it is called the Global Warming Potential (GWP). A time horizon of 100 years is taken as the default, robust scenario and a time horizon of 100 - 1000 years represents the less robust scenario. GWPs provided by the IPCC are expressed in equivalents of 1 kg CO_2 for a 100-year time horizon. By using the radiative forcing capacity and the atmospheric life time, the AGWP and GWP for other time horizons can be calculated for all GHGs except CO_2. The approach followed here (equations 2.2 and 2.3) is equal to the midpoint calculation in the most recent ReCiPe update (Huijbregts et al., 2014).

$$AGWP_{x,TH} = RF_x \cdot cv_x \cdot LT_x \cdot (1 - e^{-\frac{TH}{LT_x}})$$

Equation 2.2

$$GWP_{x,TH} = \frac{AGWP_{x,TH,}}{AGWP_{CO_2,TH}}$$

Equation 2.3

"RF is the radiative efficiency (W m^{-2}/ppb), cv is the substance-specific mass to concentration conversion factor (ppb/kg), LT is the lifetime (year) of the substance x and TH is the time horizon (year) of the assessment (in this case 1000 years). RF and LT were directly available from the fifth assessment report (IPCC, 2013). Since the values for cv are not reported separately in the fifth assessment report these were calculated from the AGWPs that were reported by IPCC (2013)."
(Equations and corresponding descriptions from Huijbregts et al., 2014)

For short-lived GHGs the AGWP for a 100 year time horizon will be almost equal to the AGWP for a 1000 year horizon, because no additional effects after 100 years are to be expected. For long-lived GHGs (including CO_2 itself) however, the $AGWP_{1000}$ is much larger than the $AGWP_{100}$ because a large fraction of the captured radiation will occur during the uncertain period between 100 and a 1000 years.

2.2.2. From AGWP to temperature increase

All midpoint-to-endpoint models start with the modelling of the effects of an increase in temperature. In this study the projected increase in temperature due to 1 kg of CO_2 was taken from Joos et al. (2013). The amount of temperature increase caused by captured cumulative radiative forcing is assumed to be equal to that of CO_2 for all GHGs (Equation 2.4). This may lead to some uncertainty because the time dimension (which is important in the climate response models) is lost after the amount of radiative forcing is integrated over time.

$$\partial Temp_{x,TH} = GWP_{x,TH}\, \partial Temp_{CO_2,TH}$$

Equation 2.4

Where dTemp is the temperature change (°C/kg) and GWP is the Global Warming Potential of GHG *x* (in kg CO_2 eq), over a time horizon TH (years) and $dTemp_{CO2}$ is the temperature change caused by 1 kg of CO_2.

2.2.3. From temperature increase to endpoint damage

The effect of a temperature increase on terrestrial ecosystems and human health was derived from De Schryver et al. (2009, 2011 respectively), while the effect on freshwater ecosystems was taken from Hanafiah et al. (2011). Equations 2.5 through 2.7 show how these effect factors were calculated.

$$EF_{HH} = \sum_{i,r} Incidence_{i,r} \cdot Severity_{i,r}$$

Equation 2.5

Where EF_{HH} (DALY/°C) is the effect factor for human health, incidence is the additional incidence of disease/flooding event *i* (incidences/°C) and severity is the damage caused by these incidences (DALY/incidence) in region *r* (Africa, Eastern Mediterranean, Latin American and the Caribbean, South

East Asia, Western Pacific and developed countries). Please note that this factor includes both the effect (incidences) and the damage (DALY).

The effect factor for terrestrial ecosystems is shown in equation 2.6.

$$EF_{TE} = \sum_{r,g} \frac{1}{\sum S} \cdot S_{r,t} \cdot Loss_{r,t}$$

Equation 2.6

Where EF_{TE} (PDF/°C) is effect factor for terrestrial ecosystems. Species is the number of species and Loss is the percentual loss of species (%/°C) within species group *t* (mammals, birds, frogs, reptiles, butterflies and plants), in region *r* (Australia, Mexico, South Africa, Brazil and Europe). Equation 2.7 shows the effect factor for aquatic ecosystems.

$$EF_{FE} = \sum_{i} \frac{1}{\sum V} \cdot dQ_{mouth,i} \cdot \frac{0.4}{Q_{mouth,i}} \cdot V_i$$

Equation 2.7

Where EF_{FE} (PDF/°C) is the effect factor for freshwater ecosystems, dQ_{mouth} is the change in river discharge (m^3 yr^{-1}/°C) Q_{mouth} is the total river discharge (m^3/yr) and V is the volume (m^3) of the river in river basin *i*.

The damage factors for terrestrial ecosystems (Urban 2015) represent the potentially disappeared fraction of species (PDF) per degree temperature increase. A value of 0.037 PDF/°C is reported (based on a meta analysis of different climate scenario studies). The studies that are included in the meta-analysis focus on global extinction risk for species, and the damage factor is thus in line with the rest of the impact categories. For freshwater ecosystems, Hanafiah et al. (2011) reported an effect factor of $2.04*10^{-9}$ PDF m^3/°C; this factor was derived by taking the sum of the potentially disappeared fractions of species per river basin multiplied by the total water volume of each river basin, based on all river basins below 42°. We modified this approach by removing duplicates from the used database. Also, we estimated the number and change of fish species in each watershed based on Xenopoulos et al. (2005) for different climate scenarios (since changes may be non-marginal in some scenarios and for some watersheds). To get to a global PDF we then divide with the total number of fish species. River basins north of a latitude of 42° are not included because recent (in evolutionary terms) glaciation during ice ages has caused the number of species there to be lower than what would be expected from the discharge. Therefore the relationship between river discharge and number of fish species does not hold for these river basins. To get an average, weighted effect factor of $1.15 *10^{-2}$ PDF/°C we average across all climate scenarios.

2.3. Uncertainties

The CFs for this impact category are based on reported data from existing literature. Assessing the sensitivity of the CFs to uncertainties in the individual parameters is therefore only possible to a limited extent and is dependent on the reported data in the original reports. For the first part of the cause-and-effect chain uncertainties in the AGWP of CO_2 are provided by Joos et al. (2013). The 90% confidence interval spans from 67.9 to $117 \cdot 10^{-15}$ yr Wm^{-2} kg-CO_2^{-1} (for a 100 year time horizon) and this range becomes larger for longer time horizons. Uncertainty estimates for the GWPs of the other

greenhouse gases are provided by the IPCC as 90% intervals. Note that these uncertainties are a combination of the uncertainty in the AGWP of CO_2 and the uncertainty in the AGWP of the GHG under consideration. For CH_4 an uncertainty estimate of ±40% is given (for a 100 year time horizon), for GHGs with a lifetime of a century or more a value ±30% is estimated to cover the 90% interval (for a 100 year time horizon). While for shorter-lived GHGs this interval is estimated to be ±35% (for a 100 year time horizon).

Such a detailed quantitative assessment of the other steps in the cause-and-effect chain is not available. Time integrated temperature factors are likely to be similar to the AGWP but with additional uncertainty, especially for longer time horizons were the climate feedbacks are highly relevant. Damage factors for human health are uncertain because of subjective choices (covered in section 2.4.2) as well as inherently uncertain due to limited knowledge. Assumptions related to the human health effects are listed in table 2.1 (from De Schryver et al. 2009). Most of the parameters used in these models are uncertain, so it is likely that the modelled relative risks also include a substantial amount of uncertainty. The same is true for the damage factors for terrestrial and aquatic ecosystems. For terrestrial species this is caused by uncertainty in the model that projects species extinction, which include many uncertain parameters among which the magnitude of possible dispersal per species and which species groups are included. For aquatic species there is uncertainty in the amount of discharge change caused by a rise in global temperature and the response of fish species to this change in discharge. Additionally it is not likely that the response of fish is representative of all aquatic species, therefore the level of robustness is considered low (see also section 2.4.2).

Table 2.1. Health effects considered, related assumptions and burden of disease type (from De Schryver et al. 2009).

Causes of health effects	Assumptions	Burden of disease
Malnutrition	Models of grain cereals and soybean to estimate the effects of change in temperature, rainfall and CO2 on future crop yields were used.	Nutritional deficiencies
Diarrhoea	Effects of increasing temperature on the incidence of all-cause diarrhoea were addressed, while effects of rainfall were excluded.	Diarrhoeal diseases
Heat stress	Temperature attributable deaths were calculated. The burden of disease of all cardiovascular diseases were used.	All cardiovascular diseases
Natural disasters	The increased incidence of coastal and inland flooding were assessed.	Drowning

2.4. Value choices

2.4.1. Time horizon

A prominent value choice in the modelling of the climate change is the time horizon. GHGs have widely different atmospheric lifetimes, making it important to properly state the time horizon over which impacts are considered. We calculated CFs for 100 years and 100 – 1000 years, thus the user can choose between using the more robust 100 year time horizon or the less robust and more uncertain, but more complete 1000 year time horizon.

2.4.2. Level of robustness

Other relevant value choices that are considered are:

- whether or not there is a strong potential for adaptation,
- whether future socio-economic developments are favourable

The human health and ecosystem effects were classified according to their level of robustness (Table 2.2). For the area of protection human health the expected increase in some diseases is dependent on the future socio-economic development. For some diseases, a positive socio-economic development thus prevents an increase in case occurrences. For others diseases like diarrhea and malaria, as well as for coastal flooding, an increase will occur even if the future socio-economic developments are positive. All these effects on human health are therefore considered to be health effects with a high level of robustness. In contrast, other effects may or may not occur and are therefore considered to have a low level of robustness. All effects on freshwater ecosystems were considered to have a low level of robustness because the CF was based on fish species only. It is uncertain whether these fish species are representative of the total freshwater ecosystem.

Table 2.2: Included effects in the core and extended versions of the CFs per area of protection

Area of protection	Core	Extended	Source
Time horizon (applies to all areas of protection)	100 years	100 - 1000 years	-
Human Health	Diarrhea Malaria Coastal flooding	Cardiovascular disease Malnutrition Inland flooding	De Schryver et al. (2011)
Terrestrial Ecosystems	All species included	Same species as high level	Urban (2015)
Freshwater Ecosystems	None	Fish as representative of the entire freshwater ecosystem, Based on global river basins below 42°	Hanafiah et al. (2011)

2.4.3. Characterization factors

Table 2.3: Characterization factors for human health (HH), terrestrial ecosystems (TE) and freshwater ecosystems (FE). Adding the CFs of high and low level of evidence results in the total CF over the complete time horizon and taking effects with both high and low levels of robustness into account. Substances with characterization factors of zero are very short-lived substances and are only relevant if the effects are studied over time periods shorter than a few years. Thus, over 100 years, their impacts disappear.

Substance	Human health Core (DALY/kg)	Human health Extended (DALY/kg)	Terrestrial ecosystems Core (PDF*y/kg)	Terrestrial ecosystems Extended (PDF*y/kg)	Aquatic ecosystems Core (PDF*y/kg)	Aquatic ecosystems Extended (PDF*y/kg)
Carbon dioxide (fossil)	4.28E-07	1.25E-05	1.76E-15	1.57E-14	0	4.87E-15
Methane	1.20E-05	5.96E-05	4.93E-14	7.47E-14	0	2.32E-14
Fossil methane	1.28E-05	6.13E-05	5.28E-14	7.67E-14	0	2.39E-14
Nitrous oxide	1.13E-04	9.86E-04	4.66E-13	1.24E-12	0	3.84E-13
Chlorofluorocarbons						
CFC-11	1.99E-03	1.10E-02	8.20E-12	1.37E-11	0	4.26E-12
CFC-12	4.36E-03	3.39E-02	1.80E-11	4.25E-11	0	1.32E-11
CFC-13	5.95E-03	1.59E-01	2.45E-11	1.99E-10	0	6.18E-11
CFC-113	2.49E-03	1.76E-02	1.02E-11	2.21E-11	0	6.87E-12
CFC-114	3.68E-03	4.37E-02	1.51E-11	5.47E-11	0	1.70E-11
CFC-115	3.28E-03	1.07E-01	1.35E-11	1.34E-10	0	4.18E-11
Hydrochlorofluorocarbons						
HCFC-21	6.33E-05	3.08E-04	2.60E-13	3.86E-13	0	1.20E-13
HCFC-22	7.53E-04	3.70E-03	3.10E-12	4.64E-12	0	1.44E-12
HCFC-122	2.52E-05	1.24E-04	1.04E-13	1.55E-13	0	4.83E-14
HCFC-122a	1.10E-04	5.41E-04	4.54E-13	6.77E-13	0	2.11E-13
HCFC-123	3.38E-05	1.66E-04	1.39E-13	2.08E-13	0	6.47E-14
HCFC-123a	1.58E-04	7.75E-04	6.51E-13	9.70E-13	0	3.01E-13
HCFC-124	2.25E-04	1.10E-03	9.27E-13	1.38E-12	0	4.30E-13
HCFC-132c	1.45E-04	7.08E-04	5.95E-13	8.87E-13	0	2.76E-13
HCFC-141b	3.35E-04	1.64E-03	1.38E-12	2.05E-12	0	6.38E-13
HCFC-142b	8.47E-04	4.16E-03	3.48E-12	5.21E-12	0	1.62E-12
HCFC-225ca	5.43E-05	2.67E-04	2.23E-13	3.35E-13	0	1.04E-13
HCFC-225cb	2.25E-04	1.10E-03	9.24E-13	1.38E-12	0	4.28E-13
(E)-1-Chloro-3,3,3-trifluoroprop-1-ene	4.28E-07	3.13E-06	1.76E-15	3.92E-15	0	1.22E-15
Hydrofluorocarbons						
HFC-23	5.31E-03	7.09E-02	2.18E-11	8.88E-11	0	2.76E-11
HFC-32	2.90E-04	1.42E-03	1.19E-12	1.78E-12	0	5.52E-13
HFC-41	4.96E-05	2.44E-04	2.04E-13	3.06E-13	0	9.52E-14
HFC-125	1.36E-03	6.84E-03	5.58E-12	8.56E-12	0	2.66E-12
HFC-134	4.79E-04	2.33E-03	1.97E-12	2.92E-12	0	9.08E-13
HFC-134a	5.56E-04	2.72E-03	2.29E-12	3.41E-12	0	1.06E-12
HFC-143	1.40E-04	6.88E-04	5.77E-13	8.61E-13	0	2.68E-13
HFC-143a	2.05E-03	1.14E-02	8.45E-12	1.43E-11	0	4.45E-12
HFC-152	6.85E-06	3.45E-05	2.82E-14	4.32E-14	0	1.34E-14
HFC-152a	5.90E-05	2.88E-04	2.43E-13	3.60E-13	0	1.12E-13
HFC-161	1.71E-06	7.61E-06	7.04E-15	9.52E-15	0	2.96E-15
HFC-227ca	1.13E-03	5.70E-03	4.65E-12	7.14E-12	0	2.22E-12
HFC-227ea	1.43E-03	7.60E-03	5.90E-12	9.52E-12	0	2.96E-12
HFC-236cb	5.18E-04	2.53E-03	2.13E-12	3.17E-12	0	9.86E-13
HFC-236ea	5.69E-04	2.80E-03	2.34E-12	3.50E-12	0	1.09E-12
HFC-236fa	3.45E-03	4.90E-02	1.42E-11	6.14E-11	0	1.91E-11
HFC-245ca	3.06E-04	1.50E-03	1.26E-12	1.88E-12	0	5.83E-13
HFC-245cb	1.98E-03	1.10E-02	8.13E-12	1.38E-11	0	4.29E-12
HFC-245ea	1.01E-04	4.93E-04	4.14E-13	6.17E-13	0	1.92E-13
HFC-245eb	1.24E-04	6.08E-04	5.10E-13	7.61E-13	0	2.37E-13
HFC-245fa	3.67E-04	1.80E-03	1.51E-12	2.25E-12	0	7.00E-13
HFC-263fb	3.25E-05	1.58E-04	1.34E-13	1.98E-13	0	6.16E-14
HFC-272ca	6.16E-05	3.02E-04	2.53E-13	3.78E-13	0	1.17E-13
HFC-329p	1.01E-03	5.09E-03	4.15E-12	6.38E-12	0	1.98E-12
HFC-365mfc	3.44E-04	1.69E-03	1.41E-12	2.11E-12	0	6.56E-13
HFC-43-10mee	7.06E-04	3.46E-03	2.90E-12	4.34E-12	0	1.35E-12
HFC-1132a	0.00E+00	0.00E+00	0.00E+00	0.00E+00	0	0.00E+00
HFC-1141	0.00E+00	0.00E+00	0.00E+00	0.00E+00	0	0.00E+00
(Z)-HFC-1225ye	0.00E+00	0.00E+00	0.00E+00	0.00E+00	0	0.00E+00
(E)-HFC-1225ye	0.00E+00	0.00E+00	0.00E+00	0.00E+00	0	0.00E+00

(Z)-HFC-1234ze	**0.00E+00**	**0.00E+00**	**0.00E+00**	**0.00E+00**	**0**	**0.00E+00**
HFC-1234yf	**0.00E+00**	**0.00E+00**	**0.00E+00**	**0.00E+00**	**0**	**0.00E+00**
(E)-HFC-1234ze	**4.28E-07**	**2.00E-06**	**1.76E-15**	**2.50E-15**	**0**	**7.77E-16**
(Z)-HFC-1336	**8.56E-07**	**3.52E-06**	**3.52E-15**	**4.40E-15**	**0**	**1.37E-15**
HFC-1243zf	**0.00E+00**	**0.00E+00**	**0.00E+00**	**0.00E+00**	**0**	**0.00E+00**
HFC-1345zfc	**0.00E+00**	**0.00E+00**	**0.00E+00**	**0.00E+00**	**0**	**0.00E+00**
3,3,4,4,5,5,6,6,6-Nonafluorohex-1-ene	**0.00E+00**	**0.00E+00**	**0.00E+00**	**0.00E+00**	**0**	**0.00E+00**
3,3,4,4,5,5,6,6,7,7,8,8,8-Tridecafluorooct-1-ene	**0.00E+00**	**0.00E+00**	**0.00E+00**	**0.00E+00**	**0**	**0.00E+00**
3,3,4,4,5,5,6,6,7,7,8,8,9,9,10,10,10-Heptadecafluorodec-1-ene	**0.00E+00**	**0.00E+00**	**0.00E+00**	**0.00E+00**	**0**	**0.00E+00**
Chlorocarbons and hydrochlorocarbons						
Methyl chloroform	**6.85E-05**	**3.35E-04**	**2.82E-13**	**4.20E-13**	**0**	**1.31E-13**
Carbon tetrachloride	**7.40E-04**	**3.70E-03**	**3.04E-12**	**4.64E-12**	**0**	**1.44E-12**
Methyl chloride	**5.13E-06**	**2.56E-05**	**2.11E-14**	**3.20E-14**	**0**	**9.96E-15**
Methylene chloride	**3.85E-06**	**1.87E-05**	**1.58E-14**	**2.34E-14**	**0**	**7.27E-15**
Chloroform	**6.85E-06**	**3.43E-05**	**2.82E-14**	**4.29E-14**	**0**	**1.33E-14**
1,2-Dichloroethane	**4.28E-07**	**1.88E-06**	**1.76E-15**	**2.36E-15**	**0**	**7.33E-16**
Bromocarbons, hyrdobromocarbons and Halons						
Methyl bromide	**8.56E-07**	**4.93E-06**	**3.52E-15**	**6.18E-15**	**0**	**1.92E-15**
Methylene bromide	**4.28E-07**	**2.13E-06**	**1.76E-15**	**2.66E-15**	**0**	**8.28E-16**
Halon-1201	**1.61E-04**	**7.87E-04**	**6.62E-13**	**9.86E-13**	**0**	**3.06E-13**
Halon-1202	**9.88E-05**	**4.84E-04**	**4.07E-13**	**6.07E-13**	**0**	**1.89E-13**
Halon-1211	**7.49E-04**	**3.67E-03**	**3.08E-12**	**4.60E-12**	**0**	**1.43E-12**
Halon-1301	**2.69E-03**	**1.68E-02**	**1.11E-11**	**2.10E-11**	**0**	**6.54E-12**
Halon-2301	**7.40E-05**	**3.64E-04**	**3.04E-13**	**4.55E-13**	**0**	**1.42E-13**
Halon-2311/Halothane	**1.75E-05**	**8.61E-05**	**7.22E-14**	**1.08E-13**	**0**	**3.35E-14**
Halon-2401	**7.87E-05**	**3.84E-04**	**3.24E-13**	**4.81E-13**	**0**	**1.49E-13**
Halon-2402	**6.29E-04**	**3.10E-03**	**2.59E-12**	**3.89E-12**	**0**	**1.21E-12**
Fully Fluorinated Species						
Nitrogen trifluoride	**6.89E-03**	**1.60E-01**	**2.83E-11**	**2.01E-10**	**0**	**6.24E-11**
Sulphur hexafluoride	**1.01E-02**	**4.30E-01**	**4.14E-11**	**5.39E-10**	**0**	**1.67E-10**
(Trifluoromethyl)sulfur pentafluoride	**7.45E-03**	**2.22E-01**	**3.06E-11**	**2.78E-10**	**0**	**8.63E-11**
Sulfuryl fluoride	**1.75E-03**	**9.16E-03**	**7.20E-12**	**1.15E-11**	**0**	**3.57E-12**
PFC-14	**2.84E-03**	**1.38E-01**	**1.17E-11**	**1.73E-10**	**0**	**5.36E-11**
PFC-116	**4.75E-03**	**2.23E-01**	**1.95E-11**	**2.79E-10**	**0**	**8.68E-11**
PFC-c216	**3.94E-03**	**1.67E-01**	**1.62E-11**	**2.09E-10**	**0**	**6.49E-11**
PFC-218	**3.81E-03**	**1.58E-01**	**1.57E-11**	**1.98E-10**	**0**	**6.14E-11**
PFC-318	**4.08E-03**	**1.74E-01**	**1.68E-11**	**2.18E-10**	**0**	**6.78E-11**
PFC-31-10	**3.94E-03**	**1.63E-01**	**1.62E-11**	**2.04E-10**	**0**	**6.34E-11**
Perfluorocyclopentene	**8.56E-07**	**3.91E-06**	**3.52E-15**	**4.89E-15**	**0**	**1.52E-15**
PFC-41-12	**3.66E-03**	**1.61E-01**	**1.50E-11**	**2.01E-10**	**0**	**6.25E-11**
PFC-51-14	**3.38E-03**	**1.44E-01**	**1.39E-11**	**1.80E-10**	**0**	**5.60E-11**
PFC-61-16	**3.35E-03**	**1.41E-01**	**1.38E-11**	**1.77E-10**	**0**	**5.51E-11**
PFC-71-18	**3.26E-03**	**1.38E-01**	**1.34E-11**	**1.73E-10**	**0**	**5.38E-11**
PFC-91-18	**3.08E-03**	**1.21E-01**	**1.27E-11**	**1.52E-10**	**0**	**4.72E-11**
Perfluorodecalin(cis)	**3.10E-03**	**1.22E-01**	**1.27E-11**	**1.53E-10**	**0**	**4.75E-11**
Perfluorodecalin(trans)	**2.69E-03**	**1.06E-01**	**1.11E-11**	**1.33E-10**	**0**	**4.14E-11**
PFC-1114	**0.00E+00**	**0.00E+00**	**0.00E+00**	**0.00E+00**	**0**	**0.00E+00**
PFC-1216	**0.00E+00**	**0.00E+00**	**0.00E+00**	**0.00E+00**	**0**	**0.00E+00**
Perfluorobuta-1,3-diene	**0.00E+00**	**0.00E+00**	**0.00E+00**	**0.00E+00**	**0**	**0.00E+00**
Perfluorobut-1-ene	**0.00E+00**	**0.00E+00**	**0.00E+00**	**0.00E+00**	**0**	**0.00E+00**
Perfluorobut-2-ene	**8.56E-07**	**3.70E-06**	**3.52E-15**	**4.63E-15**	**0**	**1.44E-15**
Halogenated alcohols and ethers						
HFE-125	**5.31E-03**	**4.58E-02**	**2.18E-11**	**5.73E-11**	**0**	**1.78E-11**
HFE-134 (HG-00)	**2.38E-03**	**1.18E-02**	**9.78E-12**	**1.48E-11**	**0**	**4.61E-12**
HFE-143a	**2.24E-04**	**1.10E-03**	**9.20E-13**	**1.37E-12**	**0**	**4.26E-13**
HFE-227ea	**2.76E-03**	**1.58E-02**	**1.14E-11**	**1.98E-11**	**0**	**6.14E-12**
HCFE-235ca2(enflurane)	**2.49E-04**	**1.22E-03**	**1.03E-12**	**1.53E-12**	**0**	**4.76E-13**
HCFE-235da2(isoflurane)	**2.10E-04**	**1.03E-03**	**8.64E-13**	**1.29E-12**	**0**	**4.00E-13**
HFE-236ca	**1.81E-03**	**8.95E-03**	**7.46E-12**	**1.12E-11**	**0**	**3.48E-12**
HFE-236ea2(desflurane)	**7.66E-04**	**3.76E-03**	**3.15E-12**	**4.70E-12**	**0**	**1.46E-12**
HFE-236fa	**4.19E-04**	**2.05E-03**	**1.72E-12**	**2.57E-12**	**0**	**7.98E-13**
HFE-245cb2	**2.80E-04**	**1.37E-03**	**1.15E-12**	**1.72E-12**	**0**	**5.33E-13**
HFE-245fa1	**3.54E-04**	**1.73E-03**	**1.46E-12**	**2.17E-12**	**0**	**6.75E-13**
HFE-245fa2	**3.47E-04**	**1.70E-03**	**1.43E-12**	**2.13E-12**	**0**	**6.62E-13**
2,2,3,3,3-Pentafluoropropan-1-ol	**8.13E-06**	**3.93E-05**	**3.34E-14**	**4.92E-14**	**0**	**1.53E-14**

HFE-254cb1	**1.29E-04**	**6.31E-04**	**5.30E-13**	**7.90E-13**	**0**	**2.45E-13**
HFE-263fb2	**4.28E-07**	**2.79E-06**	**1.76E-15**	**3.49E-15**	**0**	**1.08E-15**
HFE-263m1	**1.24E-05**	**6.17E-05**	**5.10E-14**	**7.72E-14**	**0**	**2.40E-14**
3,3,3-Trifluoropropan-1-ol	**0.00E+00**	**0.00E+00**	**0.00E+00**	**0.00E+00**	**0**	**0.00E+00**
HFE-329mcc2	**1.31E-03**	**6.51E-03**	**5.40E-12**	**8.15E-12**	**0**	**2.53E-12**
HFE-338mmz1	**1.12E-03**	**5.53E-03**	**4.61E-12**	**6.93E-12**	**0**	**2.15E-12**
HFE-338mcf2	**3.97E-04**	**1.95E-03**	**1.63E-12**	**2.44E-12**	**0**	**7.57E-13**
Sevoflurane (HFE-347mmz1)	**9.24E-05**	**4.52E-04**	**3.80E-13**	**5.66E-13**	**0**	**1.76E-13**
HFE-347mcc3 (HFE-7000)	**2.27E-04**	**1.11E-03**	**9.33E-13**	**1.39E-12**	**0**	**4.32E-13**
HFE-347mcf2	**3.65E-04**	**1.79E-03**	**1.50E-12**	**2.24E-12**	**0**	**6.96E-13**
HFE-347pcf2	**3.80E-04**	**1.86E-03**	**1.56E-12**	**2.33E-12**	**0**	**7.25E-13**
HFE-347mmy1	**1.55E-04**	**7.61E-04**	**6.39E-13**	**9.53E-13**	**0**	**2.96E-13**
HFE-356mec3	**1.66E-04**	**8.11E-04**	**6.81E-13**	**1.02E-12**	**0**	**3.16E-13**
HFE-356mff2	**7.27E-06**	**3.52E-05**	**2.99E-14**	**4.40E-14**	**0**	**1.37E-14**
HFE-356pcf2	**3.08E-04**	**1.51E-03**	**1.27E-12**	**1.89E-12**	**0**	**5.86E-13**
HFE-356pcf3	**1.91E-04**	**9.35E-04**	**7.85E-13**	**1.17E-12**	**0**	**3.64E-13**
HFE-356pcc3	**1.77E-04**	**8.66E-04**	**7.27E-13**	**1.08E-12**	**0**	**3.37E-13**
HFE-356mmz1	**5.99E-06**	**2.86E-05**	**2.46E-14**	**3.58E-14**	**0**	**1.11E-14**
HFE-365mcf3	**4.28E-07**	**1.94E-06**	**1.76E-15**	**2.43E-15**	**0**	**7.57E-16**
HFE-365mcf2	**2.48E-05**	**1.22E-04**	**1.02E-13**	**1.53E-13**	**0**	**4.76E-14**
HFE-374pc2	**2.68E-04**	**1.31E-03**	**1.10E-12**	**1.65E-12**	**0**	**5.11E-13**
4,4,4-Trifluorobutan-1-ol	**0.00E+00**	**0.00E+00**	**0.00E+00**	**0.00E+00**	**0**	**0.00E+00**
2,2,3,3,4,4,5,5-Octafluorocyclopentanol	**5.56E-06**	**2.70E-05**	**2.29E-14**	**3.37E-14**	**0**	**1.05E-14**
HFE-43-10pccc124(H-Galden 1040x,HG-11)	**1.21E-03**	**5.90E-03**	**4.96E-12**	**7.39E-12**	**0**	**2.30E-12**
HFE-449s1 (HFE-7100)	**1.80E-04**	**8.81E-04**	**7.41E-13**	**1.10E-12**	**0**	**3.43E-13**
n-HFE-7100	**2.08E-04**	**1.02E-03**	**8.55E-13**	**1.27E-12**	**0**	**3.96E-13**
i-HFE-7100	**1.74E-04**	**8.52E-04**	**7.16E-13**	**1.07E-12**	**0**	**3.32E-13**
HFE-569sf2 (HFE-7200)	**2.44E-05**	**1.19E-04**	**1.00E-13**	**1.49E-13**	**0**	**4.63E-14**
n-HFE-7200	**2.78E-05**	**1.35E-04**	**1.14E-13**	**1.69E-13**	**0**	**5.26E-14**
i-HFE-7200	**1.88E-05**	**9.27E-05**	**7.74E-14**	**1.16E-13**	**0**	**3.61E-14**
HFE-236ca12 (HG-10)	**2.29E-03**	**1.14E-02**	**9.42E-12**	**1.43E-11**	**0**	**4.44E-12**
HFE-338pcc13 (HG-01)	**1.25E-03**	**6.09E-03**	**5.12E-12**	**7.63E-12**	**0**	**2.37E-12**
1,1,1,3,3,3-Hexafluoropropan-2-ol	**7.79E-05**	**3.81E-04**	**3.20E-13**	**4.78E-13**	**0**	**1.48E-13**
HG-02	**1.17E-03**	**5.71E-03**	**4.80E-12**	**7.15E-12**	**0**	**2.22E-12**
HG-03	**1.22E-03**	**5.98E-03**	**5.02E-12**	**7.49E-12**	**0**	**2.33E-12**
HG-20	**2.27E-03**	**1.13E-02**	**9.33E-12**	**1.42E-11**	**0**	**4.40E-12**
HG-21	**1.66E-03**	**8.16E-03**	**6.85E-12**	**1.02E-11**	**0**	**3.18E-12**
HG-30	**3.14E-03**	**1.56E-02**	**1.29E-11**	**1.96E-11**	**0**	**6.09E-12**
1-Ethoxy-1,1,2,2,3,3,3-heptafluoropropane	**2.61E-05**	**1.27E-04**	**1.07E-13**	**1.59E-13**	**0**	**4.94E-14**
Fluoroxene	**0.00E+00**	**0.00E+00**	**0.00E+00**	**0.00E+00**	**0**	**0.00E+00**
1,1,2,2-Tetrafluoro-1-(fluoromethoxy)ethane	**3.73E-04**	**1.83E-03**	**1.53E-12**	**2.29E-12**	**0**	**7.11E-13**
2-Ethoxy-3,3,4,4,5-pentafluorotetrahydro-2,5-bis[1,2,2,2-tetrafluoro-1-(trifluoromethyl)ethyl]-furan	**2.40E-05**	**1.16E-04**	**9.86E-14**	**1.46E-13**	**0**	**4.52E-14**
Fluoro(methoxy)methane	**5.56E-06**	**2.63E-05**	**2.29E-14**	**3.29E-14**	**0**	**1.02E-14**
Difluoro(methoxy)methane	**6.16E-05**	**3.02E-04**	**2.53E-13**	**3.78E-13**	**0**	**1.17E-13**
Fluoro(fluoromethoxy)methane	**5.56E-05**	**2.74E-04**	**2.29E-13**	**3.43E-13**	**0**	**1.07E-13**
Difluoro(fluoromethoxy)methane	**2.64E-04**	**1.29E-03**	**1.09E-12**	**1.62E-12**	**0**	**5.03E-13**
Trifluoro(fluoromethoxy)methane	**3.21E-04**	**1.57E-03**	**1.32E-12**	**1.97E-12**	**0**	**6.13E-13**
HG'-01	**9.50E-05**	**4.64E-04**	**3.91E-13**	**5.81E-13**	**0**	**1.80E-13**
HG'-02	**1.01E-04**	**4.93E-04**	**4.15E-13**	**6.18E-13**	**0**	**1.92E-13**
HG'-03	**9.46E-05**	**4.64E-04**	**3.89E-13**	**5.81E-13**	**0**	**1.80E-13**
HFE-329me3	**1.95E-03**	**1.04E-02**	**8.01E-12**	**1.30E-11**	**0**	**4.04E-12**
3,3,4,4,5,5,6,6,7,7,7-Undecafluoroheptan-1-ol	**0.00E+00**	**0.00E+00**	**0.00E+00**	**0.00E+00**	**0**	**0.00E+00**
3,3,4,4,5,5,6,6,7,7,8,8,9,9,9-Pentadecafluorononan-1-ol	**0.00E+00**	**0.00E+00**	**0.00E+00**	**0.00E+00**	**0**	**0.00E+00**
3,3,4,4,5,5,6,6,7,7,8,8,9,9,10,10,11,11,11-Nonadecafluoroundecan-1-ol	**0.00E+00**	**0.00E+00**	**0.00E+00**	**0.00E+00**	**0**	**0.00E+00**
2-Chloro-1,1,2-trifluoro-1-methoxyethane	**5.22E-05**	**2.56E-04**	**2.15E-13**	**3.20E-13**	**0**	**9.96E-14**
PFPMIE(perfluoropolymethylisopropyl ether)	**4.15E-03**	**1.23E-01**	**1.71E-11**	**1.55E-10**	**0**	**4.80E-11**
HFE-216	**0.00E+00**	**0.00E+00**	**0.00E+00**	**0.00E+00**	**0**	**0.00E+00**
Trifluoromethylformate	**2.52E-04**	**1.23E-03**	**1.03E-12**	**1.54E-12**	**0**	**4.79E-13**
Perfluoroethylformate	**2.48E-04**	**1.21E-03**	**1.02E-12**	**1.52E-12**	**0**	**4.73E-13**
Perfluoropropylformate	**1.61E-04**	**7.88E-04**	**6.62E-13**	**9.87E-13**	**0**	**3.07E-13**
Perfluorobutylformate	**1.68E-04**	**8.21E-04**	**6.90E-13**	**1.03E-12**	**0**	**3.19E-13**
2,2,2-Trifluoroethylformate	**1.41E-05**	**7.01E-05**	**5.81E-14**	**8.78E-14**	**0**	**2.73E-14**
3,3,3-Trifluoropropylformate	**7.27E-06**	**3.65E-05**	**2.99E-14**	**4.58E-14**	**0**	**1.42E-14**
1,2,2,2-Tetrafluoroethylformate	**2.01E-04**	**9.84E-04**	**8.27E-13**	**1.23E-12**	**0**	**3.83E-13**

1,1,1,3,3,3-Hexafluoropropan-2-ylformate	**1.42E-04**	**6.97E-04**	**5.86E-13**	**8.73E-13**	**0**	**2.71E-13**
Perfluorobutylacetate	**8.56E-07**	**3.47E-06**	**3.52E-15**	**4.35E-15**	**0**	**1.35E-15**
Perfluoropropylacetate	**8.56E-07**	**3.63E-06**	**3.52E-15**	**4.55E-15**	**0**	**1.41E-15**
Perfluoroethylacetate	**8.56E-07**	**4.32E-06**	**3.52E-15**	**5.41E-15**	**0**	**1.68E-15**
Trifluoromethylacetate	**8.56E-07**	**4.34E-06**	**3.52E-15**	**5.43E-15**	**0**	**1.69E-15**
Methylcarbonofluoridate	**4.06E-05**	**2.00E-04**	**1.67E-13**	**2.50E-13**	**0**	**7.77E-14**
1,1-Difluoroethylcarbonofluoridate	**1.16E-05**	**5.62E-05**	**4.75E-14**	**7.04E-14**	**0**	**2.19E-14**
1,1-Difluoroethyl2,2,2-trifluoroacetate	**1.33E-05**	**6.46E-05**	**5.46E-14**	**8.09E-14**	**0**	**2.52E-14**
Ethyl 2,2,2-trifluoroacetate	**4.28E-07**	**2.88E-06**	**1.76E-15**	**3.60E-15**	**0**	**1.12E-15**
2,2,2-Trifluoroethyl2,2,2-trifluoroacetate	**3.00E-06**	**1.43E-05**	**1.23E-14**	**1.79E-14**	**0**	**5.57E-15**
Methyl 2,2,2-trifluoroacetate	**2.22E-05**	**1.10E-04**	**9.15E-14**	**1.37E-13**	**0**	**4.27E-14**
Methyl 2,2-difluoroacetate	**1.28E-06**	**6.85E-06**	**5.28E-15**	**8.58E-15**	**0**	**2.67E-15**
Difluoromethyl 2,2,2-trifluoroacetate	**1.16E-05**	**5.66E-05**	**4.75E-14**	**7.09E-14**	**0**	**2.20E-14**
2,2,3,3,4,4,4-Heptafluorobutan-1-ol	**1.45E-05**	**7.08E-05**	**5.98E-14**	**8.87E-14**	**0**	**2.76E-14**
1,1,2-Trifluoro-2-(trifluoromethoxy)-ethane	**5.31E-04**	**2.60E-03**	**2.18E-12**	**3.26E-12**	**0**	**1.01E-12**
1-Ethoxy-1,1,2,3,3,3-hexafluoropropane	**9.84E-06**	**4.89E-05**	**4.05E-14**	**6.12E-14**	**0**	**1.90E-14**
1,1,1,2,2,3,3-Heptafluoro-3-(1,2,2,2-tetrafluoroethoxy)-propane	**2.78E-03**	**1.75E-02**	**1.14E-11**	**2.19E-11**	**0**	**6.82E-12**
2,2,3,3-Tetrafluoro-1-propanol	**5.56E-06**	**2.72E-05**	**2.29E-14**	**3.40E-14**	**0**	**1.06E-14**
2,2,3,4,4,4-Hexafluoro-1-butanol	**7.27E-06**	**3.56E-05**	**2.99E-14**	**4.46E-14**	**0**	**1.39E-14**
2,2,3,3,4,4,4-Heptafluoro-1-butanol	**6.85E-06**	**3.40E-05**	**2.82E-14**	**4.26E-14**	**0**	**1.32E-14**
1,1,2,2-Tetrafluoro-3-methoxy-propane	**4.28E-07**	**1.10E-06**	**1.76E-15**	**1.38E-15**	**0**	**4.28E-16**
perfluoro-2-methyl-3-pentanone	**0.00E+00**	**0.00E+00**	**0.00E+00**	**0.00E+00**	**0**	**0.00E+00**
3,3,3-Trifluoropropanal	**0.00E+00**	**0.00E+00**	**0.00E+00**	**0.00E+00**	**0**	**0.00E+00**
2-Fluoroethanol	**4.28E-07**	**1.84E-06**	**1.76E-15**	**2.31E-15**	**0**	**7.17E-16**
2,2-Difluoroethanol	**1.28E-06**	**6.35E-06**	**5.28E-15**	**7.95E-15**	**0**	**2.47E-15**
2,2,2-Trifluoroethanol	**8.56E-06**	**4.18E-05**	**3.52E-14**	**5.23E-14**	**0**	**1.63E-14**
1,1'-Oxybis[2-(difluoromethoxy)-1,1,2,2-tetrafluoroethane	**2.11E-03**	**1.05E-02**	**8.66E-12**	**1.32E-11**	**0**	**4.09E-12**
1,1,3,3,4,4,6,6,7,7,9,9,10,10,12,12-hexadecafluoro-2,5,8,11-Tetraoxadodecane	**1.92E-03**	**9.62E-03**	**7.90E-12**	**1.20E-11**	**0**	**3.74E-12**
1,1,3,3,4,4,6,6,7,7,9,9,10,10,12,12,13,13,15,15-eicosafluoro-2,5,8,11,14-Pentaoxapentadecane	**1.55E-03**	**7.78E-03**	**6.39E-12**	**9.74E-12**	**0**	**3.03E-12**

2.5. References

De Schryver, A. M., Brakkee, K. W., Goedkoop, M. & Huijbregts, M. A. J. (2009) Characterization factors for global warming in life cycle assessment based on damages to humans and ecosystems Environ. Sci. Technol., 43 (6) 1689– 1695

De Schryver, A. M., Van Zelm, R., Humbert, S., Pfister, S., McKone, T. E. and Huijbregts, M. A. J. (2011). Value Choices in Life Cycle Impact Assessment of Stressors Causing Human Health Damage. Journal of Industrial Ecology 15(5): 796-815.

Hanafiah, M. M., Xenopoulos, M. A., Pfister, S., Leuven, R. S., & Huijbregts, M. A. J. (2011). Characterization factors for water consumption and greenhouse gas emissions based on freshwater fish species extinction. *Environmental science & technology*, *45*(12), 5272-5278.

Huijbregts M.A.J., Steinmann Z.J.N., Stam G., Van Zelm R. (2014). Update of emission-related impact categories in ReCiPe2008. Department of Environmental Science, Radboud University Nijmegen.

IPCC, 2013: Climate Change 2013: The Physical Science Basis. Contribution of Working Group I to the Fifth Assessment Report of the Intergovernmental Panel on Climate Change [Stocker, T.F., D. Qin, G.-K. Plattner, M. Tignor, S.K. Allen, J. Boschung, A. Nauels, Y. Xia, V. Bex and P.M. Midgley (eds.)]. Cambridge University Press, Cambridge, United Kingdom and New York, NY, USA, 1535 pp.

Joos, F., Roth, R., Fuglestvedt, J. S., Peters, G. P., Enting, I. G., Bloh, W. V., ... & Weaver, A. J. (2013). Carbon dioxide and climate impulse response functions for the computation of greenhouse gas metrics: a multi-model analysis. Atmospheric Chemistry and Physics, 13(5), 2793-2825.

Urban, M.C. (2015) Accelerating extinction risk from climate change. Science, 348, 571-573.

WMO (2011) Scientific assessment of ozone depletion: 2010, Global Ozone Research and Monitoring Project-report no.52. World Meteorological Organization, Geneva

Xenopoulos, M. A., Lodge, D. M., Alcamo, J., Märker, M., Schulze, K. and van Vuurens, D. P. (2005). "Scenarios of freshwater fish extinctions from climate change and water withdrawal." Global Change Biol. **11**: 1557-1564.

3.Stratospheric ozone depletion

Zoran Steinmann[1], Mark A.J. Huijbregts[1]

[1] Department of Environmental Science, Radboud University Nijmegen, The Netherlands

* z.steinmann@science.ru.nl

3.1. Areas of protection and environmental mechanisms covered

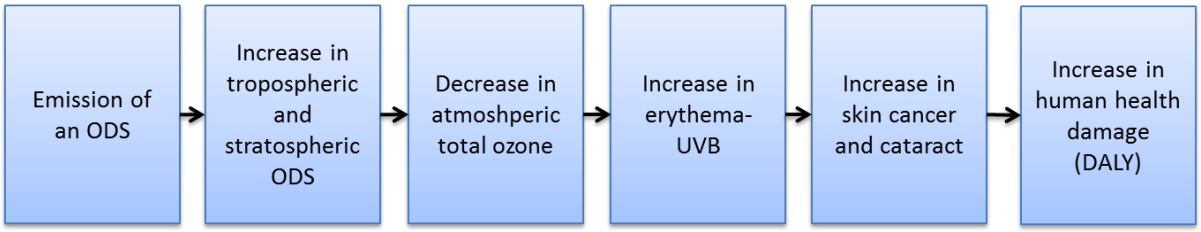

Figure 3.1: Cause-and-effect chain for emissions of ozone depleting substances (ODS) resulting in human health damage (from: Huijbregts et al. 2014)

The ozone layer in the stratosphere absorbs a large part of the harmful UV-radiation coming from the sun. In the natural situation ozone is continuously being formed and destroyed. However, a number of man-made chemicals that contain fluorine, bromine and chlorine groups, called Ozone Depleting Substances (ODS), can greatly increase the rate of destruction, leading to a reduction in the thickness of the ozone layer. With the thickness of the layer reduced, more of the UV-B radiation will reach the earth's surface. Increased exposure to UV-B radiation can lead to adverse human health effects (Figure 3.1), such as skin cancer and cataract, and effects on ecosystems. The latter are, however, not considered here, meaning that the only area of protection that is covered is human health.

3.2. Calculation of the characterization factors at endpoint level

The procedure we follow here is equal to the procedure from the latest ReCiPe report (Huijbregts et al., 2014). The World Meteorological Organization (WMO) reports the Ozone Depletion Potential (ODP) for 21 different substances (WMO, 2011) these ODPs were used for the calculation of the CFs. The ODP, as reported by the WMO, represents the amount of ozone destroyed by a substance during its entire lifetime relative to the amount of ozone destroyed by CFC-11 during its entire lifetime. Equation 3.1 shows the characterization factor CF_{end} at endpoint level. It consists of the ozone depletion potential (ODP) for substance x with time horizon TH and the effect factor EF for the reference substance CFC-11 for time horizon *TH*.

$$CF_{end,x,TH} = ODP_{x,TH} \cdot EF_{CFC-11,TH}$$

Equation 3.1

The WMO (2011) uses a semi-empirical approach to calculate the ODPs. Observational data from different air layers is used to predict the release of the bromine and chlorine groups from an ODS. Each bromine group has approximately 60 times (65 in arctic regions) more potency to destroy ozone than a chlorine group. By taking into account the release of the chlorine and bromine groups and their potencies the change in Equivalent Effective Stratospheric Chlorine (EESC) resulting from the release

of 1 kg of ODS was calculated. By dividing this value by the EESC effect of CFC-11 one can calculate the ODP as follows (equation 3.2):

$$ODP_{inf,x} = \frac{\Delta EESC_x}{\Delta EESC_{CFC-11}}$$

Equation 3.2

Where the $ODP_{inf,x}$ is the ODP for an infinite time horizon for ODS *x*, $\Delta EESC_x$ and $\Delta EESC_{cfc\text{-}11}$ are the changes in EESC caused by the emission of 1 kg of ODS *x* and 1 kg of CFC-11 respectively (Equation 3.2 and description from Huijbregts et al. 2014).

The ODPs from WMO are all based on an infinite time horizon, for a 100 year time horizon a correction is needed to calculate the fraction of the bromine and chlorine that is released during the first 100 years of the lifetime. Equal to the approach followed in ReCiPe we used the equation from De Schryver et al. (2011) (equation 3.3).

$$F_t = 1 - e^{(-t-3)\cdot k}$$

Equation 3.3

Where F_t is the fraction of the total damage caused by an ODS during the first *t* years, *k* is the removal rate of the ODS (yr^{-1}) which is the inverse of the atmospheric life time and the 3 is the average time (in years) that is needed for transport from the troposphere to the stratosphere. This fraction F_t is then multiplied with $ODP_{inf,x}$ to get to the $OPD_{x,TH}$ with a finite time horizon TH.

The amount of damage caused by exposure to UV-B radiation has been quantified by Hayashi et al. (2006), a summarizing, qualitative formula of the effect factor is shown in Equation 3.4. For more details, see Hayashi et al. (2006).

$$EF = f(OLT, UVB, s, i, j, x)$$

Equation 3.4

This equation shows that the effect factor is a function of the ozone layer thickness (*OLT*), the resulting UVB radiation (*UVB*) that reaches the surface as a response to this ozone layer thickness, the season (*s*), latitudinal zone (*i*), population number of skin type (*j*) and skin cancer type (*x*) (note: damage by cataract was calculated in a similar matter, but is independent of the skin type).

The effect of EESC on ozone layer thickness was determined by historical observational data, using year 1980 as a reference year because prior to this year anthropogenic effects on ozone layer thickness were considered negligible. The effect of EESC depends on both the season as well as the latitude. Therefore Hayashi et al. (2006) used a model with latitudinal zones of degrees and four different seasons to calculate the amount of UV-B radiation that reaches the surface. The optical thickness of the ozone layer rather than the actual thickness determines the amount of direct or scattered UV-B radiation that reaches the surface. To correct for this difference, a linear regression between actual and optical thickness was used.

Three different types of skin cancer (malignant melanoma (MM), basal cell carcinoma (BCC) and squamous cell carcinoma (SCC)) were linked to UV-B radiation. The DALY concept was used to

determine the severity of each of these cancers. The incidence rate of these cancers is inversely related to the amount of pigments in the skin. In order to take this into account, the percentage of people with different skin colours (white, yellow or black) was determined per longitudinal zone. The resulting damage in human health was 5.91E-04 yr/kg CFC-11 eq (for an infinite time horizon). For a 100 year time horizon this value is 10% lower (5.34 E-04 yr/kg CFC-11 eq). If the effect of cataract is also taken into account (infinite time horizon only) this factor increases to 1.34E-03 yr/kg CFC-11 eq. The resulting endpoints CFs are listed in table 3.1 for 22 ozone depleting substances.

3.3. Uncertainties

The CFs for this impact category are based on reported data from existing literature. Assessing the sensitivity of the CFs to uncertainties in the individual parameters is therefore only possible to a limited extent and is dependent on the reported data in the original reports. Uncertainties in the lifetimes as well as the estimated and projected emissions of the different ODSs are described by the WMO (2011). The resulting uncertainty in the projected total EESC is moderate, a clear downward trend in total EESC is observed and this trend is expected to continue in the future. The year at which the levels return to the national background concentration is dependent on both the future emissions as well as the projected climate change. According to the WMO scenario's it is likely that the EESC levels will continue to drop significantly within the coming 30 to 50 years, perhaps even to a level where there is hardly any expected negative impact form ODS emissions. It is not certain whether we will reach this level because of the expected increase in N_2O and uncertain developments in the future climate. Therefore impacts of long-lived substances integrated over time horizons longer than 100 years should be considered highly uncertain and it is likely that their impact is overestimated. Unfortunately no direct quantitative assessment of the uncertainty on the level of the ODPs is provided by the WMO. ODPs are uncertain both because of uncertainties in the fractional release of chlorine and bromine and the lifetime of the ODS compared to that of the reference substance CFC-11. In general the lifetimes and therefore the ODPs of the shorter lived substances are more uncertain than those of the longer lived ones, which would result in more uncertain ODPs.

Additional uncertainty is present in the damage factors. As Hayashi et al. (2006) state, a more detailed assessment of these uncertainties is required; unfortunately no quantitative estimates are provided in their publication. However, it is likely that there is model uncertainty in the models that project the increase in UV-B radiation reaching the surface, as well as in the fraction of people with different skin colours in each region and the additional cancer incidences resulting from that increased exposure to UV-B radiation. For future impacts, the projected population developments (and the distribution of people with different skin colours within those populations) are uncertain. The (implicit) assumption that this population remains stable is likely to cause an underestimation of the impact, especially in regions with a large projected population growth such as Africa.

3.4. Value choices

The different ODSs have widely varying atmospheric lifetimes, ranging from 0.8 years for CH_3Br to 1020 years for CFC-115. Therefore the CF is time-horizon dependent. The effects over the first 100 years are considered to be certain and robust. Effects in a longer time horizon are more uncertain, because of unknown future emissions as well as uncertain climate and population developments.

There is strong evidence of the link between UV radiation and skin cancer incidence. The evidence for a link with cataract is much weaker and these effects should therefore be considered to have a low robustness (Table 3.1). The mechanism by which bromine and chlorine containing substances destroy

ozone is well known and understood. Nitrous oxide (N_2O) also has an ozone depleting capacity (but no bromine or chlorine groups) whether or not to include this substance should be included can be seen as a value choice. In this analysis we chose to include N_2O, as also recommended in literature (Ravishankara et al. 2010; WMO, 2011). This division of the value choices gives a CF with a high level of robustness that is equal to the Hierarchist CF in the latest ReCiPe update (Huijbregts et al., 2014), while the total CF is equal to the Egalitarian CF for all substances.

Table 3.1: Value choices in the modelling of CFs for core and extended value choices (i.e. what is added to get from core to extended vaues)

Choice category	Core	Addition in extended	Source
Time horizon	100 yr	100 yr - Infinite	De Schryver et al. (2011)
Included effects	Skin cancer	Cataract	

Table 3.2: The characterization factors for ozone depleting substances at the core level (100 year time horizon, skin cancers only) and for the extended version (infinite time horizon, additional effects of skin cancers and cataract), representing human health damage expressed as DALYs (DALY/kg ODS = y/kg ODS).

Substance	HH, core [DALY/kg ODS]	HH, extended [DALY/kg ODS]
Annex A-I		
CFC-11	5.31E-04	1.34E-03
CFC-12	3.12E-04	1.10E-03
CFC-113	3.53E-04	1.14E-03
CFC-114	1.43E-04	7.80E-04
CFC-115	3.24E-05	7.67E-04
Annex A-II		
Halon-1301	7.47E-03	2.14E-02
Halon-1211	4.66E-03	1.06E-02
Halon-2402	7.64E-03	1.75E-02
Annex B-II		
CCl4	4.75E-04	1.10E-03
Annex B-III		
CH3CCl3	9.46E-05	2.15E-04
Annex C-I		
HCFC-22	2.36E-05	5.38E-05
HCFC-123	5.91E-06	1.34E-05
HCFC-124	1.18E-05	2.69E-05
HCFC-141b	7.09E-05	1.61E-04
HCFC-142b	3.54E-05	8.07E-05
HCFC-225ca	1.18E-05	2.69E-05
HCFC-225cb	1.77E-05	4.03E-05
Annex E		
CH3Br	3.90E-04	8.88E-04
Others		
Halon-1202	1.00E-03	2.29E-03
CH3Cl	1.18E-05	2.69E-05
N2O	5.64E-06	2.29E-05

3.5. References

De Schryver, A. M., Van Zelm, R., Humbert, S., Pfister, S., McKone, T. E., & Huijbregts, M. A. (2011). Value choices in life cycle impact assessment of stressors causing human health damage. Journal of Industrial Ecology, 15(5), 796-815.

Hayashi, K., Nakagawa, A., Itsubo, N., & Inaba, A. (2006). Expanded Damage Function of Stratospheric Ozone Depletion to Cover Major Endpoints Regarding Life Cycle Impact Assessment (12 pp). The International Journal of Life Cycle Assessment, 11(3), 150-161.

Huijbregts M.A.J., Steinmann Z.J.N., Stam G., Van Zelm R. (2014). Update of emission-related impact categories in ReCiPe2008. Department of Environmental Science, Radboud University Nijmegen.

Ravishankara AR, Daniel JS, Portmann RW, 2009. Nitrous oxide (N2O): the dominant ozone-depleting substance emitted in the 21st century. Science 326,123–125.

WMO (2011) Scientific assessment of ozone depletion: 2010, Global Ozone Research and Monitoring Project-report no.52. World Meteorological Organization, Geneva

4. Ionizing radiation

Zoran Steinmann[1], Mark A.J. Huijbregts[1]

[1] Department of Environmental Science, Radboud University Nijmegen, The Netherlands

* z.steinmann@science.ru.nl

4.1. Areas of protection and environmental mechanisms covered

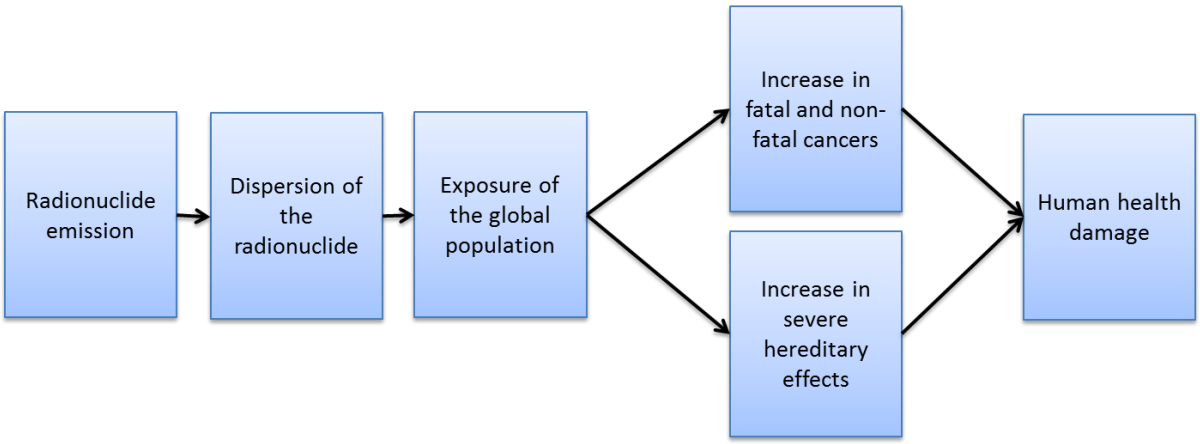

Figure 4.1: Cause-and-effect chain from an airborne or waterborne emission of a radionuclide to human health damage (from: Huijbregts et al., 2014)

Radionuclides can be released during a number of human activities. These can be related to the nuclear fuel cycle (mining, processing, use or treatment of the nuclear fuel) or during more conventional energy generation such as the burning of coal. Airborne radionuclides can be inhaled by humans, while radionuclides that end up in freshwater can be ingested during swimming in open water, via drinking water produced from surface water or can enter the food cycle via crops.

When the radionuclides decay, they release ionizing radiation. Human exposure to ionizing radiation causes alterations in the DNA, which in turn can lead to different types of cancer and birth defects. Similar effects must be expected in other living organisms, but damage to ecosystems is not quantified at the moment. Thus, the only area of protection covered is human health (Figure 4.1).

The effect factors are based on disease statistics resulting from relatively high work-related or accident-related exposure. An average approach is used to calculate the amount of additional cancer-incidences resulting from this exposure. In LCA however the exposure doses are generally very low. Therefore, the value based on relatively high exposure was corrected for the difference in cancer incidences per exposure dose, thereby approximating a marginal approach.

4.2. Calculation of the characterization factors at endpoint level

The calculation procedure here is equal to that of the latest ReCiPe update (Huijbregts et al. 2014), which in turn is based mostly on the works from De Schryver et al. (2011) and Frischknecht et al. (2000). The division of the value choices (see below) is different, meaning that the CFs with good robustness are not the same as the factors provided in ReCiPe. However, the total CFs are equal to the endpoint CFs of the Egalitarian perspective in ReCiPe, because in both methodologies these reflect all potential impacts. The endpoint CF is calculated as shown in equation 4.1, where CD stands for collective dose

of radionuclide x, and EF for effect factor for radionuclide *x,* environmental compartment *i* (air, freshwater or marine water) and time horizon *TH*

$$CF_{end,x,i,TH} = CD_{x,i,TH} \cdot EF$$

Equation 4.1

Unlike most other CFs the damage is not expressed per kg of emission but rather per kBq. The unit Becquerel (Bq) is the number of atom nuclei that decay per second. Even though the CF for every radionuclide is based on the same activity level (1kBq = a decay of 1000 nuclei per second), there are differences due to the type of radiation, the half-live of the radionuclide and the environmental fate of the radionuclide. For emissions to air a Gaussian plume model is used to describe the dispersion around the emission location for all but four radionuclides. Tritium (H-3), carbon-14, krypton-85 and iodine-129 are assumed to disperse globally. Models that cover the global water cycle, the carbon cycle, a two compartment dynamic model and a nine compartment dynamic model were used for these radionuclides respectively. Emissions to river water are modelled via a box-model with several different river compartments. By taking into account the fraction that is taken up by the human population one can calculate the collective dose (CD). As shown in equation 4.2, the collective dose (unit: man.Sv) is a measure for the total amount of exposure to a radionuclide for the entire, global population.

$$CD_{TH} = \int_{t=0}^{TH} Exposure_t \; Population_t$$

Equation 4.2

Exposure is the average exposure in Sievert (Sv=J/kg body weight) and Population represents the number of people at time *t*, integrated over time horizon TH. For the longest time horizon (100 000 years) the total human population was assumed to be stable at 10 billion people (Dreicer et al., 1995; Frischknecht et al., 2000).

The effect factor, shown in equation 4.3, combines the damages of the different disease types that can be caused by ionizing radiation.

$$EF = \sum_{i} Incidence_i \; Severity_i$$

Equation 4.3

Where Incidence is the extra incidence of disease type *i* (incidences/man.Sv) and Severity represents the human health damage caused by these diseases (DALY/incidence).

The incidence rates of the different cancer types and hereditary disease were taken from Frischknecht et al. (2000) while the corresponding human health damage (in DALY) per disease type was taken from De Schryver et al. (2011). This yields a robust damage factor of 0.617 DALY/man.Sv and a less robust factor of 1.239 DALY/man.Sv. Multiplied by the collective dose in man.Sv (taken from De Schryver et al. 2011 for almost all radionuclides, Frischknecht (2000) for the others) for emissions to the different compartments this yields the final CFs (Table 4.2).

4.3. Uncertainties

The CFs for this impact category are based on reported data from existing literature. Assessing the sensitivity of the CFs to uncertainties in the individual parameters is therefore only possible to a limited extent and is dependent on the reported data in the original reports. The uncertainties in this impact category are a combination of the uncertainty in the environmental fate and the damage factors of the different radionuclides. Because of the extremely long lifetimes of most radionuclides it is likely that the uncertainty in the first part (fate) is larger than the uncertainty in the second part (damage). Quantitative assessments are unavailable, but it is not difficult to identify potential sources of uncertainty in the fate modelling. Firstly, quite simple fate models with a limited number of compartments are used for modelling the environmental fate of the radionuclides. In contrast to other long-term effects, an important distinction for the radionuclides is that the uncertainty of the decay intensity and the type and intensity of the released radiation is negligible. The uncertainty concerns the extent to which humans will be exposed to the released radiation, which depends on the compartments where the radionuclides end up and perhaps more importantly, on the future population levels and distributions. The accuracy is highly questionable because the human exposure was modelled in quite a simplistic way. The collective dose is determined based on the assumptions that the population is evenly spread throughout the world and will remain stable at a level of 10 billion people for the next 100'000 years. Both predictions are likely to be very inaccurate. The number of 10 billion people will overestimate impacts in the short run, but potentially underestimate the future impact if the population grows beyond that number in the (distant) future.

On top of the uncertain collective dose there is also uncertainty related to the amount and types of cancer caused by exposure to radiation. Some of this uncertainty relates to whether or not different types of cancer can be caused by radiation, this is covered in the next section on value choices. Another part that is uncertain is how to adjust the factors derived from high exposure to radiation to the low exposure levels that are assessed in LCA. Partly this is a subjective choice as well, this is therefore also considered in the next section. In addition to these sources of uncertainty there is also uncertainty in the amount of DALYs caused by each cancer type. It is important to keep in mind that the values used here are representative of the current situation, if advances in medical development continue to progress it is likely that the burden of (some) types of disease decreases substantially. The longer the time horizon, the more likely it is that this will happen.

4.4. Value choices

Radioactive half-lives of radionuclides can vary from less than a second to millions of years. The harmful ionizing radiation is released during the radioactive decay. The decay is described by an exponential function, and radionuclides that decay very slowly (half-lives > 100 years) therefore release the majority of their radiation in the far future, while shorter-lived radionuclides (half-lives <100 years) will release the majority of their radiation during the first couple of years after release. It is therefore important to know over which time horizon the impact of the different radionuclides is considered. The impacts over a 100 year time horizon are considered to be robust, while the impacts occurring in a 100 000 year period after that are considered uncertain and less robust (Table 4.1).

It should be noted that even the 100.000 year time horizon is still relatively short compared to the half-life of Uranium-235 of $7.10 * 10^8$ years. However, the models that were used to derive these factors only calculated results for a time period up to 100.000 years.

While it is certain that ionizing radiation can cause hereditary disease and thyroid, bone marrow, lung and breast cancer it is less clear whether other types (bladder, colon, ovary, skin, liver, oesophagus, stomach, bone surface and remaining types) of cancer can also be caused by exposure to ionizing radiation. Therefore in the core CF only the first four types of cancer and hereditary disease are included, while for extended CF all cancer types are assumed to be caused by ionizing radiation. The incidence rate of cancer caused by ionizing radiation was determined by statistics based on accidental medium to high exposure (for example from workers in nuclear power plants). It is uncertain by how much the high to medium exposure doses should be corrected to get a CF that accurately reflects the very low exposure situations considered relevant in life cycle assessment. A factor called the Dose and dose rate effectiveness factor (DDREF) is used to correct for the fact that at higher exposures less dose is needed to result in the same effect. A factor of 10 is considered an optimistic estimate (based on animal studies), i.e. meaning that for the same cancer incidence rate caused by medium to high exposure one would need to get a dose that is 10 times higher as a result of (prolonged) low exposure (used for core CFs). A more conservative estimate is that this factor is only about 2 (used for the cancer types that are added to the extended CFs). For hereditary diseases no correction factor is applied.

Table 4.1: Value choices in the modelling for core and extended CFs. The right column shows what is added to the core values to reach the extended values.

Choice category	Core	Addition in extended
Time horizon	100 yr	100 - 100,000 years
Dose and dose rate effectiveness factor (DDREF)	10	2
Included effects	-Thyroid, bone marrow, lung and breast cancer -Hereditary disease	- bladder, colon, ovary, skin, liver, oesophagus, stomach, bone surface and remaining types of cancer

Table 4.2: Characterization factors (CF) for the core and extended values for human health damage DALY (DALY/kBq = y/kBq) for emissions to air, freshwater or the marine environment. HH stands for human health.

Emission to air	**HH, core [DALY/kBq]**	**HH, extended [DALY/kBq]**
Am-241	3.7E-07	7.6E-07
C-14	7.8E-09	1.8E-07
Co-58	1.7E-10	3.5E-10
Co-60	6.8E-09	1.4E-08
Cs-134	4.9E-09	9.8E-09
Cs-137	1.1E-08	2.2E-08
H-3	5.8E-12	1.2E-11
I-129	7.1E-08	2.8E-06
I-131	6.2E-11	1.2E-10
I-133	3.8E-12	7.7E-12
Kr-85	5.8E-14	1.2E-13
Pb-210	6.2E-10	1.2E-09
Po-210	6.2E-10	1.2E-09
Pu alpha		6.8E-08
Pu-238		5.5E-08
Pu-239	2.2E-07	4.3E-07
Ra-226		7.4E-10
Rn-222	9.9E-12	2.0E-11
Ru-106	6.8E-10	1.4E-09
Sr-90	1.7E-08	3.3E-08
Tc-99	8.0E-09	1.6E-08
Th-230		3.7E-08
U-234		7.9E-08
U-235		1.7E-08
U-238		6.7E-09
Xe-133	5.8E-14	1.2E-13
Emission to river and lakes		
Ag-110m	2.0E-10	4.1E-10
Am-241	2.3E-11	5.0E-11
C-14	4.1E-11	1.7E-10
Co-58	1.7E-11	3.3E-11
Co-60	1.8E-08	3.6E-08
Cs-134	5.9E-08	1.2E-07
Cs-137	6.8E-08	1.4E-07
H-3	2.8E-13	5.6E-13
I-129	1.9E-09	2.1E-06
I-131	2.0E-10	4.1E-10
Mn-54	1.3E-10	2.6E-10
Pu-239	2.5E-12	5.7E-12
Ra-226		1.1E-10
Ru-106	1.6E-12	3.2E-12
Sb-124	3.3E-10	6.7E-10
Sr-90	1.7E-10	3.8E-10
Tc-99	2.1E-10	4.2E-10
U-234		2.0E-09
U-235		1.9E-09
U-238		1.9E-09
Emission to ocean		
Am-241	3.3E-10	6.6E-10
C-14	1.9E-10	3.7E-10
Cm alpha		4.7E-08
Co-60	1.6E-10	3.2E-10
Cs-134	3.2E-11	6.4E-11
Cs-137	3.9E-11	7.9E-11
H-3	2.8E-14	5.5E-14
I-129	2.0E-10	2.1E-06

Pu alpha		6.1E-08
Pu-239	3.6E-11	7.8E-11
Ru-106	7.4E-12	1.5E-11
Sb-125	6.0E-12	1.2E-11
Sr-90	3.1E-12	6.2E-12
Tc-99	5.4E-13	1.5E-12
U-234		1.9E-11
U-235		2.0E-11
U-238		1.9E-11

4.5. References

De Schryver, A. M., Van Zelm, R., Humbert, S., Pfister, S., McKone, T. E., & Huijbregts, M. A. (2011). Value choices in life cycle impact assessment of stressors causing human health damage. Journal of Industrial Ecology, 15(5), 796-815

Dreicer, M., Tort, V. & Manen, P. (1995) ExternE, Externalities of Energy, Vol. 5. Nuclear, Centre d'étude sur l'Evaluation de la Protection dans le domaine Nucléaire (CEPN), edited by the European Commission DGXII, Science, Research and Development JOULE, Luxembourg, 1995.

Frischknecht, R., Braunschweig,A., Hofstetter, P. & Suter,P. (2000) Human health damages due to ionising radiation in life cycle impact assessment. *Environmental Impact Assessment Review* 20(2):159–189.

Huijbregts M.A.J., Steinmann Z.J.N., Stam G., Van Zelm R. (2014). Update of emission-related impact categories in ReCiPe2008. Department of Environmental Science, Radboud University Nijmegen.

5. Photochemical ozone formation

Rosalie van Zelm[1], Philipp Preiss[2,3], Thomas van Goethem[1], Francesca Verones[4], Rita Van Dingenen[5], Mark Huijbregts[1]*

[1] Department of Environmental Science, Radboud University Nijmegen, The Netherlands
[2] European Institute for Energy Research | EIFER, Emmy-Noether-Str. 11, 76131 Karlsruhe, Germany
[3]Institute for Energy Economics and the Rational Use of Energy, Department for Technology Assessment and Environment, Universität Stuttgart, Germany
[4] Industrial Ecology Programme and Department of Energy and Process Engineering, NTNU, Trondheim, Norway
[5]European Commission, Joint Research Centre (JRC), Environment and Sustainability (IES), Air and Climate Unit, Via Enrico Fermi, 2749, 21027 Ispra (VA), Italy
* r.vanzelm@science.ru.nl

The impact assessment method for assessing damage to human health and ecosystems due photochemical ozone formation is described based on Van Zelm et al. (2016).

5.1. Areas of protection and environmental mechanisms covered

The cause and effect pathway (Figure 5.1) of ozone formation starts with an emission of NO_x or NMVOC to the atmosphere, followed by atmospheric fate and chemistry in the air; NO_x and NMVOCs are transformed in air to ozone. Subsequently, this tropospheric ozone can be inhaled by humans or taken up by plants, leading to an increased number of mortality cases and final damage to human health, as well as disappearance of plant species and final damage to terrestrial ecosystems.

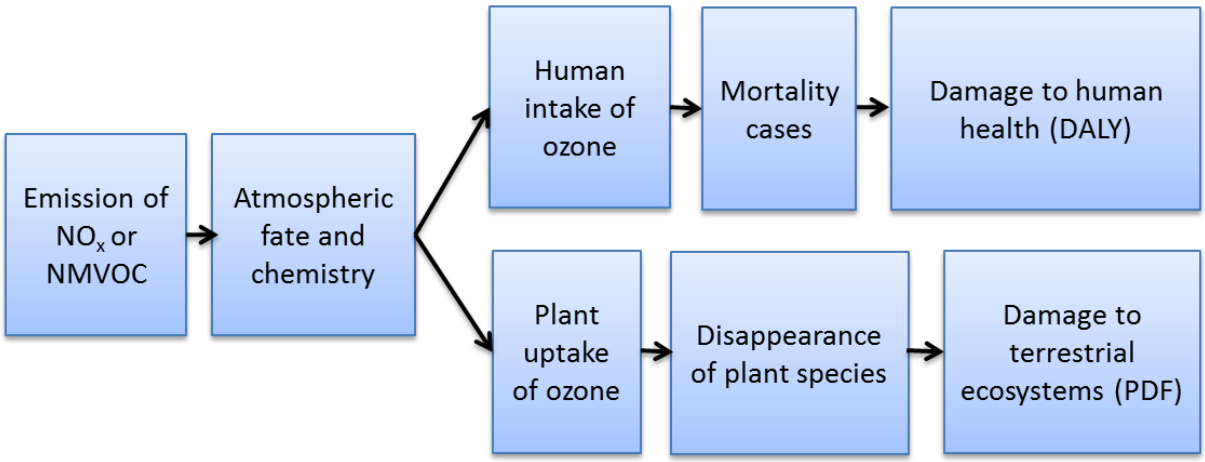

Figure 5.1: Cause and effect pathway from tropospheric ozone precursor emissions to damage to human health and terrestrial ecosystems.

The intake of a pollutant by humans is described by intake fractions (iF, in kg intake per kg emission) that quantify the relationship between an emission and intake at the population level. The environmental fate of ozone is described by fate factors (FF in ppm·hr·yr per kg emission) that quantify the relationship between an emission and subsequent concentration (Van Zelm et al. 2008). Here, a global chemical transport model was applied to determine environmental fate factors and human

intake fractions for 56 emission and receptor regions. To determine human health effect factors, region-specific mortality rates, background concentrations and years of life lost were used.

Here, we included respiratory mortality due to ozone for two reasons: first, these contribute by far the most to overall disability adjusted life years, and second, for these the most up-to-date and least uncertain data related to relative risks and years of life lost are available (see e.g. Anenberg et al. 2010, Friedrich et al. 2011, Murray et al. 2012, WHO 2013).

To determine environmental impacts on terrestrial ecosystems, grid-cell specific forest and grass shares and background concentrations were used as input for plant species sensitivity distributions (Van Goethem et al. 2013a)

5.2. Calculation of the characterization factors at endpoint level

5.2.1. Human health damage

The endpoint characterization factors (CFs) for human health damage due to ozone formation caused by emitted precursor substance x in world region i ($CF_{x,i}$ in DALY·kg^{-1}) are defined as the yearly change in Disability Adjusted Life Years (DALY) of all inhabitants (dDALY in yr·yr^{-1}) due to a change in emission of substance x in source region i ($dM_{x,i}$ in kg·yr^{-1}). This CF for human health damage is composed of a dimensionless intake fraction ($iF_{x,\,i\rightarrow j}$), providing the population intake of ozone in receptor region j (in kg/yr) following an emission change of substance x in source region i (in kg/yr), an effect factor (EF_e), describing the cases of health effect *e* per kg of inhaled ozone, and a damage factor (DF_e), which describes the years of life lost per case of health effect *e*. In equation this reads:

$$CF_{x,i} = \sum_j \left(\left(iF_{x,i\rightarrow j} \right) \cdot \sum_e \left(EF_{e,j} \cdot DF_{e,j} \right) \right) \qquad \textbf{Equation 5.1.}$$

5.2.1.1. From emission to human intake

The intake fraction is determined as the change in exposure to ozone in region j ($dEXP_j$), due to a change in emission of precursor substance x ($dM_{x,i}$). dEXP was retrieved by multiplying the change in concentration of ozone in each receptor region (dC_j) with the population (N_j) in the receptor region j and the average breathing rate per person (BR) of 4745 m^3·yr^{-1} (13 m^3·d^{-1} as recommended by USEPA (1997):

$$iF_{x,i\rightarrow j} = \frac{dEXP_j}{dM_{x,i}} = \frac{dC_j \cdot N_j \cdot BR}{dM_{x,i}} \qquad \textbf{Equation 5.2.}$$

Population numbers (year 2005) were taken from the United Nations (2011). Since all data for the effect factor are based on the population ≥ 30 years of age, the population number was adjusted for the population share ≥ 30 years of age in 2005 (United Nations 2011) assuming no effects for younger people.

The emission–concentration sensitivities matrices for emitted precursors and relevant end pollutants (or pollutant metrics) from the global source-receptor model TM5-FASST (FAst Scenario Screening Tool for Global Air Quality and Instantaneous Radiative Forcing), based on perturbation runs with TM5 (Van Dingenen et al. 2009; Krol et al. 2005) were used to derive the change in ambient concentration of a pollutant after the emission of a precursor. TM5 is a global chemical transport model hosted by the

European Commission Joint Research Center (JRC). TM5-FASST takes into account spatial features at the emission site as well as dispersion characteristics for the whole world. In this model, the world is divided into 56 emission source regions. The regions correspond to countries or a group of countries (see Table 5.1). The TM5 model output consists of the change in concentration for each region, derived from gridded 1°×1° concentration results, following a change in emission. This change is determined by lowering the year 2000 emissions (Lamarque et al. 2010) by 20% for each of the 56 source regions sequentially. The emission-normalized differences in pollutant concentration between the unperturbed and perturbed case, aggregated over each receptor region, are stored as the emission – concentration matrix elements. This procedure was performed for both NO_x and NMVOC.

5.2.1.2. From human intake to human health damage

The human effect factor (dINC/dEXP) for health effect e caused by ozone in receptor region j, representing the change in disease incidence due to a change in exposure concentration in ambient air, was determined by dividing the concentration-response function (CRF in $m^3 \cdot yr^{-1} \cdot kg^{-1}$) by the breathing rate BR ($m^3 \cdot yr^{-1}$) (Gronlund et al. 2015) (equation 5.3):

$$EF_{e,j} = \frac{dINC_j}{dEXP_j} = \frac{CRF_{e.j}}{BR} \qquad \textbf{Equation 5.3}$$

Region-specific CRFs were calculated as follows (equation 5.4):

$$CRF_{e,j} = \frac{(RR_e - 1) \cdot MR_{e,j}}{(RR_e - 1) \cdot C_j + 1} \qquad \textbf{Equation 5.4}$$

where RR_e is the relative risk to obtain health effect e due to exposure to ozone (per $\mu g \cdot m^{-3}$), $MR_{e,j}$ is the mortality rate for health effect e in region j (deaths/person/yr), and C_j is the yearly average background concentration of ozone in a region ($\mu g \cdot m^{-3}$).

We followed recommendations for RRs by Anenberg et al. (2010) and Friedrich et al. (2011), who focus on the world and Europe respectively, based on North American cohort studies. The RR for respiratory mortality (1.004 per $\mu g \cdot m^{-3}$) based on data of daily 1-hr maximum ozone levels found by Jerrett et al. (2009) in an ACS cohort study of U.S. adults ≥ 30 years of age was used. Although many daily time-series epidemiology studies demonstrate short-term ozone mortality impacts (Anderson et al. 2004; Bell et al. 2005), Jerrett et al. (2009) provide the first clear evidence for long-term impacts.

Mortality rates per health effect (year 2005) were taken from the World Health Organization (WHO 2015a), and simulated background concentrations per region for the year 2000 were taken from the TM5-CTM reference run with the Lamarque et al. (2010) year 2000 reference emission scenario.

The Damage Factor $DF_{e,j}$ is defined as the Disability Adjusted Life Years (DALY) associated to the health effect e per incidence case, which were estimated per receiving region j from the world health organization (WHO) world health estimates, year 2012 (WHO 2015b):

$$DF_{e,j} = \frac{dDALY_{e,j}}{dINC_{e,j}} \qquad \textbf{Equation 5.5}$$

For the DALY no discounting was included and uniform age weights were applied.

5.2.2. Terrestrial ecosystem damage

The endpoint characterization factors (CFs) for ecosystem damage due to ozone formation caused by emitted precursor substance x in world region i ($CF_{x,i}$ in PDF·yr·kg^{-1}) are defined as the area-integrated change in Potentially Disappeared Fraction (PDF) of forest and natural grassland species due to a change in emission of substance x in source region i ($dM_{x,i}$ in kg·yr^{-1}). This CF for ecosystem damage is composed of a Fate Factor ($FF_{x,i\rightarrow g}$, unit: ppm·h·yr·kg^{-1}), quantifying the relationship between the emission of precursor substances in region i and ozone exposure in receiving grid cell g, and an Effect Factor ($EF_{n,j}$ in PDF· ppm^{-1}·h^{-1}), quantifying the relationship between ozone exposure and the damage to natural vegetation n (forest and grassland). In equation this reads:

$$CF_{ECO,x,i} = \sum_{g}\sum_{n}\left(FF_{x,i\rightarrow g}\cdot EF_{n,g}\right) \qquad \textbf{Equation 5.6}$$

5.2.2.1. From emission to environmental concentration

To determine the ecosystem fate factor, the AOT40, i.e. the sum of the differences between the hourly mean ozone concentration and 40 ppb during daylight hours over the relevant growing season in ppm·h, was used as metric of the cumulative concentration change. The fate factor represents the sum in the change in AOT40 in grid cell g due to a change of emission of precursor x in source region i (Van Goethem et al. 2013b):

$$\mathrm{FF_{x,i\rightarrow g}} = \sum_{g}\frac{\Delta AOT40_{g}}{\Delta M_{x,i}} \qquad \textbf{Equation 5.7}$$

Monthly AOT40 concentrations per unit of emission of NO_x and NMVOC were calculated on a 1°x1° resolution from hourly ozone concentrations resulting from the year 2000 reference run with TM5 chemical transport model. For the Northern Hemisphere the same growing seasons for grassland and forest were taken as was done for Europe by Van Goethem et al. (2013), namely May till July and April till September, respectively. For the Southern Hemisphere for grassland the months November till January and for forests the months October till March were taken.

5.2.2.2. From concentration to ecosystem damage

The ecosystem effect factor (EF) was derived from Van Goethem et al. (2013), and corrected for species density:

$$\mathrm{EF_{n,g}} = \frac{\Delta PDF_{g,n}}{\Delta AOT40_{g}}\cdot A_{g,n}\cdot\frac{PRD_{g\in br}}{PR_{global}} \qquad \textbf{Equation 5.8}$$

where PRD_g is the vascular plant richness density in grid g belonging to terrestrial biogeographical region br (species/km^2), PR is the total vascular plant richness in the world (species), and $A_{g,n}$ is the area (m^2) occupied by vegetation type n in grid cell g. The effect factor was determined with data on AOT40 concentrations for which 50% reduction in productivity (EC50) was found for a number of forest or grassland species (taken from Van Goethem et al. (2013a, 2013b)). Here, we chose to use the linear ecosystem effect factor, assuming a linear change in PAF with changing AOT40 that represents the average effect between a PAF of 0.5 and 0 (Van Goethem et al. 2013b). The corresponding "AOT40 concentration per unit of yearly emission" values per grid were multiplied by the corresponding natural area of either grassland or forest (Van Zelm et al. 2016). PRD and PR were obtained from Kier et al. (2009). PR equals 315'903.

5.3. Uncertainties

The CFs were derived from emission-concentration sensitivities (dC/dM) obtained from a 20% emission perturbation. Because AOT40 is a threshold based concentration indicator, there is more uncertainty attached to it compared to the use of linear scaling concentrations (Van Dingenen et al. 2009). When a concentration is, for example, slightly above the threshold of 40 ppb and then reduced when looking at the 20% perturbation, this can have large impacts on the results. For a limited number of representative source regions the dC/dM coefficients were calculated for large perturbations of inorganic pollutants (-80%, +100%) and compared to the extrapolated 20% perturbation (Van Zelm et al. 2016). For M6M, precursor NO_x, a deviation up to 14% was seen. For AOT40, however, deviations can be large. The large deviation for AOT40 under an 80% reduction of NOx (36% average) is explained by the linear extrapolation of a threshold metric from a regime above threshold to a regime below threshold.

The negative intake fractions for ozone due to emissions of NO_x are caused by the so-called titration effect. As a result of the rapid reaction of ozone with NO to form NO_2, concentrations of ozone tend to be lower close to sources of NO emissions, such as near dense urban traffic, major highways, and industrial sources. Countries that show negative characterization factors for NO_x therefore have relatively large characterization factors for NMVOC.

5.4. Value choices

5.4.1. Time horizon

For ozone formation impacts, time horizon is not of importance as only short-living substances are involved.

5.5. Resulting characterization factors

Figure 5.2 shows the region-specific characterization factors for human health damage due to ozone precursor emissions. Lowest factors (apart from the negatives) were obtained for emissions of NMVOC in New Zealand, Australia, Indonesia, and South America, while largest factors were obtained for NOx emissions in South Asia, West-Africa, India and China. The emission weighted average for the world for NMVOC is $1.4 \cdot 10^{-1}$ yr·kton^{-1} ($8.8 \cdot 10^{-3}$ to $5.0 \cdot 10^{-1}$ yr·kton^{-1}). The emission weighted average for the world for NOx is $9.1 \cdot 10^{-1}$ yr·kton^{-1} ($-2.2 \cdot 10^{-1}$ to 5.7 yr·kton^{-1}). Negative intake fractions and thus CFs were obtained for NO_x emitted in Belgium, the Netherlands, Luxembourg, Great-Britain, and Ireland. A negative value means that the emission of NO_x leads to an overall reduction of ozone exposure.

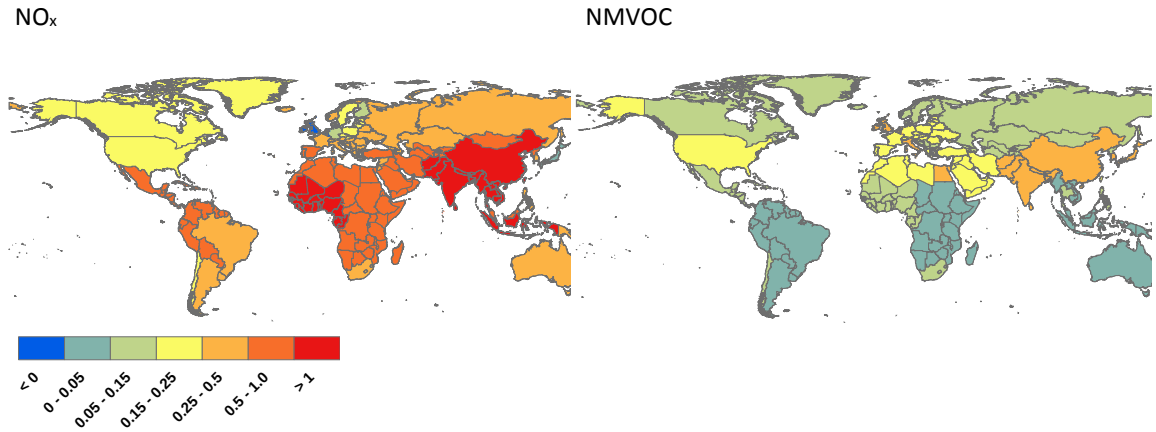

Figure 5.2.: Characterization factors for human health damage caused by ozone formation (10^{-6} DALY·kg^{-1}) (Taken from Van Zelm et al. 2016).

Figure 5.3 shows the region-specific characterization factors for ecosystem damage due to ozone precursor emissions. Lowest factors were obtained for emissions of NMVOC in New Zealand, Mongolia, and Argentina, and for NOx emissions in New Zealand, Taiwan and China. Largest factors were obtained for NOx emissions in Mid America. The emission weighted average for the world for NMVOC is $3.7 \cdot 10^{-16}$ PDF·yr·kg^{-1}. The emission weighted average for the world for NOx is $1.0 \cdot 10^{-15}$ PDF·yr·kg^{-1}.

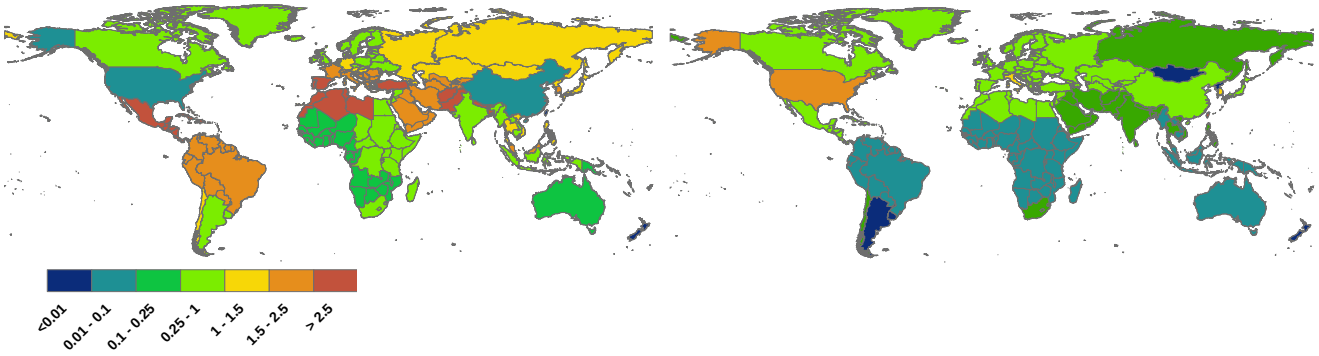

Figure 5.3.: Characterization factors for ecosystem damage caused by ozone formation (10^{-15} PDF·yr·kg^{-1}).

Table 5.1: Country-specific endpoint characterization factors for human health damage and ecosystem damage due to ozone formation.

		Human health damage (DALY·kg^{-1})		Ecosystem damage (PDF·yr·kg^{-1})	
Country	TM5 region	NO_x	NMVOC	NO_x	NMVOC
Afghanistan	RSAS	3.7E-07	5.7E-06	1.1E-16	2.9E-15
Albania	RCEU	1.4E-07	4.9E-07	4.9E-16	2.1E-15
Algeria	NOA	1.7E-07	9.9E-07	7.7E-16	4.9E-15
Angola	SAF	2.3E-08	5.8E-07	2.6E-17	1.9E-16
Argentina	ARG	3.0E-08	3.3E-07	-1.8E-17	9.5E-16
Armenia	RUS	1.4E-07	3.0E-07	4.4E-16	1.1E-15
Aruba	RCAM	5.9E-08	6.7E-07	3.0E-16	7.2E-15
Australia	AUS	1.8E-08	2.8E-07	2.4E-17	1.1E-16
Austria	AUT	1.9E-07	3.3E-07	7.7E-16	1.0E-15
Azerbaijan	RUS	1.4E-07	3.0E-07	4.4E-16	1.1E-15
Bahamas	RCAM	5.9E-08	6.7E-07	3.0E-16	7.2E-15
Bahrain	GOLF	1.6E-07	9.7E-07	2.0E-16	1.6E-15
Bangladesh	RSAS	3.7E-07	5.7E-06	1.1E-16	2.9E-15
Barbados	RCAM	5.9E-08	6.7E-07	3.0E-16	7.2E-15
Belgium	BLX	3.3E-07	-2.2E-07	6.2E-16	2.9E-16
Belize	RCAM	5.9E-08	6.7E-07	3.0E-16	7.2E-15
Benin	WAF	1.1E-07	2.4E-06	5.6E-17	2.4E-16
Bhutan	RSAS	3.7E-07	5.7E-06	1.1E-16	2.9E-15
Bolivia	RSAM	1.6E-08	5.1E-07	2.5E-17	1.6E-15
Bosnia and Herzegovina	RCEU	1.4E-07	4.9E-07	4.9E-16	2.1E-15
Botswana	SAF	2.3E-08	5.8E-07	2.6E-17	1.9E-16
Brazil	BRA	1.8E-08	4.5E-07	5.8E-17	2.5E-15
Brunei	MYS	3.0E-08	7.0E-07	5.1E-17	1.9E-15
Bulgaria	BGR	1.5E-07	3.9E-07	5.8E-16	1.5E-15
Burkina Faso	WAF	1.1E-07	2.4E-06	5.6E-17	2.4E-16
Burundi	EAF	4.3E-08	9.7E-07	5.4E-17	4.3E-16
Byelarus	UKR	1.6E-07	3.4E-07	5.0E-16	9.3E-16
Cambodia	RSEA	4.4E-08	1.8E-06	9.7E-17	8.3E-16
Cameroon	WAF	1.1E-07	2.4E-06	5.6E-17	2.4E-16
Canada	CAN	1.1E-07	2.0E-07	2.6E-16	5.9E-16
Cape Verde	WAF	1.1E-07	2.4E-06	5.6E-17	2.4E-16

		Human health damage (DALY·kg^{-1})		Ecosystem damage (PDF·yr·kg^{-1})	
Country	TM5 region	NO_x	NMVOC	NO_x	NMVOC
Central African Republic	EAF	4.3E-08	9.7E-07	5.4E-17	4.3E-16
Chad	EAF	4.3E-08	9.7E-07	5.4E-17	4.3E-16
Chile	CHL	7.6E-08	1.8E-07	1.3E-16	1.1E-15
China	CHN	2.9E-07	1.6E-06	2.9E-16	3.9E-17
China	CHN	2.9E-07	1.6E-06	2.9E-16	3.9E-17
China, Hong Kong Special Administrative Region	CHN	2.9E-07	1.6E-06	2.9E-16	3.9E-17
Colombia	RSAM	1.6E-08	5.1E-07	2.5E-17	1.6E-15
Comoros	EAF	4.3E-08	9.7E-07	5.4E-17	4.3E-16
Congo	WAF	1.1E-07	2.4E-06	5.6E-17	2.4E-16
Costa Rica	RCAM	5.9E-08	6.7E-07	3.0E-16	7.2E-15
Croatia	RCEU	1.4E-07	4.9E-07	4.9E-16	2.1E-15
Cuba	RCAM	5.9E-08	6.7E-07	3.0E-16	7.2E-15
Cyprus	GRC	2.3E-07	4.4E-07	8.2E-16	2.4E-15
Czech Republic	RCZ	1.9E-07	1.6E-07	6.1E-16	6.2E-16
Democratic Republic of the Congo	EAF	4.3E-08	9.7E-07	5.4E-17	4.3E-16
Denmark	SWE	1.5E-07	1.9E-07	4.1E-16	3.9E-16
Djibouti	EAF	4.3E-08	9.7E-07	5.4E-17	4.3E-16
Dominican Republic	RCAM	5.9E-08	6.7E-07	3.0E-16	7.2E-15
Ecuador	RSAM	1.6E-08	5.1E-07	2.5E-17	1.6E-15
Egypt	EGY	2.5E-07	6.0E-07	2.6E-16	5.2E-16
El Salvador	RCAM	5.9E-08	6.7E-07	3.0E-16	7.2E-15
Equatorial Guinea	WAF	1.1E-07	2.4E-06	5.6E-17	2.4E-16
Eritrea	EAF	4.3E-08	9.7E-07	5.4E-17	4.3E-16
Estonia	POL	1.8E-07	1.8E-07	5.5E-16	6.3E-16
Ethiopia	EAF	4.3E-08	9.7E-07	5.4E-17	4.3E-16
Fiji	PAC	1.0E-08	4.5E-07	2.0E-17	2.2E-16
Finland	FIN	1.3E-07	1.1E-07	3.6E-16	2.6E-16
France	FRA	2.4E-07	3.2E-07	8.3E-16	1.6E-15
French Guiana	RSAM	1.6E-08	5.1E-07	2.5E-17	1.6E-15
Gabon	WAF	1.1E-07	2.4E-06	5.6E-17	2.4E-16
Gambia, The	WAF	1.1E-07	2.4E-06	5.6E-17	2.4E-16
Georgia	RUS	1.4E-07	3.0E-07	4.4E-16	1.1E-15
Germany	RFA	2.5E-07	6.9E-08	6.3E-16	1.3E-15
Ghana	WAF	1.1E-07	2.4E-06	5.6E-17	2.4E-16
Greece	GRC	2.3E-07	4.4E-07	8.2E-16	2.4E-15
Greenland	CAN	1.1E-07	2.0E-07	2.6E-16	5.9E-16
Grenada	RCAM	5.9E-08	6.7E-07	3.0E-16	7.2E-15
Guadeloupe	RCAM	5.9E-08	6.7E-07	3.0E-16	7.2E-15
Guatemala	RCAM	5.9E-08	6.7E-07	3.0E-16	7.2E-15
Guinea	WAF	1.1E-07	2.4E-06	5.6E-17	2.4E-16
Guinea-Bissau	WAF	1.1E-07	2.4E-06	5.6E-17	2.4E-16
Guyana	RSAM	1.6E-08	5.1E-07	2.5E-17	1.6E-15
Haiti	RCAM	5.9E-08	6.7E-07	3.0E-16	7.2E-15
Honduras	RCAM	5.9E-08	6.7E-07	3.0E-16	7.2E-15
Hungary	HUN	1.7E-07	2.8E-07	6.0E-16	1.1E-15
Iceland	NOR	1.2E-07	4.5E-07	3.6E-16	7.7E-16
India	NDE	4.1E-07	5.2E-06	2.1E-16	5.6E-16
Indonesia	IDN	1.8E-08	1.0E-06	2.6E-17	8.0E-16
Iran	GOLF	1.6E-07	9.7E-07	2.0E-16	1.6E-15
Iraq	GOLF	1.6E-07	9.7E-07	2.0E-16	1.6E-15
Ireland	GBR	3.2E-07	-1.6E-07	6.0E-16	3.6E-16
Israel	MEME	1.8E-07	4.9E-07	4.2E-16	9.7E-16
Italy	ITA	2.7E-07	4.6E-07	1.3E-15	1.9E-15
Ivory Coast	WAF	1.1E-07	2.4E-06	5.6E-17	2.4E-16
Jamaica	RCAM	5.9E-08	6.7E-07	3.0E-16	7.2E-15
Japan	JPN	2.7E-07	2.3E-09	1.0E-15	1.1E-15
Jordan	MEME	1.8E-07	4.9E-07	4.2E-16	9.7E-16

		Human health damage (DALY·kg^{-1})		Ecosystem damage (PDF·yr·kg^{-1})	
Country	TM5 region	NO_x	NMVOC	NO_x	NMVOC
Kazakhstan	KAZ	1.0E-07	4.0E-07	2.8E-16	1.2E-15
Kenya	EAF	4.3E-08	9.7E-07	5.4E-17	4.3E-16
Kuwait	GOLF	1.6E-07	9.7E-07	2.0E-16	1.6E-15
Kyrgyzstan	RIS	1.5E-07	7.0E-07	3.6E-16	2.4E-15
Laos	RSEA	4.4E-08	1.8E-06	9.7E-17	8.3E-16
Latvia	POL	1.8E-07	1.8E-07	5.5E-16	6.3E-16
Lebanon	MEME	1.8E-07	4.9E-07	4.2E-16	9.7E-16
Lesotho	RSA	1.1E-07	4.0E-07	2.0E-16	3.7E-16
Liberia	WAF	1.1E-07	2.4E-06	5.6E-17	2.4E-16
Libya	NOA	1.7E-07	9.9E-07	7.7E-16	4.9E-15
Lithuania	POL	1.8E-07	1.8E-07	5.5E-16	6.3E-16
Luxembourg	BLX	3.3E-07	-2.2E-07	6.2E-16	2.9E-16
Macedonia	RCEU	1.4E-07	4.9E-07	4.9E-16	2.1E-15
Madagascar	EAF	4.3E-08	9.7E-07	5.4E-17	4.3E-16
Malawi	SAF	2.3E-08	5.8E-07	2.6E-17	1.9E-16
Malaysia	MYS	3.0E-08	7.0E-07	5.1E-17	1.9E-15
Maldives	NDE	4.1E-07	5.2E-06	2.1E-16	5.6E-16
Mali	WAF	1.1E-07	2.4E-06	5.6E-17	2.4E-16
Malta	ITA	2.7E-07	4.6E-07	1.3E-15	1.9E-15
Martinique	RCAM	5.9E-08	6.7E-07	3.0E-16	7.2E-15
Mauritania	WAF	1.1E-07	2.4E-06	5.6E-17	2.4E-16
Mauritius	EAF	4.3E-08	9.7E-07	5.4E-17	4.3E-16
Mexico	MEX	8.4E-08	5.8E-07	3.4E-16	1.6E-14
Moldova	UKR	1.6E-07	3.4E-07	5.0E-16	9.3E-16
Mongolia	MON	5.0E-08	5.8E-07	-2.6E-16	1.4E-15
Morocco	NOA	1.7E-07	9.9E-07	7.7E-16	4.9E-15
Mozambique	SAF	2.3E-08	5.8E-07	2.6E-17	1.9E-16
Myanmar (Burma)	RSEA	4.4E-08	1.8E-06	9.7E-17	8.3E-16
Namibia	SAF	2.3E-08	5.8E-07	2.6E-17	1.9E-16
Nepal	RSAS	3.7E-07	5.7E-06	1.1E-16	2.9E-15
Netherlands	BLX	3.3E-07	-2.2E-07	6.2E-16	2.9E-16
Netherlands Antilles	RCAM	5.9E-08	6.7E-07	3.0E-16	7.2E-15
New Zealand	NZL	8.8E-09	6.2E-08	3.0E-18	4.5E-18
Nicaragua	RCAM	5.9E-08	6.7E-07	3.0E-16	7.2E-15
Niger	WAF	1.1E-07	2.4E-06	5.6E-17	2.4E-16
Nigeria	WAF	1.1E-07	2.4E-06	5.6E-17	2.4E-16
North Korea	MON	5.0E-08	5.8E-07	-2.6E-16	1.4E-15
Norway	NOR	1.2E-07	4.5E-07	3.6E-16	7.7E-16
Oman	GOLF	1.6E-07	9.7E-07	2.0E-16	1.6E-15
Pakistan	RSAS	3.7E-07	5.7E-06	1.1E-16	2.9E-15
Panama	RCAM	5.9E-08	6.7E-07	3.0E-16	7.2E-15
Papua New Guinea	PAC	1.0E-08	4.5E-07	2.0E-17	2.2E-16
Paraguay	RSAM	1.6E-08	5.1E-07	2.5E-17	1.6E-15
Peru	RSAM	1.6E-08	5.1E-07	2.5E-17	1.6E-15
Philippines	PHL	7.2E-08	4.8E-07	2.4E-16	1.1E-15
Poland	POL	1.8E-07	1.8E-07	5.5E-16	6.3E-16
Portugal	ESP	2.2E-07	6.2E-07	9.8E-16	3.7E-15
Puerto Rico	RCAM	5.9E-08	6.7E-07	3.0E-16	7.2E-15
Qatar	GOLF	1.6E-07	9.7E-07	2.0E-16	1.6E-15
Reunion	EAF	4.3E-08	9.7E-07	5.4E-17	4.3E-16
Romania	ROM	1.6E-07	3.8E-07	5.9E-16	1.6E-15
Russia	RUE	7.7E-08	4.7E-07	2.3E-16	1.0E-15
Russia Europe	RUS	1.4E-07	3.0E-07	4.4E-16	1.1E-15
Rwanda	EAF	4.3E-08	9.7E-07	5.4E-17	4.3E-16
Saint Lucia	RCAM	5.9E-08	6.7E-07	3.0E-16	7.2E-15
Saint Vincent and the Grenadines	RCAM	5.9E-08	6.7E-07	3.0E-16	7.2E-15
Samoa	PAC	1.0E-08	4.5E-07	2.0E-17	2.2E-16

		Human health damage (DALY·kg^{-1})		Ecosystem damage (PDF·yr·kg^{-1})	
Country	TM5 region	NO_x	NMVOC	NO_x	NMVOC
Saudi Arabia	GOLF	1.6E-07	9.7E-07	2.0E-16	1.6E-15
Senegal	WAF	1.1E-07	2.4E-06	5.6E-17	2.4E-16
Serbia	RCEU	1.4E-07	4.9E-07	4.9E-16	2.1E-15
Sierra Leone	WAF	1.1E-07	2.4E-06	5.6E-17	2.4E-16
Singapore	MYS	3.0E-08	7.0E-07	5.1E-17	1.9E-15
Slovakia	RCZ	1.9E-07	1.6E-07	6.1E-16	6.2E-16
Slovenia	AUT	1.9E-07	3.3E-07	7.7E-16	1.0E-15
Solomon Islands	PAC	1.0E-08	4.5E-07	2.0E-17	2.2E-16
Somalia	EAF	4.3E-08	9.7E-07	5.4E-17	4.3E-16
South Africa	RSA	1.1E-07	4.0E-07	2.0E-16	3.7E-16
South Korea	COR	5.0E-07	4.1E-07	1.4E-15	1.9E-15
Spain	ESP	2.2E-07	6.2E-07	9.8E-16	3.7E-15
Sri Lanka	NDE	4.1E-07	5.2E-06	2.1E-16	5.6E-16
Sudan	EAF	4.3E-08	9.7E-07	5.4E-17	4.3E-16
Suriname	RSAM	1.6E-08	5.1E-07	2.5E-17	1.6E-15
Swaziland	RSA	1.1E-07	4.0E-07	2.0E-16	3.7E-16
Sweden	SWE	1.5E-07	1.9E-07	4.1E-16	3.9E-16
Switzerland	CHE	2.0E-07	4.2E-07	7.1E-16	1.9E-15
Syria	MEME	1.8E-07	4.9E-07	4.2E-16	9.7E-16
Sao Tomo and Principe	WAF	1.1E-07	2.4E-06	5.6E-17	2.4E-16
Taiwan	TWN	2.0E-07	1.0E-06	1.0E-14	-2.0E-14
Tajikistan	RIS	1.5E-07	7.0E-07	3.6E-16	2.4E-15
Tanzania, United Republic of	EAF	4.3E-08	9.7E-07	5.4E-17	4.3E-16
Thailand	THA	5.3E-08	1.2E-06	1.3E-16	1.1E-15
Togo	WAF	1.1E-07	2.4E-06	5.6E-17	2.4E-16
Tonga	PAC	1.0E-08	4.5E-07	2.0E-17	2.2E-16
Trinidad and Tobago	RCAM	5.9E-08	6.7E-07	3.0E-16	7.2E-15
Tunisia	NOA	1.7E-07	9.9E-07	7.7E-16	4.9E-15
Turkey	TUR	1.9E-07	6.2E-07	7.5E-16	3.7E-15
Turkmenistan	RIS	1.5E-07	7.0E-07	3.6E-16	2.4E-15
Uganda	EAF	4.3E-08	9.7E-07	5.4E-17	4.3E-16
Ukraine	UKR	1.6E-07	3.4E-07	5.0E-16	9.3E-16
United Arab Emirates	GOLF	1.6E-07	9.7E-07	2.0E-16	1.6E-15
United Kingdom	GBR	3.2E-07	-1.6E-07	6.0E-16	3.6E-16
United States	USA	1.9E-07	1.9E-07	1.6E-15	8.0E-17
Uruguay	ARG	3.0E-08	3.3E-07	-1.8E-17	9.5E-16
Uzbekistan	RIS	1.5E-07	7.0E-07	3.6E-16	2.4E-15
Vanuatu	PAC	1.0E-08	4.5E-07	2.0E-17	2.2E-16
Venezuela	RSAM	1.6E-08	5.1E-07	2.5E-17	1.6E-15
Vietnam	VNM	4.3E-08	1.1E-06	1.3E-16	1.3E-15
Western Sahara	NOA	1.7E-07	9.9E-07	7.7E-16	4.9E-15
Yemen	GOLF	1.6E-07	9.7E-07	2.0E-16	1.6E-15
Zambia	SAF	2.3E-08	5.8E-07	2.6E-17	1.9E-16
Zimbabwe	SAF	2.3E-08	5.8E-07	2.6E-17	1.9E-16

Table 5.2: Continent-specific endpoint characterization factors for human health damage and ecosystem damage due to ozone formation.

	Human health damage (DALY·kg^{-1})		Ecosystem damage (PDF·yr·kg^{-1})	
Continent	NO_x	NMVOC	NO_x	NMVOC
World Weighted Average	1.4E-07	9.1E-07	3.7E-16	1.0E-15
Africa	6.4E-08	1.1E-06	9.1E-17	6.0E-16
Asia	1.9E-07	2.0E-06	3.5E-16	3.6E-16
Europe	1.6E-07	3.1E-07	4.9E-16	1.4E-15
North America	1.7E-07	1.9E-07	1.3E-15	1.4E-16
Oceania	1.7E-08	2.7E-07	2.3E-17	1.1E-16
South America	3.0E-08	4.9E-07	9.8E-17	5.2E-15

5.5. References

Anderson HR, Atkinson RW, Peacock JL, Marston L, Konstantinou K (2004) Meta-analysis of time-series studies and panel studies of Particulate Matter (PM) and Ozone (O3). Report of a WHO task group. World Health Organization, London, United Kingdom.

Anenberg SC, Horowitz LW, Tong DQ, West JJ (2010) An estimate of the global burden of anthropogenic ozone and fine particulate matter on premature human mortality using atmospheric modeling. Environ Health Persp 118 (9):1189-1195.

Bell ML, Dominici F, Samet JM (2005) A meta-analysis of time-series studies of ozone and mortality with comparison to the national morbidity, mortality, and air pollution study. Epidemiology 16 (4):436-445.

Friedrich R, Kuhn A, Bessagnet B, Blesl M, Bruchof D, Cowie H, Fantke P, Gerharz L, Grellier J, Gusev A, Haverinen-Shaughnessy U, Hout D, Hurley F, Huynen M, Kampffmeyer T, Karabelas A, Karakitsios S, Knol A, Kober T, Kollanus V, Kontoroupis P, Kuder R, Kugler U, Loh M, Meleux F, Miller B, Müller W, Nikolaki S, Panasiuk D, Preiss P, Rintala T, Roos J, Roustan Y, Salomons E, Sánchez Jiménez A, Sarigiannis D, Schenk K, Shafrir A, Shatalov V, Solomou E, Theloke J, Thiruchittampalam B, Torras Ortiz S, Travnikov O, Tsyro S, Tuomisto J, Vinneau D, Wagner S, Yang A (2011) D 5.3.1/2 Methods and results of the HEIMTSA/INTARESE Common Case Study. The Institute of Occupational Medicine. Available at http://www.integrated-assessment.eu/sites/default/files/CCS_FINAL_REPORT_final.pdf.

Gronlund C, Humbert S, Shaked S, O'Neill M, Jolliet O (2015) Characterizing the burden of disease of particulate matter for life cycle impact assessment. Air Quality, Atmosphere & Health 8:29-46.

Jerrett M, Burnett RT, Pope CA, Ito K, Thurston G, Krewski D, Shi YL, Calle E, Thun M (2009) Long-Term Ozone Exposure and Mortality. New Engl J Med 360 (11):1085-1095.

Kier G, Kreft H, Lee TM, Jetz W, Ibisch PL, Nowicki C, Mutke J, Barthlott W. (2009). A Global assessment of endemism and species richness across island and mainland regions. PNAS 106 (23), 9322-9327.

Krol M, Houweling S, Bregman B, van den Broek M, Segers A, van Velthoven P, Peters W, Dentener F, Bergamaschi P (2005) The two-way nested global chemistry-transport zoom model TM5: algorithm and applications. Atmos Chem Phys 5:417-432.

Lamarque JF, Bond TC, Eyring V, Granier C, Heil A, Klimont Z, Lee D, Liousse C, Mieville A, Owen B, Schultz MG, Shindell D, Smith SJ, Stehfest E, Van Aardenne J, Cooper OR, Kainuma M, Mahowald N, McConnell JR, Naik V, Riahi K, van Vuuren DP (2010) Historical (1850-2000) gridded anthropogenic and biomass burning emissions of reactive gases and aerosols: methodology and application. Atmos Chem Phys 10 (15):7017-7039.

Murray CJL, Ezzati M, Flaxman A, Lim S, Lozano R, Michaud C, Naghavi M, Salomon J, Shibuya K, Vos T, Wikler D, Lopez A (2012) GBD 2010: design, definitions, and metrics. Lancet 380:2063-2066.

USEPA (1997) Exposure factors handbook. National Center for Environmental Assessment, office of research and development, Washington, DC

United Nations (2011) World Population Prospects: The 2010 Revision, CD-ROM Edition. - File 1: Total population (both sexes combined) by five-year age group, major area, region and country, 1950-2100 [thousands], variant "Estimates". Department of Economic and Social Affairs, Population Division, United Nations, New York, USA.

Van Dingenen R, Dentener FJ, Raes F, Krol MC, Emberson L, Cofala J (2009) The global impact of ozone on agricultural crop yields under current and future air quality legislation. Atmos Environ 43 (3):604-618.

Van Goethem T, Azevedo LB, Van Zelm R, Hayes RM, Ashmore MR, Huijbregts MAJ (2013a) Plant Species Sensitivity Distributions for ozone exposure. Environ Pollut 178:1-6.

Van Goethem T, Preiss P, Azevedo LB, Friedrich R, Huijbregts MAJ, Van Zelm R (2013b) European characterization factors for damage to natural vegetation by ozone in life cycle impact assessment. Atmos Environ 77:318-324.

Van Zelm R, Huijbregts MAJ, Den Hollander HA, Van Jaarsveld HA, Sauter FJ, Struijs J, Van Wijnen HJ, Van de Meent D (2008) European characterization factors for human health damage due to PM10 and ozone in life cycle impact assessment. Atmos Environ 42 (3):441-453.

Van Zelm R, Preiss P, Van Goethem T, Van Dingenen R, Huijbregts MAJ. 2016. Regionalized life cycle impact assessment of air pollution on the global scale: damage to human health and vegetation. Atmospheric Environment 134, 129-137.

WHO (2013). Health risks of air pollution in Europe-HRAPIE project recommendations for concentration-response functions for cost benefit analysis of particulate matter, ozone and nitrogen dioxide. World Health Organization, Geneva, Switzerland.

WHO (2015a) World Health Organization Statistical Information System. World Health Organization, accessible at http://www.who.int/healthinfo/global_burden_disease/estimates/en/index1.html
WHO (2015b) World health statistics 2015. World Health Organization, Geneva, Switzerland.

6. Particulate Matter Formation

*Rosalie van Zelm[*1], Philipp Preiss[2,3], Rita Van Dingenen[4], Mark Huijbregts[1].*

[a] Department of Environmental Sciences, Institute for Water and Wetland Research, Radboud University Nijmegen, P.O. Box 9010, 6500 GL, Nijmegen, The Netherlands
[b] European Institute for Energy Research | EIFER, Emmy-Noether-Str. 11, 76131 Karlsruhe, Germany
[c] Institute for Energy Economics and the Rational Use of Energy, Department for Technology Assessment and Environment, Universität Stuttgart, Germany
[d] European Commission, Joint Research Centre (JRC), Environment and Sustainability (IES), Air and Climate Unit, Via Enrico Fermi, 2749, 21027 Ispra (VA), Italy
* r.vanzelm@science.ru.nl

The impact assessment method for assessing damage to human health due to primary PM2.5 and PM2.5 precursor emissions is described based on Van Zelm et al. (2016).

6.1. Areas of protection and environmental mechanisms covered

The cause and effect pathway (Figure 6.1) of particulate matter formation starts with an emission of NO_x, NH_3, SO_2, or primary $PM_{2.5}$ to the atmosphere, followed by atmospheric fate and chemistry in the air; NO_x, NH_3, and SO_2 are transformed in air to secondary aerosols. Subsequently, $PM_{2.5}$ can be inhaled by the human population, leading to an increased number of mortality cases and final damage to human health.

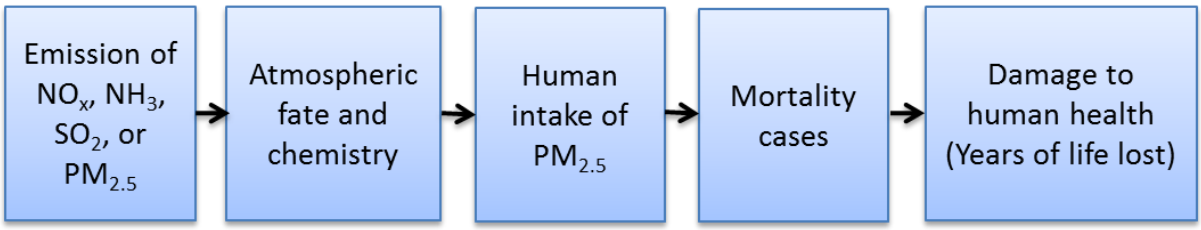

Figure 6.1: Cause and effect pathway from primary PM2.5 and PM2.5 precursor emissions to damage to human health

The intake of a pollutant by the population is described by intake fractions (iF, in kg intake per kg emission) that quantify the relationship between an emission and intake (Van Zelm et al. 2008). Here, a global chemical transport model was applied to determine human intake fractions for 56 emission and receptor regions. Second, region-specific mortality rates, background concentrations and years of life lost were used to determine human health effect factors. Here, we included cardiopulmonary and lung cancer mortality due to particulate matter with a diameter of less than 2.5µm ($PM_{2.5}$) for two reasons: first, these contribute by far the most to overall disability adjusted life years (DALYs) for these two pollutants (as e.g. shown in previous research (Van Zelm et al. 2008)), and second, for these the most up-to-date and least uncertain data related to relative risks and years of life lost are available (see e.g. Anenberg et al. 2010, Friedrich et al. 2011, Murray et al. 2012, WHO 2013).

6.2. Calculation of the characterization factors at endpoint level

The endpoint characterization factors (CFs) for human health damage due to particulate matter formation caused by emitted substance x in world region i (CFx,i in DALY·kg-1) are defined as the yearly change in Disability Adjusted Life Years (DALY) of all inhabitants (dDALY in yr·yr-1) due to a change in emission of substance x in source region i (dMx,i in kg·yr-1). This CF for human health damage is composed of a dimensionless intake fraction (iFx, i→j), providing the population intake of PM2.5 in receptor region j (in kg/yr) following an emission change of substance x in source region i (in kg/yr), an effect factor (EF_e), describing the cases of health effect *e* per kg of inhaled $PM_{2.5}$, and a damage factor (DF_e), which describes the years of life lost per case of health effect *e*. In equation this reads:

$$CF_{x,i} = \sum_j \left(\left(iF_{x,i\to j} \right) \cdot \sum_e \left(EF_{e,j} \cdot DF_{e,j} \right) \right) \qquad \textbf{Equation 6.1.}$$

6.2.1. From emission to human intake

The intake fraction is determined as the change in exposure to $PM_{2.5}$ in region j ($dEXP_j$), due to a change in emission of substance x ($dM_{x,i}$). dEXP was retrieved by multiplying the change in concentration of $PM_{2.5}$ in each receptor region (dC_j) with the population (N_j) in the receptor region j and the average breathing rate per person (BR) of 4745 $m^3 \cdot yr^{-1}$ (13 $m^3 \cdot d^{-1}$ as recommended by USEPA (1997):

$$iF_{x,i\to j} = \frac{dEXP_j}{dM_{x,i}} = \frac{dC_j \cdot N_j \cdot BR}{dM_{x,i}} \qquad \textbf{Equation 6.2.}$$

Population numbers (year 2005) were taken from the United Nations (2011). Since all data for the effect factor are based on the population ≥ 30 years of age, the population number was adjusted for the population share ≥ 30 years of age in 2005 (United Nations 2011) assuming no effects for younger people.

The emission–concentration sensitivities matrices for emitted precursors and relevant end pollutants (or pollutant metrics) from the global source-receptor model TM5-FASST (FAst Scenario Screening Tool for Global Air Quality and Instantaneous Radiative Forcing), based on perturbation runs with TM5 (Van Dingenen et al. 2009; Krol et al. 2005) were used to derive the change in ambient concentration of a pollutant after the emission of a precursor. TM5 is a global chemical transport model hosted by the European Commission Joint Research Center (JRC). TM5-FASST takes into account spatial features at the emission site as well as dispersion characteristics for the whole world. In this model, the world is divided into 56 emission source regions. The regions correspond to countries or a group of countries (see Table 6.1). The TM5 model output consists of the change in concentration for each region, derived from gridded 1°×1° concentration results, following a change in emission. This change is determined by lowering the year 2000 emissions (Lamarque et al. 2010) by 20% for each of the 56 source regions sequentially. The emission-normalized differences in pollutant concentration between the unperturbed and perturbed case, aggregated over each receptor region, are stored as the emission – concentration matrix elements. This procedure was performed for each (precursor) substance. i.e. NH_3, NO_x, SO_2, and primary $PM_{2.5}$.

6.2.2 From human intake to human health damage

The human effect factor (dINC/dEXP) for health effect e caused by $PM_{2.5}$ in receptor region j, representing the change in disease incidence due to a change in exposure concentration in ambient

air, was determined by dividing the concentration-response function (CRF in $m^3 \cdot yr^{-1} \cdot kg^{-1}$) by the breathing rate BR ($m^3 \cdot yr^{-1}$) (Gronlund et al. 2015) (equation 6.3).

$$EF_{e,j} = \frac{dINC_j}{dEXP_j} = \frac{CRF_{e.j}}{BR}$$ **Equation 6.3**

Region-specific CRFs were calculated as follows (equation 6.4):

$$CRF_{e,j} = \frac{(RR_e - 1) \cdot MR_{e,j}}{(RR_e - 1) \cdot C_j + 1}$$ **Equation 6.4**

where RR_e is the relative risk to obtain health effect e due to exposure to $PM_{2.5}$ (per $\mu g \cdot m^{-3}$), $MR_{e,j}$ is the mortality rate for health effect e in region j (deaths/person/yr), and C_j is the yearly average background concentration of $PM_{2.5}$ in a region ($\mu g \cdot m^{-3}$).

We followed recommendations for RRs by Anenberg et al. (2010) and Friedrich et al. (2011), who focus on the world and Europe respectively, based on North American cohort studies. RRs for cardiopulmonary (1.013 per $\mu g \cdot m^{-3}$), and lung cancer (1.014 per $\mu g \cdot m^{-3}$) mortality from Krewski et al. (2009) were used. This study is the latest reanalysis of the American Cancer Society (ACS) $PM_{2.5}$ studies (see e.g. Pope et al. 2002) and has by far the largest population of the available PM2.5 cohort studies, and this latest update involves better exposure data, longer follow-up (i.e. more deaths) and more comprehensive statistical analyses.

Mortality rates per health effect (year 2005) were taken from the World Health Organization (WHO 2015a), and simulated background concentrations per region for the year 2000 were taken from the TM5-CTM reference run with the Lamarque et al. (2010) year 2000reference emission scenario.

The Damage factor $D_{e,j}$ is defined as the Disability Adjusted Life Years (DALY) associated to the health effect e per incidence case, which were estimated per receiving region j from the world health organization (WHO) world health estimates, year 2012 (WHO 2015b):

$$DF_{e,j} = \frac{dDALY_{e,j}}{dINC_{e,j}}$$ **Equation 6.5**

For the DALY no discounting was included and uniform age weights were applied.

6.3. Uncertainties

The CFs were derived from emission-concentration sensitivities (dC/dM) obtained from a 20% emission perturbation. For a limited number of representative source regions the dC/dM coefficients were calculated for large perturbations of inorganic pollutants (-80%, +100%) and compared to the extrapolated 20% perturbation (Van Zelm et al. 2016). Relatively small maximum absolute deviations were seen, up to 5%.

TM5 includes the various emission stack heights. However, it does not differentiate between them to derive the CFs. Stack-height specific intake fractions can differ 2 orders of magnitude, as shown by Humbert et al. (2011).

The native TM5 resolution of 1x1 degree at the receptor level does not reflect possible sub-grid gradients in PM and ozone that are expected when large population gradients occur within the grid (like isolated urban areas), leading to a possible underestimation of exposure. Van Zelm et al. (2016) compared area-weighted and population-weighted concentration and found that, aggregated at the level of the receptor regions used in this study, the largest deviations in exposure concentrations were found for Australia, Philippines, and Japan with population-weighted concentrations 12-19% higher

compared to area-weighted concentrations. For all other regions, the deviation (over- or underestimation) between area and population-weighted PM2.5 was less than 10%.

In this research, only effects of lung cancer and cardiopulmonary mortality were included, neglecting morbidity due to, e.g. COPD and chronic bronchitis. The choice was made to include mortality with the largest share to human health damage caused by PM2.5, and of which the most certain epidemiological data are available. Due to this, total human health damage is slightly underestimated. Van Zelm et al. (2008) showed, for example, that 99% of DALYs due to PM10 is caused by chronic mortality.

6.4. Value choices

6.4.1. Time horizon

For human health damage due to fine dust, time horizon is not of importance as only short-living substances are involved.

6.4.2. Level of robustness

As outlined by De Schryver et al. (2011), evidence for effects from primary PM is available (Pope et al. 2009) and therefore considered robust. There is evidence concerning human health risks at ambient concentrations of secondary PM from SO_2, NO_x and NH_3 is available. However, the level of effect is still under debate (De Schryver et al. 2011). Reiss et al. (2007) do show that there are more studies indicating health effects from secondary PM from SO_2 than from NO_x or NH_3.

6.5. Resulting characterization factors

Figure 6.2 shows the region-specific characterization factors for human health for $PM_{2.5}$ precursor emissions. Lowest factors were obtained for emissions of NO_x on the Southern Hemisphere, while largest factors were obtained for primary $PM_{2.5}$ emissions in Central Asia. The emission weighted average for the world for $PM_{2.5}$ is $6.29 \cdot 10^{-4}$ DALY·kg^{-1} (with a minimum of $9.40 \cdot 10^{-6}$ and a maximum of $4.02 \cdot 10^{-3}$ DALY·kg^{-1}). The emission weighted average for the world for NH_3 is $1.61 \cdot 10^{-4}$ DALY·kg^{-1} ($3.30 \cdot 10^{-6}$ to $1.34 \cdot 10^{-3}$ DALY·kg^{-1}), for NO_x $7.62 \cdot 10^{-5}$ DALY·kg^{-1} ($4.43 \cdot 10^{-7}$ to $3.65 \cdot 10^{-4}$ DALY·kg^{-1}), and for SO_2 $1.83 \cdot 10^{-4}$ DALY·kg^{-1} ($1.40 \cdot 10^{-5}$ to $9.45 \cdot 10^{-4}$ DALY·kg^{-1}). For each country the region-specific factor was allocated to it. Table 6.1 provides the characterization factors for each country. Table 6.2 provides the continent-specific emission weighted average characterization factors.

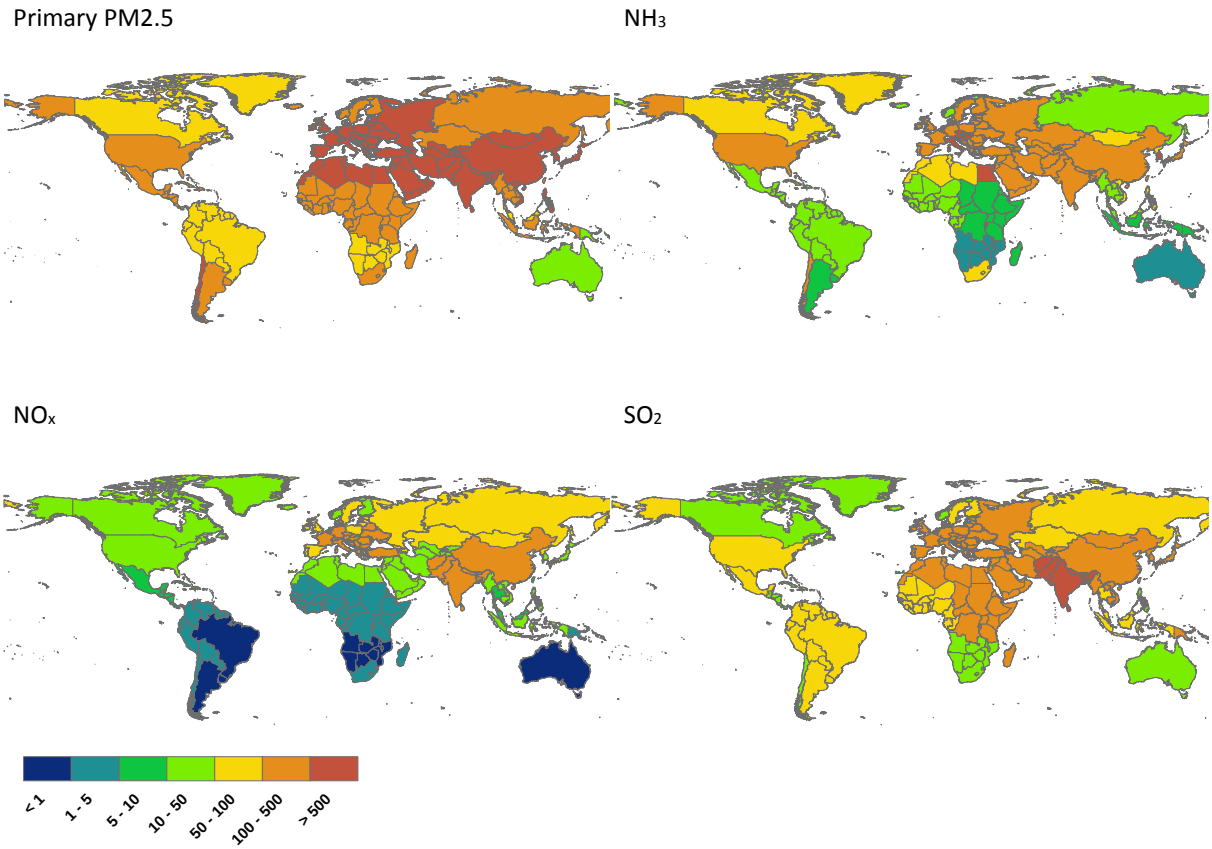

Figure 6.2.: Characterization factors for human health damage caused by fine dust formation (10^{-6} DALY·kg^{-1}) (Taken from Van Zelm et al. 2016).

Table 6.1: Country-specific endpoint characterization factors for human health damage due to particulate matter formation (DALY·kg^{-1}) (Van Zelm et al. 2016).

Country	TM5 region	$PM_{2.5}$	NH_3	NO_x	SO_2
Afghanistan	RSAS	4.02E-03	1.13E-04	3.65E-04	9.45E-04
Albania	RCEU	9.59E-04	3.56E-04	1.65E-04	1.49E-04
Algeria	NOA	6.63E-04	6.39E-05	3.39E-05	1.58E-04
Angola	SAF	6.26E-05	4.08E-06	8.46E-07	4.59E-05
Argentina	ARG	2.13E-04	6.44E-06	4.43E-07	6.34E-05
Armenia	RUS	1.35E-03	3.81E-04	7.99E-05	1.35E-04
Aruba	RCAM	1.58E-04	2.46E-05	6.85E-06	4.72E-05
Australia	AUS	2.03E-05	3.30E-06	6.90E-07	1.40E-05
Austria	AUT	1.20E-03	7.36E-04	1.59E-04	1.72E-04
Azerbaijan	RUS	1.35E-03	3.81E-04	7.99E-05	1.35E-04
Bahamas	RCAM	1.58E-04	2.46E-05	6.85E-06	4.72E-05
Bahrain	GOLF	5.63E-04	1.44E-04	4.71E-05	2.09E-04
Bangladesh	RSAS	4.02E-03	1.13E-04	3.65E-04	9.45E-04
Barbados	RCAM	1.58E-04	2.46E-05	6.85E-06	4.72E-05
Belgium	BLX	1.29E-03	7.00E-04	1.35E-04	1.36E-04
Belize	RCAM	1.58E-04	2.46E-05	6.85E-06	4.72E-05
Benin	WAF	2.44E-04	1.48E-05	3.25E-06	9.31E-05
Bhutan	RSAS	4.02E-03	1.13E-04	3.65E-04	9.45E-04
Bolivia	RSAM	7.11E-05	1.98E-05	3.52E-06	6.52E-05
Bosnia and Herzegovina	RCEU	9.59E-04	3.56E-04	1.65E-04	1.49E-04
Botswana	SAF	6.26E-05	4.08E-06	8.46E-07	4.59E-05
Brazil	BRA	9.65E-05	1.09E-05	4.87E-07	6.36E-05
Brunei	MYS	9.67E-05	1.53E-05	6.55E-06	6.03E-05
Bulgaria	BGR	1.22E-03	3.53E-04	1.99E-04	1.66E-04
Burkina Faso	WAF	2.44E-04	1.48E-05	3.25E-06	9.31E-05
Burundi	EAF	1.41E-04	7.92E-06	2.67E-06	1.08E-04
Byelarus	UKR	1.34E-03	3.91E-04	1.80E-04	1.71E-04
Cambodia	RSEA	3.37E-04	2.34E-05	2.92E-05	1.65E-04

Cameroon	WAF	2.44E-04	1.48E-05	3.25E-06	9.31E-05
Canada	CAN	8.78E-05	8.12E-05	1.93E-05	2.86E-05
Cape Verde	WAF	2.44E-04	1.48E-05	3.25E-06	9.31E-05
Central African Republic	EAF	1.41E-04	7.92E-06	2.67E-06	1.08E-04
Chad	EAF	1.41E-04	7.92E-06	2.67E-06	1.08E-04
Chile	CHL	6.57E-04	2.43E-04	3.16E-06	3.21E-05
China	CHN	1.70E-03	4.17E-04	2.26E-04	2.68E-04
China	CHN	1.70E-03	4.17E-04	2.26E-04	2.68E-04
China, Hong Kong Special Administrative Region	CHN	1.70E-03	4.17E-04	2.26E-04	2.68E-04
Colombia	RSAM	7.11E-05	1.98E-05	3.52E-06	6.52E-05
Comoros	EAF	1.41E-04	7.92E-06	2.67E-06	1.08E-04
Congo	WAF	2.44E-04	1.48E-05	3.25E-06	9.31E-05
Costa Rica	RCAM	1.58E-04	2.46E-05	6.85E-06	4.72E-05
Croatia	RCEU	9.59E-04	3.56E-04	1.65E-04	1.49E-04
Cuba	RCAM	1.58E-04	2.46E-05	6.85E-06	4.72E-05
Cyprus	GRC	6.54E-04	1.57E-04	1.42E-04	1.74E-04
Czech Republic	RCZ	1.19E-03	6.52E-04	1.41E-04	1.36E-04
Democratic Republic of the Congo	EAF	1.41E-04	7.92E-06	2.67E-06	1.08E-04
Denmark	SWE	3.10E-04	1.11E-04	9.09E-05	7.05E-05
Djibouti	EAF	1.41E-04	7.92E-06	2.67E-06	1.08E-04
Dominican Republic	RCAM	1.58E-04	2.46E-05	6.85E-06	4.72E-05
Ecuador	RSAM	7.11E-05	1.98E-05	3.52E-06	6.52E-05
Egypt	EGY	2.18E-03	7.59E-04	2.13E-05	1.69E-04
El Salvador	RCAM	1.58E-04	2.46E-05	6.85E-06	4.72E-05
Equatorial Guinea	WAF	2.44E-04	1.48E-05	3.25E-06	9.31E-05
Eritrea	EAF	1.41E-04	7.92E-06	2.67E-06	1.08E-04
Estonia	POL	8.12E-04	4.76E-04	8.95E-05	1.28E-04
Ethiopia	EAF	1.41E-04	7.92E-06	2.67E-06	1.08E-04
Fiji	PAC	1.14E-05	6.92E-06	2.52E-06	1.02E-04
Finland	FIN	2.38E-04	2.43E-04	4.21E-05	5.34E-05
France	FRA	8.16E-04	1.87E-04	1.04E-04	1.47E-04
French Guiana	RSAM	7.11E-05	1.98E-05	3.52E-06	6.52E-05
Gabon	WAF	2.44E-04	1.48E-05	3.25E-06	9.31E-05
Gambia, The	WAF	2.44E-04	1.48E-05	3.25E-06	9.31E-05
Georgia	RUS	1.35E-03	3.81E-04	7.99E-05	1.35E-04
Germany	RFA	1.33E-03	4.82E-04	1.70E-04	1.66E-04
Ghana	WAF	2.44E-04	1.48E-05	3.25E-06	9.31E-05
Greece	GRC	6.54E-04	1.57E-04	1.42E-04	1.74E-04
Greenland	CAN	8.78E-05	8.12E-05	1.93E-05	2.86E-05
Grenada	RCAM	1.58E-04	2.46E-05	6.85E-06	4.72E-05
Guadeloupe	RCAM	1.58E-04	2.46E-05	6.85E-06	4.72E-05
Guatemala	RCAM	1.58E-04	2.46E-05	6.85E-06	4.72E-05
Guinea	WAF	2.44E-04	1.48E-05	3.25E-06	9.31E-05
Guinea-Bissau	WAF	2.44E-04	1.48E-05	3.25E-06	9.31E-05
Guyana	RSAM	7.11E-05	1.98E-05	3.52E-06	6.52E-05
Haiti	RCAM	1.58E-04	2.46E-05	6.85E-06	4.72E-05
Honduras	RCAM	1.58E-04	2.46E-05	6.85E-06	4.72E-05
Hungary	HUN	1.44E-03	5.71E-04	1.33E-04	1.56E-04
Iceland	NOR	2.46E-04	3.87E-05	4.78E-05	4.80E-05
India	NDE	3.36E-03	1.73E-04	3.16E-04	8.32E-04
Indonesia	IDN	1.88E-04	6.41E-06	1.11E-05	9.44E-05
Iran	GOLF	5.63E-04	1.44E-04	4.71E-05	2.09E-04
Iraq	GOLF	5.63E-04	1.44E-04	4.71E-05	2.09E-04
Ireland	GBR	1.27E-03	3.99E-04	6.31E-05	1.07E-04
Israel	MEME	7.55E-04	1.96E-04	3.21E-05	1.78E-04
Italy	ITA	1.61E-03	5.18E-04	1.80E-04	2.17E-04
Ivory Coast	WAF	2.44E-04	1.48E-05	3.25E-06	9.31E-05
Jamaica	RCAM	1.58E-04	2.46E-05	6.85E-06	4.72E-05
Japan	JPN	1.47E-03	4.12E-04	3.68E-05	1.49E-04
Jordan	MEME	7.55E-04	1.96E-04	3.21E-05	1.78E-04
Kazakhstan	KAZ	2.41E-04	1.21E-04	6.35E-05	5.69E-05
Kenya	EAF	1.41E-04	7.92E-06	2.67E-06	1.08E-04
Kuwait	GOLF	5.63E-04	1.44E-04	4.71E-05	2.09E-04

Kyrgyzstan	RIS	1.08E-03	3.55E-04	4.20E-05	1.48E-04
Laos	RSEA	3.37E-04	2.34E-05	2.92E-05	1.65E-04
Latvia	POL	8.12E-04	4.76E-04	8.95E-05	1.28E-04
Lebanon	MEME	7.55E-04	1.96E-04	3.21E-05	1.78E-04
Lesotho	RSA	3.15E-04	5.53E-05	2.11E-06	4.64E-05
Liberia	WAF	2.44E-04	1.48E-05	3.25E-06	9.31E-05
Libya	NOA	6.63E-04	6.39E-05	3.39E-05	1.58E-04
Lithuania	POL	8.12E-04	4.76E-04	8.95E-05	1.28E-04
Luxembourg	BLX	1.29E-03	7.00E-04	1.35E-04	1.36E-04
Macedonia	RCEU	9.59E-04	3.56E-04	1.65E-04	1.49E-04
Madagascar	EAF	1.41E-04	7.92E-06	2.67E-06	1.08E-04
Malawi	SAF	6.26E-05	4.08E-06	8.46E-07	4.59E-05
Malaysia	MYS	9.67E-05	1.53E-05	6.55E-06	6.03E-05
Maldives	NDE	3.36E-03	1.73E-04	3.16E-04	8.32E-04
Mali	WAF	2.44E-04	1.48E-05	3.25E-06	9.31E-05
Malta	ITA	1.61E-03	5.18E-04	1.80E-04	2.17E-04
Martinique	RCAM	1.58E-04	2.46E-05	6.85E-06	4.72E-05
Mauritania	WAF	2.44E-04	1.48E-05	3.25E-06	9.31E-05
Mauritius	EAF	1.41E-04	7.92E-06	2.67E-06	1.08E-04
Mexico	MEX	2.20E-04	4.23E-05	9.39E-06	5.26E-05
Moldova	UKR	1.34E-03	3.91E-04	1.80E-04	1.71E-04
Mongolia	MON	7.18E-04	8.23E-05	8.82E-05	1.54E-04
Morocco	NOA	6.63E-04	6.39E-05	3.39E-05	1.58E-04
Mozambique	SAF	6.26E-05	4.08E-06	8.46E-07	4.59E-05
Myanmar (Burma)	RSEA	3.37E-04	2.34E-05	2.92E-05	1.65E-04
Namibia	SAF	6.26E-05	4.08E-06	8.46E-07	4.59E-05
Nepal	RSAS	4.02E-03	1.13E-04	3.65E-04	9.45E-04
Netherlands	BLX	1.29E-03	7.00E-04	1.35E-04	1.36E-04
Netherlands Antilles	RCAM	1.58E-04	2.46E-05	6.85E-06	4.72E-05
New Zealand	NZL	9.40E-06	5.83E-05	9.45E-07	1.08E-04
Nicaragua	RCAM	1.58E-04	2.46E-05	6.85E-06	4.72E-05
Niger	WAF	2.44E-04	1.48E-05	3.25E-06	9.31E-05
Nigeria	WAF	2.44E-04	1.48E-05	3.25E-06	9.31E-05
North Korea	MON	7.18E-04	8.23E-05	8.82E-05	1.54E-04
Norway	NOR	2.46E-04	3.87E-05	4.78E-05	4.80E-05
Oman	GOLF	5.63E-04	1.44E-04	4.71E-05	2.09E-04
Pakistan	RSAS	4.02E-03	1.13E-04	3.65E-04	9.45E-04
Panama	RCAM	1.58E-04	2.46E-05	6.85E-06	4.72E-05
Papua New Guinea	PAC	1.14E-05	6.92E-06	2.52E-06	1.02E-04
Paraguay	RSAM	7.11E-05	1.98E-05	3.52E-06	6.52E-05
Peru	RSAM	7.11E-05	1.98E-05	3.52E-06	6.52E-05
Philippines	PHL	5.61E-04	7.99E-05	1.74E-05	4.53E-05
Poland	POL	8.12E-04	4.76E-04	8.95E-05	1.28E-04
Portugal	ESP	6.10E-04	1.06E-04	6.34E-05	1.52E-04
Puerto Rico	RCAM	1.58E-04	2.46E-05	6.85E-06	4.72E-05
Qatar	GOLF	5.63E-04	1.44E-04	4.71E-05	2.09E-04
Reunion	EAF	1.41E-04	7.92E-06	2.67E-06	1.08E-04
Romania	ROM	1.71E-03	4.46E-04	2.73E-04	2.10E-04
Russia	RUE	1.27E-04	4.15E-05	6.15E-05	5.31E-05
Russia Europe	RUS	1.35E-03	3.81E-04	7.99E-05	1.35E-04
Rwanda	EAF	1.41E-04	7.92E-06	2.67E-06	1.08E-04
Saint Lucia	RCAM	1.58E-04	2.46E-05	6.85E-06	4.72E-05
Saint Vincent and the Grenadines	RCAM	1.58E-04	2.46E-05	6.85E-06	4.72E-05
Samoa	PAC	1.14E-05	6.92E-06	2.52E-06	1.02E-04
Saudi Arabia	GOLF	5.63E-04	1.44E-04	4.71E-05	2.09E-04
Senegal	WAF	2.44E-04	1.48E-05	3.25E-06	9.31E-05
Serbia	RCEU	9.59E-04	3.56E-04	1.65E-04	1.49E-04
Sierra Leone	WAF	2.44E-04	1.48E-05	3.25E-06	9.31E-05
Singapore	MYS	9.67E-05	1.53E-05	6.55E-06	6.03E-05
Slovakia	RCZ	1.19E-03	6.52E-04	1.41E-04	1.36E-04
Slovenia	AUT	1.20E-03	7.36E-04	1.59E-04	1.72E-04
Solomon Islands	PAC	1.14E-05	6.92E-06	2.52E-06	1.02E-04
Somalia	EAF	1.41E-04	7.92E-06	2.67E-06	1.08E-04

South Africa	RSA	3.15E-04	5.53E-05	2.11E-06	4.64E-05
South Korea	COR	6.96E-04	5.17E-04	2.71E-05	1.45E-04
Spain	ESP	6.10E-04	1.06E-04	6.34E-05	1.52E-04
Sri Lanka	NDE	3.36E-03	1.73E-04	3.16E-04	8.32E-04
Sudan	EAF	1.41E-04	7.92E-06	2.67E-06	1.08E-04
Suriname	RSAM	7.11E-05	1.98E-05	3.52E-06	6.52E-05
Swaziland	RSA	3.15E-04	5.53E-05	2.11E-06	4.64E-05
Sweden	SWE	3.10E-04	1.11E-04	9.09E-05	7.05E-05
Switzerland	CHE	1.48E-03	1.34E-03	2.26E-04	2.07E-04
Syria	MEME	7.55E-04	1.96E-04	3.21E-05	1.78E-04
Sao Tomo and Principe	WAF	2.44E-04	1.48E-05	3.25E-06	9.31E-05
Taiwan	TWN	3.51E-04	2.25E-04	9.01E-06	1.31E-04
Tajikistan	RIS	1.08E-03	3.55E-04	4.20E-05	1.48E-04
Tanzania, United Republic of	EAF	1.41E-04	7.92E-06	2.67E-06	1.08E-04
Thailand	THA	2.31E-04	1.11E-05	9.91E-06	8.83E-05
Togo	WAF	2.44E-04	1.48E-05	3.25E-06	9.31E-05
Tonga	PAC	1.14E-05	6.92E-06	2.52E-06	1.02E-04
Trinidad and Tobago	RCAM	1.58E-04	2.46E-05	6.85E-06	4.72E-05
Tunisia	NOA	6.63E-04	6.39E-05	3.39E-05	1.58E-04
Turkey	TUR	8.14E-04	2.28E-04	1.45E-04	1.99E-04
Turkmenistan	RIS	1.08E-03	3.55E-04	4.20E-05	1.48E-04
Uganda	EAF	1.41E-04	7.92E-06	2.67E-06	1.08E-04
Ukraine	UKR	1.34E-03	3.91E-04	1.80E-04	1.71E-04
United Arab Emirates	GOLF	5.63E-04	1.44E-04	4.71E-05	2.09E-04
United Kingdom	GBR	1.27E-03	3.99E-04	6.31E-05	1.07E-04
United States	USA	4.55E-04	1.53E-04	1.41E-05	5.29E-05
Uruguay	ARG	2.13E-04	6.44E-06	4.43E-07	6.34E-05
Uzbekistan	RIS	1.08E-03	3.55E-04	4.20E-05	1.48E-04
Vanuatu	PAC	1.14E-05	6.92E-06	2.52E-06	1.02E-04
Venezuela	RSAM	7.11E-05	1.98E-05	3.52E-06	6.52E-05
Vietnam	VNM	9.61E-04	7.21E-05	1.43E-05	2.11E-04
Western Sahara	NOA	6.63E-04	6.39E-05	3.39E-05	1.58E-04
Yemen	GOLF	5.63E-04	1.44E-04	4.71E-05	2.09E-04
Zambia	SAF	6.26E-05	4.08E-06	8.46E-07	4.59E-05
Zimbabwe	SAF	6.26E-05	4.08E-06	8.46E-07	4.59E-05

Table 6.2: Continent-specific endpoint characterization factors for human health damage due to particulate matter formation (DALY·kg^{-1}) (Van Zelm et al. 2016).

Continent	$PM_{2.5}$	NH_3	NO_x	SO_2
World Weighted Average	***6.29E-04***	***1.61E-04***	***7.62E-05***	***1.83E-04***
Africa	1.62E-04	1.75E-05	4.86E-06	8.66E-05
Asia	1.35E-03	1.92E-04	1.60E-04	3.24E-04
Europe	5.95E-04	2.71E-04	1.05E-04	1.37E-04
North America	3.09E-04	1.38E-04	1.47E-05	4.95E-05
Oceania	1.94E-05	1.05E-05	7.72E-07	1.86E-05
South America	1.24E-04	2.12E-05	3.59E-06	5.35E-05

6.6. References

Anenberg SC, Horowitz LW, Tong DQ, West JJ (2010) An estimate of the global burden of anthropogenic ozone and fine particulate matter on premature human mortality using atmospheric modeling. Environ Health Persp 118 (9):1189-1195.

De Schryver, A. M., Van Zelm, R., Humbert, S., Pfister, S., McKone, T. E. and Huijbregts, M. A. J. (2011). Value Choices in Life Cycle Impact Assessment of Stressors Causing Human Health Damage. Journal of Industrial Ecology 15(5): 796-815.

Friedrich R, Kuhn A, Bessagnet B, Blesl M, Bruchof D, Cowie H, Fantke P, Gerharz L, Grellier J, Gusev A, Haverinen-Shaughnessy U, Hout D, Hurley F, Huynen M, Kampffmeyer T, Karabelas A, Karakitsios S, Knol A, Kober T, Kollanus V, Kontoroupis P, Kuder R, Kugler U, Loh M, Meleux F, Miller B, Müller W, Nikolaki S, Panasiuk D, Preiss P, Rintala T, Roos J, Roustan Y, Salomons E, Sánchez Jiménez A, Sarigiannis D, Schenk K, Shafrir A, Shatalov V, Solomou E, Theloke J, Thiruchittampalam B, Torras Ortiz S, Travnikov O, Tsyro S, Tuomisto J, Vinneau D, Wagner S, Yang A (2011) D 5.3.1/2 Methods and results of the HEIMTSA/INTARESE Common Case Study. The Institute of Occupational Medicine. Available at http://www.integrated-assessment.eu/sites/default/files/CCS_FINAL_REPORT_final.pdf.

Gronlund C, Humbert S, Shaked S, O'Neill M, Jolliet O (2015) Characterizing the burden of disease of particulate matter for life cycle impact assessment. Air Quality, Atmosphere & Health 8:29-46.

Humbert S, Marshall JD, Shaked S, Spadaro J, Nishioka Y, Preiss P, McKone TE, Horvath A, Jolliet O (2011) Intake fraction for particulate matter: recommendations for life cycle assessment. Environ Sci Technol 45 (11):4808-4816.

Krol M, Houweling S, Bregman B, van den Broek M, Segers A, van Velthoven P, Peters W, Dentener F, Bergamaschi P (2005) The two-way nested global chemistry-transport zoom model TM5: algorithm and applications. Atmos Chem Phys 5:417-432.

Lamarque JF, Bond TC, Eyring V, Granier C, Heil A, Klimont Z, Lee D, Liousse C, Mieville A, Owen B, Schultz MG, Shindell D, Smith SJ, Stehfest E, Van Aardenne J, Cooper OR, Kainuma M, Mahowald N, McConnell JR, Naik V, Riahi K, van Vuuren DP (2010) Historical (1850-2000) gridded anthropogenic and biomass burning emissions of reactive gases and aerosols: methodology and application. Atmos Chem Phys 10 (15):7017-7039.

Murray CJL, Ezzati M, Flaxman A, Lim S, Lozano R, Michaud C, Naghavi M, Salomon J, Shibuya K, Vos T, Wikler D, Lopez A (2012) GBD 2010: design, definitions, and metrics. Lancet 380:2063-2066.

Pope CA, Burnett RT, Thun MJ, Calle EE, Krewski D, Ito K, Thurston GD (2002) Lung cancer, Cardiopulmonary mortality, and long-term exposure to fine particulate air pollution. J Am Med Assoc 287 (9):1132-1141.

Reiss, R., E.L. Anderson, C.E. Cross, G. Hidy, D. Hoel, R. McClellan and S. Moolgavkar. 2007. Evidence of Health Impacts of Sulfate-and Nitrate-Containing Particles in Ambient Air. Inhalation Toxicology: International Forum for Respiratory Research 19(5): 419 - 449.

USEPA (1997) Exposure factors handbook. National Center for Environmental Assessment, office of research and development, Washington, DC

United Nations (2011) World Population Prospects: The 2010 Revision, CD-ROM Edition. - File 1: Total population (both sexes combined) by five-year age group, major area, region and country, 1950-2100 [thousands], variant "Estimates". Department of Economic and Social Affairs, Population Division, United Nations, New York, USA.

Van Dingenen R, Dentener FJ, Raes F, Krol MC, Emberson L, Cofala J (2009) The global impact of ozone on agricultural crop yields under current and future air quality legislation. Atmos Environ 43 (3):604-618.

Van Zelm R, Huijbregts MAJ, Den Hollander HA, Van Jaarsveld HA, Sauter FJ, Struijs J, Van Wijnen HJ, Van de Meent D (2008) European characterization factors for human health damage due to PM10 and ozone in life cycle impact assessment. Atmos Environ 42 (3):441-453.

Van Zelm R, Preiss P, Van Goethem T, Van Dingenen R, Huijbregts MAJ. (2016). Regionalized life cycle impact assessment of air pollution on the global scale: damage to human health and vegetation. Atmospheric Environment 134: 129-137.

WHO (2013). Health risks of air pollution in Europe-HRAPIE project recommendations for concentration-response functions for cost benefit analysis of particulate matter, ozone and nitrogen dioxide. World Health Organization, Geneva, Switzerland.

7. Terrestrial acidification

Ligia B. Azevedo[1,2], Pierre-Olivier Roy[3], Francesca Verones[1], Rosalie van Zelm[1], Mark A. J. Huijbregts[1]*

[1] Radboud University Nijmegen, Department of Environmental Sciences, Toernooiveld 1, 6500 GL Nijmegen, the Netherlands
[2]International Institute for Applied Systems Analysis, Ecosystem Services and Management Program, Schlossplatz 1, A-2361 Laxenburg, Austria
[3] CIRAIG, Chemical Engineering Department, École Polytechnique de Montréal, P.O. Box 6079, Montréal, Québec, Canada, H3C 3A7

* azevedol@iiasa.ac.at

Based on: Roy *et al.* (2012b), Roy *et al*. (2012a), Roy et al. (2014), and Azevedo *et al.* (2013c).

7.1. Environmental mechanism and impact categories covered

Terrestrial acidification is characterized by changes in soil chemical properties following the deposition of nutrients (namely, nitrogen and sulfur) in acidifying forms. Here, we assess the environmental impact of nitrogen oxides (NO_x), ammonia (NH_3), and sulfur dioxide (SO_2), see Figure 7.1. In addition to soil pH decline (i.e. increase in hydrogen cation concentration in the soil), the increase in acidifying nutrients concentration in the soil leads to the decline in base saturation and the increase of aluminum dissolved in soil solution. This decline in soil fertility may lead to an increase in plant tissue yellowing and seed germination failure and a decrease in new root production, thereby reducing photosynthetic rates and plant biomass and, in extreme cases, plant diversity (Falkengren-Grerup 1986; Roem et al. 2000; Zvereva et al. 2008).

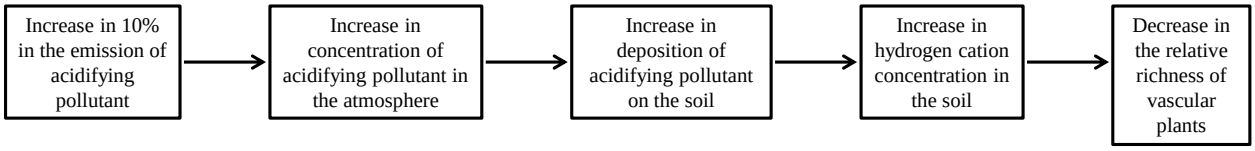

Figure 7.1: Illustration of the impact pathway represented in equation 7.1.

The impact category covered by this environmental mechanism is the ecosystem quality. The acidification impact is related to the atmospheric transport of the emitted pollutants and their subsequent impact on soil pH (described by the fate factor), and to the sensitivity of the ecosystem to soil acidity (described by the effect factor). Here, the effect factor is based on the decline in richness of vascular plants. Note that in cases where acidifying pollutants are released to human-built structures (e.g. buildings and statues) there can be aesthetic impacts of terrestrial acidification. However, this mechanism is not taken into account in this framework.

The coverage of the endpoint characterization factor (CF) is global. Of the three effect factor models (i.e. linear, marginal, and average approaches), we chose the marginal one. The spatial resolution of the CF is 2.0° x 2.5°.

7.2. Calculation of the characterization factors at endpoint level

An endpoint characterization factor (yr·kg^{-1}, see Figure 7.1 for illustration of impact pathway) for emitting cell *i* for pollutant *p* (i.e. NO_x, NH_3, or SO_2) is described as

$$CF_{end,i,p} = \sum_{j,p} AF_{i \to j,p} \cdot SF_{j,p} \cdot EF_j \qquad \textbf{Equation 7.1}$$

where $AF_{i \to j,p}$ is the atmospheric fate factor of pollutant *p* from cell *i* to receiving cell *j*, $SF_{j,p}$ is the soil sensitivity factor, and EF_j is the effect factor in cell *j*.

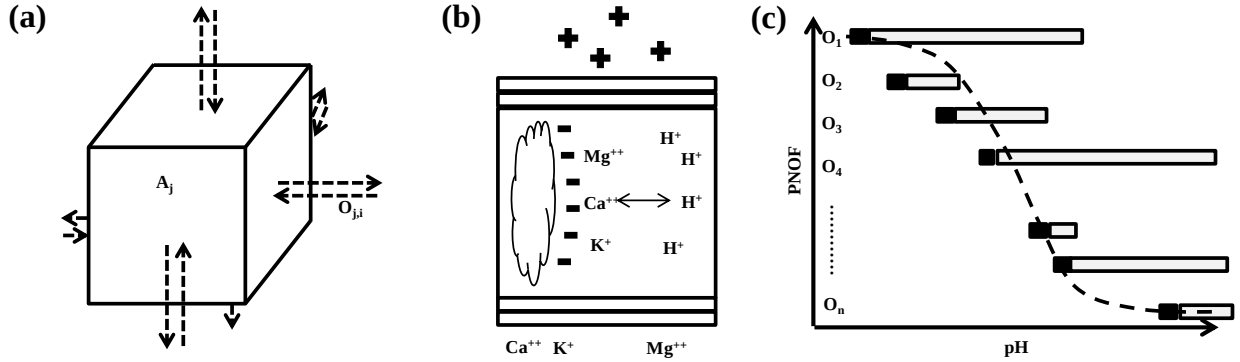

Figure 7.2: Illustration of the (a) atmospheric transport, adapted from Roy *et al.* (2012b), (b) soil chemistry, and (c) the logistic regression originating effect model, adapted from Azevedo (2014). In (a), the flows through six possible transport pathways into and out of a receiving cell *j* (one pathway represented by $O_{j,i}$) and the accumulated mass of pollutant in *j* (A_j) in the atmospheric compartment are used in a mass balance of the source-receptor matrix (SRM). In (b), the flow of positively charged ions (+) originating from the dissociation of sulfuric acid and nitrous acid and from the reduction of ammonia prompts base cations to be leached out of the soil profile (here, the middle soil layer is amplified for illustration purposes). In (c), the potentially not occurring fraction (PNOF) of species as a logistic function of pH is determined with the lowest tolerable pH condition (illustrated as the black tip of the grey bar pH range) for individual species (O_i) recorded in observational field studies.

Atmospheric fate factor

The atmospheric fate factor (keq·ha^{-1}·kg^{-1}) is described as

$$AF_{i \to j,p} = \frac{dDEP_{j,p}}{dEM_{i,p}} \qquad \textbf{Equation 7.2}$$

where dDEP (keq·yr^{-1}·ha^{-1}) is the relative increase in deposition of pollutant *p* onto the terrestrial compartment *j* following an increase in the emission of *p* from emitting cell *i*, dEM (kg^{-1}·yr), by 10% relative to a reference year (2005) (Roy et al. 2012b).

The unit of the AF is given as kiloequivalent of electric charge (keq) per mass of emitted pollutant per given area (therefore, keq·ha^{-1}·kg^{-1}). (The unit of electric charge can be converted from a mass of deposited pollutant by taking the atomic weight and the valence of the atom deposited. For example, 1 mol of sulfur is equal to 64.13eq, because the atomic weight of S is 32.07 and its valence is 2).

The AF is derived based on the tropospheric chemistry model GEOS-Chem, which is described in detail by Roy *et al.* (2012b). It considers various photochemical reactions and the flow of particles that is influenced by temperature and atmospheric pressure differences, described in detail by Evans & Jingqiu (2009). The model includes transboundary transport across countries and across continents. The inventory of emissions in 2005 includes anthropogenic sources, e.g. fossil fuel, and biofuel, and biomass burning as well as non-anthropogenic sources (for example, sulfur in volcanic ash and nitrous oxides from soils and produced with lightning). Note that the AF describes a relative change in emissions from a given year. Thereby the inclusion of natural sources of acidifying pollutants should not influence the estimation of the environmental impact as long as the reference year is

representative of other years. The year of 2005 is chosen since it is a representative average of the period from 1961 to 1990 according to the National Climatic Data Center of the National Oceanic and Atmospheric Administration (NOAA 2005).

The atmospheric fate model consists of a three-dimensional transport from emitting cell *i* to receptor cell *j* and is calculated with a source-receptor matrix (SRM) of the transport of pollutant *p* within the atmospheric compartment in six possible directions, i.e. latitude-wise (north and south), longitude-wise (east and west), and altitude-wise (upwards and downwards), with a total of 615,888 compartments included in the SRM. The SRM is the pollutant mass balance of the mass of emitting cells. The mass across all receiving compartments are equal for a given year (in this case, 2005), see illustration in Figure 7.2a.

Soil sensitivity factor

The soil sensitivity factor (mol $H \cdot L^{-1} \cdot ha \cdot keq^{-1} \cdot yr$) is described as

$$SF_{j,p} = \frac{dC_j}{dDEP_{j,p}} \qquad \textbf{Equation 7.3}$$

where dC_j is the increase in hydrogen ion concentration (mol $H \cdot L^{-1}$) following an increase in dDEP for pollutant *p* in receiving cell *j*. The SF is derived based on the steady-state soil chemistry model PROFILE and is described in detail by Roy *et al.* (2012a). It includes various parameters of soil chemistry (e.g. dissolved organic carbon, soil bulk density and texture) and climate (i.e. precipitation and temperature). The model consists of a two-dimensional mass balance of positive ions originating from atmospheric deposition. The exchanges of cations include soil chemical reactions with hydrogen ions, aluminum, base cations (i.e. potassium, calcium, and magnesium), and silicon.

The mass balance was performed in each receiving cell *j*, with resolution 2.0° x 2.5° worldwide (and, thus, 99, 515 cells in total), across five 20cm soil layers of the first meter of soil, see illustration in Figure 7.2b. The total impact on the five soil layers of cell *j* was weighted based on the fraction of roots in each layer. The distribution of roots in the first meter of soil was reported by Jackson *et al.* (1996) for each of the fourteen terrestrial world biomes. We used the biome map provided by Olson *et al.* (2001b) to define the biome occupying each cell *j*. The parameters for the SF calculation are reported by Roy *et al.* (2012a).

Effect factor

The effect factor (mol $H^{-1} \cdot L$) is described as

$$EF_j = \frac{SD_j \cdot A_j \cdot MEF_j}{S_{global}} \qquad \textbf{Equation 7.4}$$

where MEF is the marginal effect factor (mol $H^{-1} \cdot L$), A_j refers to the terrestrial ecosystem area in grid cell j (ha), SD_j is the species density of vascular plant species in grid cell j (species/ha) and S_{global} is the total number of plant species taken from Kier et al. (2009), which is 315'903.
Note that the unit of the EF is the loss of vascular plant species in *j* relative to the total number of vascular plant species worldwide per mol/l increase of H+ concentration. In this work, we equate potentially not occurring fraction with PDF. This relationship allows for an estimation of the actual potential global species loss.

The vascular plant richness density SD is derived from the vascular plant richness (see illustration in Figure 7.3), derived by Kier et al. (2009), and the area of each region.

The marginal effect factor is described as

$$MEF_j = \frac{dPDF_j}{dC_j} = \frac{dPNOF_j}{dC_j}$$ **Equation 7.5**

where dPDF and dPNOF are the marginal increase in the potentially disappearing and not occurring fractions (both dimensionless) following a marginal increase in dC_j in *j*. Since the EF describes a marginal increase to PDF, the reference state for the changes in PDF is the PNOF prior to the increase in hydrogen ion concentrations in the soil.

The EF model is based on a probabilistic model of the PNOF as a logistic function of hydrogen ions (Equation 7.6) and it is described in detail by Roy et al. (2014). The logistic function describes the cumulative fraction of absent species with increasing hydrogen ion concentration, Figure 7.2c. The inputs for the derivation of the EF are the two parameters of the logistic function, i.e. the ion concentration at which PNOF is 0.5 (α) and the slope of the function (β), and the hydrogen ion concentration resulting from the acidic deposition in receiving cell *j*, C_j.

$$PNOF_j = \frac{1}{1+e^{-\frac{log_{10}C_j-\alpha_j}{\beta_j}}}$$ **Equation 7.6**

The two logistic function parameters (α and β) were derived at resolution of biome and the hydrogen ion variable, C_j, was derived for each 2.0° x 2.5° receiving cell *j* with the PROFILE model. The biome-specific α and β parameters were derived from logistic regressions which used the maximum tolerance hydrogen ion concentration of each species subsisting in that biome, see illustration in Figure 2c. Species-specific data on minimum tolerable pH per biome (from which maximum hydrogen ion concentration in cell *j*, C_j, were derived) were reported by Azevedo *et al.* (2013c). The biome-specific parameters for the EF calculation are shown in Figure 7.5. Grid-specific CFs are shown in Figure 7.4. Country, continent, and world CFs were derived based on a weighted average of emissions of SO_2, NH_3 and NO_x repsectively (IIASA 2015), within the aggregation unit level (see Excel file and Tables 7.1 and 7.2). Global average values are 5.2E-14 PDF·kg^{-1}·yr, 2.5E-14 PDF·kg^{-1}·yr and 1.0E-14 PDF·kg^{-1}·yr for SO_2, NO_x and NH_3, respectively.

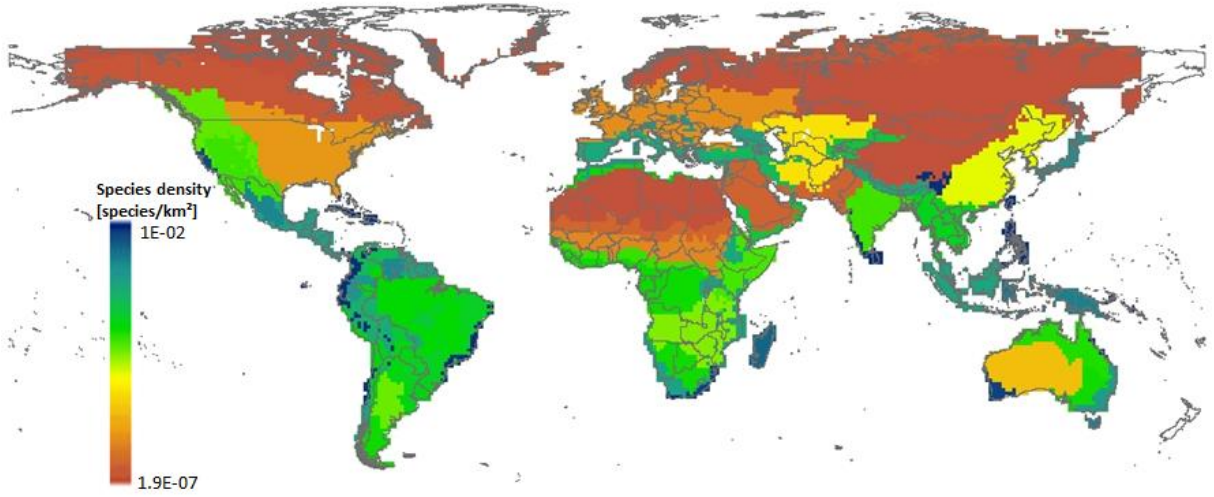

Figure 7.3: Relative species richness of vascular plants (species·km^{-2}) derived from Kier et al. (2009).

Contribution to variance

Soil chemical processes, estimated by Roy *et al.* (2012a), contribute the most to the variance in the NO_x, NH_3, and SO_2 emission impacts (Roy et al. 2014). The uncertainty in the parameters on which the EF is based contributes the most to the variability in the effect factors.

7.3. Uncertainties

The fate factors for terrestrial acidification are based on an atmospheric deposition and on a chemical soil property model, whereby an increase in 10% of atmospheric emission of an acidifying pollutant prompts an increase in atmospheric deposition and, consequently, an increase in hydrogen ions in soil solution (Roy et al. 2012a; Roy et al. 2012b). The atmospheric model includes transport across continents and it depends upon the dispersion of the pollutant, weather characteristics, and the locations of emission and deposition. The soil sensitivity model is influenced by the capacity of the receiving soil to buffer acidifying pollutants and fraction land in the receiving grid.

The atmospheric fate and soil sensitivity models can also be verified by comparison with an existing endpoint characterization model covering Europe (van Zelm et al. 2007). This comparison is skewed since the transportation pathways of N and S forms are not exactly the same for both fate models. van Zelm *et al.* (2007) do not account for transboundary atmospheric transport beyond Europe as the model is limited to that continent. Additionally, the stressor indicating acidification is not the same (base saturation in the model by van Zelm *et al.* (2007) and pH in the model of (Roy et al. 2014).

There is sufficient evidence of the detrimental impact of terrestrial acidification on the performance of plants (Falkengren-Grerup 1986; Zvereva et al. 2008). Thus, the level of robustness of impact is fairly high. However, the effect model used to derive endpoint effect factors employs observational field data whereby the absence of species resulting from decreasing pH cannot be confirmed and, thus, proof of causality is problematic. Proof for causality would only be possible if the underlying data would consist of controlled (not observational) experiments in which the high level of a stressor (in this case, high hydrogen ion levels) would be the primary cause for a species becoming absent.

The failure to record the species at a specific pH may be human related, such as (1) an incomplete survey of the existing species or of the existing pH, but also due to natural causes, such as that (2) the species may be rare and difficult to spot, (3) extreme pH may be tolerated by the species but may not be found under natural conditions, or (4) the pH is tolerated by the species but the species absence is due to another stressor. For a detailed description of the downsides of observational field data for conducting impact assessments, see Azevedo (2014). Because of the possible underestimation of the minimum pH tolerated by the species, the level of evidence of the effect model specifically employed here is considered low.

The variance across CFs is most explained by either the atmospheric fate factor or the soil sensitivity factor, depending on the pollutant considered (Roy et al. 2014).

7.4. Value Choices

The time horizon for this impact category is not relevant since it is assumed that the impact occurs at the moment of emission of NO_x, NH_3, or SO_2 to the atmospheric compartment. No choices are thus modelled for fate and effect factor for terrestrial acidification. In total, the CFs are considered as low level of robustness, mainly because one out of the two pollutants of acidification (i.e. N) is also included in terrestrial eutrophication. It is therefore not possible to disentangle if detrimental effects are due to the increase in hydrogen ions (acidification) or increase in primary productivity (eutrophication).

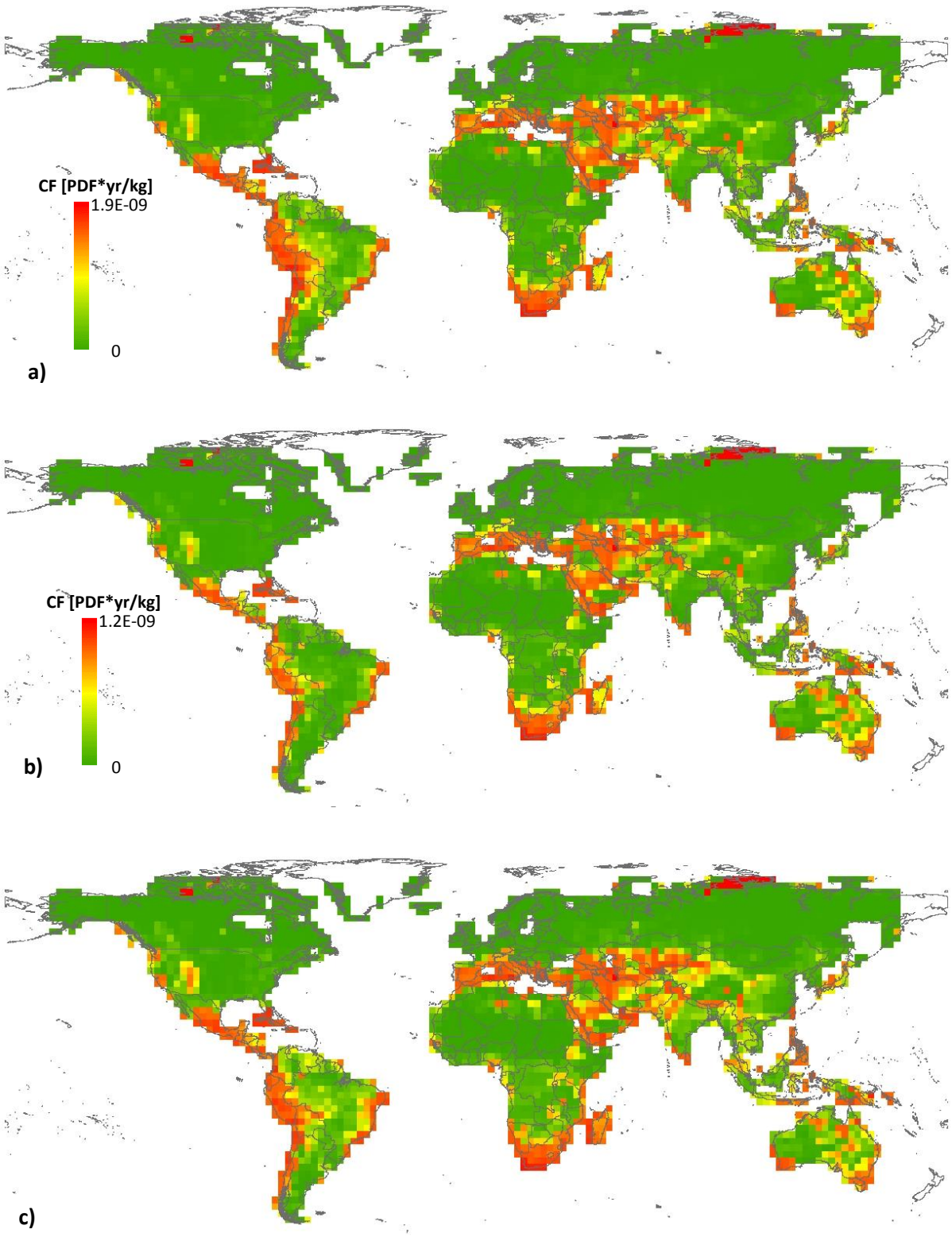

Figure 7.4: Endpoint characterization factors (PD·Fkg^{-1}·yr) based on vascular plant richness for (a) SO_2, (b) NO_x, and (c) NH_3.

Table 7.1: Global endpoint characterization factors (PD·Fkg^{-1}·yr) on a country level, based on vascular plant richness for SO_2, NO_x, and NH_3. The relevant compartment here is the soil.

COUNTRY	CF SO_2 [PDF·yr/kg]	CF NOx [PDF·yr/kg]	CF NH_3 [PDF·yr/kg]
Afghanistan	8.49E-16	8.23E-16	1.70E-15
Albania	1.32E-13	5.95E-14	4.41E-14
Algeria	3.99E-15	4.10E-15	5.97E-15
Angola	5.88E-16	8.55E-16	5.54E-16
Antarctica			
Argentina	1.27E-15	1.11E-15	3.15E-16
Armenia	0.00E+00	0.00E+00	0.00E+00
Australia	2.12E-14	6.09E-14	8.41E-15
Austria	3.86E-15	1.28E-15	2.78E-15
Azerbaijan	2.58E-14	3.38E-14	4.72E-14
Azores	0.00E+00	0.00E+00	0.00E+00
Bahamas	0.00E+00	0.00E+00	0.00E+00
Bangladesh	5.39E-17	2.46E-17	5.32E-17
Belarus	0.00E+00	4.14E-18	6.90E-18
Belgium	4.21E-17	3.19E-17	3.51E-17
Belize	0.00E+00	0.00E+00	0.00E+00
Benin	0.00E+00	0.00E+00	0.00E+00
Bhutan	0.00E+00	0.00E+00	0.00E+00
Bolivia	3.99E-12	1.07E-13	1.54E-13
Bosnia and Herzegovina	7.73E-15	1.36E-14	3.93E-14
Botswana	4.57E-16	1.33E-15	1.02E-15
Brazil	5.54E-15	3.30E-15	7.27E-15
Brunei Darussalam	0.00E+00	0.00E+00	0.00E+00
Bulgaria	4.55E-15	9.14E-15	1.08E-14
Burkina Faso	0.00E+00	0.00E+00	6.09E-18
Burundi	0.00E+00	0.00E+00	0.00E+00
Cambodia	4.81E-16	1.63E-16	5.62E-16
Cameroon	2.98E-16	1.69E-16	1.69E-16
Canada	2.28E-16	3.77E-17	3.02E-17
Canarias	0.00E+00	0.00E+00	0.00E+00
Cayman Islands	0.00E+00	0.00E+00	0.00E+00
Central African Republic	0.00E+00	1.26E-16	9.69E-17
Chad	0.00E+00	0.00E+00	6.34E-18
Chile	6.66E-14	9.48E-15	2.94E-14
China	5.04E-16	6.75E-16	2.32E-15
Colombia	5.48E-12	3.25E-13	9.80E-14
Comoros	0.00E+00	0.00E+00	0.00E+00
Congo	1.91E-15	1.41E-15	1.54E-15
Congo DRC	2.86E-16	2.25E-16	3.03E-16
Cook Islands			
Costa Rica	5.42E-15	1.54E-14	2.79E-14
Côte d'Ivoire	1.54E-16	8.63E-17	5.52E-17
Croatia	7.80E-17	9.06E-17	1.41E-16
Cuba	4.14E-12	3.58E-13	2.76E-13
Cyprus	0.00E+00	0.00E+00	0.00E+00
Czech Republic	4.24E-17	1.73E-17	1.52E-17
Denmark	0.00E+00	9.77E-18	0.00E+00
Djibouti	0.00E+00	0.00E+00	0.00E+00
Dominican Republic	0.00E+00	0.00E+00	0.00E+00
Ecuador	6.66E-14	1.76E-14	7.44E-14
Egypt	1.05E-15	2.24E-15	4.07E-16
El Salvador	0.00E+00	0.00E+00	0.00E+00
Equatorial Guinea	0.00E+00	0.00E+00	0.00E+00
Eritrea	6.69E-16	4.44E-16	2.51E-16
Estonia	0.00E+00	0.00E+00	0.00E+00
Ethiopia	1.19E-15	9.14E-16	8.58E-16
Falkland Islands	0.00E+00	0.00E+00	0.00E+00
Fiji			
Finland	0.00E+00	0.00E+00	0.00E+00

France	5.04E-16	4.19E-16	4.92E-16
French Guiana	0.00E+00	0.00E+00	0.00E+00
French Polynesia			
French Southern Territories			
Gabon	5.53E-16	5.37E-16	6.25E-16
Gambia	2.17E-13	5.08E-14	3.16E-14
Georgia	2.49E-15	4.00E-15	3.03E-15
Germany	3.57E-16	2.30E-16	5.39E-16
Ghana	4.52E-17	3.71E-17	3.13E-17
Greece	2.25E-14	4.10E-14	5.58E-14
Greenland			
Guadeloupe	0.00E+00	0.00E+00	0.00E+00
Guatemala	2.75E-14	6.05E-15	1.15E-14
Guinea	1.64E-16	6.79E-17	6.04E-17
Guinea-Bissau	0.00E+00	0.00E+00	0.00E+00
Guyana	0.00E+00	9.02E-17	4.28E-16
Haiti	3.20E-13	1.54E-13	1.14E-13
Honduras	5.45E-15	4.16E-16	2.78E-16
Hungary	3.98E-17	2.17E-17	1.62E-17
Iceland	0.00E+00	0.00E+00	0.00E+00
India	6.55E-16	3.21E-16	1.50E-15
Indonesia	8.72E-16	1.03E-15	9.22E-16
Iran	9.17E-14	2.16E-14	1.92E-14
Iraq	3.47E-15	3.89E-15	7.63E-15
Ireland	0.00E+00	0.00E+00	1.08E-17
Israel	0.00E+00	0.00E+00	0.00E+00
Italy	1.44E-12	6.15E-13	1.31E-13
Jamaica	0.00E+00	0.00E+00	0.00E+00
Japan	1.74E-15	4.31E-16	1.41E-15
Jersey	0.00E+00	0.00E+00	0.00E+00
Jordan	1.76E-15	1.17E-15	1.21E-15
Kazakhstan	1.06E-14	8.85E-15	3.31E-14
Kenya	1.26E-16	1.56E-16	4.03E-16
Kiribati			
Kuwait	0.00E+00	0.00E+00	0.00E+00
Kyrgyzstan	1.41E-15	1.62E-15	1.98E-15
Laos	8.80E-16	3.83E-16	1.15E-15
Latvia	0.00E+00	0.00E+00	0.00E+00
Lebanon	0.00E+00	0.00E+00	0.00E+00
Lesotho	1.47E-15	4.18E-15	9.32E-15
Liberia	0.00E+00	0.00E+00	0.00E+00
Libya	1.21E-15	4.53E-16	2.59E-16
Lithuania	0.00E+00	0.00E+00	0.00E+00
Luxembourg	0.00E+00	0.00E+00	0.00E+00
Madagascar	1.00E-15	1.34E-15	4.75E-15
Madeira	0.00E+00	0.00E+00	0.00E+00
Malawi	0.00E+00	0.00E+00	0.00E+00
Malaysia	9.96E-16	6.05E-16	1.15E-15
Maldives			
Mali	0.00E+00	0.00E+00	4.86E-18
Mauritania	0.00E+00	0.00E+00	1.90E-17
Mauritius	0.00E+00	0.00E+00	0.00E+00
Mexico	7.02E-13	4.89E-14	7.46E-14
Moldova	1.57E-16	7.78E-17	1.18E-16
Mongolia	9.35E-18	1.24E-17	2.07E-17
Montenegro	0.00E+00	0.00E+00	0.00E+00
Morocco	1.58E-15	1.32E-15	3.83E-15
Mozambique	9.06E-15	1.68E-14	3.37E-14
Myanmar	2.16E-16	1.79E-16	4.40E-16
Namibia	6.72E-15	6.41E-15	1.28E-15
Nepal	1.99E-16	1.42E-16	8.49E-16
Netherlands	0.00E+00	2.12E-17	3.04E-17
New Caledonia			

New Zealand	0.00E+00	0.00E+00	0.00E+00
Nicaragua	2.07E-15	5.54E-16	3.92E-15
Niger	0.00E+00	0.00E+00	0.00E+00
Nigeria	9.61E-16	8.41E-16	2.26E-16
North Korea	1.44E-16	9.88E-17	2.13E-16
Norway	0.00E+00	0.00E+00	0.00E+00
Oman	1.01E-12	3.10E-13	1.57E-13
Pakistan	9.27E-15	5.46E-15	1.08E-14
Palestinian Territory	0.00E+00	0.00E+00	0.00E+00
Panama	0.00E+00	0.00E+00	0.00E+00
Papua New Guinea	0.00E+00	0.00E+00	0.00E+00
Paraguay	3.88E-16	4.66E-17	1.98E-16
Peru	8.40E-13	2.49E-14	1.31E-13
Philippines	9.77E-15	1.34E-14	2.85E-14
Poland	2.98E-17	1.45E-17	2.09E-17
Portugal	0.00E+00	0.00E+00	0.00E+00
Puerto Rico	0.00E+00	0.00E+00	0.00E+00
Qatar	0.00E+00	0.00E+00	0.00E+00
Réunion	0.00E+00	0.00E+00	0.00E+00
Romania	7.65E-17	3.40E-17	2.14E-17
Russian Federation	1.02E-15	1.32E-15	1.53E-15
Rwanda	4.20E-16	4.55E-16	2.50E-15
Saint Vincent and the Grenadines	0.00E+00	0.00E+00	0.00E+00
Samoa			
Saudi Arabia	1.02E-13	8.11E-14	1.03E-13
Senegal	3.53E-16	8.60E-16	1.43E-15
Serbia	5.69E-17	7.11E-17	1.41E-16
Sierra Leone	2.15E-16	1.04E-16	1.47E-16
Slovakia	3.67E-17	2.29E-17	3.58E-17
Slovenia	0.00E+00	0.00E+00	0.00E+00
Solomon Islands			
Somalia	0.00E+00	4.42E-17	3.66E-17
South Africa	3.39E-14	8.56E-14	2.40E-13
South Georgia			
South Korea	1.57E-17	7.37E-18	4.55E-17
South Sudan	0.00E+00	3.12E-17	3.67E-17
Spain	2.27E-15	5.23E-15	1.08E-14
Sri Lanka	1.40E-14	6.31E-15	2.70E-14
Sudan	5.80E-17	3.77E-17	7.07E-18
Suriname	7.18E-16	5.19E-16	1.26E-15
Swaziland	0.00E+00	0.00E+00	0.00E+00
Sweden	4.11E-17	1.34E-17	2.32E-17
Switzerland	0.00E+00	0.00E+00	0.00E+00
Syria	1.31E-13	9.38E-14	3.15E-14
Tajikistan	0.00E+00	0.00E+00	0.00E+00
Tanzania	6.03E-16	4.24E-16	4.65E-16
Thailand	2.95E-16	1.40E-16	4.63E-16
The Former Yugoslav Republic of Macedonia	0.00E+00	0.00E+00	0.00E+00
Timor-Leste	0.00E+00	0.00E+00	0.00E+00
Togo	0.00E+00	6.03E-17	4.91E-17
Trinidad and Tobago	0.00E+00	0.00E+00	0.00E+00
Tunisia	2.70E-15	1.67E-15	6.98E-16
Turkey	1.52E-14	1.68E-14	1.39E-14
Turkmenistan	1.45E-13	5.79E-14	6.18E-14
Turks and Caicos Islands			
Uganda	1.69E-15	1.27E-15	1.25E-15
Ukraine	3.78E-17	6.49E-17	3.74E-17
United Arab Emirates	4.53E-12	2.62E-12	4.83E-13
United Kingdom	6.89E-18	7.54E-18	1.59E-17
United States	6.76E-16	3.22E-16	3.03E-16
Uruguay	8.95E-16	1.96E-16	3.05E-16

US Virgin Islands	0.00E+00	0.00E+00	0.00E+00
Uzbekistan	3.06E-13	1.33E-13	1.70E-13
Vanuatu			
Venezuela	3.26E-15	7.76E-16	4.68E-16
Vietnam	2.08E-16	9.75E-17	2.50E-16
Yemen	5.56E-15	7.64E-14	6.88E-14
Zambia	1.41E-16	7.49E-16	6.26E-16
Zimbabwe	1.18E-16	3.62E-16	6.02E-16

Table 7.2: Global endpoint characterization factors (PD·Fkg^{-1}·yr) on a continental level, based on vascular plant richness for SO_2, NO_x, and NH_3.

CONTINENT	CF SO_2 [PDF·yr/kg]	CF NOx [PDF·yr/kg]	CF NH_3 [PDF·yr/kg]
Asia	2.14E-14	2.69E-14	5.73E-15
North America	1.08E-13	7.75E-15	1.82E-14
Europe	2.40E-14	3.89E-14	1.21E-14
Africa	1.65E-14	2.02E-14	1.22E-14
South America	7.07E-13	2.83E-14	2.23E-14
Australia	4.60E-14	9.58E-14	1.32E-14

7.5. References

Azevedo, L. B. (2014). Development and application of stressor – response relationships of nutrients. Chapter 8. Ph.D. Dissertation, Radboud University Nijmegen, The Netherlands. http://repository.ubn.ru.nl.

Azevedo, L. B., van Zelm, R., Hendriks, A. J., Bobbink, R. and Huijbregts, M. A. J. (2013). "Global assessment of the effects of terrestrial acidification on plant species richness." Environmental Pollution **174**(0): 10-15.

Evans, M. and Jingqiu, M. (2009). "Updated Chemical Reactions Now Used in GEOS-Chem v8-02-01 Through GEOS-Chem v8-02-03." Oxidants and Chemistry Working Group Retrieved June 6th, 2011, from http://acmg.seas.harvard.edu/geos/wiki_docs/chemistry/chemistry_updates_v5.pdf.

Falkengren-Grerup, U. (1986). "Soil acidification and vegetation changes in deciduous forest in Southern-Sweeden." Oecologia **70**(3): 339-347.

IIASA. (2015). "ECLIPSE V5 global emission fields." Retrieved 10 September, 2016, from http://www.iiasa.ac.at/web/home/research/researchPrograms/air/ECLIPSEv5.html.

Jackson, R. B., Canadell, J., Ehleringer, J. R., Mooney, H. A., Sala, O. E. and Schulze, E. D. (1996). "A global analysis of root distributions for terrestrial biomes." Oecologia **108**(3): 389-411.

Kier, G., Kreft, H., Lee, T. M., Jetz, W., Ibisch, P. L., Nowicki, C., Mutke, J. and Barthlott, W. (2009). "A global assessment of endemism and species richness across island and mainland regions." PNAS **106**(23): 9322-9327.

NOAA. (2005). "National Climatic Data Center State of the Climate: Global Analysis for Annual 2005." Retrieved June 5th, 2011, from www.ncdc.noaa.gov/sotc/global/2005/13.

Olson, D. M., Dinerstein, E., Wikramanayake, E. D., Burgess, N. D., Powell, G. V. N., Underwood, E. C., D'Amico, J. A., Itoua, I., Strand, H. E., Morrison, J. C., Loucks, C. J., Allnutt, T. F., Ricketts, T. H., Kura, Y., Lamoreux, J. F., Wettengel, W. W., Hedao, P. and Kassem, K. R. (2001). "Terrestrial ecoregions of the worlds: A new map of life on Earth." Bioscience **51**(11): 933-938.

Roem, W. J. and Berendse, F. (2000). "Soil acidity and nutrient supply ratio as possible factors determining changes in plant species diversity in grassland and heathland communities." Biological Conservation **92**(2): 151-161.

Roy, P.-O., Azevedo, L. B., Margni, M., van Zelm, R., Deschênes, L. and Huijbregts, M. A. J. (2014). "Characterization factors for terrestrial acidification at the global scale: A systematic analysis of spatial variability and uncertainty." Science of The Total Environment **500–501**: 270-276.

Roy, P.-O., Deschênes, L. and Margni, M. (2012a). "Life cycle impact assessment of terrestrial acidification: Modeling spatially explicit soil sensitivity at the global scale." Environmental Science & Technology **45**(15): 8270–8278.

Roy, P.-O., Deschênes, L., Margni, M. and Huijbregts, M. A. J. (2012b). "Spatially-differentiated atmospheric source-receptor relationships for nitrogen oxides, sulfur oxides and ammonia emissions at the global scale for life cycle impact assessment." Atmospheric Environment **62**: 74-81.

van Zelm, R., Huijbregts, M. A. J., Van Jaarsveld, H. A., Reinds, G. J., De Zwart, D., Struijs, J. and Van de Meent, D. (2007). "Time horizon dependent characterization factors for acidification in life-cycle assessment based on forest plant species occurrence in Europe." Environmental Science & Technology **41**(3): 922-927.

Zvereva, E. L., Toivonen, E. and Kozlov, M. V. (2008). "Changes in species richness of vascular plants under the impact of air pollution: a global perspective." Global Ecology and Biogeography **17**(3): 305-319.

7.6. Appendix

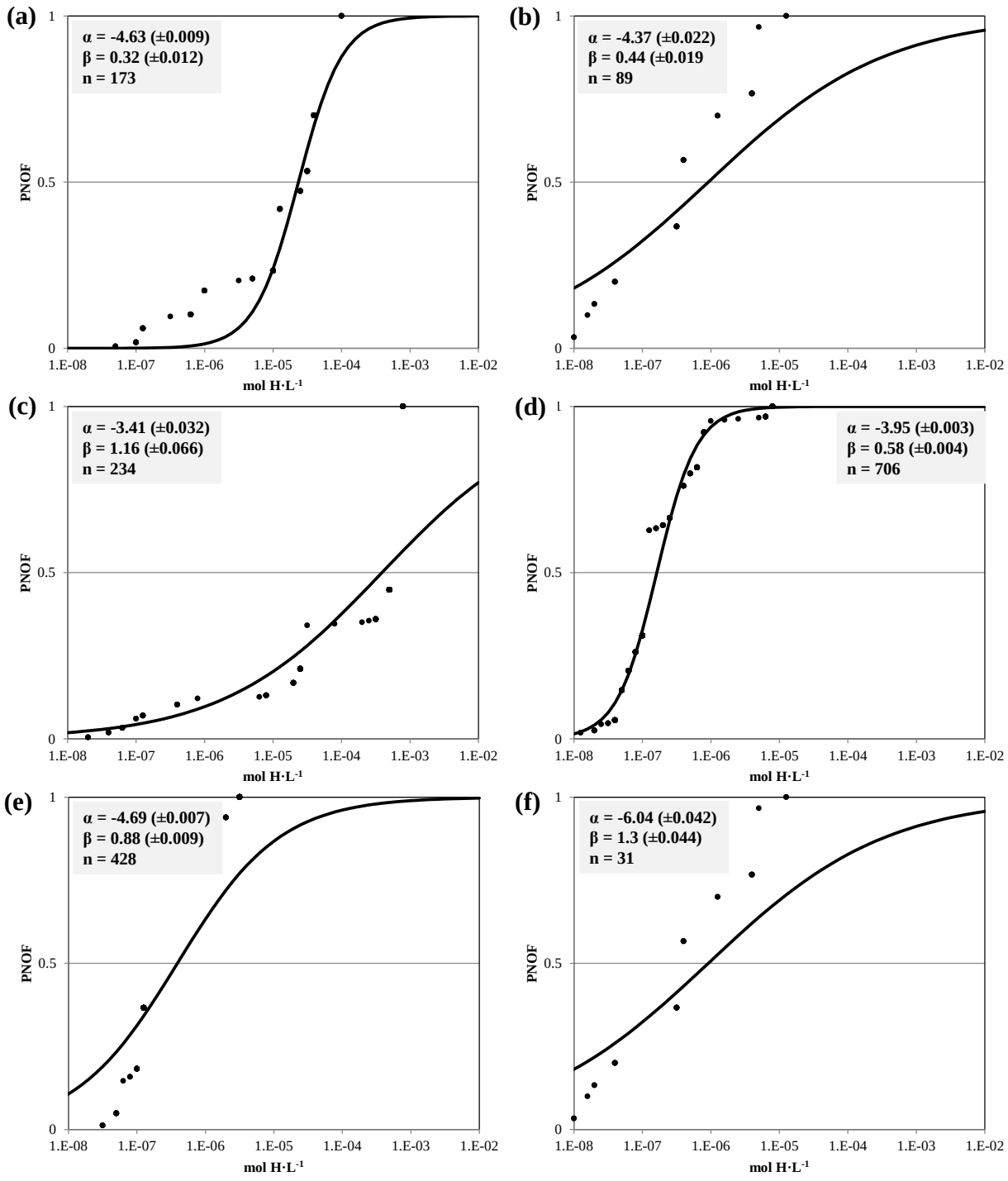
(a)
α = -4.63 (±0.009)
β = 0.32 (±0.012)
n = 173
(b)
α = -4.37 (±0.022)
β = 0.44 (±0.019
n = 89
(c)
α = -3.41 (±0.032)
β = 1.16 (±0.066)
n = 234
(d)
α = -3.95 (±0.003)
β = 0.58 (±0.004)
n = 706
(e)
α = -4.69 (±0.007)
β = 0.88 (±0.009)
n = 428
(f)
α = -6.04 (±0.042)
β = 1.3 (±0.044)
n = 31
PNOF
mol H·L-1
1.E-08
1.E-07
1.E-06
1.E-05
1.E-04
1.E-03
1.E-02
0
0.5
1

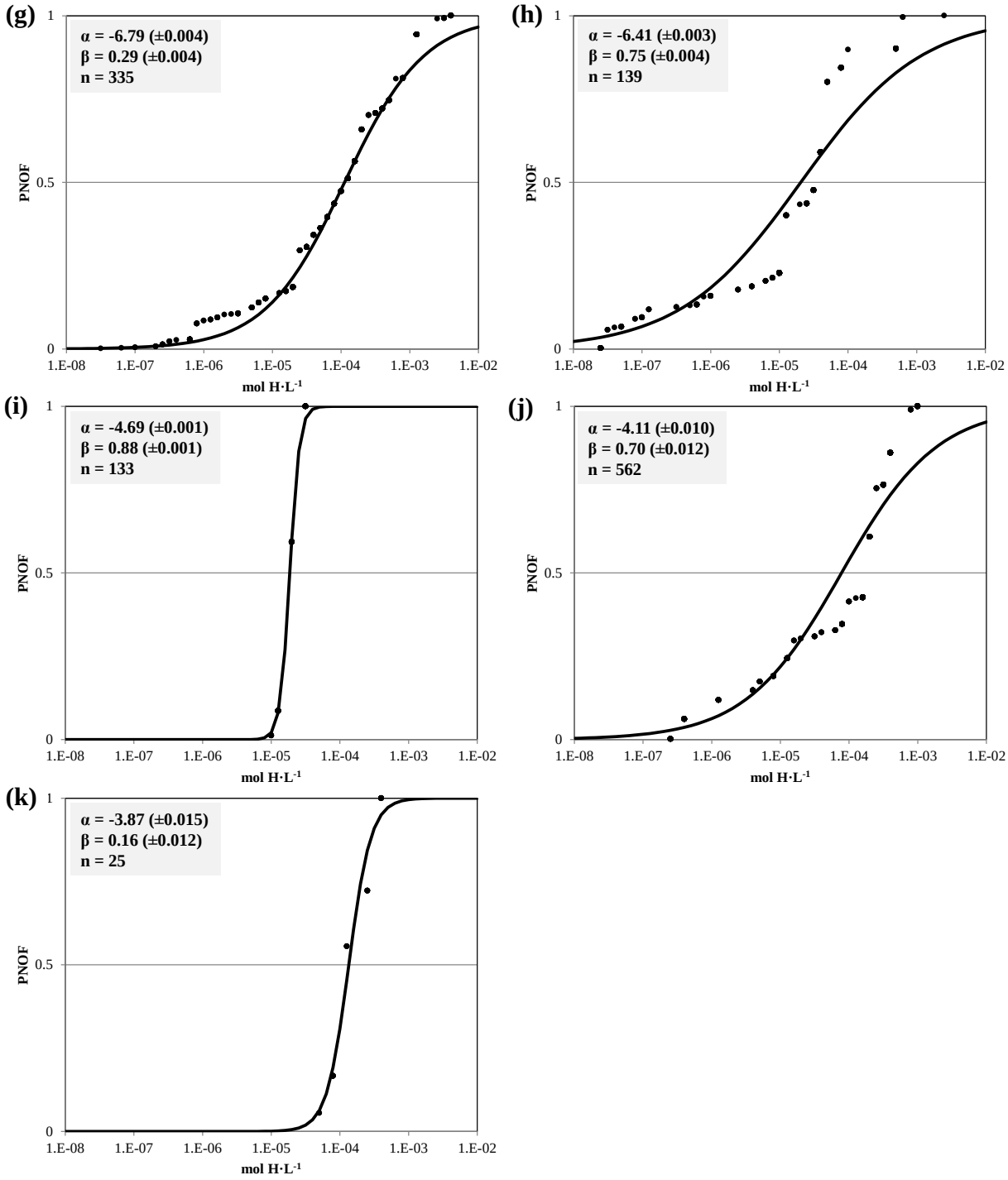

Figure 7.5: Coefficients α and β of the potentially not occurring fraction (PNOF) of vascular plant species as a logistic function of hydrogen ions (H, mol·L^{-1}) in the (a) tundra and alpine lands, (b) boreal forest and taiga, (c) temperate coniferous forest, and (d) temperate broadleaf mixed forest, (e) temperate grassland, savanna, and shrubland, (f) mediterranean forest, woodland, and scrub, (g) desert and xeric shrubland, (h) (sub)tropical dry broadleaf forest, (i) (sub)tropical grassland, savanna, and shrubland, (j) (sub)tropical moist broadleaf forest, and (k) mangrove.

8. Freshwater eutrophication

Ligia B. Azevedo[1,2], Francesca Verones[1,3], Andrew D. Henderson[4,5], Rosalie van Zelm[1], Olivier Jolliet[4], Laura Scherer[6], Mark A. J. Huijbregts[1]*

[1] Department of Environmental Science, Institute for Water and Wetland Research, Radboud University Nijmegen, P.O. Box 9010, 6500 GL, Nijmegen, the Netherlands
[2] International Institute for Applied Systems Analysis, Ecosystem Services and Management Program, Schlossplatz 1, A-2361 Laxenburg, Austria
[3] Industrial Ecology Programme, Department for Energy and Process Technology, Norwgian University of Science and Technology, Trondheim, Norway
[4] Department of Environmental Health Sciences, School of Public Health, University of Michigan, 1415 Washington Heights, Ann Arbor, MI 48109, USA
[5] Division of Epidemiology, Human Genetics and Environmental Sciences, School of Public Health, The University of Texas Health Science Center at Houston, 1200 Herman Pressler, Houston, Texas 77030, USA
[6] Institute of Environmental Engineering, ETH Zurich, 8093 Zurich, Switzerland

* azevedol@iiasa.ac.at

Based on: Helmes *et al.* (2012), Azevedo *et al.* (2013a), Azevedo *et al.* (2013b), Azevedo (2014), and Scherer and Pfister (2015).

8.1. Areas of protection and environmental mechanisms covered

Freshwater eutrophication occurs due to the discharge of nutrients into soil or into freshwater bodies and the subsequent rise in nutrient levels (namely, of phosphorus and nitrogen). Environmental impacts related to freshwater eutrophication are numerous. They follow a sequence of ecological impacts offset by increasing nutrient emissions into freshwater, thereby increasing nutrient uptake by autotrophic organisms such as cyanobacteria and algae and, ultimately, potential losses to biodiversity. In this work, emission impacts to freshwater are based on the transfer of phosphorus from the soil to freshwater bodies, its residence time in freshwater systems and on the potentially disappeared fraction (PDF) following an increase in phosphorus concentrations in freshwater (Figure 8.1). The detailed sequence of impacts related with freshwater eutrophication is described next.

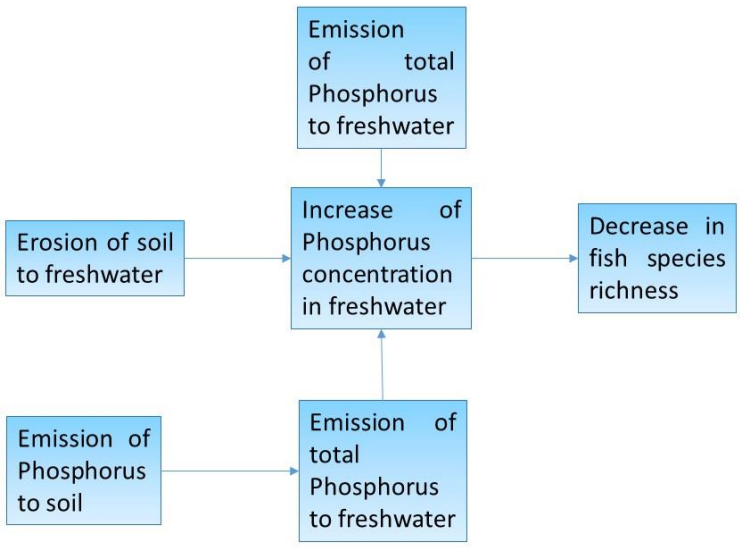

Figure 8.1: Illustration of impact pathway represented in equations 8.1 and 8.2.

Ecological impacts from freshwater eutrophication are initialized by the increase in primary productivity resulting from enhanced nutrient uptake by autotrophs, thereby prompting the increase in water turbidity, odor, and, subsequently, the decomposition of organic matter, water temperatures, and the depletion of dissolved oxygen. The latter is particularly detrimental to heterotrophic species. The depletion of sunlight caused by increased water turbidity also enhances competition for light by photosynthesizing organisms, which, in some cases, may lead to the synthesis of toxic substances (allelochemicals) by competing phytoplankton (Carpenter et al. 1998; Leflaive et al. 2007). Ultimately, they may prompt losses in biodiversity, e.g. decline in genera richness (Struijs et al. 2011b). In this report, we only include the environmental impact of emissions of phosphorus as increases in phosphorus levels in freshwaters seem to instigate primary production more than those of nitrogen (Schindler 2012).

The area of protection covered for this environmental mechanism is the ecosystem quality. The freshwater eutrophication impact is determined by the fraction of P emitted to soil or erosion of soil that reaches the freshwater compartment, the residence time of phosphorus (P) in freshwater (described by the fate factor) and by the sensitivity of the ecosystem to P levels (described by the effect factor). Here, the effect factor is based on a probabilistic model of a decline in richness of freshwater fish species with increasing emissions of P in freshwater systems. Note that, in cases where allelochemicals are released in the environment and these are also toxic to humans, there can be a direct impact to human health. However, this environmental mechanism is not taken into account in this chapter.

The geographical coverage of the endpoint characterization factor is global. The effect factor is based on a linear approach (see description of the effect factor below). The spatial resolution of the fate factor for direct emissions to water is 0.5° x 0.5°, the one for the fate factor for emissions to soil is 5 arc-minutes and the spatial resolution of the effect factor is biogeographical habitats (defined by the Freshwater Ecoregions of the World project, www.feow.org). Here, we use a modified version of the ecoregion classification (Azevedo et al. 2013b), where freshwater habitats are divided into cold, temperate, (sub)tropical, and xeric systems. The spatial resolution for the endpoint characterization factors is 0.5° x 0.5°.

8.2. Calculation of the characterization factors at endpoint level

Characterization factor

The characterization factor for freshwater eutrophication (PDF·yr·kg^{-1} or PDF·yr·m^{-2}·yr^{-1}) caused by emissions of P to compartment e (agricultural soil or freshwater) or by erosion of soil to compartment e were calculated for every freshwater ecoregion in the world, denoted with subscript r (Abell et al. 2008). It is described as

$$CF_{FW,e,r} = \frac{1}{\sum_{i \in r} w_{i \in r}} \sum_{i \in r} w_{i \in r} \cdot CF_{FW,e,i \in r}$$

Equation 8.1

where

$CF_{FW,e,r}$ = the characterisation factor of freshwater eutrophication of P emitted to compartment e in ecoregion r (PDF·yr·kg^{-1} or PDF·yr·m^{-2}·yr^{-1} for erosion)

$w_{i \in r}$ = the weighting factor of grid cell i situated in ecoregion r, which is phosohorus emissions for P emissions to freshwater and for P emissions to agricultural soil and cropland for erosion

$CF_{FW,e,i \in r}$ = the characterisation factor of freshwater eutrophication of P emitted to compartment e in grid cell i situated in ecoregion r(PDF·yr·kg^{-1} or PDF·yr·m^{-2}·yr^{-1} for erosion)

The characterisation factor for a P emission in grid cell i is derived via

$$CF_{FW,e,i \in r} = \sum_{j \in r} FF_{e,i,j \in r} \cdot \overline{EF_{j \in r}}$$

Equation 8.2

where

$FF_{e,i,j \in r}$ = the partial fate factor of P emitted to compartment e in grid cell i that travels to grid cell j situated in ecoregion r (year or kg·yr·m^{-2}·yr^{-1})

$EF_{j \in r}$= the average effect factor of grid cell j situated in ecoregion r (PDF/kg).

Note that we did not derive CFs if the emitting cell *i* was entirely deprived of water.

Fate factor

The partial fate factor of P emitted to compartment e (agricultural soil or freshwater) in grid cell i and transfered to grid cell j which are situated in ecoregion r. $FF_{e,i \to j \in r}$ is described as

$$FF_{e,i \to j \in r} = f_{e \to i \in r} \cdot f_{i \to j \in r} \cdot \tau_{j \in r}$$

Equation 8.3

where

$f_{e \to i \in r}$ = the fraction of P transported from compartment e to cell *i* in ecoregion r (dimensionless). Note that this fraction is by definition 1 for an emission to freshwater. Note that the for erosion this fraction has unit kg/m^2

$f_{i \to j \in r}$ = the fraction of P transported from cell *i* to *j* in ecoregion r (dimensionless),

$\tau_{j \in r}$ = the retention of P in grid cell j situated ecoregion r (year) (as derived by Helmes et al. 2012). The persistence of P is based on the rate at which P is removed from the freshwater compartment by three different processes, i.e. advection, water use, and retention (Figure 8.2a).

The fraction of P transferred from agricultural soil to freshwater was derived from a combination of two models. The Universal Soil Loss Equation (USLE) for the estimation of soil erosion was coupled with the

Swiss Agricultural Life Cycle Analysis (SALCA) model to determine the emissions from soil to the aquatic environment (Scherer and Pfister 2015). Two separate P transfer fractions from soil to freshwater are provided:
i) for erosion as a result of land use (kg P_{water} / (ha·yr)); and
ii) for runoff, drainage and groundwater leaching as a result of fertilizer application (kg P_{water} / kg $P_{fertilizer}$).
While the original grid-specific fraction transferred from soil to freshater was crop specific (Scherer and Pfister 2015), here it is crop independent by using a generic crop factor C_1 of 0.3 in the USLE.

Effect factor

The average effect factor of grid cell j as part of ecoregion r is averaged over the types of freshwater w (rivers or lakes), based on the fraction of their presence in that grid cell:

$$\overline{EF}_{j\in r} = \sum_{w} f_{w,j\in r} \cdot EF_{w,r}$$

Equation 8.4

where
$f_{w,j\in r}$ = the fraction of freshwater type w (river or lake) in grid cell j of ecoregion r;
$EF_{w,r}$ = the effect factor of freshwater type w (river or lake) in ecoregion r (PDF/kg).

The effect factor for a specific water type in a specific ecoregion is described as

$$EF_{w,r} = \frac{FRD_r \cdot LEF_{w,r}}{FR_{global}}$$

Equation 8.5

where
FRD_r = the fish richness density (species/l, see Figure 8.3 for illustration) in each ecoregion r,
$LEF_{w,r}$ = the linear effect factor describing the increase in the potentially disappeared fraction (PDF) of heterotrophic species in freshwater type *w* due to an increase in the total P level (PDF.m^3.kg^{-1}), and
FR = the total fish richness in the world (species). FR equals 15'000 and was determined by counting the total number of every "non-extinct" and "non-extinct in the wild" fish species living in streams and freshwater lakes listed by the International Union for Conservation of Nature (IUCN 2014).

Here, we assumed that the probabilistic model for heterotrophic species (including fishes and invertebrates) from which the LEF was derived is representative for the PDF of fish species. Also, we do not account for seasonal variation (e.g. summer versus winter) in the response of species to increasing P levels. We employ a linear effect model since P concentrations are unfrequently reported on a global scale and, as opposed to marginal and average effect factors, linear modelling does not require the environmental concentration of total P as an input variable.

The fish richness density (Figure 8.3) is described as

$$FRD_r = \frac{FSR_r}{\sum_{j\in r} V_{j,r}}$$

Equation 8.6

The fish species richness FSR_r in ecoregion r was obtained from data from Abell et al. (2008). The freshwater water volume in each ecoregion ($V_{j,r}$) was obtained from the model derived by Helmes *et al.*

(2012) on a pixel basis and summed per ecoregion. We assumed no difference between FRD across the two freshwater types lakes and rivers in an ecoregion.

The linear effect factor is described as

$$LEF_{w,r} = \frac{0.5}{10^{\alpha_{w,r}}}$$

Equation 8.7

where
$\alpha_{w,r}$ = the total P level (log m^3/kg) in water type w in ecoregion r at which the potentially not occurring fraction (PNOF) of heterotrophic species equals 50% in water type.

The effect factor is based on a probabilistic model of the cumulative PNOF as a logistic function of total P concentration (Azevedo et al. 2013a) and is illustrated in Figure 8.2b. In this work, we equate PNOF with PDF. The effect factor depends both on the climate type (warm, temperate or cold) and the water type (river vs. lake). The climate type per ecoregion was identified based on geographical location of each pixel and the respective effect factor was used. The effect factors for every climate-water type combination are given in Table 8.1. The parameter logistic function parameter α was derived for four biogeographic regions, i.e. cold, temperate, (sub)tropical, and xeric, as well as for lakes and streams separately. The empirical data employed in the derivation of the logistic regressions consisted of the maximum tolerance total P concentration of each heterotrophic species subsisting in freshwater *w* in the biogeographic region occupied by cell *j* as described by the Freshwater Ecoregions of the World project, FEOW (http://www.feow.org). Species-specific data on maximum tolerable total P concentration were given by Azevedo *et al.* (2013b) and the α coefficients for the four biogeographic regions and two freshwater types are shown in Figure 6. For xeric lakes as well as for cold and (sub)tropical streams, the α coefficient could not be determined. In those cases, the α parameters of (sub)tropical lakes and streams were employed as the α for xeric lakes and streams, respectively, and the α for temperate streams was employed as the α for cold streams. Grid-specific CFs are shown in Figure 8.4. The global average CF is for emissions to water 1.81E-12 PDF·yr·kg^{-1} and for emissions to soil and erosion 1.76E-13 PDF·yr·kg^{-1} and 3.88E-12 PDF·yr/m^2·yr. Country, continent, and world CFs were derived based on a emission-based or area-based average. For emission to water and fertilizer applications combined fertilizer and manure applications are used for weighting. For the factors related to erosion we used as a proxy for weighting the crop area (both fertilizer and cropland information from Scherer et al. (2015))(see Excel file and Table 8.2 and 8.3).

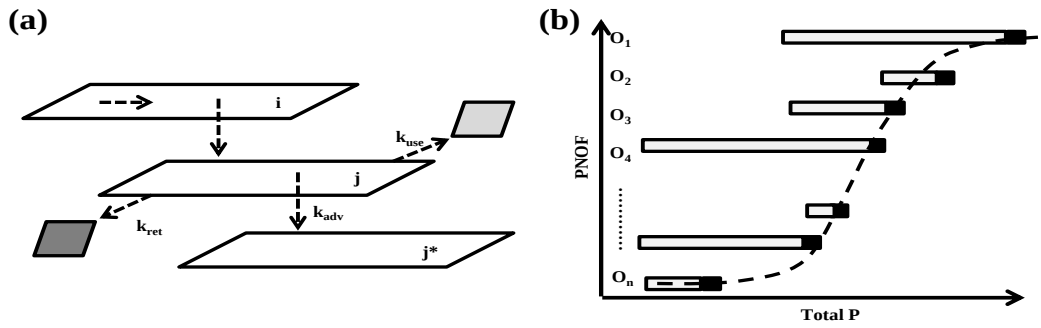

Figure 8.2: (a) fate transport, adapted from Helmes *et al.* (2012), and (b) the logistic regression originating the linear effect model, adapted from Azevedo (2014). (a) shows the flow of P from the soil compartment into the freshwater compartment within emitting cell *i* and from emitting cell *i* into *j* and the flow through three pathways of P removal from the freshwater compartment of, i.e. advection k_{adv} to cell *j downstream of j, retention k_{ret} to the sediment (dark grey) compartment of *j* and water use k_{use} to the soil (light grey) compartment of *j*. In (b), the potentially not occurring fraction (PNOF) of species as a logistic function of total P is determined with the highest tolerable total P condition (illustrated as the black tip of the grey bar total P range) for individual species (O_i) recorded in observational field studies.**

Table 8.1: Linear effect factors for streams and lakes for the different climate zones. See also explanations in text.

	Lake [PDF·m³/kg]	Stream [PDF·m³/kg]
subtropical	13457.67	777.98
tropical	13457.67	777.98
temperate	1253.05	674.48
cold	18279.74	674.48
xeric	13457.67	777.98

8.3. Uncertainties

The transfer model of phosphorus from soils to freshwater bodies relies on multiple assumptions. As such, it was assumed that soil phosphorus is equally distributed between surface and sub-surface soil layers and that all phosphorus from fertilizers is bioavailable. However, we do not include phosphorus impacts to groundwater. Emissions caused by wind erosion (i.e., via dust uplift) were neglected. Furthermore, the crop factor C_1 was here assigned to a fixed number whereas it actually varies according to the crops, chemical and physical soil properties, and agricultural management (including P inputs and soil conservation strategies) (Kleinmann et al. 2011; Vadas et al. 2010).

It is not possible to provide evidence of the actual phosphorus residence times unless P transport is measured in the field and then compared with the fate factors. Another option is the comparison with an independent phosphorus fate model. Helmes *et al.* (2012) compared their FF results with those reported by Struijs *et al.* (2011a) for Europe. This comparison may be skewed since P flows are not the same for both fate models. The fate model employed in this report is that of Helmes *et al.* (2012), who include water retention and use. However, Struijs *et al.* (2011a) do not include these two P transport pathways.

The level of robustness of the effects of freshwater eutrophication on fish species is high. The effect of increasing P levels on net primary productivity has been verified at multiple spatial scales, see meta-analyses by Wilson *et al.* (2006) and Elser *et al.* (2007) for laboratory and whole-field experiment examples, respectively. Additionally, the effect of a nutrient discharge to freshwater, particularly to lakes,

has been demonstrated for short term response (within days) (Schindler 1977) and long term response as well (decades) (Marsden 1989). Our method is based on field surveys consisting of records whereby a freshwater species is observed and the concentration of total P is measured at the same location and at the same time (Azevedo et al. 2013b). Although the presence of the species at a specific P level and at a certain P range is confirmed, the absence of that species at levels below or above that specified range is less certain. (The species may indeed be present beyond the registered P levels but it may go unrecorded.)

The failure to record the species at a specific P level may be human related, such as (1) an incomplete survey of the existing species or of the existing P levels, but also due to natural causes, such as that (2) the species may be rare and difficult to spot, (3) extreme P levels may be tolerated by the species but it may not be found under natural conditions, or (4) the level of P is tolerated by the species but the species absence is due to another stressor. For a detailed description of the downsides of observational field data for conducting impact assessments, see Azevedo (2014). Because of the possible underestimation of the maximum P level tolerated by the species, the uncertainty of the effect model specifically employed here is considered high.

Nearly 50% of the variance in CF results is attributed to the difference in freshwater types. This difference is determined by the residence time of P in the water (i.e. the fate factor) (Azevedo et al. 2013a). In turn, the fate factors are primarily dependent upon water advection and, to a lower extent, to water use (Helmes et al. 2012).

8.4. Value Choices

The time horizon for this impact category is not relevant since it is assumed that the impact occurs at the moment of emitting phosphorus to freshwater bodies. No choices are thus modelled for fate and effect factors for freshwater eutrophication. The level of robustness for the CFs is considered to be high, since the effects on freshwater fish are certain.

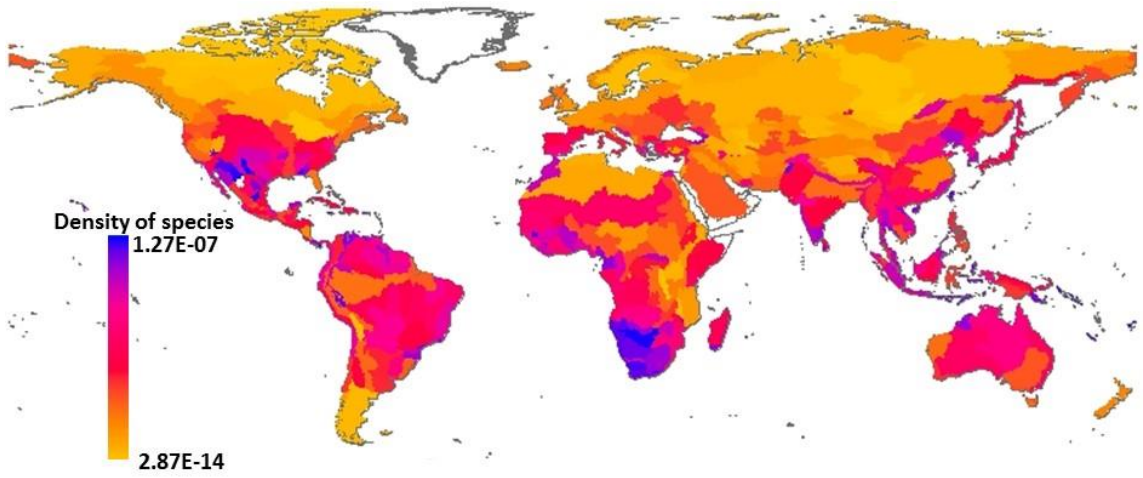

Figure 8.3: Freshwater fish density (species·m^{-3}) based on data from Abell et al. (2008) and freshwater volumes of Helmes *et al.* (2012).

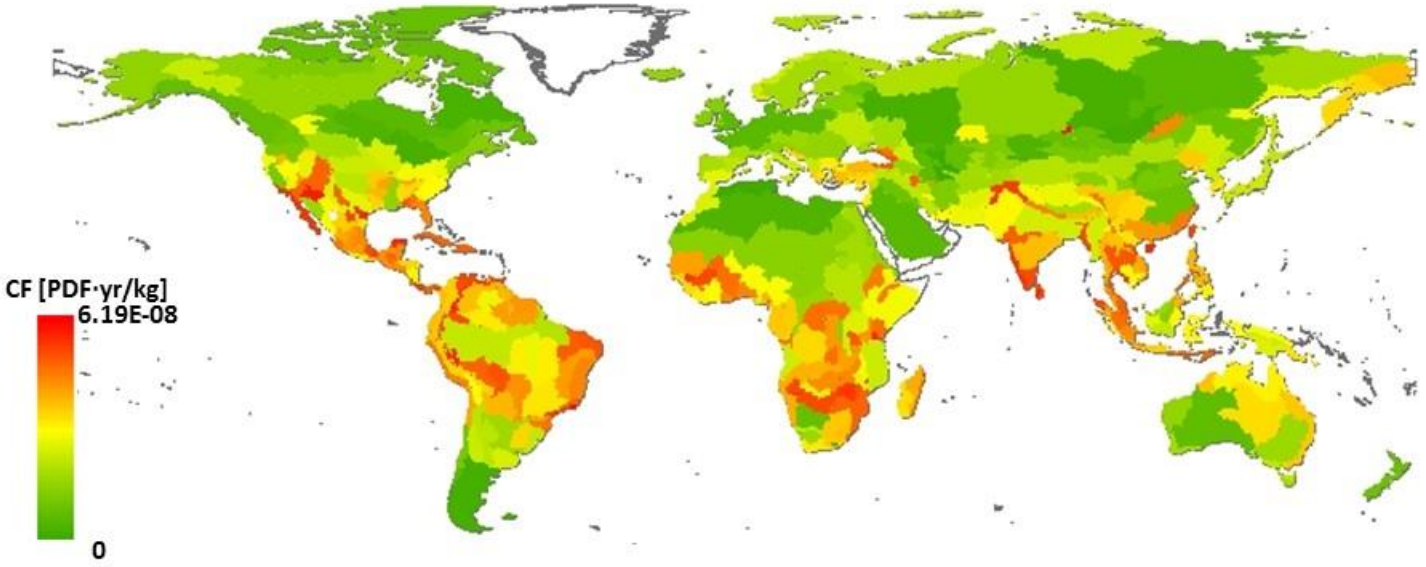

Figure 8.4: Endpoint characterization factors for emissions of P to freshwater ($CF_{freshwater}$, PDF·yr·kg^{-1}) based on fish richness.

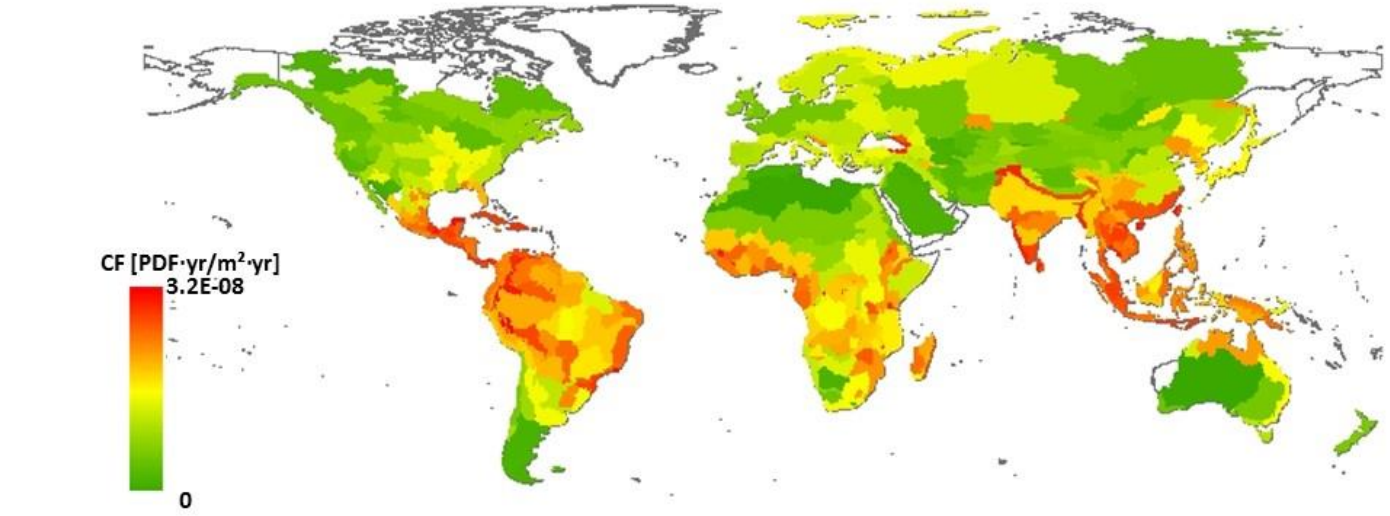

a)

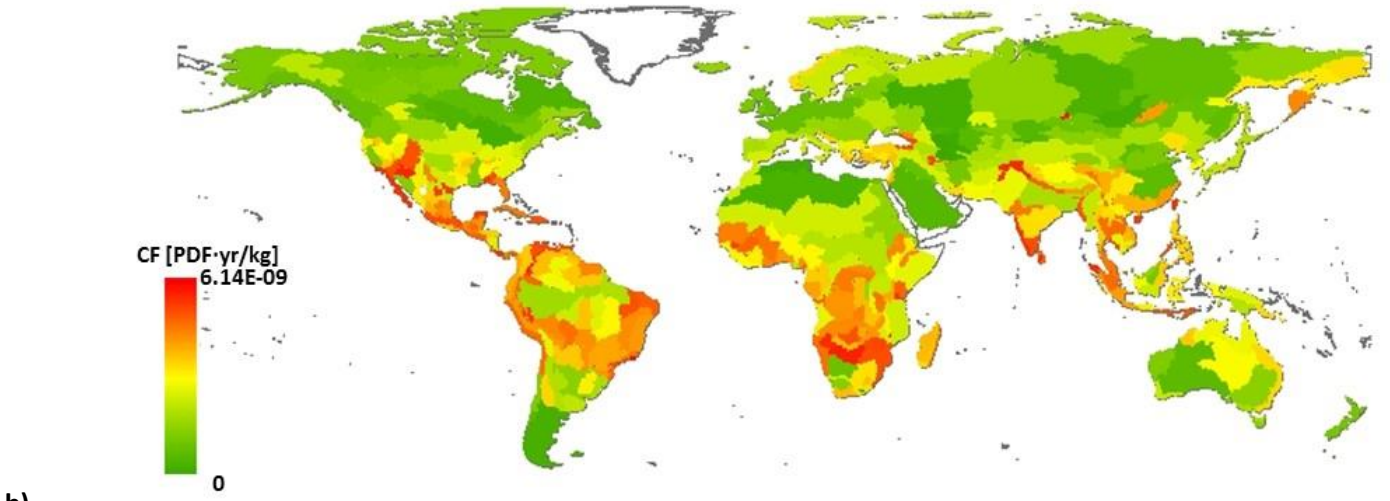

b)

Figure 8.5: Endpoint characterization factors for emissions of P to soil and erosion based on fish richness. A) for P from erosion and B) for P from fertilizer application.

Table 8.1: Global endpoint characterization factors for emissions to freshwater ($CF_{freshwater}$, PDF·yr·kg^{-1}), for emissions to soil (CF_{soil}, PDF·yr·kg^{-1}) and for impacts from erosion ($CF_{erosion}$, PDF·yr/m^2·yr) on a country level, based on fish richness. This is the CF for total phosphorus, reported as P. The emissions all go to the freshwater compartment.

Country	$CF_{freshwater}$ [PDF·yr/kg]	CF_{soil} [PDF·yr/kg]	$CF_{erosion}$ [PDF·yr/m2·yr]
Afghanistan	7.66E-12	1.06E-12	6.27E-12
Albania	5.20E-13	7.51E-14	1.38E-12
Algeria	6.36E-15	6.44E-16	6.58E-16
Andorra	3.37E-13	3.11E-14	2.16E-13
Angola	4.73E-12	9.04E-13	1.96E-12
Argentina	5.61E-13	4.18E-14	7.22E-13
Armenia	2.15E-13	3.29E-14	3.53E-13
Australia	7.05E-13	4.97E-14	1.13E-13
Austria	2.33E-13	2.18E-14	3.17E-13
Azerbaijan	2.61E-13	3.74E-14	3.85E-13
Bahrain	3.45E-14	1.92E-15	2.95E-15
Bangladesh	1.16E-12	7.35E-14	4.36E-12
Belgium	3.56E-14	5.43E-15	2.58E-14
Belize	4.24E-12	3.64E-13	1.26E-11
Benin	3.40E-12	2.78E-13	9.30E-12
Bhutan	2.16E-12	3.02E-13	5.43E-11
Bolivia	5.57E-12	3.94E-13	7.89E-12
Bosnia and Herzegovina	9.69E-13	9.19E-14	1.90E-12
Botswana	2.13E-11	3.79E-12	3.29E-12
Brazil	3.18E-12	3.47E-13	6.69E-12
Brunei	2.49E-13	1.72E-14	1.41E-12
Bulgaria	7.58E-13	7.13E-14	2.94E-13
Burkina Faso	4.63E-12	4.18E-13	3.99E-12
Burundi	2.02E-12	1.42E-13	2.06E-12
Belarus	2.91E-13	2.60E-14	4.08E-13
Cambodia	3.11E-12	2.07E-13	1.57E-11
Cameroon	1.45E-12	1.62E-13	2.23E-12
Canada	2.46E-13	1.88E-14	6.81E-14
Central African Republic	9.12E-13	1.62E-13	5.62E-13
Chad	1.93E-13	4.37E-14	2.45E-13
Chile	1.78E-13	2.13E-14	3.75E-13
China	1.18E-12	8.96E-14	2.89E-12
Colombia	6.02E-12	7.69E-13	1.85E-11
Congo	3.26E-12	8.44E-13	8.18E-12
Costa Rica	6.56E-12	8.01E-13	3.23E-11
Croatia	7.50E-13	7.19E-14	1.97E-12
Cuba	7.01E-12	4.83E-13	2.76E-11
Czech Republic	1.02E-13	1.13E-14	1.23E-13
Denmark	5.86E-14	9.44E-15	8.91E-14
Djibouti	3.11E-13	3.37E-14	3.16E-14
Dominican Republic	7.24E-12	9.67E-13	3.98E-11
Ecuador	2.59E-12	3.12E-13	1.39E-11
Egypt	1.79E-13	1.16E-14	6.53E-14
El Salvador	4.07E-12	7.89E-13	1.97E-11
Equatorial Guinea	1.97E-12	1.80E-13	8.43E-12
Eritrea	9.30E-13	7.94E-14	1.70E-12
Estonia	1.46E-13	1.21E-14	4.62E-13
Ethiopia	3.39E-12	3.01E-13	6.61E-12
Finland	2.87E-13	4.86E-14	3.38E-13
France	1.15E-13	1.53E-14	1.17E-13
French Guiana	3.48E-12	4.17E-13	2.63E-12
Gabon	2.03E-12	2.63E-13	1.08E-11
Gambia, The	3.33E-12	4.71E-13	2.39E-12
Gaza Strip	9.55E-13	7.96E-14	3.36E-13
Georgia	3.61E-12	4.56E-13	1.58E-11
Germany	6.52E-14	7.88E-15	6.38E-14
Ghana	6.17E-12	5.62E-13	6.71E-12
Greece	1.15E-12	1.28E-13	4.42E-13

Guatemala	4.82E-12	5.93E-13	1.98E-11
Guinea	1.14E-11	9.45E-13	2.16E-11
Guinea-Bissau	2.75E-12	3.54E-13	4.44E-12
Guyana	2.86E-12	2.54E-13	3.50E-12
Haiti	7.25E-12	9.69E-13	3.88E-11
Honduras	2.78E-12	4.14E-13	1.36E-11
Hungary	2.26E-13	2.07E-14	2.90E-13
Iceland	1.86E-13	1.64E-14	0.00E+00
India	3.15E-12	2.68E-13	8.61E-12
Indonesia	2.88E-12	3.51E-13	1.20E-11
Iran	9.74E-13	1.46E-13	3.59E-13
Iraq	1.90E-13	2.20E-14	9.38E-14
Ireland	1.46E-13	9.91E-15	6.22E-14
Israel	1.05E-12	1.18E-13	2.12E-13
Italy	2.98E-13	3.57E-14	2.84E-13
Ivory Coast	3.00E-12	2.43E-13	4.46E-12
Japan	5.41E-13	4.51E-14	1.03E-12
Jordan	9.88E-13	1.58E-13	2.68E-14
Kazakhstan	1.90E-13	1.59E-14	4.30E-13
Kenya	2.76E-12	2.83E-13	2.68E-12
Kuwait	3.92E-14	3.15E-15	2.56E-15
Kyrgyzstan	1.89E-13	2.93E-14	9.18E-14
Laos	5.06E-12	3.51E-13	1.65E-11
Latvia	1.53E-13	1.26E-14	4.65E-13
Lebanon	1.29E-12	1.25E-13	2.39E-13
Lesotho	2.24E-12	2.15E-13	4.52E-12
Liberia	1.45E-12	1.02E-13	7.40E-12
Libya	2.38E-14	1.58E-15	0.00E+00
Liechtenstein	3.55E-14	5.44E-15	2.61E-14
Lithuania	7.07E-14	7.84E-15	1.88E-13
Luxembourg	3.62E-14	5.52E-15	2.73E-14
Macedonia	5.63E-13	7.72E-14	4.84E-13
Madagascar	2.25E-12	2.24E-13	5.88E-12
Malawi	1.80E-11	1.80E-12	6.48E-11
Malaysia	3.88E-12	3.28E-13	1.12E-11
Mali	6.24E-12	5.19E-13	4.33E-12
Mauritania	2.64E-12	3.68E-13	2.05E-12
Mexico	6.96E-12	8.73E-13	2.20E-11
Moldova	2.04E-13	1.86E-14	2.63E-13
Mongolia	2.65E-13	2.43E-14	2.60E-13
Montenegro	4.15E-13	4.52E-14	2.14E-12
Morocco	5.93E-13	4.64E-14	7.67E-14
Mozambique	8.45E-12	1.03E-12	1.69E-11
Myanmar (Burma)	2.95E-12	2.17E-13	6.91E-12
Namibia	9.28E-12	2.11E-12	1.42E-12
Nepal	3.20E-12	4.72E-13	1.52E-11
Netherlands	3.44E-14	5.25E-15	2.52E-14
New Zealand	6.25E-14	9.36E-15	3.31E-14
Nicaragua	1.59E-12	1.33E-13	1.43E-11
Niger	4.36E-13	6.60E-14	9.16E-13
Nigeria	1.14E-12	1.16E-13	3.32E-12
North Korea	5.64E-13	3.95E-14	2.66E-12
Norway	3.94E-13	8.36E-14	3.76E-13
Oman	1.58E-14	1.29E-15	1.27E-16
Pakistan	3.45E-12	4.06E-13	7.51E-12
Panama	1.26E-11	1.56E-12	4.71E-11
Papua New Guinea	8.21E-13	6.86E-14	5.75E-12
Paraguay	2.78E-12	2.66E-13	4.96E-12
Peru	5.53E-12	8.29E-13	1.88E-11
Philippines	2.35E-12	2.17E-13	6.58E-12
Poland	3.65E-14	5.55E-15	2.60E-14
Portugal	3.68E-13	3.36E-14	1.50E-13
Qatar	3.24E-14	2.64E-15	0.00E+00

Romania	2.04E-13	1.85E-14	2.64E-13
Russia	4.66E-13	5.10E-14	4.47E-13
Rwanda	7.45E-13	5.37E-14	9.57E-13
San Marino	1.60E-13	2.67E-14	1.58E-13
Saudi Arabia	3.01E-14	2.46E-15	2.23E-15
Senegal	3.22E-12	4.57E-13	2.39E-12
Serbia	2.35E-13	2.32E-14	3.15E-13
Sierra Leone	1.64E-12	1.13E-13	8.22E-12
Singapore	9.07E-12	6.17E-13	2.25E-11
Slovakia	2.26E-13	2.13E-14	2.98E-13
Slovenia	4.59E-13	5.91E-14	4.05E-13
Somalia	7.15E-13	5.04E-14	3.67E-13
South Africa	4.31E-12	3.83E-13	1.54E-12
South Korea	9.71E-13	6.71E-14	1.95E-12
Spain	4.68E-13	4.03E-14	1.78E-13
Sri Lanka	1.80E-11	1.50E-12	4.27E-11
Sudan	3.77E-13	3.46E-14	6.24E-13
Suriname	3.52E-12	4.22E-13	2.62E-12
Swaziland	5.40E-12	7.50E-13	3.26E-12
Sweden	2.83E-13	4.82E-14	3.42E-13
Switzerland	4.94E-14	7.46E-15	2.93E-14
Syria	7.24E-13	7.75E-14	1.43E-13
Taiwan	1.52E-11	2.45E-12	8.50E-11
Tajikistan	2.56E-13	3.41E-14	7.81E-14
Tanzania, United Republic of	5.00E-12	3.72E-13	7.11E-12
Thailand	8.52E-12	5.79E-13	2.28E-11
Togo	5.43E-12	4.45E-13	8.99E-12
Trinidad and Tobago	1.10E-11	1.08E-12	1.64E-11
Tunisia	4.77E-15	3.92E-16	6.57E-16
Turkey	2.15E-12	2.05E-13	2.67E-12
Turkmenistan	2.24E-13	2.38E-14	4.53E-14
Uganda	6.47E-13	4.61E-14	9.83E-13
Ukraine	3.76E-13	3.22E-14	4.88E-13
United Arab Emirates	5.84E-16	4.75E-17	0.00E+00
United Kingdom	8.74E-14	7.58E-15	3.50E-14
United States	1.27E-12	1.10E-13	4.75E-13
Uruguay	1.35E-12	9.02E-14	3.48E-12
Uzbekistan	2.02E-13	2.30E-14	5.58E-14
Venezuela	9.72E-12	9.98E-13	2.52E-11
Vietnam	2.16E-12	1.59E-13	1.26E-11
West Bank	1.25E-12	1.62E-13	1.90E-13
Western Sahara	5.50E-13	4.26E-14	0.00E+00
Yemen	3.32E-15	2.71E-16	1.11E-17
Zaire	3.69E-12	3.87E-13	2.12E-12
Zambia	4.08E-12	4.46E-13	2.51E-12
Zimbabwe	1.40E-11	1.22E-12	1.08E-11

Table 8.2: Global endpoint characterization factors for emissions to freshwater ($CF_{freshwater}$, PDF·yr·kg^{-1}), for emissions to soil (CF_{soil}, PDF·yr·kg^{-1}) and for impacts from erosion ($CF_{erosion}$, PDF·yr/m^2·yr) on a continental level based on fish richness.

Continent	$CF_{freshwater}$ [PDF·yr/kg]	CF_{soil} [PDF·yr/kg]	$CF_{erosion}$ [PDF·yr/m^2·yr]
Africa	2.75E-12	2.85E-13	3.67E-12
Asia	1.94E-12	1.71E-13	5.84E-12
Australia	7.05E-13	4.98E-14	1.13E-13
Europe	2.20E-13	2.28E-14	3.47E-13
North America	1.86E-12	1.95E-13	3.85E-12
Oceania	6.34E-14	9.50E-15	1.17E-13
South America	3.18E-12	3.47E-13	6.03E-12

8.5. References

Abell, R., Thieme, M. L., Revenga, C., Bryer, M., Kottelat, M., Bogutskaya, N., Coad, B., Mandrak, N., Balderas, S. C., Bussing, W., Stiassny, M. L. J., Skelton, P., Allen, G. R., Unmack, P., Naseka, A., Ng, R., Sindorf, N., Robertson, J., Armijo, E., Higgins, J. V., Heibel, T. J., Wikramanayake, E., Olson, D., López, H. L., Reis, R. E., Lundberg, J. G., Sabaj Pérez, M. H. and Petry, P. (2008). "Freshwater Ecoregions of the World: A New Map of Biogeographic Units for Freshwater Biodiversity Conservation." BioScience **58**(5): 403-414.

Azevedo, L. B. (2014). Development and application of stressor – response relationships of nutrients. Chapter 8. Ph.D. Dissertation, Radboud University Nijmegen, The Netherlands. http://repository.ubn.ru.nl.

Azevedo, L. B., Henderson, A. D., van Zelm, R., Jolliet, O. and Huijbregts, M. A. J. (2013a). "Assessing the Importance of Spatial Variability versus Model Choices in Life Cycle Impact Assessment: The Case of Freshwater Eutrophication in Europe." Environmental Science & Technology **47**(23): 13565-13570.

Azevedo, L. B., van Zelm, R., Elshout, P. M. F., Hendriks, A. J., Leuven, R. S. E. W., Struijs, J., de Zwart, D. and Huijbregts, M. A. J. (2013b). "Species richness–phosphorus relationships for lakes and streams worldwide." Global Ecology and Biogeography **22**(12): 1304-1314.

Carpenter, S. R., Caraco, N. F., Correll, D. L., Howarth, R. W., Sharpley, A. N. and Smith, V. H. (1998). "Nonpoint pollution of surface waters with phosphorus and nitrogen." Ecological Applications **8**(3): 559-568.

Elser, J. J., Bracken, M. E. S., Cleland, E. E., Gruner, D. S., Harpole, W. S., Hillebrand, H., Ngai, J. T., Seabloom, E. W., Shurin, J. B. and Smith, J. E. (2007). "Global analysis of nitrogen and phosphorus limitation of primary producers in freshwater, marine and terrestrial ecosystems." Ecology Letters **10**(12): 1135-1142.

Helmes, R. J. K., Huijbregts, M. A. J., Henderson, A. D. and Jolliet, O. (2012). "Spatially explicit fate factors of phosphorous emissions to freshwater at the global scale." International Journal of Life Cycle Assessment **17**(5): 646-654.

IUCN (2014). International Union for Conservation of Nature. Red List of Threatened Species. Version 2010.1. Downloaded on 30 June 2014 at www.iucnredlist.org.

Leflaive, J. and Ten-Hage, L. (2007). "Algal and cyanobacterial secondary metabolites in freshwaters: a comparison of allelopathic compounds and toxins." Freshwater Biology **52**(2): 199-214.

Kleinman, P., Sharpley, A., Buda, A., McDowell, R., and Allen, A. (2011): *Soil controls of phosphorus in runoff: Management barriers and opportunities.* Canadian Journal of Soil Science. **91**(3): 329-338.

Marsden, M. W. (1989). "Lake restoration by reducing external phosphorus loading: the influence of sediment phosphorus release." Freshwater Biology **21**(2): 139-162.

Scherer, L. and Pfister, S. (2015). "Modelling spatially explicit impacts from phosphorus emissions in agriculture." International Journal of Life Cycle Assessment **20**(6): 785–795.

Schindler, D. W. (1977). "Evolution of phosphorus limitation in lakes." Science **195**(4275): 260-262.

Schindler, D. W. (2012). "The dilemma of controlling cultural eutrophication of lakes." Proceedings of the Royal Society B: Biological Sciences.

Struijs, J., Beusen, A., de Zwart, D. and Huijbregts, M. (2011a). "Characterization factors for inland water eutrophication at the damage level in life cycle impact assessment." International Journal of Life Cycle Assessment **16**(1): 59-64.

Struijs, J., De Zwart, D., Posthuma, L., Leuven, R. S. E. W. and Huijbregts, M. A. J. (2011b). "Field sensitivity distribution of macroinvertebrates for phosphorus in inland waters." Integrated Environmental Assessment & Management **7**(2): 280-286.

Vadas, P.A. and J, W.M. (2010): *Validating soil phosphorus routines in the SWAT model.* Transactions of the ASABE **53**: 1469-1476.

Wilson, A. E., Sarnelle, O. and Tillmanns, A. R. (2006). "Effects of cyanobacterial toxicity and morphology on the population growth of freshwater zooplankton: Meta-analyses of laboratory experiments." Limnology and Oceanography **51**(4): 1915-1924.

8.6. Appendix

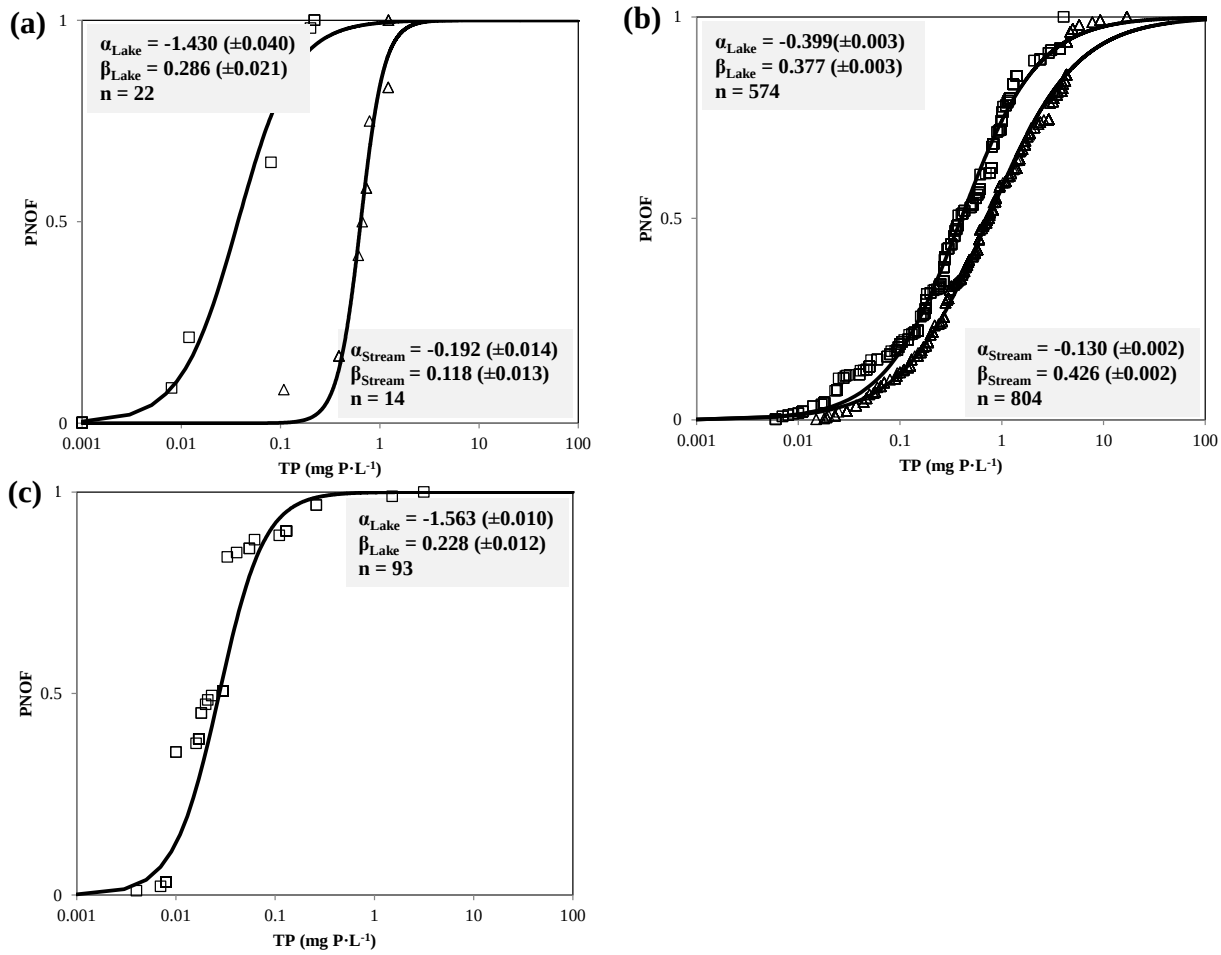

Figure 8.6: Coefficients α and β of the potentially not occurring fraction (PNOF) of heterotrophic species in lake (squares) and streams (triangles) as a logistic function of total P (TP, mg P·L^{-1}) in the (a) (sub)tropical, (b) temperate, and (c) cold. The PNOF is a logistic function of α, β, and TP, i.e. $PNOF = \frac{1}{1+e^{-\left(\frac{log_{10}TP-\alpha}{\beta}\right)}}$. Although β is not used in the derivation of effect factors in our work, it can later be employed in future LCAs in the derivation of average or marginal effect factors.

9. Marine eutrophication

coming soon

10. Toxicity

coming soon

11. Land stress: Potential species loss from land use (global; PSSRg)

Abhishek Chaudhary[1], Francesca Verones[2], Laura de Baan[1], Stephan Pfister[1], Stefanie Hellweg[1]*

[1]Institute of Environmental Engineering, ETH Zurich, 8093 Zurich, Switzerland

[2]Industrial Ecology Programme, Department of Energy and Process Engineering, NTNU, 7491 Trondheim, Norway

*Corresponding author email: abhinain2010@yahoo.com

11.1. Areas of protection and environmental mechanisms covered

The method is based on the UNEP-SETAC guideline on global land use impact assessment on biodiversity in LCA (Koellner et al. 2013a) concerning the area of protection of ecosystem quality. The approach proposed by Chaudhary et al. 2015 using countryside species-area relationship (SAR) is used for calculating ecoregion specific marginal and average characterization factors (CFs) for biodiversity loss for both land occupation and transformation.

Description of impact pathway

Land use is a main driver of global biodiversity loss (MAS 2005). Within a product's life cycle, the land use impacts can represent a significant portion of their total environmental burden, e.g. for forestry and agriculture based products. Two types of land use interventions are usually considered in life cycle inventories and impact assessments; land transformation (also called land use change) and land occupation (Milà i Canals 2007). During transformation, the land is modified to make it suitable for an intended use, such as deforesting to make space for agriculture. During land occupation, land is used in the intended productive way (e.g. agriculture) and the land cannot develop towards a "natural reference state" (i.e. the regrowth of forest is avoided). The land use impacts result from both land transformation (because the ecosystems characteristics are changed) and land occupation (because ecosystem quality is kept at a different level than its natural state). As biodiversity shows a strong spatial heterogeneity and responds differently to land transformation and occupation in different parts of the world, a regionalized assessment is required (Koellner et al., 2013a).

Modeling the ecosystem quality damage due to land use impact on biodiversity is done in four steps (see Figure 11.1). In the first step *relative* changes in species richness is calculated by comparing the *local* species richness of different land use types with the (semi-)natural regional reference situation (de Baan 2013b, Koellner 2013a). A global literature review was carried out to select studies that report such comparisons. Data from existing databases such as GLOBIO (Alkamade et al. 2010), or the Swiss biodiversity monitoring (BDM 2004) were also imported. Differences across land use types, biogeographic regions (i.e. biomes) and species groups were statistically analyzed. Based on these data, damage scores (so called *local* characterization factors) for six land use types and five taxa in different biomes were calculated.

In the second step, above local CFs are fed into the 'Countryside species area relationship model' to calculate species extinctions due to land use. The model predicts the *absolute* loss of species for each of the five taxa and provides the *regional* characterization factors (CFs) in the unit 'regional species lost per unit of land occupied or transformed' in 804 terrestrial ecoregions.

However, the CFs calculated using SAR treat all species equally, whether the species present in an ecoregion are critically threatened or widely distributed. In the third step, these CFs are weighted with

vulnerability scores (Verones et al. 2013) of each species present in a particular region to derive *weighted CFs* in the unit 'global species eq. lost per unit of land occupied or transformed' in 804 terrestrial ecoregions. The CFs calculated in step-2 using SAR and without vulnerability scores are referred to as *unweighted* CFs.

Finally, in step-4, the modelled species lost for each taxon are aggregated using Eq. 1.3 (chapter 1), to derive the ecosystem quality loss in the final endpoint unit- global fraction of potentially disappeared species (PDF). The impact pathway is described in figure 11.1 and equations 11.1 – 11.12. The detailed methodology is explained in Chaudhary et al. 2015.

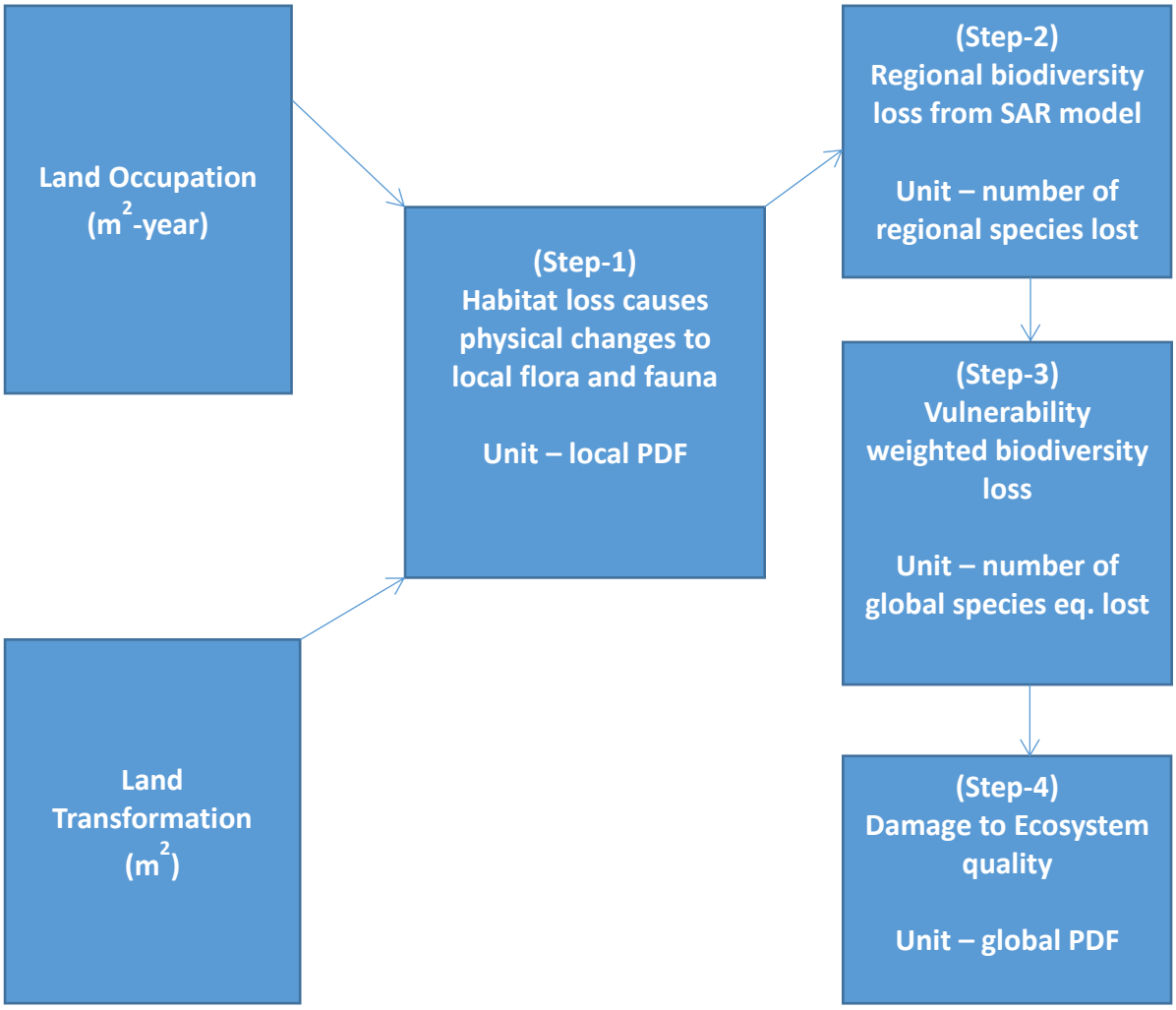

Figure 11.1: Cause-effect chain for ecosystem quality impacts caused by land use and the modeled impact pathway (following ILCD). Land transformation and land occupation causes physical changes to flora and fauna locally, which leads to an altered species composition and species richness on the occupied land itself. If too much suitable habitat is lost, this leads to species extinction on regional or global scales, which in turn negatively affects ecosystem quality. The unit of corresponding biodiversity damage at each step is also shown. PDF is potentially disappeared fraction.

Description of all related impact categories

This impact pathway addresses biodiversity loss and, thus, changes in ecosystem quality.

Methodological choice

Two different sets of CFs are available: (1) marginal CFs, which are typically used in LCA to address impacts of additional land use and (2) average CFs, which are used to assess total impacts of land use within a region.

In ecological and conservation studies, the use of models describing species-area relationships (SARs) is common to predict biodiversity impacts resulting from habitat loss in terrestrial systems (Brook et al 2003). The *classic SAR* model (Arrhenius 1921) is the most commonly used model and defines species richness as a power function, $S = cA^z$, where A is the area, S is the number of species, and c and z are parameters depending on the taxonomic group, region under study, sampling scale and regime (Rosenzweig 1995). This approach of assessing extinction risk is based on the assumption of a binary landscape of either habitat (such as an old-growth forest) or non-habitat (e.g., farmland). In other words, it assumes that the human-dominated areas, such as agriculture and forestry, are totally hostile to biodiversity (Pereira et al. 2012). Therefore, the model has been criticized for overestimation of extinction risk (He & Hubbel 2011). There is a growing recognition that that the human-modified habitats also play an important role in the conservation of biodiversity (Karp et al. 2012). It has been recognized that while some species are highly sensitive to habitat loss and only occur in native habitats, many other species show partial or total tolerance to human-modified habitats, and still other species even benefit from the conditions found in human-modified habitats (Barlow et al. 2007; Proenca et al. 2010).

Alternative models that account for habitat heterogeneity have been proposed to assess patterns of species richness in multi-habitat landscapes. The *matrix SAR* model is one such example where the matrix effects (i.e., the habitat provided by human-modified land) are incorporated into the SAR by calibrating the z value of the power model accounting for taxon-specific sensitivity to each land use type within a heterogeneous landscape (Koh and Gouzoul 2010). However, the matrix SAR model predicts that no species will survive if all *natural* habitat within a region disappears. It predicts very high rates of extinction as the natural undisturbed area within a region tends towards zero. This model outcome is unrealistic for some species which survive in human-modified habitat as well (de Baan 2013b). The *countryside SAR model* has been proposed as an alternative to matrix SAR, recognizing the fact that species adapted to human-modified habitats also survive in the absence of natural habitat (Pereira & Daily 2006). Here, we use the countryside SAR because it is known to outperform both the matrix-calibrated SAR and classic SAR models as shown by Pereira et al. 2014 for projecting tropical bird extinctions.

We first calculate regional CFs using the countryside SAR for five taxa (mammals, birds, reptiles, amphibians, and vascular plants) and six land use types (annual crops, permanent crops, pastures, urban, extensive forestry and intensive forestry). Definitions of each of the land use types are taken from Koellner et al. 2013b. The CFs weighted with vulnerability scores of taxa are then calculated. Ecoregions are used as spatial units because their boundaries approximate the original extent of natural ecosystems before major land use changes and distinct communities of species are known to exist within a given ecoregion (Olson et al 2001).

Spatial detail

The method was applied to 804 ecoregions with varying sizes, resulting in a global coverage. A global average is not considered meaningful but provided for background processes. Country and continental averages are provided based on the share of ecoregions within them.

11.2. Calculation of the characterization factors at endpoint level

Unweighted characterization factors using countryside SAR

The countryside species-area relationship (SAR) model predicts the number of species S_{new} in the remaining habitat area A_{new} as a function of the number of species S_{org} occurring in the original habitat area A_{org} as presented in equation 11.1 (Pereira et al. 2014; Chaudhary et al. 2015; Chaudhary et al. 2016a). The species are classified into species groups sharing similar habitat affinities (h_i) for different habitats in the landscape, given by equation 11.2.

$$\frac{S_{new}}{S_{org}} = \left(\frac{A_{new} + \sum_{i=1}^{n} h_i A_i}{A_{org}}\right)^z$$

Equation 11.1

$$h_i = \left(1 - CF_{loc,i}\right)^{1/z}$$

Equation11.2

Habitat affinities (h_i) are a function of $CF_{loc,i}$ (*local* land occupation characterization factor) which is the relative decrease in species richness (*S*) between a land use type *i* and the regional reference habitat (de Baan et al. 2013a). $CF_{loc,i}$ were available on the resolution of biomes.

The species lost $S_{lost,j,g}$ per taxonomic group *t* due to cumulative land use in an ecoregion *j* is thus given for countryside SAR (equation 11.3) by equation 11.3 (Chaudhary et al.2015):

$$S_{lost,j,t}^{countryside} = S_{org,t,j} - S_{new,t,j} = S_{org,t,j} - S_{org,t,j} * \left(\frac{A_{new,j} + \sum_{i=1}^{n} h_{t,i,j} \cdot A_{i,j}}{A_{org,j}}\right)^{z_j}$$

Equation 11.3

Equation (11.3) calculates the total number of species lost after conversion of the natural habitat to the current land use mix (*average* assessment). This average assessment refers to past conversion of land and not to future conversions, which would be possible as well using the same equations, if the land use of a future point in time is known. In the *marginal* assessment, the impact caused by one additional m^2 of land converted from the current land use mix for the production of a product is calculated. The marginal damage function for the SAR model is given by equation (11.4) as the first derivative of its average damage function by the area lost (de Baan et al. 2013(b)).

$$\frac{dS_{lost,t,j}}{dA_{lost,t,j}} = z_j * \frac{S_{org,t,j}}{A_{org,j}} * \left(\frac{A_{new,j} + \sum_{i=1}^{n} h_{t,i,j} \cdot A_{i,j}}{A_{org,j}}\right)^{z_j - 1}$$

Equation 11.4

This regional damage is then allocated to the different land use types *i* in the ecoregion *j* according to their relative frequency $p_{i,j}$ and the local characterization factor $CF_{loc,t,i,j}$. The allocation factor $a_{i,j}$ for each land use type *i* and ecoregion *j* is given by equation (11.5) (de Baan et al. 2013a):

$$a_{i,j} = \frac{(1 - h_{t,i,j}) * A_{i,j}}{\sum_{i=1}^{n}((1 - h_{t,i,j}) * A_{i,j})}$$

Equation 11.5

Regional characterization factors for occupation of each land use type for the average assessment are calculated by multiplying the species lost per region *j* with the corresponding allocation factor $a_{i,j}$ and dividing this by the area occupied by the land use type, $A_{i,j}$ (equation 11.6) (de Baan et al. 2013(b)). The unit of the CF is *Regional species lost/m^2.*

$$CF_{avg,occ,t,i,j} = \frac{\Delta S_{lost,t,j} * a_{i,j}}{A_{i,j}}$$

Equation 11.6

The regional occupation CFs for *marginal assessment* are calculated using equation 11.7 as a marginal loss of species due to a marginal increase in human used area $\Delta A_{lost,t,j} = 1\ m^2$(de Baan et al. 2013(b)).

$$CF_{marg,occ,t,i,j} = \frac{a_{i,j} * \Delta S_{lost,t,j}}{p_{i,j} * \Delta A_{lost,t,j}}$$

Equation 11.7

For land transformation the regional characterization factors are calculated as a multiplication of $CF_{reg,occ,t,i,j}$ with half the regeneration time (Koellner et al. 2013a, de Baan 2013a), as shown in equation 11.8. The unit is *Regional species lost*years/m².*

$$CF_{trans,t,i,j} = 0.5 * CF_{occ,t,i,j} * t_{reg,t,i,j}$$

Equation 11.8

To calculate impacts, the $CF_{reg\ ,occ}$ is multiplied by the inventory flow of occupation, that is, the land requirements of a product given in *m²·years*. The $CF_{reg,trans}$ is multiplied by the inventory flow of transformation, that is, the amount of land use change per product in *m²*. The two impacts can be summed up into the total regional biodiversity depletion potential (de Baan et al. 2013a) for each taxonomic group *g* expressed in the unit *Regional species lost*years.*

Vulnerability Scores

The vulnerability of the taxonomic groups was quantified with a vulnerability score (VS) as an indicator for global extinction risk (Chaudhary et al. 2015). The VS is a function of the geographic range (GR) of each species and a threat level (TL). The latter indicates the degree of threats the species is already facing, while the former acts as a proxy for potential susceptibility to new anthropogenic threats. This means that small-ranged and endemic species are considered intrinsically rare.

For each animal species the TL was obtained by linearly rescaling the categories defined by the IUCN Red List of threatened species. It varies from 0.2 to 1 (0.2-least concern, 0.4-near threatened, 0.6-vulnerable, 0-8-endangered, 1- critically endangered). The GR (in km²) of each species was obtained from maps provided by IUCN and Birdlife international.

From GR and TL, the VS were calculated as global maps for each species *k* in taxon *t*, and each pixel *p* (0.05° × 0.05°) as the area of the respective pixel ($RA_{k,p}$) where species *k* occurs divided by the total GR of the species (the sum of $RA_{k,p}$) and multiplied with TL_k.

The total $VS_{g,p}$ of each animal taxon *t* in a pixel *p* is obtained by summing values for all species *k* of that taxon which occur in pixel *p* and dividing by the number of species of the taxon present in pixel *p* ($n_{g,p}$, eq. 11.9). The numerator of the equation 11.9 without the threat level has also been referred to as “endemic richness” (see Kier & Barthlott 2001 and Kier et al. 2009) or “global biodiversity fraction” (Waldron et al. 2013).

$$VS_{t,p} = \frac{\sum_{k=1}^{m} \frac{TL_k \cdot RA_{k,p}}{\sum_{p=1}^{r} RA_{k,p}}}{n_{t,p}}$$

Equation 11.9

Using ArcGIS 10.2 (ESRI 2013), the individual $VS_{g,p}$ for all the pixels that occur in an ecoregion *j* are used to calculate the $VS_{g,j}$ for that ecoregion for each taxon *g* (eq. 11.10). $n_{g,j}$ in the equation 11.10 is actually the original species richness ($S_{org,g,j}$) from equation 11.3.

$$VS_{t,j} = \frac{\sum_{p=1}^{n}(VS_{t,p} \cdot n_{t,p})}{n_{t,j}}$$

Equation 11.10

Vulnerability Scores for plants

Vulnerability score for plants are calculated using the approach by Verones et al. 2015 (in preparation). They used global maps of vascular plant species richness (VPSR; Kreft et al.2007) and species range equivalents (endemic richness, $EVPSR_{bioregion}$ from Kier et al. 2009) per 10,000 km² for 90 biogeographic regions. The vascular plant species richness for each biogeographic region ($VPSR_{bioregion}$) was first calculated. The VS was then calculated from Equation 11.11.

$$VS_{plants,bioregion} = \frac{EVPSR_{bioregion}}{VPSR_{bioregion}}$$

Equation 11.11

VS_{plants} is then implemented to the VPSR map on 30 arc minutes resolution. The fraction in equation 11.11 approximates the expression for calculating VS for animal taxa in equation 11.9 by implicitly assuming that the threat level for all plants is equal to 1. Finally the vulnerability score of plants per ecoregion are calculated in the same way as for animal taxa (eq. 11.10), i.e. the ratio of threatened endemic richness to species richness.

VS-weighted Characterization Factors

The unweighted CFs calculated using SARs (equations 11.6, 11.7 and 11.8) for each taxon *t* per ecoregion *j* and land use type *i* are multiplied by VS of that taxa in that ecoregion (eq. 11.10) to obtain weighted-CFs (equation 11.12) for both land occupation and transformation.

$$CF_{weighted,t,i,j} = CF_{unweighted,t,i,j} \cdot VS_{t,j}$$

Equation 11.12

Using the terminology of Kier et al. 2009, the weighted CFs thus gives an estimate of global threatened endemic richness (of taxa *t*) lost per unit of land use. In Waldron et al. 2013 words, it will be global threatened biodiversity fraction lost per unit of land use for the individual taxa *t*. We denote the units of weighted CFs as – Global species eq. lost/m^2 (for land occupation) and Global species eq. lost*years/m^2 (for land transformation).

Damage to the area of protection ecosystem quality

The damage to ecosystem quality due to a land use type *i* in ecoregion *j* is calculated using equations 11.13 -11.15. The weighted CFs from equation 11.12 for each animal taxa *t* and plants are multiplied by factors W_t and W_{plants} respectively. Global potentially disappeared fraction (PDF_{global}) is then obtained by giving equal weighting to plants and animal taxa (see Chapter 1).

$$W_t = \frac{1}{N \cdot (S_{t,world} \times VS_{t,world})}$$

Equation 11.13

$$W_{plants} = \frac{1}{(S_{t,plants,world} \times VS_{plants,world})}$$

Equation 11.14

$$CF_{weighted,aggregated,i,j} = 0.5 \cdot \left(\sum_{t=1}^{4} CF_{weighted,t,i,j} \cdot W_t \right) + 0.5 \cdot \left(CF_{weighted,plants,i,j} \cdot W_{plants} \right)$$

Equation 11.15

Here N = 4 is no. of animal taxa and $S_{t,world}$ is the total global species richness of taxa *t* and is equal to 5,490 for mammals, 10,104 for birds, 9,084 for reptiles, 6,433 for amphibians and 321,212 for plants (WWF Wildfinder 2006).

$VS_{t,world}$ is the world average vulnerability score for taxa *t* calculated from species richness ($S_{org,t,j}$) and vulnerability scores of taxa *g* per ecoregion *j* ($VS_{t,j}$) and divided by their global species richness $S_{t,world}$ (see Chaudhary et al. 2015 – equation S7 of supporting information-1 for more details on calculating taxa-aggregated CFs along with $VS_{t,world}$).

$$VS_{t,world} = \frac{\sum_{j=1}^{804} VS_{g,j} \times S_{org,g,j}}{S_{t,world}}$$

Equation 11.16

$VS_{t,world}$ is equal to 0.44 for mammals, 0.29 for birds, 0.59 for amphibians, 0.46 for reptiles and $VS_{plants,world}$ is equal to 1.0. We denote the unit of these taxa-aggregated CFs as global PDF/m^2 for occupation impacts and global PDF*years/m^2 for transformation impacts.

Taxa-aggregated CFs compatible with other impact categories and for use in full LCA studies

For case studies interested in knowing the biodiversity loss due to land use only, we recommend taxa-aggregated CFs calculated using Eq. 11.15 above.

However, the case studies that apply full LCA of product/processes and are interested in comparing the biodiversity loss due to different drivers or impact categories such as land use, water use, climate change, eutrophication, acidification etc., we recommend using taxa-aggregated CFs calculated using Eq. 11.17 below. In order to make the above taxa-aggregated CFs for land use impacts compatible with other impact categories where so far just the regional species loss is quantified (i.e. without the vulnerability score), we adapted the CFs with a constant *C.* The constant *C* is the median of the ratios of regional and global PDFs across all ecoregions and land-use types calculated using the expression in Eq. 11.15 above. The resulting conversion factor of C = 40 was applied to all CFs. CFs are called global PDF equivalents ($PDF_{global,eq.,i,j}$).

$$CF_{compatible,aggregated,i,j} = CF_{weighted,aggregated,i,j} \times C$$

Equation 11.17

The CFs provided as Excel and maps on the LC-IMPACT homepage rerfer to the CFs calcualted according to Equation 11.17. If the original global species loss fraction is of interest (Eq. 11.15), the results need to be back-converted by dividing them by the factor of 40.

World-average CFs

In many LCA studies, the geographic location of land use for background processes is unknown. For these cases, world average CFs per land use type *i* and taxa *t* are obtained by weighting the CF of each ecoregion by their global area share (Equation 11.18). Also the CFs for some land use types could not be calculated (denoted by NaN in the excel file) because that land use type didn't exist in the ecoregion.

For such cases, the world average CF could be applied (in the maps offered on the Webpage this was not done).

$$CF_{i,t,globalavg} = \sum_{j=1}^{804} CF_{i,t,j} \cdot \frac{A_j}{A_{global}}$$

Equation 11.18

Input Data for Model Parameters

The estimates of model parameters were derived from published empirical data and existing databases. For local characterization factors ($CF_{loc,g,i,j}$), data from global reviews conducted by de Baan et al. 2013b (for all land use types), Elshout et al. 2014 (for agriculture land) and Aronson et al. 2014 (for urban areas) was imported. For z-values (z_j), estimates of Drakare et al. 2006 were used by differentiating between forest, non-forest and island ecoregions. Original species richness ($S_{org,g,j}$) per ecoregion for all taxa were obtained from Olson et al. 2001, Kier et al. 2005 and WWF wildfinder database. Original natural habitat area ($A_{org,j}$), remaining natural habitat area ($A_{new,j}$), and area per land use type for all 804 ecoregions ($A_{i,j}$), were derived from LADA and Anthrome maps (Ellis & Ramankutty 2010). Data for calculating vulnerability scores ($VS_{g,p}$) was imported from IUCN and Birdlife international databases. Finally the regeneration times ($t_{reg,g,i,j}$) calculated by Curran et al. 2014 were used for the calculation of transformation CFs. All the above 8 model parameters were fed into the countryside SAR model to calculate the CFs using equations 11.1 to 11.12 (see Chaudhary et al. 2015 for details).

11.3. Uncertainties

We propagated the parameter uncertainty into the characterization factors using Monte Carlo simulation (1,000 iterations). Triangular probability distribution was assumed for the model parameters - area estimates and z-values per ecoregion. The local CFs were assumed to have non-parametric kernel density and the regeneration times were assumed to follow a lognormal distribution (see de Baan 2013a). Median values along with 95% confidence intervals were calculated for both weighted and unweighted characterization factors for each of the five taxa per land use type and ecoregion. Contribution to variance analysis was carried out to assess the influence of each of the model input parameter on the uncertainty of characterization factors results.

11.4. Value choices

Time horizon

One value choice in the modelling of the land transformation impacts is the time horizon. As explained in the section 1.5 of framework chapter, the further away in time the impact is, the more uncertain its value is, (i.e. lower the level of robustness; see equation 1.4). Biodiversity recovery time (t_{reg}) in a region following the abandonment of human land use ranges from ~80 years to up to ~1200 years depending upon the ecosystem, taxa or the prior land use (Curran et al. 2014). We calculated two sets of transformation CFs. The user can choose between short-term "core" CFs (i.e. those calculated using the 100 year time horizon cut-off, equation 11.19) or CFs "after 100 years" (i.e. after 100 year time horizon). The "core" and "after 100y" CF add up to the total extended transformation CFs (calculated using total recovery times, equation 11.8).

$$CF_{trans,g,i,j} = \begin{cases} 0.5 * CF_{occ,g,i,j} * t_{reg,g,i,j} & \text{for } t_{reg,g,i,j} \leq 100 \\ 100 * CF_{occ,g,i,j} - 0.5 * 100 * \left(\frac{100 * CF_{occ,g,i,j}}{t_{reg,g,i,j}}\right) & \text{for } t_{reg,g,i,j} > 100 \end{cases}$$

Equation 11.19

Level of robustness

The modeling pathway for assessing land use impact on biodiversity relies on ecological models (species area relationship (SAR)) and global datasets and statistical analysis. Therefore, the level of robustness is high for the whole characterization model. As new datasets come along, the estimates of input model parameters can be improved, thereby reducing the uncertainty in the final characterization factors. Further, for the transformation CFs, we provide both the extended CFs and the core CFs (i.e. $t_{reg} \leq 100\ years$). For occupation CFs the time horizon doesn't apply as the impact is typically occurring in less than 100 years.

11.5. Results

The unweighted and weighted characterization factors (CFs) for land occupation and transformation, calculated using both marginal and average approach are presented in Excel files for all 804 ecoregions and 245 countries. In general, the CFs calculated using marginal approach were higher than those with the average approach, but still within the same order of magnitude. Table 11.1 shows the world average CFs calculated using equation 11.18 and average approach.

The CFs for different taxa for most ecoregions were within one order of magnitude across different land use types. The CFs for a particular land use type for a given ecoregion varied by approximately 2 orders of magnitude across five taxa. However, for a given taxa and land use type, the occupation CFs varied by ~5 orders of magnitude across 804 ecoregions. This underscores the importance of regionalized impact assessment within LCA.

Table 11.1: World average endpoint CFs calculated using average approach for land occupation and transformation. Weighted CFs per ecoregion and taxa were first calculated using eq. 11.12. Aggregation across taxa was done using eq. 11.15. CF referring to eq 11.15 are shown in italics, converted CF according to 11.17 in bold. World average values per land use type were finally obtained using eq. 11.18. Mean CFs along with 2.5 & 97.5 percentile values are shown. *

Characterization Factors		Annual crops	Permanent crops	Pasture	Urban	Extensive forestry	Intensive forestry
Occupation (PDF/m^2)	Mean	*2.1*10^{-15}* **8.4*10^{-14}**	*1.5*10^{-15}* **6.0*10^{-14}**	*1.3*10^{-15}* **5.2*10^{-14}**	*2.4*10^{-15}* **9.8*10^{-14}**	*3.7*10^{-16}* **1.5*10^{-14}**	*1.1*10^{-15}* **4.3*10^{-14}**
	2.5%	*-2.0*10^{-16}* **-8.1*10^{-15}**	*-6.9*10^{-16}* **-2.8*10^{-14}**	*-4.9*10^{-16}* **-1.9*10^{-14}**	*2.7*10^{-17}* **1.1*10^{-15}**	*-6.3*10^{-16}* **-2.5*10^{-14}**	*-7.1*10^{-16}* **-2.8*10^{-14}**
	97.5%	*4.7*10^{-15}* **1.9*10^{-13}**	*4.9*10^{-15}* **2.0*10^{-13}**	*4.2*10^{-15}* **1.7*10^{-13}**	*4.9*10^{-15}* **2.0*10^{-13}**	*2.8*10^{-15}* **1.1*10^{-13}**	*4.1*10^{-15}* **1.7*10^{-13}**
Transformation Core (PDF*year /m^2)	Mean	*1.5 *10^{-13}* **6.1*10^{-12}**	*1.1*10^{-13}* **4.3*10^{-12}**	*9.0*10^{-14}* **3.6*10^{-12}**	*1.7*10^{-13}* **6.9*10^{-12}**	*2.7*10^{-14}* **1.1*10^{-12}**	*7.8*10^{-14}* **3.1*10^{-12}**
	2.5%	*-3.2*10^{-14}* **-1.3*10^{-12}**	*-8.9*10^{-14}* **-3.6*10^{-12}**	*-7.8*10^{-14}* **-3.1*10^{-12}**	*1.7*10^{-15}* **6.8*10^{-14}**	*-8.9*10^{-14}* **-3.6*10^{-12}**	*-1.0*10^{-13}* **-4.1*10^{-12}**
	97.5%	*3.6*10^{-13}* **1.4*10^{-11}**	*3.6*10^{-13}* **1.5*10^{-11}**	*3.2*10^{-13}* **1.3*10^{-11}**	*3.7*10^{-13}* **1.5*10^{-11}**	*2.1*10^{-13}* **-** **8.6*10^{-12}**	*3.1*10^{-13}* **-** **1.2*10^{-11}**
Transf. Extended (PDF*year /m^2)	Mean	*2.5 *10^{-13}* **1.0*10^{-11}**	*1.8*10^{-13}* **7.2*10^{-12}**	*1.5*10^{-13}* **5.8*10^{-12}**	*2.9*10^{-13}* **1.2*10^{-11}**	*4.2*10^{-14}* **1.7*10^{-12}**	*1.1*10^{-13}* **4.6*10^{-12}**
	2.5%	*-3.0*10^{-14}* **-1.2*10^{-12}**	*-8.8*10^{-14}* **-3.5*10^{-12}**	*-7.7*10^{-14}* **-3.1*10^{-12}**	*2.8*10^{-15}* **1.1*10^{-13}**	*-8.9*10^{-14}* **-3.6*10^{-12}**	*-1.0*10^{-13}* **-4.0*10^{-12}**
	97.5%	*6.6*10^{-13}* **2.6*10^{-11}**	*6.7*10^{-13}* **2.7*10^{-11}**	*5.9*10^{-13}* **2.4*10^{-11}**	*6.8*10^{-13}* **2.7*10^{-11}**	*3.9*10^{-13}* **1.5*10^{-11}**	*5.5*10^{-13}* **2.2*10^{-11}**

***** The complete list of CFs per taxa, per ecoregion and uncertainty ranges are provided in Excel files. Global CFs calculated using the *marginal* approach and compatible CFs along with the transformation CFs with high level of robustness scenario are also provided in online Excel files.

Two sets of CF were calculated: one average (retrospective) and one marginal set of CF. Both sets of CF did not differ much from each other. It would also be possible to calculate average CF comparing the current situation to a potential future situation of land use. However, to do so scenarios of future land conversion would need to be set up, which would be uncertain in itself.

Further, owing to the lack of species richness and geographic range (GR) data in the IUCN database, characterization factors (CFs) for other species groups such as arthropods, fungi or bacteria could not be calculated. Once the above data gaps for these species groups are filled through research efforts, the calculated CFs can be calculated for them.

The input data used to calculate species extinctions through SAR model come with uncertainties and limitations that should be considered when interpreting the results obtained after applying the CFs provided in this study. Although using the latest published data for input parameters, the calculated CFs still have considerable uncertainty and range from positive to negative (Table 11.1). Contribution to variance analysis showed that the model parameter *local* characterization factors ($CF_{loc,g,i,j}$) contributed the most to the variance of both occupation and transformation regional CFs (see Chaudhary et al. 2015 for details). The local CFs were only available at biome level and their values were assumed to be same for all ecoregions within a biome. More global biodiversity monitoring surveys or meta-analysis (e.g. Chaudhary et al. 2016b) comparing species richness in human-modified land with natural/undisturbed land are needed in future to reduce this uncertainty.

Similarly, area parameters also contributed to uncertainty in final CFs. We could only calculate area share of six broad land use types per ecoregion. As more detailed global land use classification maps differentiating between management practices (e.g. organic vs. conventional agriculture, dense vs. vegetated urban etc.) come along, the accuracy of CFs can be improved.

Finally, other aspects of model uncertainty have been addressed in a previous publication such as the comparison between different SAR models, in particular the matrix and countryside SAR (Chaudhary et al. 2015). Alternative models could be included in the future, e.g. considering habitat suitability models (de Baan et al. 2015). However, for the latter, more data is needed before such an approach can be used on a worldwide scale and for taxa other than mammals.

11.6. References

Alkemade R, van Oorschot M, Miles L, Nellemann C, Bakkenes M, ten Brink B (2009) GLOBIO3: a framework to investigate options for reducing global terrestrial biodiversity loss. Ecosystems 12 (3):374–390.

Aronson, M.F.J., La Sorte, F.A., Nilon, C.H. et al. (2014) A global analysis of the impacts of urbanization on bird and plant diversity reveals key anthropogenic drivers. Proceedings of the Royal Society B: Biological Sciences, 281, 20133330.

Arrhenius, O. 1920. Distribution of the species over the area. Meddelanden fran K. Vetenskapsakademiens Nobelinstitut 4:1–6.

Barlow, J., Gardner, T. A., Araujo, I. S., Ávila-Pires, T. C., Bonaldo, A. B., et al. (2007). Quantifying the biodiversity value of tropical primary, secondary, and plantation forests. Proceedings of the National Academy of Sciences, 104, 18555–18560.

BDM (2004) Biodiversity monitoring Switzerland. Indicator Z9: species diversity in habitats. Bundesamt für Umwelt, BAFU. http:// www.biodiversitymonitoring.ch

BirdLife International;Nature Serve. Bird Species Distribution Maps of the World; BirdLife International: Cambridge, UK and NatureServe: Arlington, USA, 2011.

Brook, B.W., N. S. Sodhi, and P. K. L. Ng. 2003. Catastrophic extinctions follow deforestation in Singapore. Nature 424:420–423.

Chaudhary, A., Verones, F., de Baan, L., and Hellweg, S. (2015). Quantifying Land Use Impacts on Biodiversity: Combining Species-Area Models and Vulnerability Indicators. *Environ. Sci. Technol.*, *49* (16), 9987–9995.

Chaudhary, A., Pfister, S., & Hellweg, S. (2016a). Spatially Explicit Analysis of Biodiversity Loss Due to Global Agriculture, Pasture and Forest Land Use from a Producer and Consumer Perspective. *Environ. Sci. Technol.*, 50(7), 3928-3936.

Chaudhary, A., Burivalova, Z., Koh, L.P. , & Hellweg, S. (2016b). Impact of Forest Management on Species Richness: Global Meta-Analysis and Economic Trade-Offs. *Sci. Rep.* **6**, 23954; doi: 10.1038/srep23954 (2016).

Curran M, Hellweg S, Beck J, Is there any empirical support for biodiversity offset policy? Ecological Applications 24 (4), 617–632, 2014.

de Baan, L., Mutel, C. L., Curran, M., Hellweg, S., & Koellner, T. (2013a). Land use in life cycle assessment: global characterization factors based on regional and global potential species extinction. *Environ. Sci. Technol.*, 47(16), 9281-9290.

de Baan, L.; Alkemade, R.; Koellner, T. (2013b). Land use impacts on biodiversity in LCA: a global approach. Int. J. Life Cycle Assess. 18 (6), 1216−1230.

de Baan, L., Curran, M., Rondinini, C., Visconti, P., Hellweg, S., & Koellner, T. (2015). High-resolution assessment of land use impacts on biodiversity in life cycle assessment using species habitat suitability models. *Environ. Sci. Technol.*, *49*(4), 2237-2244.

Drakare, S.; Lennon, J.; Hillebrand, H. The imprint of the geographical, evolutionary and ecological context on species-area relationships. Ecol. Lett. 2006, 9 (2), 215−227.

Ellis, E.; Ramankutty, N. Putting people in the map: anthropogenic biomes of the world. Frontiers Ecol. Environ. 2008, 6 (8), 439−447.

Elshout, P. M., van Zelm, R., Karuppiah, R., Laurenzi, I. J., & Huijbregts, M. A. (2014). A spatially explicit data-driven approach to assess the effect of agricultural land occupation on species groups. The International Journal of Life Cycle Assessment, 19(4), 758-769.

ESRI. 2013. ArcGIS Desktop, v10.2. Redlands CA, Environmental Systems Research Institute.

Goedkoop, M.; Heijungs, R.; Huijbregts, M.; De Schryver, A.; Struijs, J.; van Zelm, R. ReCiPe 2008 - A life cycle impact assessment method which comprises harmonised category indicators at the midpoint and the endpoint level. Available at: http://lcia.wik.is.

He, F.; Hubbell, S. P. Species-area relationships always overestimate extinction rates from habitat loss. Nature 2011, 473 (7347), 368−371.

IUCN, (International Union for Conservation of Nature and Natural Resources). IUCN Red List of Threatened Species. Version 2012.1. http://www.iucnredlist.org (accessed 26 June 2014).

Karp, D. S., A. J. Rominger, J. Zook, J. Ranganathan, P. R. Ehrlich, and G. C. Daily. 2012. Intensive agriculture erodes β-diversity at large scales. Ecology Letters 15:963–970.

Kier, G., & Barthlott, W. (2001). Measuring and mapping endemism and species richness: a new methodological approach and its application on the flora of Africa. *Biodiversity & Conservation*, *10*(9), 1513-1529.

Kier, G., Kreft, H., Lee, T. M., Jetz, W., Ibisch, P. L., Nowicki, C., ... & Barthlott, W. (2009). A global assessment of endemism and species richness across island and mainland regions. Proceedings of the National Academy of Sciences, 106(23), 9322-9327.

Kier, G.; Mutke, J.; Dinerstein, E.; Ricketts, T.; Kuper, W.; Kreft, H.; Barthlott, W., Global patterns of plant diversity and floristic knowledge. J. Biogeogr. 2005, 32, (7), 1107-1116.

Koellner T, Scholz RW (2008) Assessment of land use impacts on the natural environment. Part 2: generic characterization factors for local species diversity in Central Europe. Int J Life Cycle Assess 13(1):32–48.

Koellner, T., de Baan, L., Beck, T., Brandão, M., Civit, B., Goedkoop, M., Margni, M., Milà i Canals, L., Müller-Wenk, R., Weidema, B., Wittstock, B., 2013a. Principles for life Cycle Inventories of land use on a global scale. Int. J. LCA. Published online March 2012.

Koellner, T.; de Baan, L.; Beck, T.; Brandão, M.; Civit, B.; Margni, M.; Milài Canals, L.; Saad, R.; de Souza, D. M.; Müller-Wenk, R. UNEP-SETAC guideline on global land use impact assessment on biodiversity and ecosystem services in LCA. Int. J. Life Cycle Assess. 2013a, 18 (6), 1188−1202.

Koh, L. P.; Ghazoul, J. A matrix-calibrated species-area model for predicting biodiversity losses due to land-use change. Conserv. Biol. 2010, 24 (4), 994−1001.

Kreft, H. &. Jetz, W. (2007). Global patterns and determinants of vascular plant diversity. In: Proceedings of the National Academy of Sciences 104, 5925–5930.

LADA, Mapping Land use Systems at global and regional scales for Land Degradataion Assessment Analysis. Nachtergaele, F., Petri, M. In LADA Technical Report n.8, version 1.1; UNEP/GEF; 2008.

Milài Canals, L.; Bauer, C.; Depestele, J.; Dubreuil, A.; Knuchel, R.; Gaillard, G.; Michelsen, O.; Müller-Wenk, R.; Rydgren, B. Key elements in a framework for land use impact assessment within LCA. Int. J. Life Cycle Assess. 2007, 12 (1), 5−15.

Millennium Ecosystem Assessment (2005) Millennnium Ecosystem Assessment. Ecosystems and human well-being: biodiversity synthesis. World Resources Institute, Washington.

Olson, D.; Dinerstein, E.; Wikramanayake, E.; Burgess, N.; Powell, G.; Underwood, E.; D'Amico, J.; Itoua, I.; Strand, H.; Morrison, J.; Loucks, C.; Allnutt, T.; Ricketts, T.; Kura, Y.; Lamoreux, J.; Wettengel, W.; Hedao, P.; Kassem, K. Terrestrial ecoregions of the worlds: A new map of life on Earth. BioScience 2001, 51 (11), 933− 938.

Pereira, H. M., Ziv, G., & Miranda, M. (2014). Countryside Species–Area Relationship as a Valid Alternative to the Matrix-Calibrated Species–Area Model. Conservation Biology, 28(3), 874-876.

Pereira, H.; Daily, G. Modeling biodiversity dynamics in countryside landscapes. Ecology 2006, 87, 1877−1885.

Pereira, H.M., Borda-de-Agua, L. & Martins, I.S. (2012). Geometry and scale in species-area relationships. Nature, 482, E3–E4.

Proenca, V. M., Pereira, H. M., Guilherme, J., & Vicente, L. (2010). Plant and bird diversity in natural forests and in native and exotic plantations in NW Portugal. Acta Oecologica, 36, 219–226.

Rosenzweig ML (1995) Species diversity in space and time. Cambridge: Cambridge University Press.

Schmidt J (2008) Development of LCIA characterisation factors for land use impacts on biodiversity. J Clean Prod 16:1929–1942.

Sørensen, T. A method of establishing groups of equal amplitude in plant sociology based on similarity of species content. *Biol. Skr. - K. Dan. Vidensk. Selsk*. 1948, *5* (1-34), 4-7.

The World Conservation Union. 2010. IUCN Red List of Threatened Species. Summary Statistics for Globally Threatened Species. Table 1: Numbers of threatened species by major groups of organisms (1996–2010).

Verones, F., Pfister, S., van Zelm, R., and Hellweg, S. 2015 (in preparation): Biodiversity impacts from water consumption on a global scale for use in life cycle assessment.

Verones, F., Saner, D., Pfister, S., Baisero, D., Rondinini, C., & Hellweg, S. (2013). Effects of consumptive water use on biodiversity in wetlands of international importance. Environmental science & technology, 47(21), 12248-12257.

Waldron, A., Mooers, A. O., Miller, D. C., Nibbelink, N., Redding, D., Kuhn, T. S., ... & Gittleman, J. L. (2013). Targeting global conservation funding to limit immediate biodiversity declines. *Proceedings of the National Academy of Sciences*, *110*(29), 12144-12148.

World Wildlife Fund WildFinder: Online database of species distributions, ver. Jan-06; 2006. http://www.worldwildlife.org/ WildFinder (accessed July 30, 2014).

12.Water stress

Stephan Pfister[1], Francesca Verones[2+], Chris Mutel[3]*

[1]ETH Zurich, Switzerland
[2]NTNU, Trondheim, Norway
[3]Laboratory for Energy Systems Analysis, Paul Scherrer Institute (PSI), Villigen, Switzerland
* pfister@ifu.baug.ethz.ch
[+] francesca.verones@ntnu.no

12.1. Water consumption impacts on human health

12.1.1. Areas of protection and environmental mechanisms covered

The impact assessment method for assessing water consumption concerning the area of protection of human health is described based on Pfister et al. (2009) for the impact pathway (marginal CF), Pfister and Hellweg (2011) for uncertainty assessment, and Pfister and Bayer (2013) for average CFs.

Description of impact pathway

Water for food is one of the main global issues and irrigation is a limiting factor in agricultural production. Food supply is a vital human need and insufficient nutrition accounts for ~3% of overall global health impacts (WHO 2014) and further contributes to impacts form other diseases. While many factors contribute to this issue, reduced water availability caused by water consumption leads to reduced availability for food production and consequent yield losses. The impact pathway for this issue is addressing lack of water for agricultural food production and consequent effects on human health caused by water consumption as described in figure 12.1 and equation 12.1. There are two main parts: (1) a fate factor for water consumption coupled with an exposure factor of for agricultural water consumption, which is summarized as water deprivation factor on watershed level (WDF [$m^3_{deprived}/m^3_{consumed}$]) and (2) the effect factor (EF [cases· yr/$m^3_{deprived}$]), which relates malnutrition cases to a lack of water in agriculture. The fate and exposure is modeled by the water stress index (WSI), which indicates general water deprivation (affecting all users) and the share of water used in agriculture ($WU_{\%A}$) in order to account for the share that agriculture is affected by water deprivation, both ranging from zero to one.

The effect model relates lack of water in food production to malnutrition cases using statistical data analysis and minimum water requirements for personal food provision (WR_{MN}), resulting in a malnutrition potential caused by a lack of water for agriculture. The second part of the effect model accounts for the fact that reduced food production might be compensated by advanced means of technology to enhance food production (e.g. fertilization or irrigation with desalinated water) or imports from other regions. For this purpose the human development factor (HDF) ranging from zero to one, is derived based on the regression analysis of the human development index (HDI, a socio-economic development indicator) of a region and related malnutrition occurrence.

Finally, a damage factor (DF_{MN} [DALY/(yr·case)]) is applied, which relates disability-adjusted life years lost (DALY) from malnutrition to cases of undernourished person.

The counterintuitive fact that irrigated food production might lead to malnutrition due to a lack of water for other agricultural production is due to the fact that in LCA beneficial services of the system are covered in the functional unit (e.g. a kg of potato) and not discounted from the impact assessment. The overall effect of food production might therefore be beneficial for human health. However, whether the output is used for local food supply (directly avoiding the impact pathway), international food markets or biofuel production is part of the system definition and interpretation and therefore all potential impacts should be addressed by this impact pathway, even if water is consumed for crop

production and not just for industrial or municipal purposes, especially when comparing two crops with different origins and life cycle water consumption.

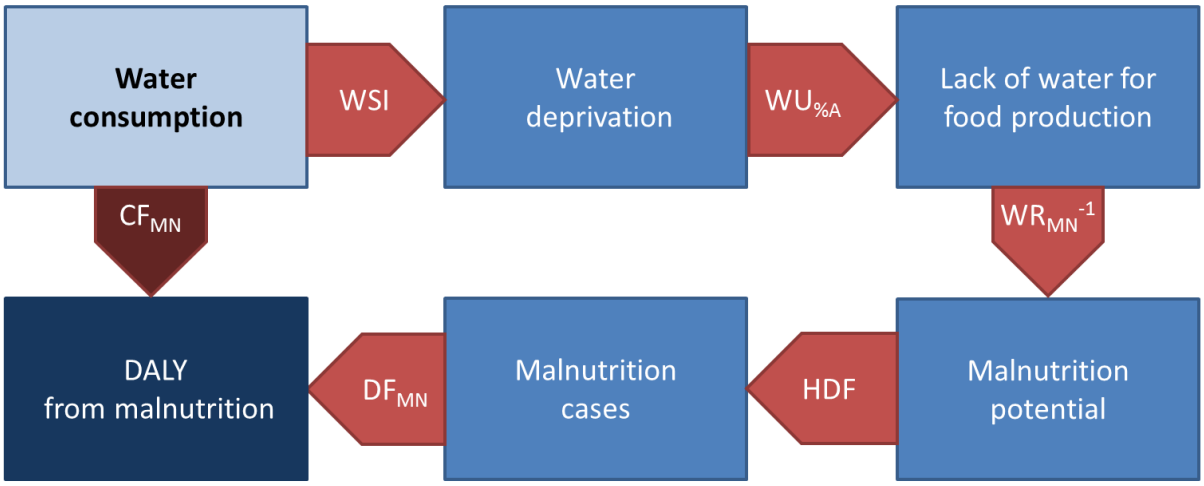

Figure 12.1: Cause-effect chain for human health impacts caused by water consumption. The interim steps of the impact pathways are depicted and the factors leading to them are described in equation 12.1.

$$CF_{end,MN,i} = \underbrace{WSI_i \cdot WU_{\%A,i}}_{WDF_i} \cdot \underbrace{HDF_i \cdot WR_{MN}^{-1}}_{EF_i} \cdot DF_{MN}$$

Equation 12.1

where $CF_{end,MN,i}$ [DALY/$m^3_{consumed}$] is the expected specific endpoint damage per unit of water consumed in watershed i (as specified in the LCI-phase) for malnutrition (MN).

Description of all related impact categories

This impact pathway only affects human health.

Methodological choice

Two different methods are available: (1) marginal CFs, which are typically used in LCA to address impacts of additional water consumption (marginal change in water consumption rate) and (2) average CFs , which are used to assess total impacts of water consumption within a region and to characterize the impact of an activity proportionally to the impact of total water consumption.

Spatial detail

The method was applied to >11'000 watersheds with varying sizes, resulting in a global coverage. Country-average CFs are available too. A global average is not considered meaningful but provided for background processes.

12.1.2. Calculation of the characterization factors at endpoint level

Marginal effect

The characterization factor is defined at the endpoint level in terms of DALY related to water consumption as described in figure 12.1 and equation 12.1. The specific factors are described below.

The water stress index (WSI) is used to indicate the ratio of water consumed that deprives other users in the same watershed of water. Water stress is commonly defined by the ratio of total annual

freshwater withdrawals to hydrological availability (WTA), with moderate and severe water stress occurring above a threshold of 20% and 40%, respectively (Vorosmarty et al. 2000, Alcamo et al. 2000). However, such stress values on global level are expert judgments and thresholds for severe water stress might vary from 20% to 60% (Alcamo et al. 2000) if local conditions are accounted for. For this CF, the concept is extended to calculate a water stress index (WSI) for LCIA, ranging from zero to one. To calculate WSI, the WTA ratio of more than 10'000 individual watersheds described in WaterGAP2 global model (Alcamo et al. 2003) was used. This data is based on annual averages, but both monthly and annual variability of precipitation may lead to changed water stress during specific periods. Especially insufficient water storage capacities or evaporation of stored water may increase the stress. Such increased stress cannot be fully compensated by periods of low water stress (Alcamo et al. 2000). Therefore a variation factor (VF) is introduced to calculate a modified WTA (WTA^*, equation 12.2, figure 12.2), which differentiates watersheds with strongly regulated flows (SRF) from others, as defined by Nilsson et al. (2005). For SRF's, storage structures weaken the effect of variable precipitation significantly, but may cause increased evaporation and a reduced correction factor was applied (square-root of VF):

$$WTA^* = \begin{cases} \sqrt{VF} \times WTA & for\ SRF \\ VF \times WTA & for\ non\text{-}SRF \end{cases}$$

Equation 12.2

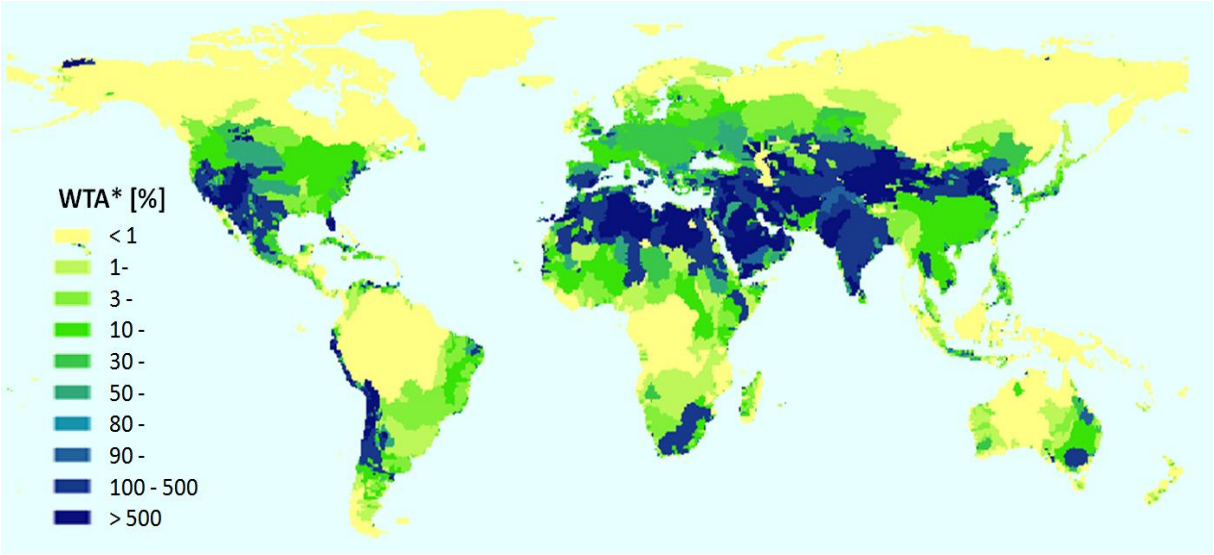

Figure 12.2: WTA^* calculated for each watershed in %. Adopted from Pfister et al. (2009).

VF was derived from the standard deviation of the monthly precipitation time series of CRU TS2.0 (Mitchell and Jones 2005). Since log-normal distribution was found to match better than normal distribution, VF was defined as the aggregated measure of dispersion of the multiplicative standard deviation of monthly (s^*_{month}) and annual precipitation (s^*_{year}), assuming a log-normal distribution and considering precipitation data from 1961-1990 (Mitchell and Jones 2005):

$$VF = e^{\sqrt{\ln(s^*_{month})^2 + \ln(s^*_{year})^2}}$$

Equation 12.3

Variation factors for each grid cell i (VF_i) are aggregated on a watershed-level (VF_{ws}, figure 12.3), weighted by the mean annual precipitation P_i [m] in grid cell i:

$$VF_{WS} = \frac{1}{\sum P_i} \sum_{i=1}^{n} VF_i \cdot P_i$$

Equation 12.4

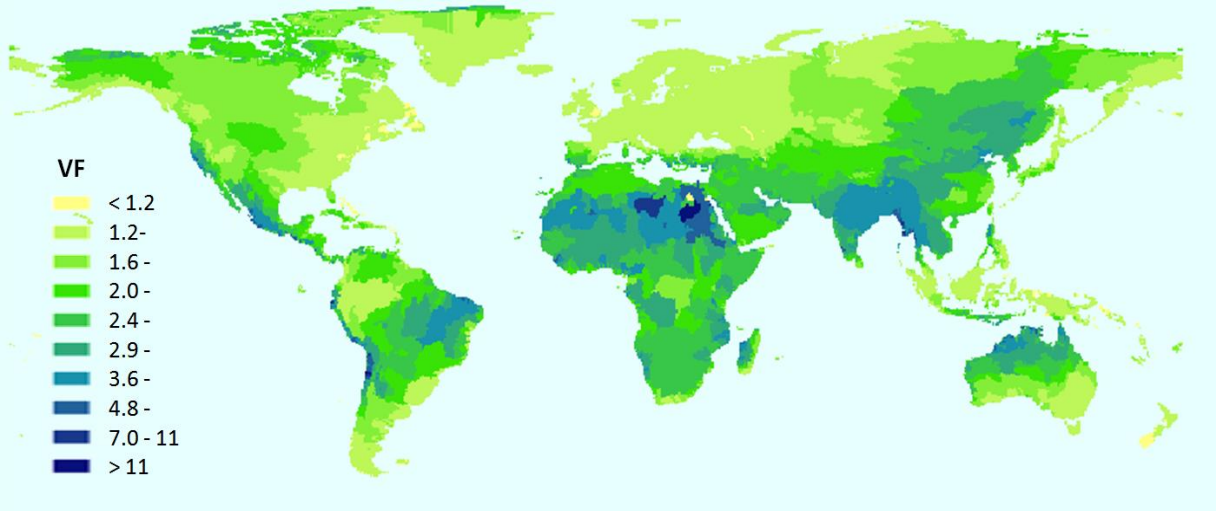

Figure 12.3: VF calculated for each watershed based on data for each 0.5° grid cell. Adopted from Pfister et al. (2009).

Water stress is an indicator for competition and therefore effects are not linear to WTA^* as also indicated by the water stress definitions. The water stress index (WSI, figure 12.4) is therefore adjusted to a logistic function to achieve continuous values between 0.01 (marginal effect in all regions) and 1:

$$WSI = \frac{1}{1 + e^{-6.4 \cdot WTA^*} \left(\frac{1}{0.01} - 1\right)}$$

Equation 12.5

The curve is tuned to result a WSI of 0.5 for a WTA of 0.4, which is the threshold between moderate and severe water stress, when applying the median variation factor of all watersheds (VF_{median} = 1.8, WTA^* = 0.72). Accordingly, WTA of 0.2 and 0.6 result in WSI of 0.09 and 0.91, respectively (Figure 12.5a).

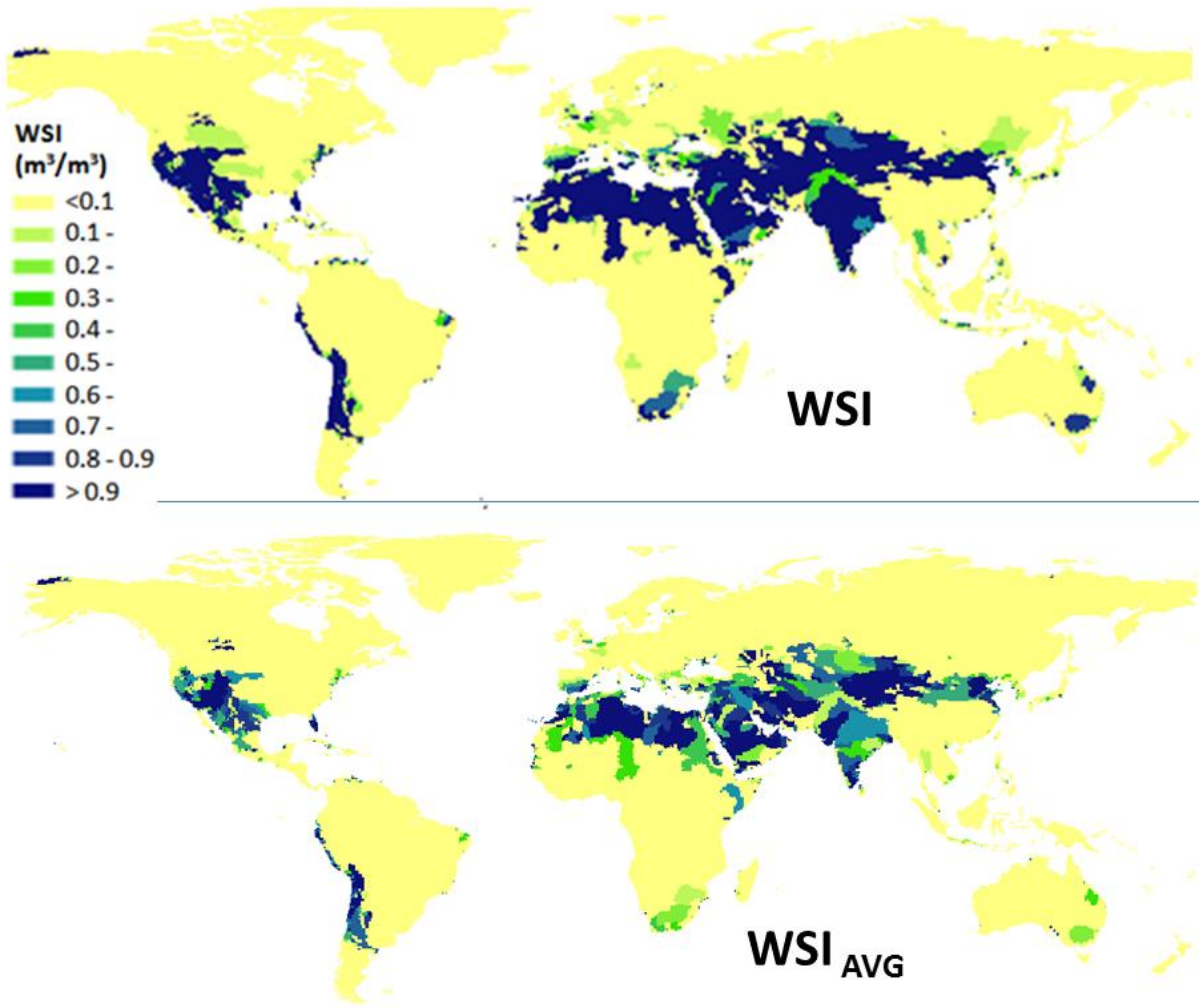

Figure 12.4: Top: Water stress index (WSI) indicating water deprivation potential (adopted from Pfister et al. 2009). Bottom: Average WSI (WSI_{AVG}, equation 12.8)

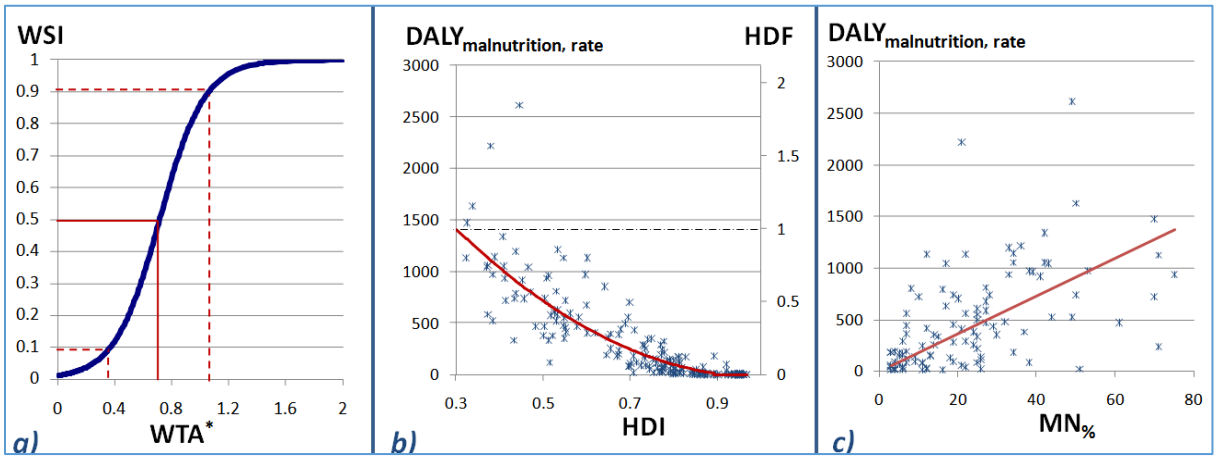

Figure 12.5: Inputs to the impact pathway: a) relation between WSI and WTA^* (blue line, logistic function), b) $DALY_{malnutrition,rate}$ for each country (blue stars) and HDF modeled (red line, $R^2 = 0.71$) based on HDI, c) $DALY_{malnutrition,rate}$ for each country (blue stars) against corresponding $MN_{\%}$ and linear regression (red line, $R^2 = 0.26$). Adopted from Pfister et al. (2009).

Agricultural water use share ($WU_{\%,A,i}$) is calculated for each watershed based on 0.5° grid-data (Vorosmarty et al. 2000) and aggregated without further changes (figure 12.6). It accounts for the fact that agricultural water users might only be affected by the share of agricultural water use. In general agriculture is the most important user except in urban areas.

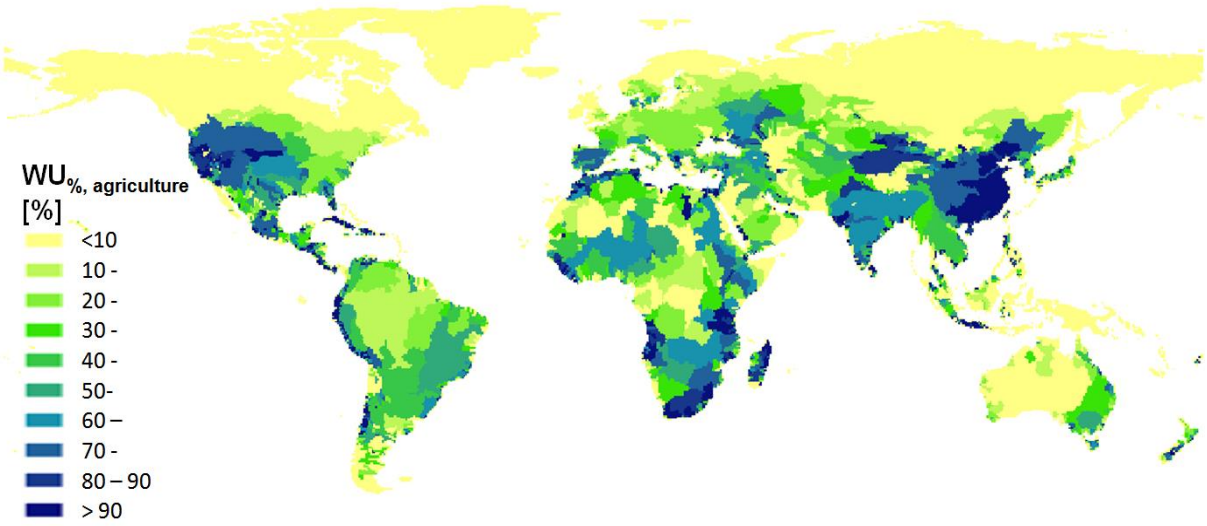

Figure 12.6: Agricultural water use ($WU_{\%,A}$) for each watershed (adopted from Pfister et al. 2009)

The human development factor ($HDF_{MN,i}$) relates the human development index (HDI) to malnutrition vulnerability. National HDIs are reported for all countries (UNDP 2008) and regional HDIs are applied for the large and spatially diverse emerging economies of India, Brazil, China, and Russia (see Pfister et al. 2009 for details). HDF_{MN} is derived from a polynomial fit of DALY values for malnutrition per 100'000 people in 2002 (WHO 2008) with corresponding HDI data (Figure 12.5b):

$$HDF_{MN} = \begin{cases} 1 & for\ HDI < 0.30 \\ 2.03\ HDI^2 - 4.09\ HDI + 2.04 & for\ 0.30 \le HDI \le 0.88 \\ 0 & for\ HDI > 0.88 \end{cases}$$

Equation 12.6

Regions with HDI > 0.88 are considered to have no direct local human health impacts due to adaptation capacity. The regional HDI values are attributed to watershed level based on the area intersections for cross-regional watersheds.

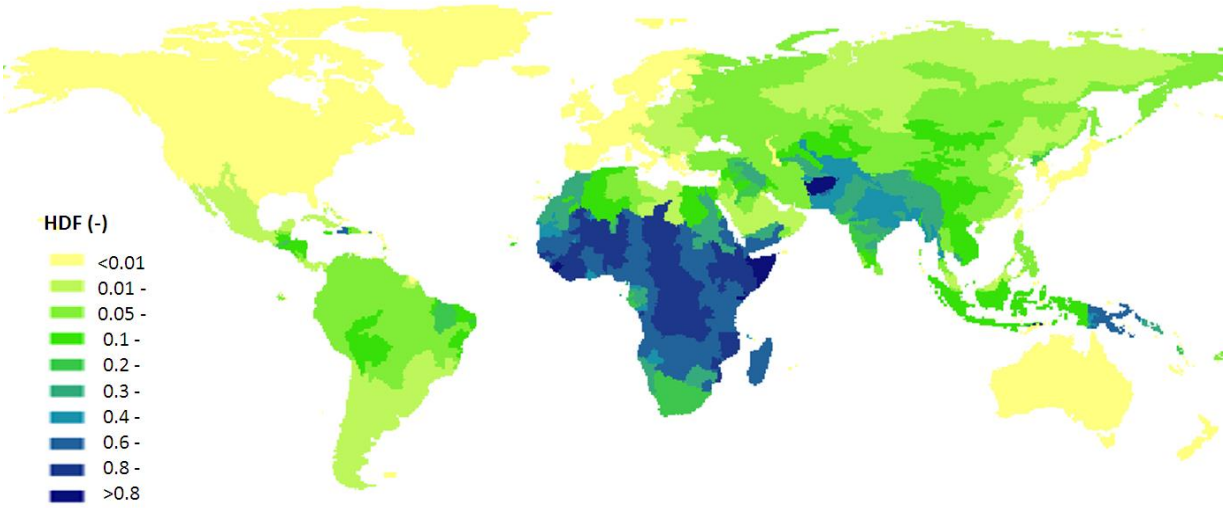

Figure 12.7: HDF_{MN} on watershed level (adopted from Pfister et al. 2009).

Water requirements (WR_{MN}) are used to relate cases of malnutrition to the lack of water for food production. WR_{MN} is set equal to 1,350 m^3/(yr·capita), which is the minimum direct human dietary requirement, including blue and green water (Falkenmark and Rockstrom 2004), accounting for food demand and water productivity of crops. This value matches modeled water resource thresholds for food security (Yang and Abbaspour 2003). While malnutrition already occurs before a person is completely deprived of food (e.g. at a lack of 20%), other compensation effects are assumed to happen (e.g. land use expansion, diet changes). The regression analysis of irrigation water consumption and malnutrition in water scarce developing countries on a global level by Pfister and Hellweg (2011) supported this value, resulting 0.0007 malnourished capita·yr per m^3 of water consumption, which corresponds to a WR_{MN} of ~1400 m^3/(yr·capita). $WR_{malnutrition}$ is a global factor and independent of location.

The damage factor (DF_{MN}) denotes the damage caused by malnutrition and is derived from linear regression of the malnutrition rate ($MN_{\%}$, Nilsson and Svedmark 2002) and $DALY_{malnutrition,rate}$ on country level (WHO 2008, Figure 12.5c) resulting in a per-capita malnutrition damage factor of $1.84 \cdot 10^{-2}$ DALY/(yr·capita).
DALY without age-weighting and discounting for malnutrition are 2.0 times the standard DALYs (3% discounting; age-weighting) originally used in Pfister et al. (2009), based on malnutrition DALY analysis from WHO reports (WHO 2008; WHO 2014)

Average effect

The characterization factor described above defines the marginal effect and is therefore a marginal CF. For the average CF ($CF_{end,MN,AVG}$), the average water stress index (WSI_{AVG}) is applied to quantify the average deprivation of other users. The other elements are already regional averages and do not have to be changed:

$$CF_{end,MN,AVGi} = WSI_{AVG,i} \cdot WU_{\%A,i} \cdot HDF_i \cdot WR_{MN}^{-1} \cdot DF_{MN}$$

Equation 12.7

$$WSI_{AVG} = \frac{\ln\left(e^{-6.4 \cdot WTA^{*}_{monthly}} + \left(\frac{1}{0.01} - 1\right)\right) - \ln\left(e^{-0} + \left(\frac{1}{0.01} - 1\right)\right)}{6.4 \bullet WTA^{*}}$$

Equation 12.8

12.1.3. Uncertainties

Available in second batch (tentative date: end of 2014/beginning of 2015)

12.1.4. Value choices

There are two sets of CFs available for (1) a marginal approach and (2) an average approach. However, within both sets there are no value choices.

Time horizon

The time horizon is infinite, assuming steady-state conditions. The effect of water consumption is described through competition for a renewable resource and therefore current stress levels are relevant. Monthly WSI assessment compatible to this approach have been recently published (Pfister and Bayer 2013) but the impact on human health through food production is based on annual water stress since food production is often based on different crops with different growth periods over several months and therefore a monthly assessment is difficult with currently existing data and is not considered to improve the results significantly.

Level of robustness

The model for human health impacts relies on global datasets and statistical analysis. There is no experimental data for this impact pathway and epidemiological data cannot definitely answer the cause-effect relation. Therefore the level of robustness is moderate for the whole characterization model and in comparison to other impact categories considered to have high level of robustness.
Excluded, due to a low level of robustness, is the effect of decreased food production on international markets and consequent effects in other countries through increased prices in globalized markets, as described in Motoshita et al. (2010b). They assume that if a loss in food production is not leading to local malnutrition effects it will lead to additional food import or reduced food exports and therefore affect countries with lower purchase power and lead to consequent effects on malnutrition in these countries. It might be included in future in the extended CF, once a full publication is available.
The level of robustness for impacts on human health due to a lack of water for domestic use (and consequent impacts on communicable diseases), as partially addressed by Motoshita et al. (2010a) and Boulay et al. (2011), are considered to be very low (Rijsberman 2006, Mila i Canals 2009, UNESCO 2003) and therefore this potential cause-effect chain is excluded.

12.1.5. Results

The range of CFs is from zero in economically developed regions up to ~10^{-4} DALY per m^3 of water consumed in economically less developed regions. In order to properly apply the CFs the geographic location needs to be known for attributing the proper watershed to the inventory. In cases where only national geographic information is available, country average CFs can be applied. Watershed characterization factors are aggregated to country level as withdrawal-weighted average based on the withdrawal data reported by WaterGAP2 (Alcamo et al. 2003) on watershed level. For cross-boundary watersheds, the withdrawal data has been allocated to countries according to the area share in each country. The results of the spatially explicit marginal and average CF are presented in Figure 12.8 on watershed level and. Country-aggregated CFs are provided as Excel table and in Table 12.1. The global average marginal CF 1.8 E-07 DALY /m^3 and the average CF is 1.3 E-07 DALY /m^3.

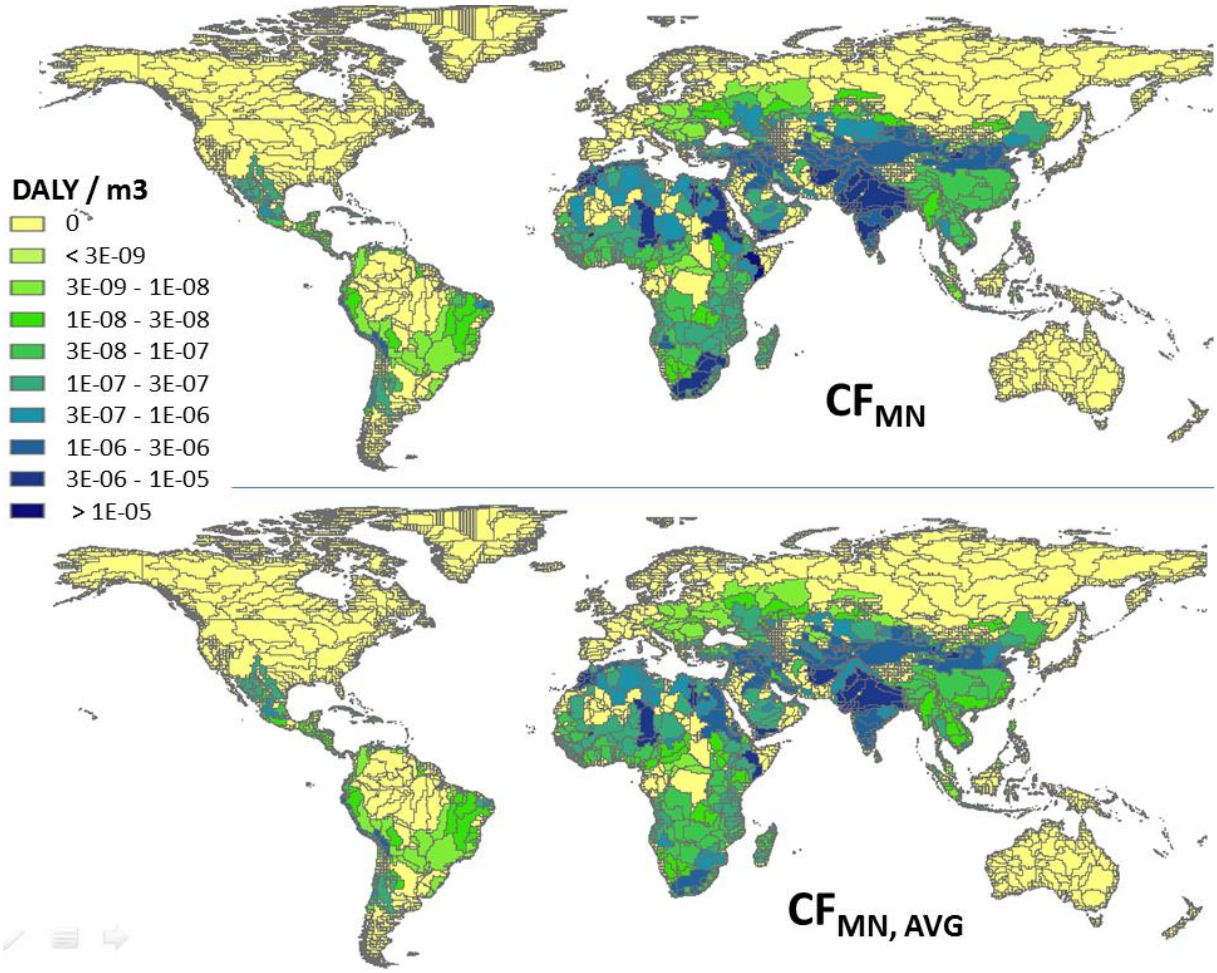

Figure 12.8: CFs for human health impacts caused by water consumption (adapted from Pfister et al. 2009). Top: Marginal CF ($CF_{MN, AVG}$); bottom: average CF ($CF_{MN, AVG}$).

Table 12.1: Overview of CFs on country basis for both marginal and average approach. All CFs are the same for the core and the extended version (see also Excel file).

Country	$CF_{marginal,HH}$ [DALY/m³]	$CF_{average,HH}$ [DALY/m³]
Afghanistan	3.2E-06	3.2E-06
Albania	1.1E-07	5.0E-08
Algeria	1.5E-06	1.5E-06
Angola	1.7E-07	1.3E-07
Argentina	7.2E-08	3.2E-08
Armenia	1.3E-06	1.3E-06
Australia	0.0E+00	0.0E+00
Austria	8.6E-09	3.8E-09
Azerbaijan	1.2E-06	1.2E-06
Bangladesh	4.3E-06	1.9E-06
Belarus	9.8E-09	4.3E-09
Belgium	0.0E+00	0.0E+00
Belize	9.6E-09	9.4E-09
Benin	1.2E-07	1.0E-07
Bhutan	8.0E-08	6.6E-08
Bolivia	9.4E-07	4.1E-07
Bosnia and Herzegovina	6.8E-09	3.0E-09
Botswana	2.3E-06	2.3E-06
Brazil	3.9E-08	3.9E-08
Brunei	0.0E+00	0.0E+00
Bulgaria	1.6E-07	7.2E-08
Burkina Faso	8.2E-08	6.7E-08
Burundi	9.8E-08	9.0E-08

Cambodia	1.3E-07	5.9E-08
Cameroon	2.7E-08	2.6E-08
Canada	0.0E+00	0.0E+00
Central African Republic	5.0E-09	5.0E-09
Chad	1.7E-07	1.4E-07
Chile	3.1E-07	3.1E-07
China	6.3E-07	2.8E-07
Colombia	2.9E-08	2.9E-08
Congo (Democratic Republic of the)	2.6E-08	2.6E-08
Congo (Republic of the)	3.5E-08	3.5E-08
Costa Rica	1.8E-08	1.5E-08
Cote d'Ivoire	5.4E-08	5.0E-08
Croatia	8.8E-09	8.8E-09
Cuba	2.0E-07	9.0E-08
Cyprus	0.0E+00	0.0E+00
Czech Republic	2.5E-09	1.1E-09
Denmark	0.0E+00	0.0E+00
Djibouti	4.6E-07	4.6E-07
Dominican Republic	2.5E-07	1.1E-07
Ecuador	4.0E-07	1.8E-07
Egypt	3.5E-06	3.5E-06
El Salvador	4.7E-08	3.9E-08
Equatorial Guinea	5.3E-11	5.2E-11
Eritrea	1.0E-06	4.5E-07
Estonia	8.2E-10	6.7E-10
Ethiopia	1.5E-06	6.7E-07
Fiji	1.8E-08	1.8E-08
Finland	8.8E-11	3.9E-11
France	0.0E+00	0.0E+00
French Guiana	1.8E-12	1.8E-12
Gabon	1.1E-09	1.1E-09
Gambia, The	6.5E-08	5.3E-08
Georgia	9.1E-07	9.1E-07
Germany	1.0E-09	4.4E-10
Ghana	2.5E-07	2.5E-07
Greece	5.6E-08	5.6E-08
Guatemala	3.3E-08	3.0E-08
Guinea	1.5E-07	1.2E-07
Guinea-Bissau	1.4E-07	1.3E-07
Guyana	2.0E-08	1.9E-08
Haiti	3.8E-07	3.8E-07
Honduras	4.7E-08	4.5E-08
Hungary	8.8E-09	3.9E-09
Iceland	0.0E+00	0.0E+00
India	4.5E-06	4.5E-06
Indonesia	3.9E-07	1.7E-07
Iran	1.4E-06	1.4E-06
Iraq	2.1E-06	2.1E-06
Ireland	0.0E+00	0.0E+00
Israel	2.2E-07	2.2E-07
Italy	0.0E+00	0.0E+00
Jamaica	2.0E-08	1.8E-08
Japan	0.0E+00	0.0E+00
Jordan	8.8E-07	8.8E-07
Kazakhstan	4.9E-07	2.2E-07
Kenya	1.2E-07	9.8E-08
Korea, Democratic People's Republic of	1.2E-06	5.5E-07
Korea, Republic of	0.0E+00	0.0E+00
Kuwait	1.3E-08	1.3E-08
Kyrgyzstan	1.6E-06	1.6E-06
Laos	3.6E-08	2.9E-08
Latvia	9.2E-10	7.5E-10

Lebanon	1.1E-06	1.1E-06
Lesotho	3.2E-06	3.2E-06
Liberia	1.2E-07	1.2E-07
Libya	9.4E-07	9.4E-07
Lithuania	1.1E-09	1.1E-09
Luxembourg	0.0E+00	0.0E+00
Macedonia	4.4E-07	1.9E-07
Madagascar	2.2E-07	1.8E-07
Malawi	1.1E-07	1.0E-07
Malaysia	8.4E-09	8.4E-09
Mali	3.1E-06	1.4E-06
Mauritania	1.4E-07	6.2E-08
Mexico	3.4E-07	3.4E-07
Moldova	7.2E-08	3.2E-08
Mongolia	2.9E-08	2.9E-08
Morocco	3.9E-06	3.9E-06
Mozambique	9.7E-07	4.3E-07
Myanmar (Burma)	4.8E-08	3.9E-08
Namibia	5.4E-08	4.4E-08
Nepal	5.8E-06	5.8E-06
Netherlands	0.0E+00	0.0E+00
New Zealand	0.0E+00	0.0E+00
Nicaragua	7.0E-08	5.7E-08
Niger	1.2E-06	5.5E-07
Nigeria	2.4E-06	1.0E-06
Norway	0.0E+00	0.0E+00
Oman	7.7E-07	7.7E-07
Pakistan	4.4E-06	4.4E-06
Palestine Territory (West Bank)	4.2E-07	4.2E-07
Panama	1.3E-08	1.2E-08
Papua New Guinea	0.0E+00	0.0E+00
Paraguay	7.4E-09	7.1E-09
Peru	1.3E-06	1.3E-06
Philippines	3.1E-07	1.4E-07
Poland	3.9E-09	3.9E-09
Portugal	0.0E+00	0.0E+00
Puerto Rico	0.0E+00	0.0E+00
Qatar	2.4E-07	2.4E-07
Romania	1.3E-08	5.5E-09
Russia	1.1E-07	4.8E-08
Rwanda	6.8E-08	5.5E-08
Saudi Arabia	1.1E-06	1.1E-06
Senegal	1.3E-07	5.9E-08
Serbia and Montenegro	1.4E-08	6.2E-09
Sierra Leone	1.9E-07	1.9E-07
Slovakia	8.4E-09	3.7E-09
Slovenia	8.8E-09	3.9E-09
Solomon Islands	0.0E+00	0.0E+00
Somalia	1.8E-06	7.8E-07
South Africa	2.4E-06	2.4E-06
Spain	0.0E+00	0.0E+00
Sri Lanka	1.9E-06	8.3E-07
Sudan	9.8E-07	4.3E-07
Suriname	1.4E-08	1.3E-08
Swaziland	3.1E-07	2.5E-07
Sweden	0.0E+00	0.0E+00
Switzerland	1.9E-10	8.3E-11
Syria	1.9E-06	1.9E-06
Tajikistan	2.6E-06	2.6E-06
Tanzania, United Republic of	1.3E-07	1.3E-07
Thailand	3.2E-07	1.4E-07
Timor Leste	0.0E+00	0.0E+00
Togo	6.0E-08	5.1E-08

Trinidad and Tobago	2.0E-07	8.7E-08
Tunisia	1.8E-06	1.8E-06
Turkey	1.1E-06	1.1E-06
Turkmenistan	1.8E-06	1.8E-06
Uganda	6.8E-08	5.5E-08
Ukraine	2.9E-07	1.3E-07
United Arab Emirates	4.3E-07	4.3E-07
United Kingdom	0.0E+00	0.0E+00
United States	4.3E-09	1.9E-09
Uruguay	4.6E-09	4.5E-09
Uzbekistan	2.2E-06	2.2E-06
Vanuatu	0.0E+00	0.0E+00
Venezuela	2.3E-07	1.0E-07
Vietnam	7.8E-07	3.4E-07
Western Sahara	4.2E-10	1.9E-10
Yemen	5.2E-06	5.2E-06
Zambia	9.6E-08	9.4E-08
Zimbabwe	7.2E-07	3.2E-07

12.1.6. References

Alcamo J, Henrichs T, Rösch T (2000) World water in 2025: Global modeling and scenario analysis. In: Rijsberman F (ed) World water scenarios. Earthscan Publications, London, pp 243-281

Alcamo J, Doll P, Henrichs T, Kaspar F, Lehner B, Rosch T, Siebert S (2003) Development and testing of the watergap 2 global model of water use and availability. Hydrological Sciences Journal 48 (3):317-337

Boulay A-M, Bulle C, Bayart J-B, Deschênes L, Margni M (2011) Regional Characterization of Freshwater Use in LCA: Modeling Direct Impacts on Human Health Environmental Science & Technology 45:8948-8957 doi:10.1021/es1030883

Falkenmark M, Rockstrom J (2004) Balancing water for humans and nature: The new approach in ecohydrology. Earthscan, London

Mila i Canals L, Chenoweth J, Chapagain A, Orr S, Anton A, Clift R (2009) Assessing freshwater use impacts in LCA: Part I-inventory modelling and characterisation factors for the main impact pathways International Journal of Life Cycle Assessment 14:28-42 doi::10.1007/s11367-008-0030-z

Mitchell TD, Jones PD (2005) An improved method of constructing a database of monthly climate observations and associated high-resolution grids. International Journal of Climatology 25 (6):693-712

Motoshita M, Itsubo N, Inaba A (2010a) Development of impact factors on damage to health by infectious diseases caused by domestic water scarcity. *The International Journal of Life Cycle Assessment*, vol. 16, no. 1, pp. 65–73, 2010a.

Motoshita M, Itsubo N, Inaba A (2010b) Damage assessment of water scarcity for agricultural use 1. in *Proceedings of 9th international conference on EcoBalance.*, 2010b, pp. 3–6.

Nilsson C, Svedmark M (2002) Basic principles and ecological consequences of changing water regimes: Riparian plant communities. Environ Manage 30 (4):468-480

Nilsson C, Reidy CA, Dynesius M, Revenga C (2005) Fragmentation and flow regulation of the world's large river systems. Science 308 (5720):405-408

Pfister S, Koehler A, Hellweg S (2009) Assessing the Environmental Impacts of Freshwater Consumption in LCA Environmental Science & Technology 43:4098-4104 doi:10.1021/es802423e

Pfister S, Hellweg S (2011) Surface water use – human health impacts. Report of the LC-IMPACT project (EC: FP7). . http://www.ifu.ethz.ch/ESD/downloads/Uncertainty_water_LCIA.pdf

Pfister S, Bayer P (2013) Monthly water stress: spatially and temporally explicit consumptive water footprint of global crop production Journal of Cleaner Production doi:http://dx.doi.org/10.1016/j.jclepro.2013.11.031

Rijsberman, F.R., (2006). Water scarcity: Fact or fiction? Agricultural Water Management 80 (1-3), 5-22.UNDP (2008) Human development statistical tools. http://hdr.undp.org/en/statistics/.

UNESCO (2003) Water for people - water for life. The united nations world water development report. UNESCO, and Berghahn Books, Paris

Vorosmarty CJ, Green P, Salisbury J, Lammers RB (2000) Global water resources: Vulnerability from climate change and population growth. Science 289 (5477):284-288

WHO (2008) Death and DALY estimates for 2002 by cause for WHO Member States (2008) http://www.who.int/healthinfo/bodestimates/en/index.html. Accessed 22 February 2008

WHO (2014) GLOBAL HEALTH ESTIMATES 2014 SUMMARY TABLES: DALY BY CAUSE, AGE AND SEX, BY WHO REGION, 2000-2012 (2014) http://www.who.int/healthinfo/bodestimates/en/index.html. Accessed 22 June 2014

Yang H RP, Abbaspour K C, B ZAJ (2003) A water resources threshold and its implications for food security. Environ Sci Technol 37 (14):3048

12.2. Water consumption impacts on ecosystems

12.2.1. Areas of protection and environmental mechanisms covered

The description of the impact assessment approach for quantifying impacts from water consumption on biodiversity is based on Verones et al. (submitted), which is a continuation from Verones et al. (2013a) and Verones et al. (2013b), as well as Chaudhary et al. (2015).

Description of impact pathway

Water is one of the most important resources for both humans and ecosystems. The human population consumes 1-2 trillion m^3 of water each year (WATCH 2011). Of all water used ~70% are used for agriculture as irrigation water, of which 71 % is withdrawn from surface water (World Water Assessment Programme 2009). It is expected that water for crop production will keep increasing in many parts of the world, because of climate change as well as a growing population with consequently larger food demands (Palmer et al. 2009). This might increase irrigation water consumption by ~60% by 2050 (Pfister et al. 2011b). The expansion of human water consumption, increases the pressure on ecosystems that are competing for the same resource (Vörösmarty et al. 2005), which is already highly problematic in many regions. Here, we cover biodiversity impacts of water consumption in wetlands as proxies for aquatic and riparian habitat, as well as impacts of water consumption on vascular plants as proxy for more terrestrial systems. According to the Ramsar Convention, wetlands are defined as "areas of marsh, fen, peatland, or water, whether natural or artificial, permanent or temporary, with water that is static or flowing, fresh, brackish, or salt, including areas of marine water the depth of which at low tide does not exceed six metres" (Ramsar Convention 1994). We only include freshwater systems in our wetland assessment and thus exclude marine and coastal, saltwater influenced wetlands. In these coastal systems a lack of water is often less of a problem, since missing freshwater can be replaced by saltwater. This changes the salinity of the wetlands, which is another impact pathway (Amores et al. 2013) than the one described here, which is focusing on the physical availability of water only. In order to represent biodiversity as good as possible it is advantageous to use a combination of multiple taxonomic groups (Larsen et al. 2012). Species from 5 taxonomic groups were included as proxies for biodiversity (amphibians, reptiles, birds, mammals and vascular plants).

<u>Aquatic and riparian habitats</u>

The quantification of impact consists of a fate and an effect part (Figure 12.9). The fate factor (FF) [$m^2 \cdot yr/m^3$] quantifies the potential change in wetland area[1] due to an increase of water consumption. We distinguish between changes in either groundwater table or surface water volume that both ultimately lead to change in wetland area. The effect factor (EF) [species-eq/m^2] quantifies the potential loss of species diversity on each square meter of lost wetland area. In addition to counting the number of species that is lost, we also introduce a vulnerability score for each species (VS) into the effect factor. VS is informing about the global vulnerability of species to extinction, by taking into account the threat levels of the IUCN Redlist and the individual geographic range area of each species (IUCN 2012). Aggregating the species-equivalents, as described in the framework chapter, results in the CFs being in PDF·yr/m^3. Both fate and effect factors are calculated for more than 20'000 wetlands globally and then assigned to watersheds based on the individual catchment of each wetland, in order to account for the spatial aspect of water consumption. Some wetlands are not included and therefore CF may underestimate the impacts in some areas.

[1] note that we use the term "wetland" for all waterbodies, according to the Ramsar convention, i.e. for lakes, rivers, swamps, etc.

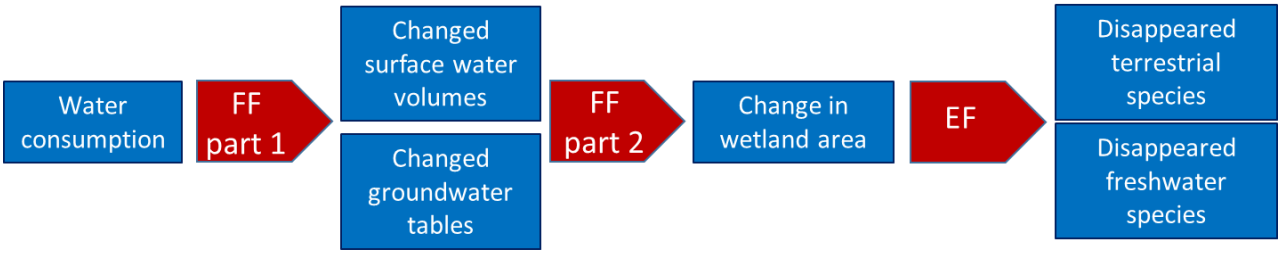

Figure 12.9: Cause-effect chain for modelling the potential loss of species due to water consumption in aquatic and riparian habitat.

The characterization factor at endpoint level ($CF_{end,\ i,t}$) for each watershed i and taxonomic group t is thus calculated according to equation 12.9. Taxonomic groups used are birds, mammals, reptiles and amphibians.

$$CF_{end,i,t} = \frac{\sum_{i,k=1}^{n} FF_{k,t} \cdot EF_{k,t}}{S_t \cdot VS_t}$$

Equation 12.9

Where $FF_{k,t}$ is the fate factor of wetland k and taxonomic group t and $EF_{k,t}$ is the effect factor of wetland k and taxonomic group t. S and VS are the species richness and vulnerability score of taxonomic group t, respectively and are used to transform the species-equivalents to PDF again. Keep in mind that these are global extinctions. These CFs have a spatial coverage indicating the "catchment" area of each wetland (i.e. the area that has an influence on the respective wetland). Note that the CF can vary within one watershed, since not all wetlands are affected by all water consumption in the watershed (i.e. they are not affected if they lie upstream of the location where water consumption happens) (see also explanation further below and figures 12.13 and 12.14).

Terrestrial habitats

The characterization factor consists of a fate and an effect part (Figure 12.10).

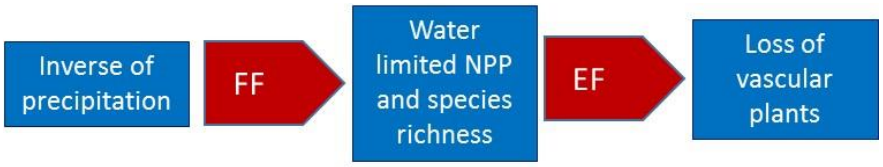

Figure 12.10: Cause-effect chain for modelling the potential loss of species due to water consumption in terrestrial habitat.

The FF [m^2·yr/m^3] indicates for each watershed the land occupation required to generate a volume of water consumed as the inverse of precipitation (see also Pfister et al. (2009)). The FF thereby accounts for the fact, that the water cycle includes interactions with soil and terrestrial ecosystems from a more conceptual perspective. The EF [species-eq/m^2] is quantifying vascular plant species loss per region, based on the water limited share of net primary productivity of plants, endemic species richness and the regional species accumulation factor z (Pfister et al. 2010). The CFs are calculated on a watershed basis w for the taxonomic group of vascular plants. In order to derive global PDF, we divide with the global richness of vascular plants (equation 12.10)

$$CF_{end,w} = \frac{FF_w \cdot EF_w}{S_{plants}}$$

Equation 12.10

Where FF_w is the average fate factor on a watershed basis and EF_w is the effect factor on a watershed basis for vascular plants. S is the global species number of vascular plants. Due to unavailability of data VS was assumed to be 1 for plants.

Description of all related impact categories

This impact pathway only affects ecosystem quality.

Methodological choice

There is one method available, which assesses impacts on wetland biodiversity (animal species) from marginal changes in water consumption and one that assesses the marginal impacts on vascular plants species. We include a vulnerability score for animal species. The aggregation procedure between the taxonomic groups is described in the framework chapter. The aggregation between plants and animals is achieved by taking the average between the aggregated animal CF and the plant CF.

Spatial detail

Characterization factors (CFs) are available for the globe with a resolution of 0.05° x 0.05° (see also explanation on assigning wetland specific factors to hydrologically relevant units below). Country-averaged CFs and continental averages are available too. A global average is provided for background processes. Averaging was based on total consumption of the year 2010 (for irrigation, livestock, municipal use, electricity generation and manufacturing) based on Pfister et al. (2011a) and WATCH (2011).

12.2.2. Calculation of the characterization factors at endpoint level – animal species

The fate factor (FF) is used to indicate the change in wetland area due to water consumption. In the modelling procedure we distinguish between wetlands that are fed by surface water (e.g. by rivers and creeks, precipitation or snowmelt) and wetlands that are predominantly fed by groundwater. The former are only affected by surface water consumption, the latter only by groundwater abstraction. We assume that there is no interaction between surface and groundwater and a wetland is either purely dependent on surface water or purely dependent on groundwater, in order to account for the dominant hydrological process. All wetlands are modelled as circular cones. A graphical representation of the modelling procedure is shown in Figure 12.11.

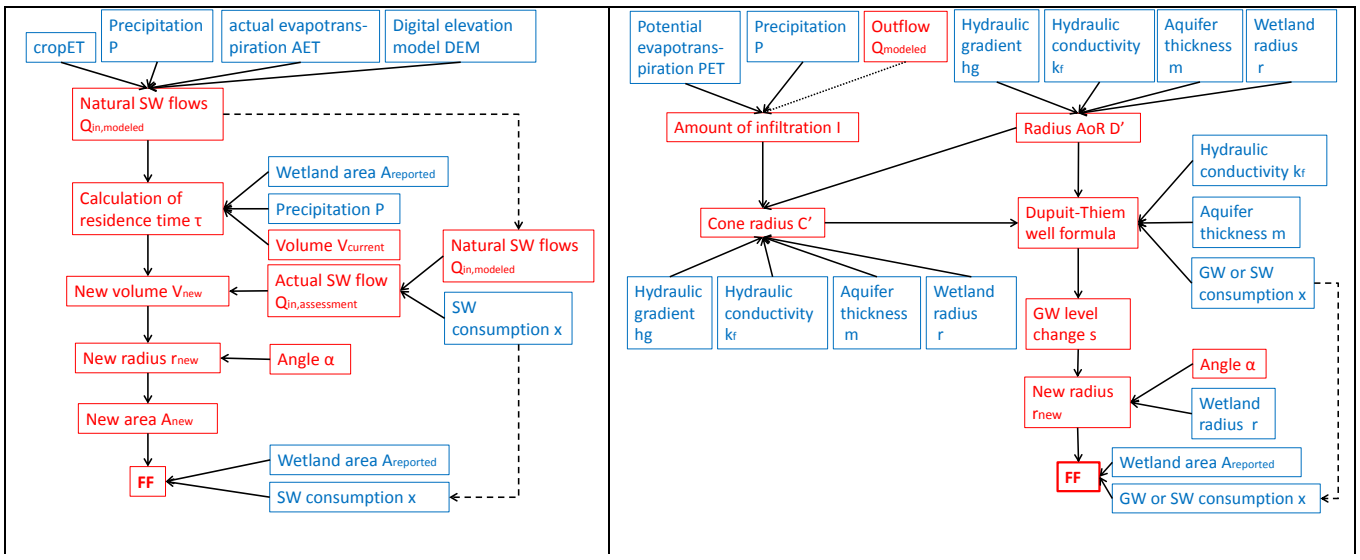

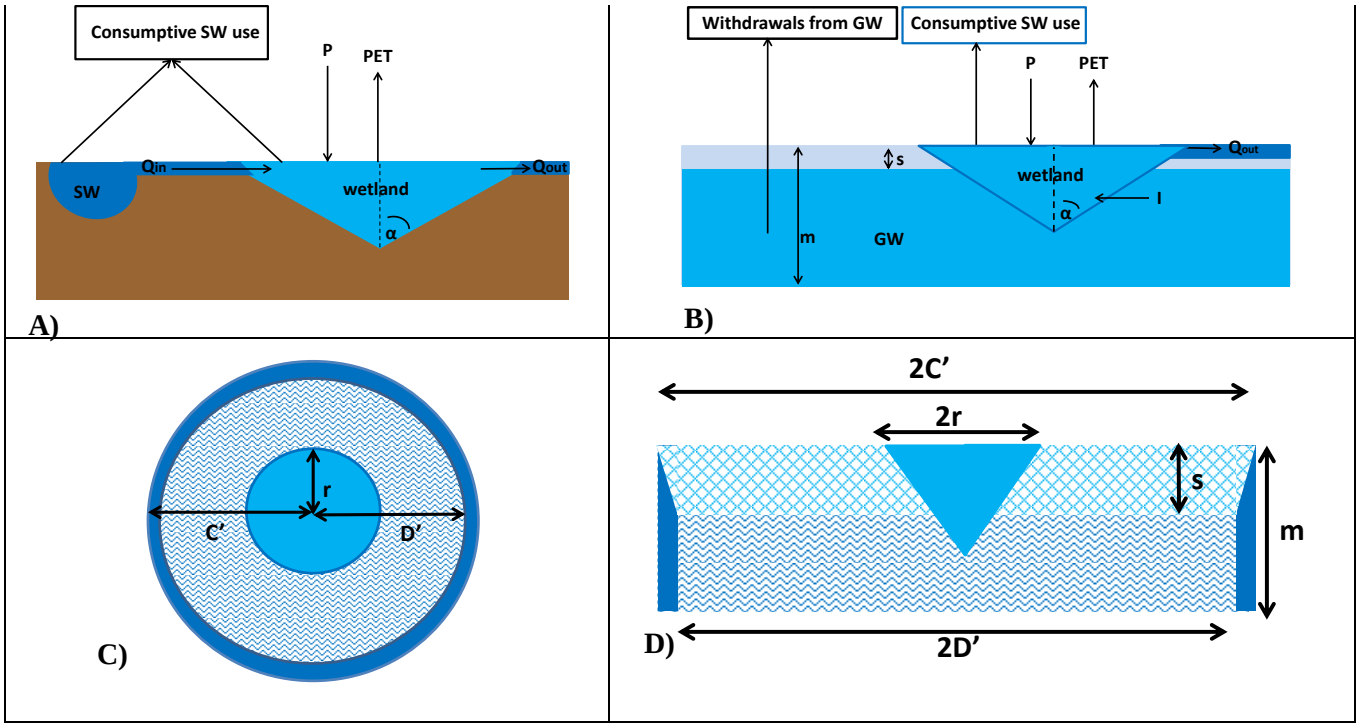

Figure 12.11: Schematic representation of the calculation procedure of the FF for A) surface water-fed (SW) wetlands and B) groundwater-fed (GW) wetlands. Red boxes show modelled parameters, blue boxes show empirical data inputs (for data sources see Verones et al. (2013a)). The dotted lines in pictures A) and B) show that this parameter is only required in some cases. The dashed lines show that parameters in those boxes are the same. Pictures C and D show schematically the way of calculating groundwater drawdowns. The radius of the wetland is r. The defined area of relevance (radius D') is assumed as the hypothetical well, leading to a depression cone with radius C'. In picture D a cross section of the situation in C is shown, with the aquifer thickness m. The wetland is shown as blue triangle. Picture adopted from Verones et al. (2013a).

The FF for both surface water (SW)-fed and groundwater (GW)-fed wetlands is calculated for each wetland k as shown in equation 12.11 where $A_{reported}$ is the reported, empirically known wetland area and A_{new} is the modelled wetland area after water consumption x. We assume x to be an increase in consumption of 1000 m^3/yr.

$$FF_k = \frac{\left(A_{reported,k} - A_{new,k}\right)}{x_k}$$

Equation 12.11

For SW-fed wetlands A_{new} is calculated according to equation 12.12, based on a new wetland radius r_{new}. The new wetland volume V_{new} is estimated based on a change in residence time τ and a change in water inflow, due to water consumption x. Angle α is the angle between the embankment of the wetland and an imaginary, vertical line at the center of the wetland, estimated from actual wetland depth and size.

$$A_{new} = r_{new}^2 \cdot \pi = \left(\left(\frac{3}{\pi} \cdot V_{new} \cdot \tan(\alpha)\right)^{\frac{1}{3}}\right)^2 \cdot \pi$$

Equation 12.12

For groundwater-fed wetlands we assume that the wetland is acting like a pump (through evapotranspiration and outflow). Thereby the evapotranspiration is the driving force and causes water from a certain area around the wetland (denoted area of relevance, AoR) to flow towards the wetland.

The AoR is at least the size of the wetland itself and is calculated based on the infiltration into a wetland, hydraulic conductivity and aquifer thickness of at each wetland's site. Both hydraulic conductivity and aquifer thickness are empirical data inputs. The new wetland area A_{new} is calculated as shown in equation 12.13 where $r_{reported}$ is the radius from the reported wetland area and s is the drawdown of the water level in the wetland that is created due to water abstraction.

$$A_{new} = r_{new}^2 \cdot \pi = \left(-s \cdot tan(\alpha) + r_{reported}\right)^2 \cdot \pi$$

Equation 12.13

Assuming steady-state conditions the depth of the depression cone stems from equation 12.14, which is the well formula of Thiem-Dupuit (Stelzig 2012). We set x_{GW} to 1000 m^3/yr and used this equation to determine the drawdown s.

$$x_{GW} = k_f \cdot \pi \cdot \frac{m^2 - (m-s)^2}{ln\frac{C'}{D'}}$$

Equation 12.14

C' and D' are the radius of the depression cone and the radius of the area of relevance, respectively. The latter is calculated based on the amount of infiltration I that reaches the wetland in a given hydrogeological setting with hydraulic conductivity k_f, aquifer thickness m and a pre-defined minimal hydraulic gradient to have an influence (a gradient is needed for water to flow). The radius of the area of relevance D' is at least the same value like the wetland radius r before water consumption. D' is used to determine the area of the respective CF. The radius of the cone C' is calculated analogously, but in addition to the infiltration amount required to sustain the wetland at the area it is now, also the amount x_{GW} has to be covered and therefore the CF is non-linear and depending on the x_{GW} used. Further details and formulae can be found in Verones et al. (2013a).

The effect factor (EF) is based on the species-area relationship for estimating the potential loss in species. The number of lost species is quantified with equation 12.15 where S_{lost} is the number of lost species, A_{new} and $A_{reported}$ are the new and empirically reported wetland area and $S_{original}$ is the original species richness. The exponent z indicates the slope of the species-area relationship and differs for each taxonomic group (birds: 0.37, mammals: 0.34, amphibians: 0.2, reptiles: 0.33). We calculated these values from Drakare et al. (2006), as explained in further detail in Verones et al. (2013b).

$$S_{lost} = \left(1 - \left(\frac{A_{new}}{A_{reported}}\right)^z\right) \cdot S_{original}$$

Equation 12.15

The values for $S_{original}$ are taken from global species maps that we calculated from IUCN data on geographical ranges of individual species (IUCN 2013b). Note that these maps (see example in Figure 12.12) are based on current species richness, i.e. species that are already extinct are excluded.

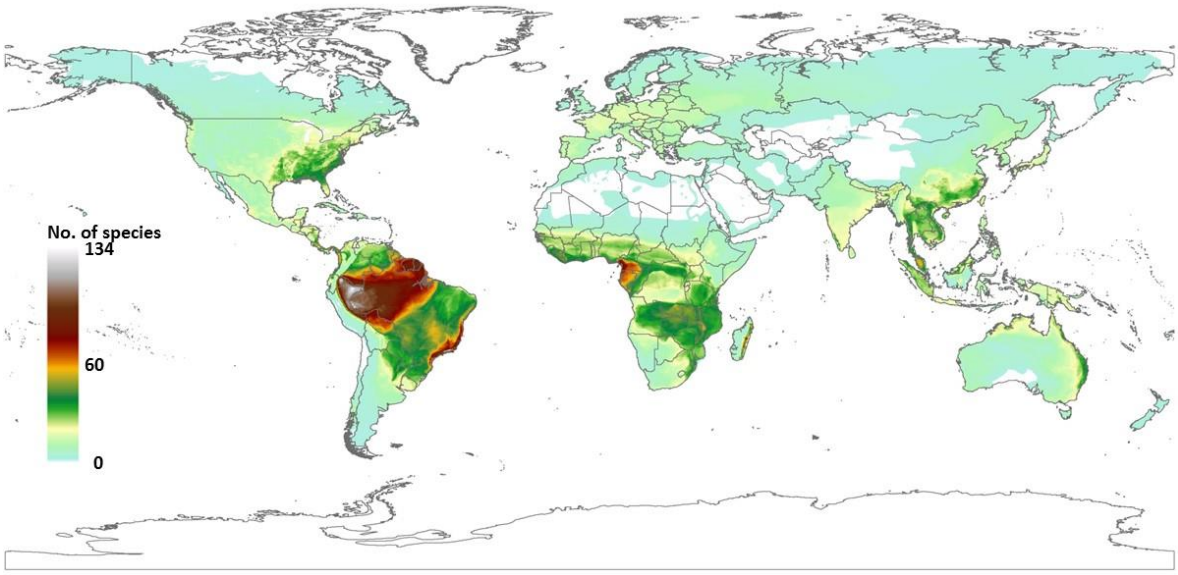

Figure 12.12: Map showing the species numbers of amphibians with a resolution of 0.05° x 0.05°. Data from IUCN (2013b). Adopted from Verones et al. (submitted).

The EF of wetland k for taxonomic group t is then calculated as shown in equation 12.16 based on the numbers of lost species S_{lost} per taxonomic group t and the loss in area that has already been calculated in the fate factor calculation. $VS_{k,t}$ is the vulnerability score of taxonomic group t in wetland k. This is important to translate local sepcies loss into global species loss equivalents.

$$EF_{k,t} = \frac{S_{lost,k,t}}{A_{reported,k} - A_{new,k}} \cdot VS_{k,t}$$

Equation 12.16

The vulnerability score is derived from information on IUCN threat levels (IUCN 2013a) and the geographical range areas of species (IUCN 2013b) for each taxonomic group t according to equation 12.17. TL is the threat level of species i and GR is the geographical range of species i. The average VS of all species within a taxa is calculated on a pixel level (0.05° x 0,05°), denoted j. VS varies between 0 and 1. The values for the TL are chosen on a linear scale: 0.2-least concern, 0.4-near threatened, 0.6-vulnerable, 0.8-endangered, 1-critically endangered.

$$VS_{t,j} = \frac{\sum_{i=1}^{n} \frac{TL_{i,j} \cdot GR_{i,j}}{\sum_{i,j=1}^{m} GR_{i,j}}}{S_{t,j}}$$

Equation 12.17

An example of a vulnerability score map with resolution 0.05° x 0.05° is shown in Figure 12.13. Table 12.2. shows the used species numbers and global vulnerability scores for animal species.

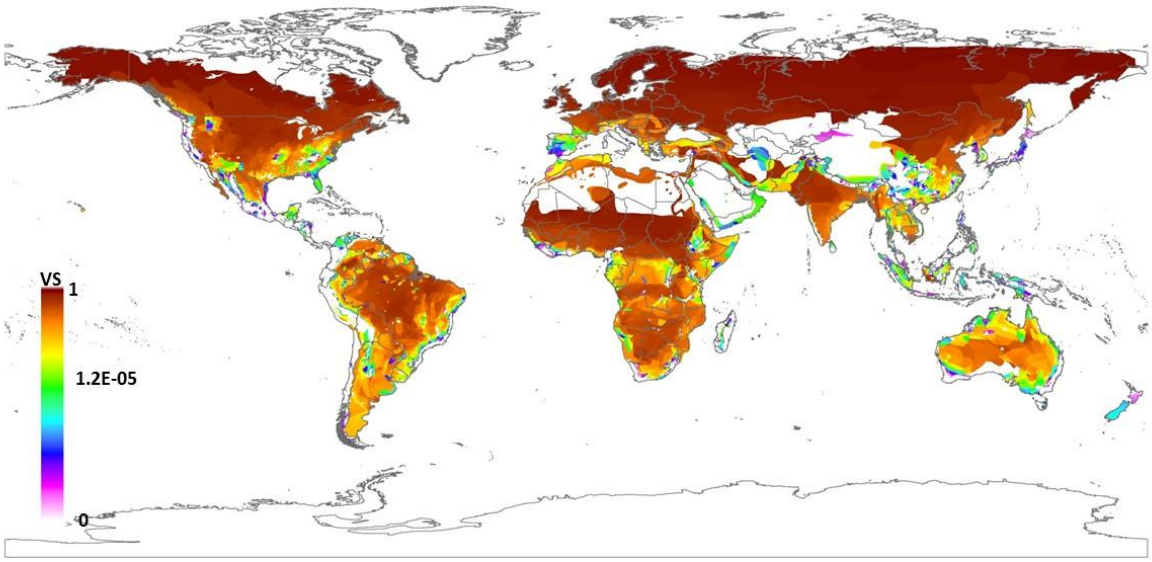

Figure 12.13: Vulnerability score for amphibians with a resolution of 0.05° x 0,05°. Data from IUCN (2013b) and (IUCN 2012). Adopted from Verones et al. (submitted).

Table 12.6: Global species richness $S_{t,world}$ and global vulnerability scores ($VS_{t,world}$), as considered for calculating aggregated characterization factors. Data from IUCN.

Taxon t	$S_{t,world}$	$VS_{t,world}$
Birds	10104	1.58E-04
Mammals	5386	1.93E-04
Amphibians	6251	1.07E-03
Reptiles	3384	4.09E-04

Characterization factors (CFs) are calculated for each wetland individually (multiplication of fate and effect factor). Then, these values are assigned to the hydrologically relevant parts of major watersheds. For surface water-fed wetlands these relevant regions within a major watershed are determined from a hydrologically corrected digital elevation model. We selected all parts of a major watershed that were at the same or at higher elevation that the wetland itself, excluding parts that do not have a physical connection to the wetland in question. The CF of a wetland is applicable in that area, since any upstream water consumption deprives the wetland of water. The areas with CFs of all wetlands in a specific location are superimposed and summed. This is schematically shown in Figure 12.14.

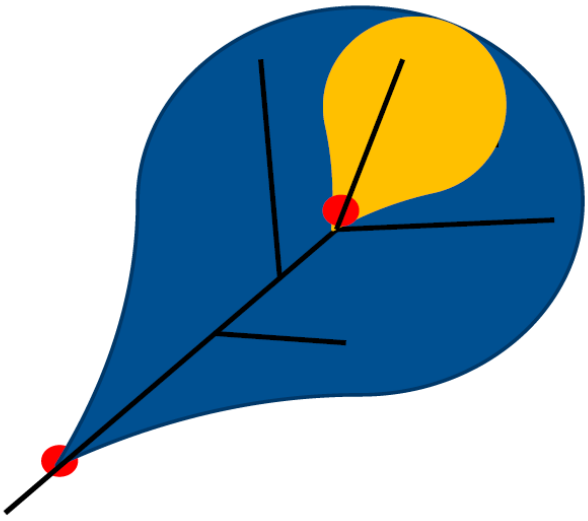

Figure 12.14: Schematic representation of the procedure for assigning values to watersheds for surface water-fed wetlands. Two wetlands are depicted with red dots; the river network is shown in black. The individual catchment of the

two wetlands are shown in orange and blue. Where the orange and blue catchments overlap the CFs of both wetlands are summed. Water consumption in that area will deprive both wetlands of water and thus damages both. Water consumption in the blue area, does not affect the wetland with the orange catchment, thus in this area inly the CF of the second wetland is applicable. Adopted from Verones et al. (2013b).

For groundwater-fed wetlands a similar procedure is used. The characterization factor is assumed to be applicable in the whole area of relevance (AoR) around the wetland, i.e. within the area from which water is drawn towards the wetland. If two or more of these areas of relevance overlap, the respective CFs are summed, since water consumption in that area would damage multiple wetlands (Figure 12.15).

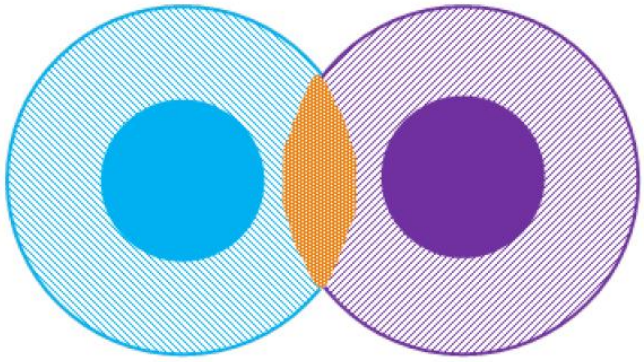

Figure 12.15: In solid blue and solid violet two groundwater-fed wetlands are shown. The hatched areas around them are the areas of relevance, in which the CF of each wetland is applicable. In the orange part the two areas of relevance overlap and the CFs of both wetlands is summed. Adopted from Verones et al. (2013b).

Note that CFs are first calculated for each taxonomic group separately in spercies-eq·yr/m^3. In order to be consistent with all impact categories, we follow the aggregation procedure described in the framework chapter, to provide final CFs in PDF·yr/m^3, aggregated over all taxonomic groups considered.

12.2.3. Calculation of the characterization factors at endpoint level – vascular plants

The fate factor is taken from Pfister et al. (2009). They assume that in water-limited environments plant growth may be obstructed by water consumption, since plants will be deprived of the water they need for growing by avoided floods or decreased groundwater levels. There is no distinction between the source of water. The fate factor is calculated as the inverse of spatially-differentiated precipitation with a minimum of 10^{-2} m/year), which is used to indicate the area-time that is affected by a certain water consumption volume for each watershed. By doing so, it is a rather conservative approach.

The effect factor for vascular plants is taking the plant species richness S,, the endemism richness factor ERF the water-limited net primary productivity $NPP_{water\text{-}limited}$ and a species accumulation factor z into account (equation 12.18). This effect factor thus gives the potential damage in endemic species-equivalents.

$$EF_i = NPP_{water-limited} \cdot z_i \cdot S_{vascular\ plant,i}$$

Equation 12.18

The $NPP_{water-limited}$ is the net primary productivity (NPP) share that is water-limited (see Pfister et al. (2009). The species accumulation factor z is used to account for regional species loss by the species-area relationship, as described in ReCiPe method (Goedkoop et al. 2009), and is depending on ecosystem conditions (Pfister et al. 2010). In order to account for the total of potentially lost species, we apply species richness S of vascular plants taken from Kreft et al.(2007).

The characterization factor is calculated by multiplying effect and fate factors on a watershed level. For this, the regional EFs and FFs are averaged on a watershed level. In order to transform the unit to PDF, we use the global species richness of vascular plants (315'903, Kier et al. (2009)).
Characterization factors for animals and plants were aggregated as described in chapter 1.

12.2.4. Uncertainties

Sensitivity analyses were performed for water depth, the chosen wetland geometry, and the amount of water consumed (10 m^3/yr and 1'000'000 m^3/yr instead of 1000 m^3/yr). For surface water-fed wetlands the amount of water inflow was changed from the own model to WaterGap values (WATCH 2011) and for groundwater-fed wetlands we also tested the influence of the hydraulic conductivity.

The sensitivity of the groundwater-fed wetlands was much larger than for the surface water-fed wetlands. CFs can vary more than 1000% in extreme cases, depending on the parameter changed (Verones et al. 2013b). Largest influence had the amount of water consumed, because of the non-linear character of the Dupuit-Thiem well formula. Also the hydraulic conductivity leads to substantial influence on the groundwater-fed wetlands, leading to less robust values for groundwater consumption than for surface water consumption (see also the Supporting Information of Verones et al. (Verones et al. 2013b)).

Surface water-fed wetlands proved to be only slightly sensitive to changes in water depth (less than 1%, see Verones et al. (Verones et al. 2013a)). Hydrological inflow data did have implication (up to 100% difference, see Verones et al. (Verones et al. 2013a)), especially because of differences in river width and the exact geographical course of the river (based on hydrologically corrected DEMs)

Differences between an ellipsoid or a straight cone assumption for the wetland geometry proved to be marginal. An overview of all other tested parameters and their influence is shown in the appendix. It is not possible to quantitatively analyse all of the identified uncertainties. Monte Carlo simulations are for example not automatically possible for groundwater-dependent wetlands, because the CFs cannot be derived in an analytical way, but need numerical iterations. However, we attempted to highlight relevant uncertainties and, if possible assess their impact in a qualitative way.

For the effect factor uncertainties are due to the range models of the taxonomic groups. Geographical ranges overestimate the species richness present in a certain location and thus we have to assume that our values are rather high.

12.2.5. Value choices

Time horizon

There are no value choices to be made for the time horizon. It is an infinite time horizon, assuming steady-state conditions.

Level of robustness

The level of robustness varies strongly between surface water-fed wetlands, groundwater-fed wetlands and terrestrial habitats, and hence between surface water consumption and groundwater consumption. It is recommended to use aggregated characterization factors for surface water consumption and terrestrial habitats as default, core values and only include groundwater-fed wetlands if the complete impact shall be assessed (extended version). We consider groundwater-fed wetlands to be of low level of robustness since they have much larger uncertainties and considerably less data available.

12.2.6. Results

The CFs range from 1.4E-18 PDF·yr/m^3 to 1.2E-11 PDF·yr/m^3 for the core values and from 1.4E-18 PDF·yr/m^3 to 6.4E-11 PDF·yr/m^3 for the extended CFs. Both are considering vulnerabilities of animal taxa. CF maps are shown in Figure 12.16 and 12.17. Global averages are shown in Table 12.3. In Table 12.4 and in the associated Excel files country averages for the CFs are listed. Table 12.5 shows continental averages. Spatially explicit characterization factors are available as Google Earth layers (on a country level) and as ArcGIS raster files (pixel specific).

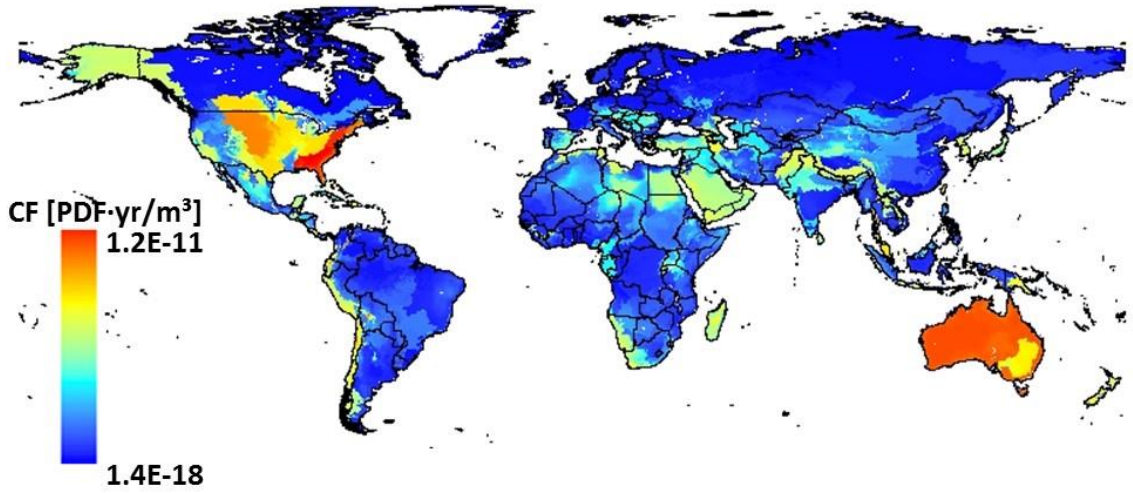

Figure 12.16: Core characterization factors for impacts from surface water consumption on all animal taxa and impacts from water consumption on vascular plants. Aggregated across taxa as described in the framework document.

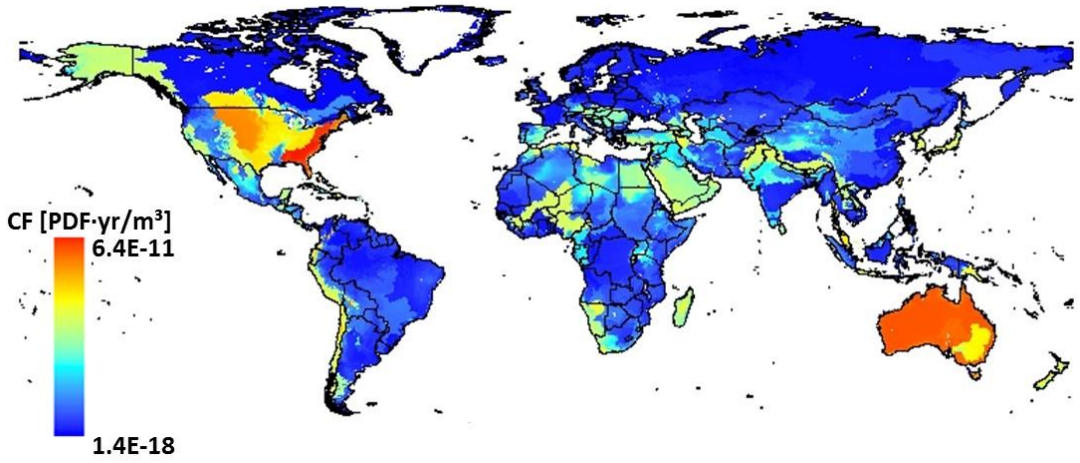

Figure 12.17: Extended characterization factors. In addition to the values from Figure 12.16, also impacts from groundwater consumption on animal taxa is included here.

Table 12.3: Global averages for the CFs.

	CF_{SW} core [PDF·yr/m³]	CF extended [PDF·yr/m³]
Ecosystem quality	1.63E-13	1.65E-13

Table 12.4: CFs per country. For the core, only surface water consumption (SW) is considered fpr anima taxa, in addition to water consumption impacts on vascular plants. Groundwater consumption (GW) is considered only in the extended CF. The unit is always [PDF·yr/m³]. Values shown here include vulnerabilities of animal species.

Country	**CF core [PDF·yr/m³]**	**CF extended [PDF·yr/m3]**
Afghanistan	1.57E-14	1.57E-14
Albania	3.15E-15	3.24E-15
Algeria	4.93E-14	7.70E-14
Angola	3.00E-15	4.28E-15
Argentina	2.52E-15	2.63E-15
Armenia	1.05E-13	1.13E-13
Australia	2.25E-12	2.34E-12
Austria	1.60E-14	3.56E-13
Azerbaijan	1.39E-14	2.11E-14
Bahamas, The	8.80E-12	8.80E-12
Bangladesh	3.73E-15	4.04E-15
Belarus	3.69E-16	6.24E-16
Belgium	3.31E-16	3.31E-16
Belize	5.21E-15	7.74E-15
Benin	5.25E-16	1.26E-14
Bhutan	2.97E-14	3.06E-14
Bolivia	1.36E-13	1.36E-13
Bosnia and Herzegovina	7.99E-15	1.24E-14
Botswana	3.12E-15	3.12E-15
Brazil	2.76E-15	2.85E-15
Brunei	2.68E-15	2.68E-15
Bulgaria	9.50E-15	1.75E-14
Burkina Faso	1.57E-15	1.58E-14
Burundi	2.82E-14	2.82E-14
Cambodia	1.63E-15	1.63E-15
Cameroon	1.29E-14	2.97E-14
Canada	2.83E-13	2.85E-13
Cape Verde	0.00E+00	0.00E+00
Central African Republic	4.09E-15	4.09E-15
Chad	4.37E-15	9.44E-15
Chile	8.86E-14	8.86E-14
China	2.32E-15	2.35E-15
Colombia	6.94E-14	6.94E-14
Comoros	0.00E+00	0.00E+00
Congo	2.93E-15	2.93E-15
Congo DRC	2.16E-15	2.16E-15
Cook Islands	0.00E+00	0.00E+00
Costa Rica	2.12E-14	2.12E-14
Croatia	8.66E-15	1.34E-14
Cuba	1.07E-14	1.07E-14
Cyprus	5.51E-14	5.51E-14
Czech Republic	4.08E-15	5.39E-15
Denmark	4.91E-16	4.91E-16
Djibouti	6.42E-15	6.43E-15
Dominican Republic	1.17E-13	1.18E-13
Ecuador	1.83E-13	1.83E-13
Egypt	1.73E-14	1.74E-14
El Salvador	6.31E-15	8.92E-15
Equatorial Guinea	1.28E-14	1.28E-14
Eritrea	5.86E-15	5.86E-15
Estonia	2.82E-16	2.95E-16
Ethiopia	6.60E-15	6.63E-15
Falkland Islands (Islas Malvinas)	0.00E+00	0.00E+00
Faroe Islands	0.00E+00	0.00E+00
Fiji	4.84E-14	4.84E-14
Finland	3.68E-16	8.99E-16

France	6.19E-16	7.03E-16
French Guiana	2.39E-15	2.39E-15
French Polynesia	0.00E+00	0.00E+00
Gabon	9.24E-15	9.24E-15
Gambia, The	1.82E-15	1.82E-15
Georgia	1.25E-14	1.75E-14
Germany	4.21E-15	5.12E-15
Ghana	9.01E-16	9.01E-16
Greece	5.52E-15	5.54E-15
Greenland	7.10E-17	7.10E-17
Guadeloupe	0.00E+00	0.00E+00
Guatemala	1.52E-14	1.60E-14
Guinea	7.77E-15	2.89E-14
Guinea-Bissau	5.49E-16	5.49E-16
Guyana	1.30E-15	1.30E-15
Haiti	8.42E-14	8.43E-14
Honduras	7.88E-15	9.36E-15
Hungary	1.30E-14	2.05E-14
Iceland	4.90E-16	4.90E-16
India	1.12E-14	1.12E-14
Indonesia	2.92E-14	2.92E-14
Iran	2.31E-14	2.47E-14
Iraq	1.00E-14	1.08E-14
Ireland	7.59E-16	5.48E-15
Israel	1.77E-14	1.77E-14
Italy	3.41E-15	3.48E-15
Ivory Coast	5.06E-15	8.66E-15
Jamaica	6.40E-15	6.40E-15
Japan	1.28E-14	5.25E-14
Jordan	3.47E-13	3.48E-13
Kazakhstan	1.93E-15	1.93E-15
Kenya	5.74E-15	5.75E-15
Kiribati	0.00E+00	0.00E+00
Kuwait	2.53E-14	2.55E-14
Kyrgyzstan	7.61E-15	7.61E-15
Laos	2.42E-14	2.42E-14
Latvia	2.42E-16	4.32E-16
Lebanon	5.86E-14	5.86E-14
Lesotho	1.46E-15	1.46E-15
Liberia	3.31E-15	3.31E-15
Libya	4.26E-14	4.88E-14
Lithuania	2.74E-16	2.74E-16
Luxembourg	5.65E-15	5.65E-15
Macedonia	2.77E-15	2.79E-15
Madagascar	9.74E-14	9.75E-14
Malawi	1.99E-15	1.99E-15
Malaysia	2.40E-13	2.40E-13
Mali	1.60E-15	4.54E-14
Mauritania	1.13E-15	1.49E-15
Mauritius	0.00E+00	0.00E+00
Mexico	1.24E-14	1.25E-14
Moldova	2.22E-15	5.17E-15
Mongolia	3.72E-15	3.72E-15
Montenegro	5.77E-15	7.12E-15
Morocco	8.61E-15	1.63E-14
Mozambique	2.81E-15	2.81E-15
Myanmar (Burma)	1.63E-14	1.63E-14
Namibia	1.88E-14	6.65E-14
Nepal	1.33E-14	1.42E-14
Netherlands	5.24E-16	5.32E-16
New Caledonia	1.23E-14	1.23E-14
New Zealand	4.08E-14	4.87E-14
Nicaragua	6.54E-15	6.80E-15

Niger	2.22E-15	3.59E-14
Nigeria	3.11E-15	2.88E-14
North Korea	3.78E-14	3.79E-14
Norway	4.00E-16	4.00E-16
Oman	3.36E-14	3.39E-14
Pakistan	3.58E-14	3.59E-14
Panama	8.56E-15	8.56E-15
Papua New Guinea	4.57E-14	4.57E-14
Paraguay	3.30E-15	3.50E-15
Peru	5.76E-14	5.76E-14
Philippines	2.69E-14	2.69E-14
Poland	4.30E-16	5.64E-16
Portugal	4.23E-15	5.99E-15
Puerto Rico	2.57E-12	2.57E-12
Qatar	1.83E-14	1.85E-14
Reunion	0.00E+00	0.00E+00
Romania	4.21E-15	9.86E-15
Russia	3.74E-15	3.75E-15
Rwanda	3.07E-14	3.07E-14
Sao Tome and Principe	0.00E+00	0.00E+00
Saudi Arabia	2.89E-14	2.91E-14
Senegal	6.20E-16	6.20E-16
Serbia	1.29E-14	2.00E-14
Sierra Leone	5.26E-15	5.26E-15
Slovakia	1.07E-14	1.67E-14
Slovenia	2.67E-14	4.19E-14
Solomon Islands	2.36E-15	2.36E-15
Somalia	3.21E-15	3.21E-15
South Africa	1.76E-14	1.76E-14
South Korea	3.99E-14	4.75E-14
Spain	1.18E-14	1.45E-14
Sri Lanka	2.25E-14	2.25E-14
St. Vincent and the Grenadines	0.00E+00	0.00E+00
Sudan	5.37E-15	5.38E-15
Suriname	9.48E-16	9.48E-16
Svalbard	1.15E-16	1.15E-16
Swaziland	5.43E-15	5.43E-15
Sweden	4.63E-16	5.11E-16
Switzerland	7.66E-15	7.73E-15
Syria	4.16E-14	4.19E-14
Taiwan	2.96E-13	2.96E-13
Tajikistan	3.60E-15	3.60E-15
Tanzania, United Republic of	4.65E-15	4.66E-15
Thailand	3.41E-14	3.41E-14
Togo	3.84E-16	3.84E-16
Trinidad and Tobago	1.78E-15	1.78E-15
Tunisia	6.21E-14	1.01E-13
Turkey	1.92E-14	1.95E-14
Turkmenistan	1.22E-14	1.22E-14
Uganda	1.13E-14	1.13E-14
Ukraine	1.02E-15	1.43E-15
United Arab Emirates	3.95E-14	3.98E-14
United Kingdom	6.32E-16	2.68E-15
United States	1.15E-12	1.15E-12
Uruguay	1.77E-15	1.91E-15
Uzbekistan	4.07E-15	4.07E-15
Vanuatu	0.00E+00	0.00E+00
Venezuela	2.33E-15	2.33E-15
Vietnam	3.36E-15	3.36E-15
Virgin Islands	0.00E+00	0.00E+00
West Bank	2.20E-14	2.20E-14
Western Sahara	2.01E-15	2.60E-15
Western Samoa	0.00E+00	0.00E+00

Yemen	5.81E-14	5.87E-14
Zambia	2.94E-15	2.94E-15
Zimbabwe	2.54E-15	2.54E-15

Table 12.5: CFs per continent. For the core, only surface water consumption (SW) is considered fpr anima taxa, in addition to water consumption impacts on vascular plants. Groundwater consumption (GW) is considered only in the extended CF. The unit is always [PDF·yr/m³]. Values shown here include vulnerabilities of animal species.

Continent	CF core [PDF·yr/m³]	CF extended [PDF·yr/m3]
Africa	1.58E-14	1.96E-14
Antarctica	0.00E+00	0.00E+00
Asia	1.46E-14	1.52E-14
Australia	2.23E-12	2.32E-12
Europe	4.57E-15	9.02E-15
North America	9.83E-13	9.84E-13
Oceania	4.22E-14	5.05E-14
South America	3.19E-14	3.20E-14

12.2.7. References

Abell, R., Thieme, M. L., Revenga, C., Bryer, M., Kottelat, M., et al. (2008). "Freshwater Ecoregions of the World: A New Map of Biogeographic Units for Freshwater Biodiversity Conservation." BioScience **58**(5): 403-414.

Amores, M. J., Verones, F., Raptis, C., Juraske, R., Pfister, S., Stoessel, F., Antón, A., Castells, F. and Hellweg, S. (2013). "Biodiversity Impacts from Salinity Increase in a Coastal Wetland." Environ. Sci. Technol. **47**(12): 6384-6392.

Azevedo, L. B. (2014). Development and application of stressor – response relationships of nutrients. Chapter 8. Ph.D. Dissertation, Radboud University Nijmegen, The Netherlands. http://repository.ubn.ru.nl.

Azevedo, L. B., Henderson, A. D., van Zelm, R., Jolliet, O. and Huijbregts, M. A. J. (2013a). "Assessing the Importance of Spatial Variability versus Model Choices in Life Cycle Impact Assessment: The Case of Freshwater Eutrophication in Europe." Environmental Science & Technology **47**(23): 13565-13570.

Azevedo, L. B., van Zelm, R., Elshout, P. M. F., Hendriks, A. J., Leuven, R. S. E. W., Struijs, J., de Zwart, D. and Huijbregts, M. A. J. (2013b). "Species richness–phosphorus relationships for lakes and streams worldwide." Global Ecology and Biogeography **22**(12): 1304-1314.

Azevedo, L. B., van Zelm, R., Hendriks, A. J., Bobbink, R. and Huijbregts, M. A. J. (2013c). "Global assessment of the effects of terrestrial acidification on plant species richness." Environmental Pollution **174**(0): 10-15.

Carpenter, S. R., Caraco, N. F., Correll, D. L., Howarth, R. W., Sharpley, A. N. and Smith, V. H. (1998). "Nonpoint pollution of surface waters with phosphorus and nitrogen." Ecological Applications **8**(3): 559-568.

Chaudhary, A., Verones, F., De Baan, L. and Hellweg, S. (2015). "Quantifying Land Use Impacts on Biodiversity: Combining Species-Area Models and Vulnerability Indicators." Environ. Sci. Technol. **49**(16): 9987-9995.

CIESIN, (Center for Interantional Earth Science Information Network, Columbia University) and CIAT, (Centro Internacional de Agricultura Tropical) (2005). Gridded Population of the World, Version 3 (GPWv3): Population Density Grid. Palisades,NY: NASA Socieoeconomic Data and Applictions Center (SEDAC). http://dx.doi.org/10.7927/H4XK8CG2 (03.09.2014).

Drakare, S., Lennon, J. and Hillebrand, H. (2006). "The imprint of the geographical, evolutionary and ecological context on species-area relationships." Ecology Letters **9**: 215-227.

Elser, J. J., Bracken, M. E. S., Cleland, E. E., Gruner, D. S., Harpole, W. S., Hillebrand, H., Ngai, J. T., Seabloom, E. W., Shurin, J. B. and Smith, J. E. (2007). "Global analysis of nitrogen and phosphorus limitation of primary producers in freshwater, marine and terrestrial ecosystems." Ecology Letters **10**(12): 1135-1142.

Evans, M. and Jingqiu, M. (2009). "Updated Chemical Reactions Now Used in GEOS-Chem v8-02-01 Through GEOS-Chem v8-02-03." Oxidants and Chemistry Working Group Retrieved June 6th, 2011, from http://acmg.seas.harvard.edu/geos/wiki_docs/chemistry/chemistry_updates_v5.pdf.

Falkengren-Grerup, U. (1986). "Soil acidification and vegetation changes in deciduous forest in Southern-Sweeden." Oecologia **70**(3): 339-347.

Gerst, M. D. (2008). "Revisiting the cumulative grade-tonnage relationship for major copper ore types." Economic Geology **103**(3): 615-628.

Goedkoop, M. (2000). The Eco-indicator 99 LCIA methodology - an introduction. Eco-Indicator 99 - eine schadensorientierte Bewertungsmethode. Nachbereitung zum 12. Diskussionsforum Ökobilanzen vom 30. Juni and der ETH Zürich. T. Baumgartner and A. Braunschweig. Zurich, Switzerland.

Goedkoop, M., Heijungs, R., Huijbregts, M. A. J., De Schryver, A., Struijs, J. and van Zelm, R. (2009). ReCiPe 2008: A life cycle impact assessment method which comprises harmonised category

indicators at the midpoint and endpoint levels. First edition. Report i: Characterization. The Netherlands, Ruimte en Milieu, Ministerie van Volkshuisvesting, Ruimtelijke Ordening en Milieubeheer.

Helmes, R. J. K., Huijbregts, M. A. J., Henderson, A. D. and Jolliet, O. (2012). "Spatially explicit fate factors of phosphorous emissions to freshwater at the global scale." International Journal of Life Cycle Assessment **17**(5): 646-654.

Huijbregts, M. A. J., Hellweg, S. and Hertwich, E. (2011). "Do We Need a Paradigm Shift in Life Cycle Assessment?" Environ. Sci. Technol. **45**: 3833-3834.

IIASA. (2015). "ECLIPSE V5 global emission fields." Retrieved 10 September, 2016, from http://www.iiasa.ac.at/web/home/research/researchPrograms/air/ECLIPSEv5.html.

ISO (2006a). Environmental Management - Life Cycle Assessment - Principles and Framework. International Standard ISO 14040. International Organisation for Standardisation. Geneva, Switzerland.

ISO (2006b). Environmental management - Life Cycle Assessment - Requirements and guidelines. International Standard ISO 14044, International Organisation for Standardisation. Geneva, Switzerland.

IUCN (2014). International Union for Conservation of Nature. Red List of Threatened Species. Version 2010.1. Downloaded on 30 June 2014 at www.iucnredlist.org.

IUCN, (International Union for Conservation of Nature and Natural Resources). (2012). "The IUCN Red List of Threatened Species. Version 2012.2." Retrieved 25 October, 2012, from www.iucnredlist.org

IUCN, (International Union for Conservation of Nature and Natural Resources). (2013a). "The IUCN Red List of Threatened Species." Retrieved 11 November, 2013, from http://www.iucnredlist.org/.

IUCN, (International Union for Conservation of Nature and Natural Resources). (2013b). "Spatial Data Download." Retrieved 3 October, 2013, from http://www.iucnredlist.org/technical-documents/spatial-data.

Jackson, R. B., Canadell, J., Ehleringer, J. R., Mooney, H. A., Sala, O. E. and Schulze, E. D. (1996). "A global analysis of root distributions for terrestrial biomes." Oecologia **108**(3): 389-411.

Kier, G., Kreft, H., Lee, T. M., Jetz, W., Ibisch, P. L., Nowicki, C., Mutke, J. and Barthlott, W. (2009). "A global assessment of endemism and species richness across island and mainland regions." PNAS **106**(23): 9322-9327.

Kreft, H. and Jetz, W. (2007). "Global patterns and determinants of vascular plant diversity." PNAS **104**(14): 5925-5930.

Krewski, D., Jerrett, M., Burnett, R. T., Ma, R., Hughes, E., Shi, Y., Turner, M. C., Pope, C. A., Thurston, G. D., Calle, E. E. and Thun, M. J. (2009). Extended follow-up and spatial analysis of the American Cancer Society study linking particulate air pollution and mortality. Boston, Massachusetts, USA, Health Effects Institute. **Research Report 140**.

Lamarque, J. F., Bond, T. C., Eyring, V., Granier, C., Heil, A., et al. (2010). "Historical (1850-2000) gridded anthropogenic and biomass burning emissions of reactive gases and aerosols: methodology and application." Atmos. Chem. Phys. **10**(15): 7017-7039.

Larsen, F. W., Bladt, J., Balmford, A. and Rahbek, C. (2012). "Birds as biodiversity surrogates: will supplementing birds with other taxa improve effectiveness?" Journal of Applied Ecology **49**: 349-356.

Leflaive, J. and Ten-Hage, L. (2007). "Algal and cyanobacterial secondary metabolites in freshwaters: a comparison of allelopathic compounds and toxins." Freshwater Biology **52**(2): 199-214.

Marsden, M. W. (1989). "Lake restoration by reducing external phosphorus loading: the influence of sediment phosphorus release." Freshwater Biology **21**(2): 139-162.

MathWorks (2013). "Matlab Version 2013b."

Mutel, C. L. and Hellweg, S. (in preparation). "Computational Methods for Regionalized Life Cycle Assessment." Environmental Science and Technology.

NOAA. (2005). "National Climatic Data Center State of the Climate: Global Analysis for Annual 2005." Retrieved June 5th, 2011, from www.ncdc.noaa.gov/sotc/global/2005/13.

Oberdorff, T., Guégan, J.-F. and Hugueny, B. (1995). "Global scale patterns of fish species richness in rivers." Ecography **18**: 345-352.

Olson, D. M., Dinerstein, E., Wikramanayake, E. D., Burgess, N., Powell, G. V. N., Underwood, E., D'Amico, J. A., Itoua, I., Strand, H. E., Morrison, J. C., Loucks, C. J., Allnutt, T. F., Ricketts, T. H., Kura, Y., Lamoreux, J. F., Wettengel, W. W., Hedao, P. and Kassem, K. R. (2001a). "Terrestrial Ecoregions of the World: A New Map of Life on Earth (Note: data update from 2004 used)." BioScience **51**(11): 933-938.

Olson, D. M., Dinerstein, E., Wikramanayake, E. D., Burgess, N. D., Powell, G. V. N., Underwood, E. C., D'Amico, J. A., Itoua, I., Strand, H. E., Morrison, J. C., Loucks, C. J., Allnutt, T. F., Ricketts, T. H., Kura, Y., Lamoreux, J. F., Wettengel, W. W., Hedao, P. and Kassem, K. R. (2001b). "Terrestrial ecoregions of the worlds: A new map of life on Earth." Bioscience **51**(11): 933-938.

Palmer, M. A., Lettenmaier, D. P., Poff, N. L., Postel, S. L., Richter, B. and Warner, R. (2009). "Climate change and river ecosystems: protection and adaptation options." Environ. Manag. **44**: 1053-1068.

Pfister, S., Bayer, P., Koehler, A. and Hellweg, S. (2011a). "Environmental Impacts of Water Use in Global Crop Production: Hotspots and Trade-Offs with Land Use." Environ. Sci. Technol. **45**(13): 5761-5768.

Pfister, S., Bayer, P., Koehler, A. and Hellweg, S. (2011b). "Projected water consumption in future global agriculture: Scenarios and related impacts." Science of the total environment **409**: 4206-4216.

Pfister, S., Curran, M., Koehler, A. and Hellweg, S. (2010). Trade-offs between land and water use: regionalized impacts of energy crops. Proceedings of the 7th International Conference on LCA in the Agri-Food Sector.

Pfister, S., Koehler, A. and Hellweg, S. (2009). "Assessing the Environmental Impacts of Freshwater Consumption in LCA." Environ. Sci. Technol. **43**(11): 4098-4104.

Prior, T., Giurco, D., Mudd, G., Mason, L. and Behrish, J. (2012). "Resource depletion, peak minerals and the implications for sustainable resource management." Global Environmental Change **22**(3): 577-587.

Ramsar Convention (1994). Convention on Wetlands of International Importance especially as Waterfowl Habitat. The Convention on Wetlands text, as amended in 1982 and 1987. Paris, Director, Office of International Standards and Legal Affairs; United Nations Educational, Scientific and Cultural Organization (UNESCO).

Roem, W. J. and Berendse, F. (2000). "Soil acidity and nutrient supply ratio as possible factors determining changes in plant species diversity in grassland and heathland communities." Biological Conservation **92**(2): 151-161.

Roy, P.-O., Azevedo, L. B., Margni, M., van Zelm, R., Deschênes, L. and Huijbregts, M. A. J. (2014). "Characterization factors for terrestrial acidification at the global scale: A systematic analysis of spatial variability and uncertainty." Science of The Total Environment **500–501**: 270-276.

Roy, P.-O., Deschênes, L. and Margni, M. (2012a). "Life cycle impact assessment of terrestrial acidification: Modeling spatially explicit soil sensitivity at the global scale." Environmental Science & Technology **45**(15): 8270–8278.

Roy, P.-O., Deschênes, L., Margni, M. and Huijbregts, M. A. J. (2012b). "Spatially-differentiated atmospheric source-receptor relationships for nitrogen oxides, sulfur oxides and ammonia emissions at the global scale for life cycle impact assessment." Atmospheric Environment **62**: 74-81.

Scherer, L. and Pfister, S. (2015). "Modelling spatially explicit impacts from phosphorus emissions in agriculture." The International Journal of Life Cycle Assessment **20**(6): 785-795.

Schindler, D. W. (1977). "Evolution of phosphorus limitation in lakes." Science **195**(4275): 260-262.

Schindler, D. W. (2012). "The dilemma of controlling cultural eutrophication of lakes." Proceedings of the Royal Society B: Biological Sciences.

Stelzig, S. (2012). Berechnung der Grundwasserabsenkung für stationäre Verhältnisse. Handbuch Geotechnik. Grundlagen- Anwendungen-Praxiserfahrungen. C. Boley, Vieweg&Teubner.

Struijs, J., Beusen, A., de Zwart, D. and Huijbregts, M. (2011a). "Characterization factors for inland water eutrophication at the damage level in life cycle impact assessment." International Journal of Life Cycle Assessment **16**(1): 59-64.

Struijs, J., De Zwart, D., Posthuma, L., Leuven, R. S. E. W. and Huijbregts, M. A. J. (2011b). "Field sensitivity distribution of macroinvertebrates for phosphorus in inland waters." Integrated Environmental Assessment & Management **7**(2): 280-286.

United Nations and Department of Economic and Social Affairs, Population Divison, (2011). "World Population Prospectes: The 2010 Revision, CD-ROM edition."

Van Goethem, T., Preiss, P., Azevedo, L. B., Friedrich, R., Huijbregts, M. A. J. and Van Zelm, R. (2013). "European characterization factors for damage to natural vegetation by ozone in life cycle impact assessment." Atmospheric Environment **77**: 318-324.

van Zelm, R., Huijbregts, M. A. J., Van Jaarsveld, H. A., Reinds, G. J., De Zwart, D., Struijs, J. and Van de Meent, D. (2007). "Time horizon dependent characterization factors for acidification in life-cycle assessment based on forest plant species occurrence in Europe." Environmental Science & Technology **41**(3): 922-927.

Verones, F., Huijbregts, M. A. J., Chaudhary, A., De Baan, L., Koellner, T. and Hellweg, S. (2015). "Harmonizing the Assessment of Biodiversity Effects from Land and Water Use within LCA." Environ. Sci. Technol. **49**(6): 3584-3592.

Verones, F., Pfister, S. and Hellweg, S. (2013a). "Quantifying area changes of internationally important wetlands due to water consumption in LCA." Environ. Sci. Technol. **47**(17): 9799-9807.

Verones, F., Pfister, S., van Zelm, R. and Hellweg, S. (submitted). "Biodiversity impacts from water consumption on a global scale for use in life cycle assessment."

Verones, F., Saner, D., Pfister, S., Baisero, D., Rondinini, C. and Hellweg, S. (2013b). "Effects of consumptive water use on wetlands of international importance." Environ. Sci. Technol. **47**(21): 12248-12257.

Vieira, M. D. M., Goedkoop, M. J., Storm, P. and Huijbregts, M. A. J. (2012). "Ore Grade Decrease As Life Cycle Impact Indicator for Metal Scarcity: The Case of Copper." Environmental Science & Technology **46**(23): 12772-12778.

Vörösmarty, C. J., Lévêque, C. and Revenga, C. (2005). Chapter 7 - Fresh water. Volume 1. Millennium Ecosystem Assessment, Island Press.

WATCH. (2011). "Water and global change." Retrieved August, 2012, from http://www.eu-watch.org/; download of data from: https://gateway.ceh.ac.uk/terraCatalog/Start.do.

Wegener Sleswijk, A., van Oers, L. F. C. M., Guinée, J. B., Struijs, J. and Huijbregts, M. A. J. (2008). "Normalisation in product life cycle assessment: An LCA of the global and European economic systems in the year 2000." Science of the total environment **390**(1): 227-240.

WHO, (World Health Organization). (2014). "Estimaters for 2002-2012: Disease burden." Retrieved 1 December, 2014, from http://www.who.int/healthinfo/global_burden_disease/estimates/en/index2.html.

Wilson, A. E., Sarnelle, O. and Tillmanns, A. R. (2006). "Effects of cyanobacterial toxicity and morphology on the population growth of freshwater zooplankton: Meta-analyses of laboratory experiments." Limnology and Oceanography **51**(4): 1915-1924.

World Water Assessment Programme (2009). The United Nations World Water Development Report 3: Water in a Changing World. Paris: UNESCO and London:Earthscan.

Xenopoulos, M. A., Lodge, D. M., Alcamo, J., Märker, M., Schulze, K. and van Vuurens, D. P. (2005). "Scenarios of freshwater fish extinctions from climate change and water withdrawal." Global Change Biol. **11**: 1557-1564.

Zvereva, E. L., Toivonen, E. and Kozlov, M. V. (2008). "Changes in species richness of vascular plants under the impact of air pollution: a global perspective." Global Ecology and Biogeography **17**(3): 305-319.

12.2.7. Appendix

Overview of assumptions and possible implications for the outcome of the FF calculation. Taken from Verones et al. (2013a)

Assumption/uncertainty	Implications for outcome	Tested/described?	Justification
Wetland areas as circles	area loss might be different with different form fragmentation of wetland area is not included	not tested, described in SI	Some wetlands in Germany and Florida modelled as "ideal" or "circular" cones. For GW-fed wetlands: depression cone around pumping well is also a circle, thus geomteric form used for both. Cannot be tested for GW-fed wetlands, since depression cones could not be rectangles (e.g.) Fragmentation is important for wetlands but cannot be modelled on a global scale
Cone	volume can be different and thus loss of wetland area	tested, described in SI	Difference between ellipsoid or straight cone is marginal, problems as for circle areas remain (see above)
Dupuit-Thiem well formula	strong implications, because non-linear	discussed, parameters within formula varied	We varied parameters within the formula, however, we did not test replacement of the formula itself. It is a commonly used formula for unconfined aquifers and steady-state conditions. Unless groundwater models are established for every single wetland, this is the simpification that can be used.
Steady-state assumption GW	Fate might be occurring over longer or shorter time scales and affect the effect factor	not specifically described/tested	steady-state assumptions are common in hydrology and do not need further justification. In LCA, impacts are generally aggregated over time
Delineation of AoR	influence on the Dupuit-Thiem well formula, thus influence potentially high (non-linear influence)	described	We did not test alternative approaches for the AoR delineation. Again, simple equations are almost non-existent for the complex topic of groundwater and aquifers. Unless groundwater models are established for every single wetland, simplifications are necessary.
Surface water flows	large implications, depending on the river courses, width of rivers and amounts of water	tested and described	We used our own model (whose uncertainty we did not quantify, since we do not have the uncertainty of the underlying data) and WaterGap, in order to test their influence.
Water consumption	large implications for GW-fed wetlands	tested and described	We calculated for each wetland two different FFs with different water consumption, thus testing the influence of this parameter on the FFs.
Residence time constant	Small implications	tested and described	We assumed the residence time to remain constant and tested this assumption. We only found negligible differences.
Hydraulic gradient	Potentially larger implications because it enters a non-linear equation	not tested	We chose a conservative value that is in the range of the natural hydraulic gradients

Uncertainty in underlying data	P, PET, AET, A, water source, depth kf, m could influence the FF	- A changed from Ramsar to waterbody area - global flows used from two different models - k_f varied by factor 100 - depth varied - water source not varied - m not varied Those that were changed were described and tested	We varied some of the parameters that we used, such as water depth, underlying area or also the surface water volumes used. However, we did not vary the aquifer thickness m for example. We also do not know the uncertainty if the data itself, i.e. the uncertainty of the precipitation, Ramsar areas or potential evapotranspiration and thus cannot check for further uncertainties.

13.Mineral resource scarcity

Marisa Vieira[1,2], Mark A.J. Huijbregts[1]*

[1] Department of Environmental Science, Radboud University Nijmegen, The Netherlands

[2] PRé Consultants b.v., The Netherlands

* vieira@pre-sustainability.com

Based on: Vieira *et al.* (2012) and Vieira *et al.* (2016).

13.1. Areas of protection and environmental mechanisms covered

Description of impact pathway

Mineral resources are key raw materials in many industrial sectors and hence their demand is increasing. Although it has been argued that mineral resources are available in almost infinite amounts in the earth crust, the actual availability of a mineral primarily depends on ore grades (Gerst 2008). The impact patway of mineral resource extraction is illustrated in Figure 13.1 and described in equation 13.1. When a mineral is extracted (ME), the overall ore grade of that mineral declines (OG) (Mudd 2007; Prior et al. 2012). This mechanism can be captured by cumulative grade-tonnage relationships, as shown by Vieira et al. (2012). The smaller the ore grade, the larger the amount of ore that needs to be produced for extracting the same amount of mineral resource (OP). According to Prior et al. (2012), ore grade decline can be used as an indicator for a range of societal impacts. For instance, larger amounts of ore produced for the same unit of mineral output, implies more waste (waste rock, tailings) to be handled. The larger the future mineral resource extraction (R) the larger becomes the overall increase of ore produced. Consequently, the future metal extraction is relevant and should be considered. The average increase in ore amount per kg of mineral extracted considering all future mineral resource yet to be extracted is defined as the surplus ore potential, here the life cycle impact indicator.

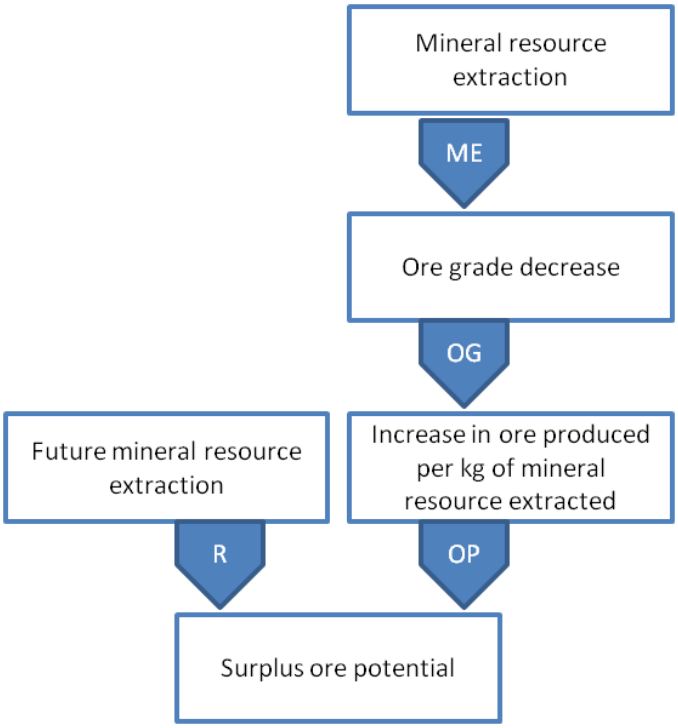

Figure 13.1: Cause-effect chain for natural resource impacts caused by mineral resource extraction. The interim steps of the impact pathway are depicted and the factors leading to them are described in equation 13.1.

Description of all related AoPs

This impact pathway only affects natural resources.

Methodological choice

An average approach is used to calculate the characterization factors. By calculating on basis of cumulative grade-tonnage relationships the increase in ore amount for all future mineral extraction and then dividing it by the future mineral extraction, average CFs are derived. These CFs are used to assess the potential impacts of mineral resource extraction worldwide.

Spatial detail

Mineral resource scarcity is a global phenomenon because there is a global market for these type of resources. As a result, no spatial detail was defined for this method.

13.2. Calculation of the characterization factors at endpoint level

The endpoint CF, expressed as the surplus ore potential (SOP), is defined as the extra amount of ore produced in the future per unit of mineral extracted, which is calculated by Equation 13.1.

$$\mathrm{CF}_{\mathrm{end},x} = \frac{\int_{CME}^{MME}(\Delta \mathrm{OP}_x)dCME}{R_x} = \frac{\int_{CME}^{MME}(\Delta \mathrm{OP}_x)dCME}{MME_x - CME_x}$$

Equation 13.1.

where $\mathrm{CF}_{\mathrm{end},x}$ ($\mathrm{kg_{ore}/kg}_x$) is the average Surplus Ore Potential of mineral x, OP_x is the ore produced per amount of mineral resource x extracted ($\mathrm{kg_{ore}/kg}_x$), and R_x (kg_x) is the actual reserve of the mineral x, defined as the maximum amount to be extracted of that mineral (MME_x) and the difference between the current amount of mineral x extracted (CME_x).

The ore extracted per amount of mineral resource x produced (OP_x in kg_{ore}/kg_x) is equal to the inverse of the ore grade of the mineral (OG_x in fraction). The ore grade of a mineral can be derived with a cumulative grade-tonnage relationship, as previously shown by Musgrove (1965), Gerst (2008), and Vieira et al. (2012). A cumulative grade-tonnage relationship reflects the relationship between the cumulative extraction of a mineral x and its ore grade and can be derived as (Vieira et al., 2012):

$$\mathrm{OG}_x = \frac{1}{\mathrm{OP}_x} = \exp(\alpha_x) \cdot \left(\frac{\mathrm{MME}_x - \mathrm{CME}_x}{\mathrm{CME}_x}\right)^{\beta_x}$$

Equation 13.2.

where OG_x is the ore grade of mineral x (in kg_x/kg_{ore}), MME_x (in kg_x) is the maximum amount of mineral x that can be extracted, CME_x (in kg_x) is the cumulative amount of mineral x extracted, and α_x and β_x are respectively the location parameter and scale parameter of the loglogistic distribution of the cumulative grade-tonnage relationship for the mineral x.

There is sufficient information to derive SOP values for 18 mineral resources, namely aluminium, antimony, chromium, cobalt, copper, gold, iron, lead, lithium, manganese, molybdenum, nickel, niobium, phosphorus, silver, tin, uranium, and zinc (Vieira et al. 2016). For the minerals for which SOP values could not be derived on the basis of empirical cumulative grade-tonnage relationships, we used the price of the mineral resource to estimate its SOP value. Price data of 2013 was retrieved from Kelly and Matos (2013) in U.S. dollars reference year 2013 (USD2013) except for the platinum group metals and uranium. For palladium, platinum, and rhodium, average price data for 2013 was retrieved from Kitco Metals Inc. (2015). The ESA spot U_3O_8 data (a weighted average of triuranium octoxide prices paid by EU utilities for uranium delivered under spot contracts during the reference year) published by the Euratom Supply Agency (2015) was used to calculate the price for uranium. As shown in figure 13.2, the price of a mineral can be considered as a good predictor for SOP (explained variance of the regressions equals 90-91%).

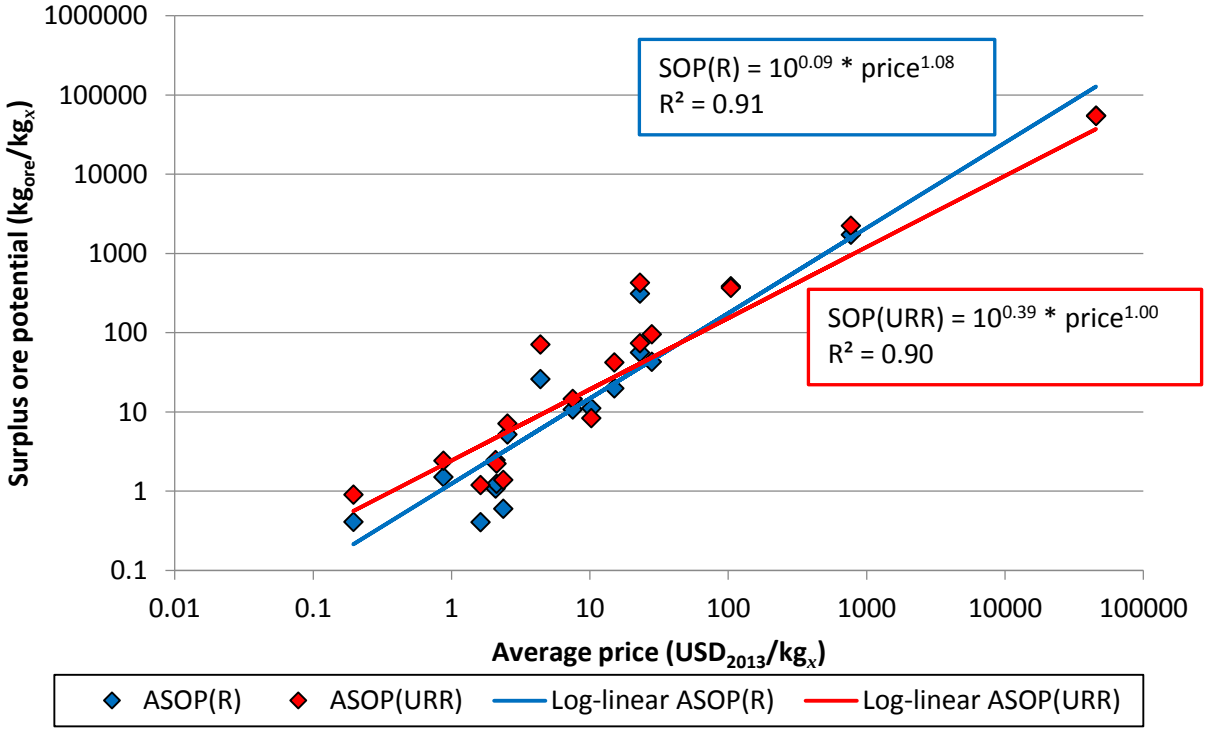

Figure 13.2: Relationship between average price in 2013 (USD_{2013}/kg_x) and surplus ore potential (kg_{ore}/kg_x). The surplus ore potential have been calculated for two different future production estimates, reserves (R) and ultimate recoverable resource (URR).

13.3. Uncertainties

The uncertainty of the characterization factors was not calculated. However, there is information of the coefficient of correlation (R^2) of the cumulative grade-tonnage curves of each mineral resource covered and these provide a good indication of the uncertainty in the CFs derived. As such, we decided to qualitatively cluster all minerals in the three classes of uncertainty depending on each R^2:

- low uncertainty if $0.9 \leq R^2 \leq 1$: aluminium, cobalt, iron, molybdenum, nickel, and phosphorus
- medium uncertainty if $0.8 \leq R^2 < 0.9$: antimony, chromium, gold, lead, and uranium
- high uncertainty if $R2 < 0.8$ or derived on basis of price: remaining mineral resources.

13.4. Value choices

Time horizon

There is no value choice related to the time horizon considered as this is infinite for this method. This means that all mineral resources to be extracted in the future are considered. No discounting to future effects is applied.

Future mineral resource extraction

One value choice that has to be made for this method is the definition of the maximum amount of a mineral resource x to be extracted (MME_x) as this is dependent on the future mineral resource to be extracted. Two different reserve estimates were applied in the calculations of the endpoint characterization factors to understand to what extent the results depend on the definition of mineral reserves. The first type of reserve estimate, used to calculate CFcore, is the 'Reserves (R)' which is defined as that part of a mineral resource "which could be economically extracted or produced at the time of determination", meaning at current prices and state of technology (U.S. Geological Survey 2015). The 'Ultimate recoverable reource (URR)', used to calculate CFextended, refer to "the amount available in the upper earth's crust that is ultimately recoverable". The definition of URR as used by UNEP (2011), there called ultimately extractable reserves, will be used here which is 0.01 % of the total amount in the crust to 3 km depth.

Table 13.1: Included effects with CFcore and CFextended.

Choice category	CFcore	CFextended
Reserve estimate	Reserves	Ultimate recoverable resource

Table 13.2: Characterization factors for natural resources.

Elementary flow	CFcore [kg_{ore}/kg]	CFextended [kg_{ore}/kg]
Aluminium	1.09E+00	2.48E+00
Antimony	1.11E+01	8.36E+00
Arsenic*	9.59E-01	1.92E+00
Ball clay*	4.16E-02	1.04E-01
Barite*	1.46E-01	3.34E-01
Bauxite*	2.60E-02	6.69E-02
Bentonite clay*	6.55E-02	1.58E-01
Beryllium*	9.09E+02	1.12E+03
Bismuth*	2.99E+01	4.68E+01

Boron*	8.39E-01	1.69E+00
Cadmium*	2.51E+00	4.68E+00
Cesium*	2.05E+05	1.73E+05
Chromium	6.01E-01	1.39E+00
Chrysolite*	2.38E+00	4.46E+00
Clay, unspecified*	6.31E-02	1.53E-01
Cobalt	4.32E+01	9.60E+01
Copper	1.08E+01	1.46E+01
Diamond (industrial)*	1.10E+03	1.34E+03
Diatomite*	3.32E-01	7.14E-01
Feldspar*	9.60E-02	2.25E-01
Fire clay*	2.10E-02	5.50E-02
Fuller's earth*	9.29E-02	2.19E-01
Gallium*	1.00E+03	1.23E+03
Germanium*	4.19E+03	4.64E+03
Gold	5.52E+04	5.46E+04
Graphite*	1.44E+00	2.80E+00
Gypsum*	1.55E-02	4.14E-02
Hafnium*	1.17E+03	1.41E+03
Ilmenite*	2.59E-01	5.68E-01
Indium*	1.25E+03	1.50E+03
Iodine*	7.02E+01	1.04E+02
Iron	4.12E-01	9.06E-01
Iron ore*	1.10E-01	2.55E-01
Kaolin*	1.58E-01	3.58E-01
Kyanite*	3.40E-01	7.31E-01
Lead	5.21E+00	7.18E+00
Lime*	1.28E-01	2.95E-01
Lithium	2.61E+01	7.10E+01
Magnesium*	6.63E+00	1.16E+01
Manganese	4.06E-01	1.20E+00
Mercury*	9.03E+01	1.31E+02
Molybdenum	3.13E+02	4.27E+02
Nickel	2.00E+01	4.23E+01
Niobium	4.81E+01	7.61E+01
Palladium*	6.88E+04	6.25E+04
Perlite*	5.48E-02	1.34E-01
Phosphorus	1.51E+00	2.44E+00
Platinum*	1.49E+05	1.28E+05
Potash*	7.48E-01	1.52E+00
Pumice and pumicite*	3.33E-02	8.42E-02
Rhenium*	7.25E+03	7.72E+03
Rhodium*	1.05E+05	9.27E+04
Rutile*	1.34E+00	2.62E+00
Selenium*	1.38E+02	1.94E+02
Silicon*	3.43E+00	6.26E+00
Silver	1.74E+03	2.24E+03
Strontium*	6.21E-01	1.28E+00
Talc*	2.52E-01	5.53E-01
Tantalum*	6.10E+02	7.74E+02
Tellurium*	1.99E+02	2.73E+02
Thallium*	1.76E+04	1.76E+04
Tin	5.65E+01	7.35E+01
Titanium*	7.43E+00	1.28E+01
Titanium dioxide pigment*	4.18E+00	7.53E+00
Tripoli*	2.30E-01	5.09E-01
Tungsten*	7.75E+01	1.14E+02
Uranium	3.86E+02	3.69E+02
Vanadium*	3.76E+01	5.81E+01
Wollastonite*	2.38E-01	5.24E-01

Zinc	1.25E+00	2.24E+00
*Garnets**	3.23E-01	6.97E-01
*Gemstones**	1.35E+05	1.17E+05
Platinum-group metals	5.99E+04	5.50E+04
*Rare earth metals**	2.97E+01	4.66E+01
*Zirconium minerals**	1.31E+00	2.56E+00

13.5. References

Euratom Supply Agency. 2015. ESA average uranium prices. Accessed 3 June 2015 at http://ec.europa.eu/euratom/observatory_price.html.

Gerst, M.D. 2008. Revisiting the cumulative grade-tonnage relationship for major copper ore types. *Economic Geology* 103(3): 615–628.

Kelly, T. D., Matos, G. R. 2013. *Historical statistics for mineral and material commodities in the United States (2013 version)*: Reston, Virginia: U.S. Geological Survey Data Series 140. Accessed 3 June 2015 at http://minerals.usgs.gov/minerals/pubs/historical-statistics/.

Kitco Metals Inc. 2015. Historical Charts and Data – London Fix. Accessed 3 June 2015 at http://www.kitco.com/charts/.

Mudd, G. M. 2007. An analysis of historic production trends in Australian base metal mining. *Ore Geology Reviews* 32(1-2): 227-261.

Musgrove, P. 1965. Lead: grade-tonnage relation. *Mining Magazine* 112(4): 249–251.

Prior, T., D. Giurco, G. Mudd, L. Mason, and J. Behrisch. 2012. Resource depletion, peak minerals and the implications for sustainable resource management. *Global Environmental Change* 22(3): 577-587.

UNEP. 2011. *Estimating long-run geological stocks of metals*. Working paper, April 6, 2011. Paris: UNEP International Panel on Sustainable Resource Management, Working Group on Geological Stocks of Metals.

U.S. Geological Survey. 2015. Mineral commodity summaries 2015. U.S. Geological Survey, 196p.

Vieira, M. D. M., T. C. Ponsioen, M. J. Goedkoop, and M. A. J. Huijbregts. 2012. Ore Grade Decrease As Life Cycle Impact Indicator for Metal Scarcity: The Case of Copper. *Environmental Science & Technology* 46(23): 12772-12778.

Vieira, M. D. M., T. C. Ponsioen, M. J. Goedkoop, and M. A. J. Huijbregts. 2016. Surplus Ore Potential as a Scarcity Indicator for Resource Extraction. *Journal of Industrial Ecology*. Advance online publication. doi: 10.1111/jiec.12444.

14.Normalization

coming soon